The development and performance of anodic biofilms in microbial fuel cells

IAIN MICHIE

A submission presented in partial fulfilment of the requirements of the

University of Glamorgan / Prifysgol Morgannwg for the degree of

Doctor of Philosophy

June 2012

Abstract

Microbial fuel cell (MFC) systems capable of both treating wastewaters and recovering energy have the potential for successful scale-up as a low carbon technology. These systems utilize microorganisms residing in biofilms as biocatalytic agents in the conversion of reduced substrates to electrical energy. As such, it is important to understand how MFC anodic biofilms develop over time and also how environmental parameters such as substrate type, temperature, carbon support material, anode architecture and optimized applied potentials also affect electrogenic performance.

The type of substrate was found to have a large impact on the acclimation and performance of electrogenic biofilms. Acetate produced the highest power density of 7.2 W m^{-3} and butyrate the lowest at 0.29 W m^{-3}, but it was also found that biofilm acclimation to these different trophic conditions also determined the MFC response to different substrate types i.e. both acetate and butyrate substrates produced power densities of 1.07 and 1.0 W m^{-3} respectively in a sucrose enriched reactor.

The use of MFCs for wastewater treatment in temperate regions requires the development of reactor systems that are robust to seasonal fluctuations and are energy efficient. As such, system performance was examined at three different operating temperatures (10°C, 20°C and 35°C). At each temperature a maximum steady-state voltage of 0.49 V ± 0.02V was achieved after an operational period of 47 weeks, with the time to reach steady-state voltage being dependent on acclimation temperature. The highest COD removal rates of 2.98g COD $L^{-1}d^{-1}$ were produced in the 35°C reactor but coulombic efficiencies (CE) were found to be significantly higher at pyschrophilic temperatures. Acclimation at different operating temperatures was found to a have a significant effect on the dynamic selection of psychrophilic, psychrotolerant and mesophilic anode respiring bacteria (ARB) and also influence the development of biofilm biomass, methanogenesis and electrogenic activity. Although start-up times were inversely influenced by temperature the amount of biomass accumulation increased with higher operational temperatures and this had a direct impact on biocatalytic performance.

The three dimensional structure and porosity of different carbon anode materials affected anodic performance by determining the levels of surface area available for biofilm growth and the capacity for mass transfer to occur. Novel helical electrode configurations were used to look at the effect of altering turbulent flows to increase mass transfer rates and carbon surface areas available

for electrogenic growth. The spiral with the highest amount of carbon veil and the smallest gap produced the highest power production of 11.63 W m^{-3}.

Comparative studies of a logic controlled and un-controlled external load impedance showed that control affected the biocatalyst development and hence MFC performance. The controlled MFC better optimized the electrogenic anodic biofilm for power production, indicating that improved power and substrate conversion can be achieved by ensuring sustainable current demand, applied microbial selection pressures and near-optimal impedance for power transference.

Acknowledgements

The author wishes to express his gratitude to the EPSRC through their RCUK Energy Programme, SUPERGEN Biological Fuel Cell project, for funding this work (grant number EP/D047943/1 and EP/H019480/1).

Special thanks also goes to the technical staff at the University of Glamorgan for all their help and advice, notably the expert guidance offered by my project supervisors Dr Jung-Rae Kim, Prof Giuliano Premier, Prof Alan Guwy and Prof Richard Dinsdale. Overriding thanks must also go to my parents, Anne and Alan Michie, for a life-time of unquestioning belief and support.

Contents

List of Figures

List of Tables

List of Equations

List of Abbreviations

AD	anaerobic digestion
ARB	Anode respiring bacteria
ATP	adenosine triphosphate
BES	bioelectrochemical system
BOD	biological oxygen demand
CE	coulombic efficiency
CLSM	confocal laser scanning microscope
COD	chemical oxygen demand
DECC	Department of Energy and Climate Change
DGGE	denaturing gradient gel electrophoresis
EAB	electrochemically active bacteria
EPS	exopolymeric substances
ETC	electron transport chain
FID	flame ionisation detector
FISH	fluorescent in-situ hybridisation
GC	gas chromatograph
HPLC	high performance liquid chromatography
HRT	hydraulic retention time
IPCC	Intergovernmental Panel on Climate Change
MEC	microbial electolysis cell
MFC	microbial fuel cell
NAD	nicotinamide adenine dinucleotide
NADH	reduced NAD
OECD	Organization for economic cooperation and development
OLR	organic loading rate

PCR	polymerase chain reaction
VFA	volatile fatty acids
VSS	volatile suspended solids
WTI	World Trade Institute

1. Introduction

1.1 Overview of Microbial Fuel Cell Technology

1.1.1 The global energy challenge

Even considering the current economic slow-down (following on from the 2007 banking crisis), the rapid economic expansion of developing nations, as set out by the New Policies Scenario, outlines that world energy demand is set to grow by an average of 1.2% per year: of this 93% will be due to growth from non-OECD countries (Tanaka 2010) and it is predicted that 80-85% of this energy demand will still be derived from fossil fuels. These figures include measures to curb CO_2 greenhouse gas emissions, as set out by the Kyoto Protocol 1997, to levels of just 450 parts per million of CO_2 equivalent which in itself would only look to maintain projected increases in global temperature to 2°C. Predictions from the IPCC fourth assessment report in 2007 however state that levels of 800 parts per million of CO_2 equivalent and world temperature rises of 1.1 – 6.4°C could occur by the year 2100 (Intergovernmental et al. 2007). In order to achieve these targets it will be necessary to impose both restrictions on carbon emissions and carbon penalties, the result of which will be an economically driven progressive increase in the oil price over time. As of February 2012 the WTI crude oil price is currently over $100 dollars a barrel, an increase of $40 dollars in 5 years. These factors, together with requirements for energy security, have focused governmental thinking on the need to develop alternative low carbon renewable energy sources. Technologies such as wind, solar, hydro and wave are likely to meet the bulk of the UK government targets to achieve a 20% level of electricity from renewable sources by 2020. However, no one solution is likely to be the answer to replace fossil fuels in their entirety. Instead a number of different solutions will have to be found to suit specific tasks and niche applications in order to find a best overall solution, and it is possible that technologies based on bioelectrochemical fuel cell technology could play a part in this low carbon renewable environment.

1.1.2 Wastewater treatment in the UK: energy burden or energy resource?

Wastewater treatment is a process that uses high amounts of energy, it is estimated that it takes approximately 6.34 gigawatt hours of energy to treat 10 billion litres per day of sewage, almost 1% of the average daily electricity consumption of England and Wales based on DECC regional electricity

consumption statistics (Anon 2005). This aerobic energy demand process is centered on the requirement for mass transfer of oxygen from the air to the water phase. Whilst mechanical energy is expended in supplying oxygen this process is limited by its efficiency of transfer to bacteria present in the wastewater in aerobic systems. This is not the case in anaerobic processes where hydrogen or electron transfer occurs directly and is therefore not subject to these mass transfer limitations. However wastewater also has an intrinsic energetic value. This can be considered by looking at sucrose as an example, as this contains 4.41 kWh of energy per kg but can also be viewed as water pollutant having a chemical oxygen demand of 1.06 kg. Indeed it was estimated by Shizas and Bagley (2004) that the energetic content of wastewater exceeds the energetic value to treat it by 9.3 fold. It is this approach that has driven the current development of renewable energy production from sewage processes via gasification, pyrolysis and anaerobic digestion (AD); as of 2005 – 2006, the amount of renewable energy generated on water industry sites was 493 gigawatt hours or 6.4% of the total energy used to treat water and wastewater according to a recent Parliamentary office for Science and Technology report (Anon 2007). However alternative technologies such as Microbial Fuel Cells (MFC) could provide additional and complementary treatment strategies by facilitating simultaneous treatment of wastewaters whilst also further recovering additional energy. BES type systems have also been investigated as potential systems that can enable the bioelectrochemical synthesis of important industrial chemicals/polymers that would otherwise require fossil based materials (Rabaey and Rozendal 2010).

1.1.3 100 years: the development of MFC technology

The origins of MFC technology lie in the discovery of "bioelectricity" by Luigi Galvani and the invention of early batteries by Alesandro Volta in late 18th Century Bologna. However it is now 100 years since M.C. Potter described the first actual MFC using *E.coli* as a biocatalyst to generate electricity. Since this point, MFC technology advanced sporadically with Cohen et al (1931) expanding the range of bacteria that could be demonstrated to exhibit low levels of electrogenic activity to include *Bacillus.dysenteriae, Corynebacterium.diphileriae, Bacillus.subtilis* and *Proteus.vulgaris*; and in 1962 Davis and Yarbrough (1962) then linked the metabolic activity of microorganisms growing on a low potential anode to the collection of electrons at a high potential cathode. The discovery of exocellular respiratory processes and the use of exogenous synthetic mediators in the 1980's led to further advances in MFC understanding (Allen and Bennetto 1993), this work also showed that it may be possible to apply these reactors as practical large scale systems. It was subsequently discovered that MFCs did not require mediators (Kim et al. 2002) and

that wastewater may be used as a fuel and also treated at the same time (Liu et al. 2004). Since this period there has been a rapid development of improved MFCs system architectures that has led to a steep rise in maximum power outputs (Logan 2010). MFCs, or more specifically Bioelectrochemical systems (BES), over the last 10 years are now producing power densities increases of 5-6 orders-of-magnitude through improvements in the physical and chemical characteristics associated with these MFC designs and developments involving material technology. Although MFCs could be used as a stand-alone energy-generating system, the technology seems more suited as a polishing step and energy recovery system associated with the treatment of anaerobic sludge fermentation (Aelterman et al. 2006). These systems now have the potential to be scaled up as an environmentally sustainable technology. Suitable applications include not only wastewater treatment and subsequent bioenergy recovery but also hydrogen production through the use of Microbial Electrolysis Cells (MEC) and the bioelectrosynthesis of value added chemicals such as butanol, succinate and polyhydroxybutyrate (PHB) (Rabaey and Rozendal 2010).

1.1.4 Bioelectrochemical Systems (BES)

1.1.4.1 Overview

These systems are characterized by a capability, under pH neutral ambient conditions, to biologically catalyze the conversion of chemical energy in reduced organic material to electrical energy in the form of electrons that can then be harvested via an anode. Whilst MFCs involved in energy generation are the archetypal microbial BES and have attracted the majority of recent research efforts, a number of BES applications relating to systems with cathodic catalytic capabilities have recently been described. These systems share similar architectures when compared to MFCs, utilizing a microbial anode to biocatalyze substrate oxidation they are able to harness the reductive energy in the cathode for the production of energy rich chemicals i.e. H_2, CH_4 and H_2O_2, reductive remediative processes and even act as desalination cells. These applications have been termed MECs, MRCs and MDCs respectively, or generically termed MXCs (Harnisch and Schroder 2010). Although applicable to all these systems the anodic work carried out in this thesis was based on MFC architecture.

1.1.4.2 Principle of operation

Bio-electrochemical systems utilize micro-organisms to catalyze the anaerobic oxidation of organic materials into useful energy carriers or products such as electricity, hydrogen and peroxide.

As part of these anodic redox processes, electrochemically active bacteria (EAB) present within the anodic chamber generate electrons along with a commensurate production of protons, CO_2 and microbial biomass. As such, the EAB act as whole cell biocatalysts which are employed in the transformation of chemical energy to electrical energy, and are typically able to offer stable and robust fixed biofilms that can facilitate a continuous processing of wastewaters (Pant et al. 2010; Pant et al. 2011). The oxidation reaction occurs in the anode compartment where bacteria can extract energy for the purposes of cell maintenance and cell growth by oxidizing organic substrate to carbon dioxide, whilst also directly donating electrons to a solid anode. These electrons can then pass through a closed circuit to a cathode to participate in the reduction of oxygen to water. This flow of electrons can thus generate electrical energy subject to the presence of a suitable external resistive load. In order to sustain the flow of electrons the cell has to balance the ionic charge between the two half-cells. This is achieved by the flow of charged ions, notably protons generated in the anodic reaction. Whilst ion exchange membranes (cation, proton, bipolar or anion exchange membranes) have been commonly used to separate anodic and cathodic processes, notably to avoid coulombic losses due to aerobic metabolism and maintain the integrity of anodic chambers in air cathode systems (Kim et al. 2007), it has also been demonstrated that BESs may operate without such membranes or with alternative separators such as glass fiber (Zhang et al. 2011b). With these types of arrangements coulombic efficiencies will typically decrease, but it has also been observed that power densities can increase due to reduced ohmic overpotentials that result from improved ionic mass transfers (Clauwaert et al. 2008) and a reduced potential for pH differences to build up between separated cells (Harnisch et al. 2008).

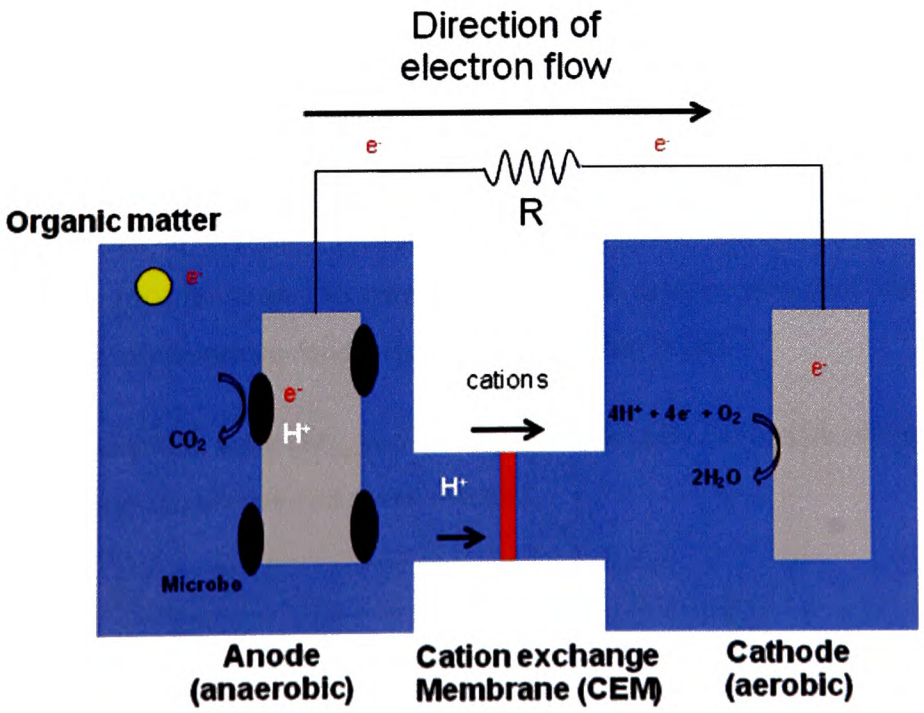

Figure 1-1. Schematic drawing of the basic features and operation of an MFC system

Tubular microbial fuel cells used as part of this project are particularly suited to operational scale-up. They are composed of an internal anodic chamber through which the waste material/electrolyte can flow; the electrical circuit is completed via an external air cathode. The anode operates under anoxic conditions and acts to accept electrons directly from microorganisms, via reduced products of metabolism or through electron transfer mediators. These electrons then flow from the anode to the cathode whilst protons migrate through a cation-exchange membrane to the cathodic chamber to complete the electrical circuit. In the cathode, oxygen is reduced at the terminal electron acceptor as illustrated by the electrode reactions for e.g. a glucose fed system.

Anode: $C_6H_{12}O_6 + 6H_2O \rightarrow 6CO_2 + 24H^+ + 24e^-$

Equation 1

Cathode: $24H^+ + 24e^- + 6O_2 \rightarrow 12H_2O$

Equation 2

Theoretical $\Delta G = -2840$ kJ/mol

1.1.5 Microbial Anodic Catabolism

1.1.5.1 Thermodynamic overview

The total voltage (V) or electromotive force (E_{emf}) in a MFC can be defined as the potential difference that exists between the anodic (E_{anode}) and cathodic ($E_{cathode}$) electrodes

$$E_{emf}\,(V) = E_{cathode}\,(V) - E_{anode}\,(V)$$

Equation 3

The likelihood of any given reaction occurring can be evaluated by looking at the Gibbs Free Energy change (ΔG) (Bard and Faulkner 2001). In MFC systems electrical energy will be generated when energetically favorable conditions prevail, i.e. when $\Delta G<0$.

Also the maximum work (W_{max}) an MFC system can carry out can be related to E_{emf} and the total amount of charge (Q) transferred in the reaction.

$$W_{max} = E_{emf} \cdot Q$$

Equation 4

The total charge (Coulombs) can thus be related to the number of electrons transferred in the reaction (n) and the Faraday constant (F = 96,485 C mol^{-1})

$$E_{emf} \cdot Q = n \cdot F \cdot E_{emf}$$

Equation 5

As the work done is related to the change in Gibbs Free Energy, the following equation can be arranged as (Logan et al. 2006) :-

$$E_{emf} \cdot n \cdot F = -\Delta G$$

Equation 6

Thus the E_{emf} of any given reaction can be calculated according to the Nernst equation based on standard E^{o}_{emf} values (1 atmosphere pressure, 298K temperature, 1M concentrations) for a reaction $A^A + B^B = C^C + D^D$

$$E = E^{\theta} \times \frac{RT}{nF} \ln\left[\frac{[A]^A [B]^B}{[C]^C [D]^D}\right]$$

Equation 7

It can be seen that using acetate as an anodic substrate enables a thermodynamically favourable reaction to occur providing a suitable external load is present in the cell circuit.

Anode: $CO_2 + 7H^+ + 8e^- \rightleftharpoons CH_3COO^- + 4H_2O$ $\quad E_{(anode)} = -280mV$

Equation 8

Cathode: $4H^+_{(aq)} + O_{2(g)} \rightleftharpoons 2H_2O$ $\quad E_{(cathode)} = 820mV$

Equation 9

Overall: $CH_3COO^- + O_2 \rightleftharpoons 2CO_2 + 3H^+$ $\quad E_{(emf)} = 1.1V$

Equation 10

$\Delta G^O = -849$ kJ mol^{-1}

1.1.5.2 The bacterial biocatalytic process

Key to environmental biotechnology in the context of MFC anode biofilms is the ability to manage mixed microbial communities so that they can effectively act as biocatalysts in the oxidation of (waste) substrates, whilst also harvesting electrical energy in the form of electrons. The ecology of anodic bacterial communities will be determined by the ability of the microorganisms to maximize growth rates, achieve cellular division and establish robust biofilms in the engineered environment. In environments where the availability of electron acceptors are limited bacteria can generate energy via fermentative metabolism but this process is energetically less favourable than respiration. In the latter case, electrons from the oxidation process are not used directly for energy generation but are instead used to create proton gradients across cell membranes using ATPase synthase complexes to regenerate the energy carrier molecule ATP (Mitchell 1961); this allows the potential difference between the electron donor (substrate) and the electron acceptor component of the microbial cell to be utilized. Microorganisms have the ability to use a range of terminal electron acceptors; whilst oxygen has the highest redox potential (highest potential free energy gain) nitrate, iron, manganese and sulphate ions may also be used as alternative acceptors in the absence of oxygen (Madigan and Brock 2009). Whilst these electron transfers allow bacteria to conserve energy, the level of energy is in theory proportional to the redox potential difference between the electron donor and the electron acceptor. However, whilst glucose may have a theoretical $\Delta G = -2840$ kJ/mol (Equation 1 and 2) in the presence of no suitable electron donors microbial metabolism utilizes the less energetically efficient substrate level phosphorylation via fermentative glycolytic pathways, meaning that only a percentage of this energy may be used for electron transfer to generate proton gradients (facilitated by electron harvesting): low metabolic Gibbs free energy values reflect the production of fermentation products such as volatile fatty acids, hydrogen and alcohols which are excreted as metabolically derived electron acceptors. Another key aspect of fermentative bacteria is a general ability to hydrolyze polymeric compounds into monomers that can then be readily metabolized via glycolysis, however other groups such as sulphate reducing bacteria may also contribute to this process.

1.1.5.3 Intracellular and extracellular electron transfer: dependency on bacterial species and environmental conditions

The transfer of metabolically derived electrons from cytoplasmic NADH via dehydrogenases to menaquinone and ubiquinones intracellular mediators enables electrons to pass to a number of different potential c-type cytochromes. Genetic analysis has found that there are respectively 39 and 111 putative *c*-type cytochromes found within *S. oneidensis* and *G. sulfurreducens* genomes. This

suggests that a number of potential electron pathways exist both within and between different bacterial species (Heidelberg et al. 2002; Methe et al. 2003). When pure culture *G. sulfurreducens* anode biofilms have been cultured at different potentials it has been observed that electrochemical properties also differed strongly suggesting an ecophysiological adaptive response to environmental conditions (Busalmen et al. 2008). Figure 1.2 shows a list of different redox active species present in bacterial cells; it can be observed that cytochrome redox potentials range from -0.29 to +0.385. A c-type cytochrome, OmcZ, has been found to play crucial part in high current *G. sulfurreducens* electrogenic activity; electrochemical characterisation showed that this protein contains 8 haem groups with potentials ranging from -0.42 to -0.06V, again showing the potential for bacteria to environmentally adapt to a diverse range of potential electron acceptors (Inoue et al. 2010). In order for the cell to gain energy, electron transfer must pass from a negative to a more positive electrode potential. The fact that acetate has been found to be a good substrate for *Geobacter spp.* to carry out electrogenesis shows that these cells are able to change the redox potential of NADH from a value more negative than acetate (-0.32 to a value more positive than -0.28). An explanation of this process was given by Logan (2008) who demonstrated, using the Nernst equation (Equation 7), that it may be possible for a cell to manipulate the pH (proton concentration) and to favourably alter cellular redox potentials. It is therefore possible that cellular metabolism may also be manipulated through the cell actively regulating NAD^+/NADH ratios to achieve a similar result.

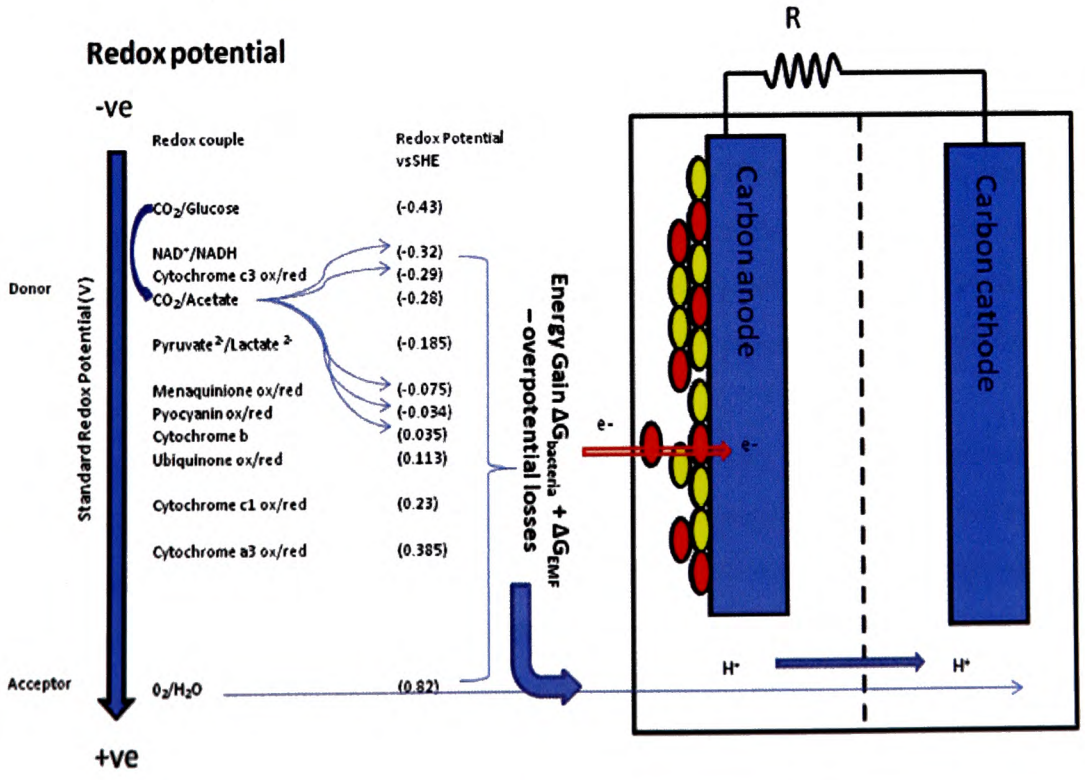

Figure 1-2. Standard reduction potentials of biological redox couples inherent to MFC electron transfer. Thermodynamic relationships demonstrate electron flow from donor substrate to terminal electron acceptor with concomitant Gibbs free energy production (bacterial and MFC cell emf) and overpotential losses.

1.1.5.4 Electron transfer mechanisms

Models for electron transfer differ between *S. oneidensis* and *G. sulfurreducens,* the two most widely studied electrogenic bacteria, and this seems to be directly related to their differing mechanisms of electron transfer to solid electron acceptors (Weber et al. 2006). Although both species have been observed to produce conductive nanowires that are capable of facilitating direct electron transfer from bacteria to a solid electrode (Reguera et al. 2005; Gorby 2006; Gorby 2007), only in *Geobacter spp.* have deletion studies shown that these pili structures are essential to electrogenic activity. OmcZ cytochromes have been observed to accumulate on the outside of bacterial cells and these are thought to play an interfacial role in the transfer of electrons to solid surfaces, however a different cytochrome OmcS has been associated with exocellular electron transfer from pili (Leang et al. 2010). Indeed it has been suggested that in engineered environments with high concentrations of VFAs such as acetate, this can directly lead bacteria such as *Geobacter spp.* to over-produce these types of external cytochromes. It is possible that this process could be more pronounced when bacteria present in a biofilm are sited remotely from the solid anode. In *Shewanella oneidensis* external surface cytochromes are able to directly reduce solid surfaces but it has been found that the bacteria also secrete flavins which act as electron mediators. Measurement of electron transfer kinetics and mutation analysis has demonstrated that the latter mechanism is probably the most important in terms of electron transfer (Baron et al. 2009). Indeed it is possible that the main function of the external cytochromes is to facilitate redox activity with these mediators. Other bacterial species also produce external mediators notably pyocyanin, a phenazine produced by *Pseudomonas spp.* (Rabaey et al. 2004).

The abundance of external cytochromes with a capacity for electron transfer suggests that within an electrogenic biofilm a network of electron transfer strategies are employed/utilized to maximize rates of electron transfer and therefore the overall energy gains of the biofilm (Fig 1.2). Hence it is feasible that electrically active pili could interact together, with cell surface cytochromes and also with diffusible electroactive elements. This could take the form of diffusible mediators secreted by bacteria and charged components of the biofilm matrix (proteins, carbohydrates and DNA), including cytochromes released after bacterial cell death. However it is currently unclear as to whether this electrically active exocellular component

forms part of an organized electrogenic biofilm structure or is simply a result of cellulytic processes (Magnuson 2011). The wide range of potentially different redox charges will undoubtedly lead to a hetrogenous redox/electrochemical environment at the sub-micro level throughout a biofilm, with the degree of biofilm conductivity thus being dependent on the resident biofilm community and the biological/environmental processes active at any given time.

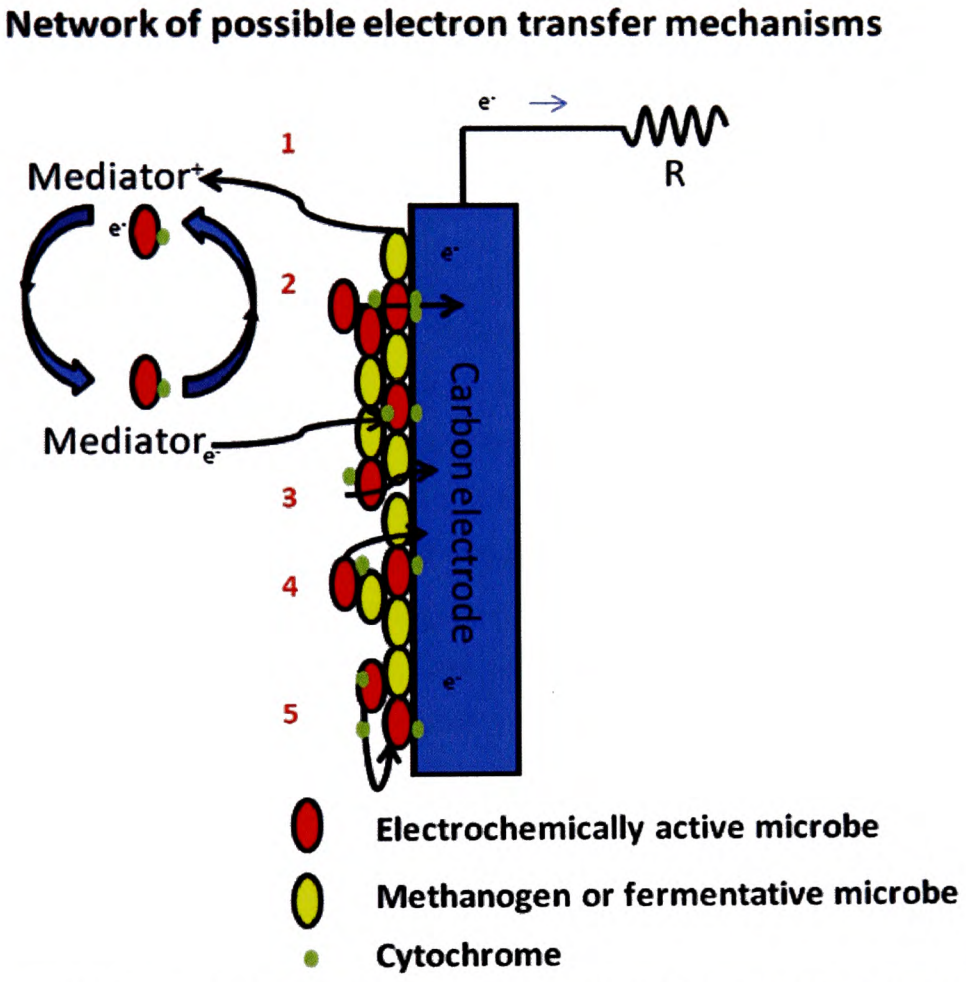

Figure 1-3. A generalized schematic of possible electron transfer mechanisms that may be active in an MFC electrogenic biofilm. Possible electron routes are indicated by the arrows, even though these are depicted as discrete events it is expected each process will interact electrochemically to differing degrees with all the stated mechanisms in an overall net movement of electrons to the solid anode. 1) Oxidized mediator 2) Direct cell:cell transfer 3) Reduced mediator 4) Direct electron transfer through the biofilm 5) Electrically conductive pili

1.1.5.5 Voltage, resistance and bacterial energy gain

The development of an electrochemically active biofilm directly results in a decrease in anode potential by reducing the anode internal resistance, the level of decrease being thermodynamically

dependent on the electron acceptors/donors present and the prevalent environmental conditions. Changing the external resistance values will also accordingly affect the set anode potentials as reducing the resistance will increase the cell potential and/or increase the electron flow (current), which although not affecting the cell potentials directly will have an overall effect on the electron transfer kinetics by allowing increased bacterial metabolic rates. Hence, in terms of maximizing the amount of electrical energy recovered, the Gibbs free energy consumed by the bacteria and the overpotential losses should be minimized. Overpotential losses can be categorized as activation losses (potential losses occurring at electrode surfaces), ohmic losses (due to resistance associated with current flow) and concentration polarization (mass transfer flow effects) (Logan et al. 2006), indeed much of the recent improvement in reported power densities has been achieved through optimizing aspects of the MFC architecture that contribute to overpotential losses (Logan 2009).

It is clear from Figures 1.2 and 1.3 that any energy gain for bacteria will lead to overall energy losses in terms of the cell EMF voltage. Figure 1.4 demonstrates that the relative Gibbs free energy gain is much higher for the total cell potential when compared to the bacterial energy gains, 767kJ and 61.7kJ respectively; a representative anode voltage of -0.2V was used in the figure (1.4) as this has been reported to produce optimal MFC operation (Aelterman et al. 2008a). The ecological survival of microorganisms dictates that energy gain be maximized but this can be viewed as being at odds with maximizing the total energy gain from the MFC. Thus any excess energy gain for the bacteria could lead to both energy and electrons being used in anabolic assimilation and the production of biomass. The ideal situation is therefore to maintain a low operating anode potential whilst allowing sufficient energy for bacterial maintenance and cell growth.

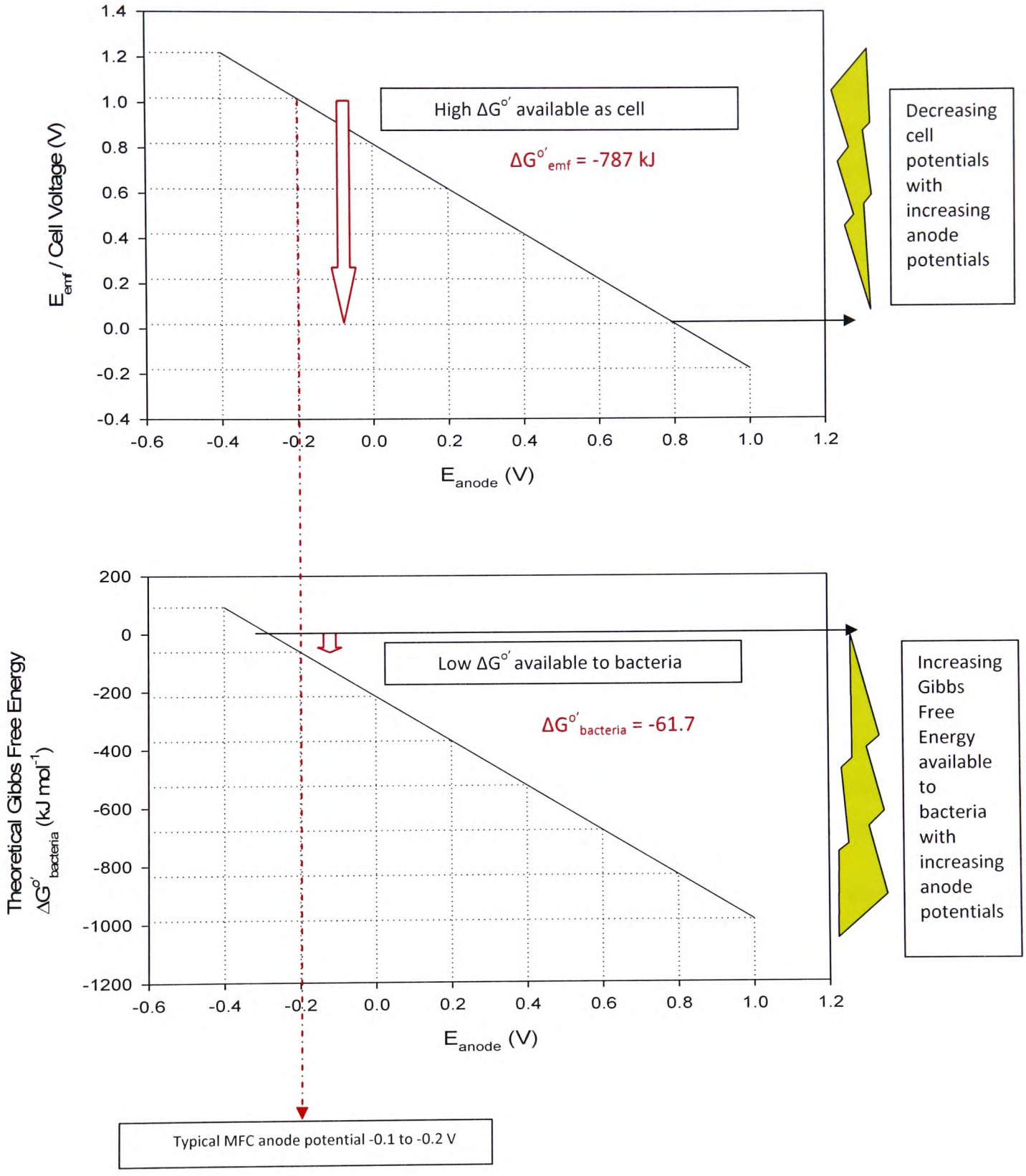

Figure 1-4. The effects of anode potential (V) on the theoretical E_{EMF}/Cell voltages and bacterial Gibbs free energy gain. An anode potential of -0.2 was used to highlight the relative Gibbs free energy gains at this point. Acetate was used as a basis for the calculations and standard conditions were used (pH 7 and 298K). Anode potentials were calculated vs SHE values

1.2 Microbiology of MFC anodes

1.2.1 Anodic Microbial Ecology

Microorganisms play an important role in biogeochemical cycles, especially through the anaerobic respiratory metabolism of minerals which act as Terminal Electron Acceptors (TEA) (Hernandez and Newman 2001). This process involves the transfer of reducing power, derived from substrate metabolism, through electron carrier proteins to a range of terminal TEAs. A diverse number of bacteria have been shown to transfer electrons to minerals (Lonergan et al. 1996) and it is this capacity that has led to the recent development of high current density bio-electrochemical systems (BES), where bacteria interact with electrodes to donate or accept electrons through an electrical circuit (Rabaey 2007). As in complex biogeochemical processes, microbial activity in MFCs are not likely to be catalyzed by individual microorganisms but by cooperating populations or consortia (Madsen 2005). MFC solid conductive anodes are engineered environments that allow materials such as carbon to act as terminal electron acceptors. Hence, bacteria that colonize the anode effectively function as a biocatalyst in the substrate oxidation process, acting to generate electrons that can produce electrical energy in an external circuit. This process is analogous to the dissimalatory reductive metabolic activity undertaken by bacteria that reside in geochemical environments, notably by *Geobacter spp.* and *Shewanella spp.,* although the phylogenic composition of the bacteria inhabiting marine sediments and underground aquifers will be dependent on the prevailing environmental conditions. The integral nature of this metabolic activity to the ecology of these microorganisms can be observed through chemotaxic responses of these types of organisms to reduced minerals in natural environments (Lovley 1997; Childers et al. 2002; Lovley et al. 2004).

It is known that many phylogenically diverse microorganisms can contribute to electricity production within MFCs and a number of recent studies have looked to characterise electrochemically active anodic communities (Logan and Regan 2006a). Bacteria identified from MFC reactors include species such as *Geobacter spp.* (Stams et al. 2006), and *Pseudomonas spp.* which are thought to both produce and use phenazine mediator molecules to facilitate electron transfer (Rabaey et al. 2005a). However, a range of diverse bacterial species have been identified in mature anode biofilms and it is likely that these act as part of a consortium to help generate a stable electrical output. Through molecular characterization studies it has been shown that these diverse electrochemically active microbial communities develop over time (Logan and Regan 2006a), and after inoculation, the MFC anode actively enriches organisms capable of mediating electron transfer. The formation of complex planktonic and biofilm communities can however maintain other

organisms that are able to utilize other electron acceptors or metabolize substrates or metabolic intermediates by fermentation or methanogenesis.

The types of dominant microorganism present at the anode will result from the given operating conditions in the MFC system. Community analysis from sludge inoculated MFCs incubated for extended periods have identified bacteria belonging to the Taxa *Firmicutes, γ-Proteobacteria, β-Proteobacteria* and *α-Proteobacteria* (Rabaey et al. 2004). The growth and selection of these electrochemically active bacteria (EAB) during anode enrichment is thus commonly associated with an increasing output of power from MFC systems. A positive anode potential (relative to a standard reference electrode) facilitates bacteria to use the electrode as a terminal electron acceptor and may promote electrostatic attachment. A large redox potential difference can provide a greater potential energy gain for the EAB and drive electrogenic activity (Liu et al. 1997; Rabaey et al. 2005b) as demonstrated by Fig 1.4. However, direct competition for electrons, VFAs/the reduced products of substrate catabolism by fermentative bacteria, can occur when bacteria utilize alternative metabolic pathways i.e. methanogenesis or through the production of biomass (an electron sink). Syntrophic, competitive and successive processes that energetically drive changing population dynamics of resident microorganisms within anode biofilms are not fully understood; but based on MFC operational parameters, environmental conditions and substrate type, a complex interaction of methanogenic, fermentative and anaerobic respiratory metabolic activities will interact to drive microbial community development and MFC performance.

1.2.2 Electrogenic Biofilms

1.2.2.1 Anodic Biofilm Overview

Microorganisms can be viewed as existing in either planktonic or sessile states, in the former they are free floating in solution and in the latter they are attached to a surface. The process of attachment is known to initiate genetic and physiological changes on the microorganisms; in many cases, notably in the case of marine bacteria, it has been observed that this is the preferential mode of growth (Zobell 1943). A key feature of all biofilm growth is the production of exopolymeric substances (EPS), this 'slimy' layer facilitates microorganisms to form multicellular organizational structures and provides inherent protection to the many environmental stresses that can occur in environmental conditions (when compared to planktonic populations) i.e. the effects of pH, drying, antibiotics, high shear rates, low nutrient stress and disinfectants (Stewart and William Costerton 2001; Shirtliff et al. 2002). The formation and structure of biofilms have been observed to vary with

different environmental conditions and will also depend on the constituent microbial species present. This means that biofilms that develop in diverse environments such as ship hulls or in water distribution pipes are very different to those found in microbial fuel cells (Spormann and Romeo 2008). Similarly, it is expected that anodic biofilm development is dependent on the type and prevalent environmental conditions present in any given MFC.

1.2.2.2 Electrogenic Biofilm Development

The development of biofilms is a complex process but can be broken down to a number of distinct stages. Prior to the attachment of microorganisms, the surface first undergoes a form of conditioning due to the adsorption of macromolecules; this will typically be composed of small organic molecules such as proteins, polysaccharides, glycoproteins and humic acids as was demonstrated by an investigation into the kinetics of conditioning layer formation on stainless steel sections immersed in seawater (Compare et al. 2001). The initial adhesion of bacteria to the surface can be driven by non-specific Van der Waal forces, but it is also necessary to overcome electrostatic forces which may occur at distances of 10-20nm. This can be achieved through bacterial expression of specific adhesion receptors, such as bacterial pili and fimbriae, which allow the initial repulsive forces to be overcome (Busscher et al. 1992), the expression and presence of these receptors in different bacterial groups dictate the bacterial colonization process. In MFC anodes this colonization process is likely to be important as for optimal electrogenic performance those bacteria that can undergo direct electron transfer are known to produce the highest power densities, notably members of the *Geobacteriaceae* family which have been observed to produce pili type appendages.

Once a biofilm is established it may then continue to colonize a surface through a number of mechanisms; namely bacterial motility of attached cells due type IV pili twitching motility, binary division of microbial cells and the possible recruitment of cells from the planktonic phase: how these mechanisms develop and how they are controlled will also determine the biofilm structure. The first key step after irreversible bacterial attachment before bacterial cells can develop into a complex mature biofilm is the production of extracellular polymeric substances (EPS). This matrix is made up of exopolysaccharides, proteins and DNA which can all act to maintain the structural and organizational components of the biofilm (Hall-Stoodley et al. 2004). The matrix composition and rates of EPS production will thus determine the biofilm function, this again being dependent on the types of microbial species present and prevalent environmental factors. Within electrogenic biofilms, bacterial development and growth on electrode surfaces involves the initiation of bacterial attachment and subsequent production of EPS to create complex and electro-facilitating

environments. However, a conductive reticular/extra-cellular matrix is also possible through syntrophic direct electron transfer between members of the biofilm consortium (Summers et al. 2010). In order for microorganisms to act as effective biocatalysts in MFCs it is necessary to use a conductive electrode as the terminal electron acceptor to drive cellular catabolism. To achieve maximum current density, bacteria should be in direct electrical contact with the solid electrode to enable efficient electron transfer, preferably as a cellular monolayer. However in developed and mature fixed anodic biofilms complex 3-dimensional structures of >50μm thickness are known to form over time (Reguera et al. 2006). This has been demonstrated by real-time imaging of anode biofilms which show that the most active cellular respiration is associated with microorganisms in close proximity to the anode interface (Franks et al. 2009). However, the generation of high current densities requires electrogenic biofilm development which allows respiratory activity to continue via more remote electron transfer mechanisms to the anode. Several mechanisms have been suggested to allow EAB to respire remotely to the anode, as previously discussed in section 1.1.5.4 (Lies et al. 2005; Gorby et al. 2006; Stams et al. 2006). The connection between the overall conductivity of the biofilm matrix and the ability of anode respiring bacteria to produce high current densities was established as being of critical importance in MFC systems (Torres et al. 2009b) and follows work that has established links between anode biofilm development and MFC performance (Ramasamy et al. 2008).

1.2.2.3 Microbial groups within the electrogenic biofilm

The development of enriched electrochemically active biofilms has successfully demonstrated a capacity to remove organic compounds whilst also being able to generate electricity. More complex and fermentable substrates were shown to produce different and more complex microbial profiles (Lee, 2003). It has been further observed that loosely associated bacterial clumps within the anode biofilm can form when MFCs are fed with fermentable substrate. DGGE analysis has shown that these clumps consist of community profiles distinct from the main body of the anode biofilm. It has been suggested that the clumps functionally act to ferment complex electron donors to produce volatile fatty acids that can be utilized by the EAB in the anode biofilm, and so facilitate the donation of electrons to the electrode (Kim et al. 2004). The view that fermentative processes are not competing with anodophiles but facilitating an energetically favourable syntrophic association was examined by looking at electron fluxes associated with glucose conversion pathways. It was found that the majority of glucose is first converted to hydrogen and acetate but electron flow to the anode could be lost to other electron sinks notably

methanogenesis (Freguia et al. 2008) but will also include losses to biomass and residual organic acids (Lee et al. 2008). However it has been found that acetate oxidizing EAB will out-compete acetoclastic methanogens present but not hydrogenotrophic methanogens, which will actively compete for electrons derived from hydrogen produced within the anode biofilm consortia (Prathap Parameswaran et al. 2009).

1.2.2.4 Advantages of a diverse mixed culture biofilm

Despite the number of different bacteria that have demonstrated a capacity of EAB activity, reports generally concur that pure culture MFCs produce less power than mixed culture systems (Logan 2009). Where higher power densities have been reported using pure cultures, experiments have been carried out under specific conditions i.e. using *G.sulfurreductans* an MFC that used a ferricyanide catholyte and a cathode eight times larger than the anode produced more power using a pure culture ($1.9Wm^2$) compared with a mixed culture ($1.6Wm^2$) (Nevin et al. 2008). This would seem to indicate that electrogenic biofilms are able to utilize and structure the networks of biofilm electron transfer mechanisms (previously described) to produce these higher power densities, this has been shown to be achieved through the reduction in the internal resistance in mixed culture biofilms (Watson and Logan 2009). However even more crucial to the successful operation of MFCs is the capacity to breakdown complex substrates/waste materials. Whilst a number of common EAB can demonstrate a wide metabolic diversity, diversity in terms of numbers of different bacterial species and the development of an ecological functional redundancy has been shown to be important in engineered systems (Briones and Raskin 2003). This was demonstrated by LaPara et al (2002) who subjected a wastewater community to decreasing nutrient concentrations, this resulted in a maintenance of functionality but it was found that redundant populations were eliminated. However decreasing microbial diversity has also been linked to a decreased community stability and functional resilience to perturbation events (Girvan et al. 2005).

1.2.2.5 Molecular analysis of EAB biofilms

A key aspect of environmental biotechnology is gaining an understanding of the microbial ecology of given systems, how microbial communities develop and interact together (Rittmann 2006). The use of molecular methods can provide useful information about microbial diversity and links between function, community structure and system performance. Using such culture-independent methods is particularly important as many major groups of both Bacteria and Archaea are only known from genetic sequences isolated from environmental samples (Gray and Head 2001).

This approach is particularly important in MFC anodes as these systems are generally both complicated and poorly understood from a microbial point of view. Polymerase Chain Reaction (PCR) has been used as the predominant genetic amplification approach, although it is also known this technique can introduce discrepancies due to the differential activities of *Taq* polymerases with template DNA samples of varying GC content (Baker et al. 2003). Furthermore it has been shown that poor complimentarity with target environmental DNA when using domain based 'universal' primers can lead to under representation of some amplified sample DNA, and if within the microbial community similar phylotypes exist chimeric sequences may arise as artifacts of the PCR process (Osborne et al. 2005). A number of techniques are available to analyze the amplified microbial community DNA, these are generally based on physical characteristics of the DNA (melting point or secondary structure) or the use of specific sequences to create fingerprint profiles. These finger-printing methods use restriction enzymes to generate profiles of either full 16S RNA genes (Amplified Ribosomal DNA Restriction Analysis) or just the terminal restriction fragments (Terminal Restriction Fragment Length Polymorphism (Liu et al. 1997). Denaturing Gradient Gel Electrophoresis (DGGE) uses a formamide/urea gradient to analyze the melting characteristics of bacterial community DNA based on the GC composition of the DNA amplicons. A GC clamp (GC rich tail) is added to the amplified DNA to ensure that full melting/strand dissociation in the gel does not occur (Muyzer and Smalla 1998) . By looking at the intensity of individual bands (semi-quantitatively) DGGE is suitable for following dynamic changes in complex microbial communities through time and space. When band intensities are ordered Pareto-Lorenz curves can be generated which can be then used to indicate the functional organization of the community, however this will only provide an indication of the community functional status due to biases inherent in the PCR-DGGE method and the potential for co-migration of different bands. The phylogenic range or degree of microbial 'richness' can also be assessed by the range and number of bands present (Marzorati et al. 2008). In MFC reactors, a number of studies have been carried out using PCR-DGGE techniques to investigate microbiological profiles and population dynamics within fuel cell anode chambers. However limitations associated with this technique must be understood within the operational context of the MFC. Coulombic efficiencies in MFCs may typically vary between 2 and 75% depending on the reactor architecture and environmental conditions. This means that of the bands identified only a proportion will originate from electrogenic bacteria, which has implications for the interpretation of diversity and dynamic measures. Also the relationship between diversity and the number of DGGE bands may not being simple when large numbers of bacterial taxa are present as DGGE primers will only detect bacterial species at levels of >1% (Boon et al. 2002). Interpretation of banding profiles will also be influenced by the clustering analytical method utilized, i.e. the Dice similarity is known to

be influenced by presence or absence of a single band which will be subject to the associated limitations discussed above. A statistical approach may also be used to examine community shifts using Principle component analysis where banding intensities and location are then converted into 2 or 3 dimensional plots (Jung and Regan 2011). A number of studies have used 16S clone library analysis techniques to investigate the development of biofilm bacterial communities (Kim et al. 2004; Aelterman et al. 2006; Logan and Regan 2006a); this technique is particularly interesting as it allows both a measure of abundance and identification of the key bacterial species present. This is carried out by inserting 16S PCR amplified DNA fragments into a competent vector where the recombinant plasmid is multiplied via cell division to a concentration that enables direct sequencing after the plasmid DNA has been extracted from the host cells. However, pyrosequencing techniques allow a more detailed understanding of anode microbial populations and community dynamics as this method allows the rapid sequencing of a large number of 16S DNA which substantially increases the sensitivity of the community analysis and reduces any bias associated with clone analysis.

Fluorescent in-situ hybridization techniques can be useful to both quantify numbers of key target biofilm micro-organisms and also provide an understanding of their in-situ spatial organization. This technique uses DNA probes to directly target cellular rDNA and, as such, does not require any PCR step as individual cells can be visualized microscopically. However an understanding of the key groups or species of interest is necessary so that specific probes can be designed/utilized. Thus, FISH provides a useful non-PCR based technique that can be used to verify community analysis and microbial abundance results.

1.3 The Effect of Environmental Conditions on Electrogenic Activity

Operational environmental conditions such as substrate type, substrate concentration temperature, pH, anode architecture, buffering capacity/conductivity and flow rate will all effect anodic/MFC performance (Feng et al. 2008) and the potential power densities achievable from the MFCs. This is directly related to the anode and cathode electrode potentials (Equation 3) and subject to parameters set by the Nernst equation (Equation 7) (Thauer et al. 1977) and overpotentials in MFC which also have a direct effect on the internal resistance. Even though each of these factors will have a direct influence on EAB activity all parameters may also exhibit a degree of operational interdependency.

1.3.1 Operation at Psychrophilic, Mesophilic Temperatures

The effects of temperature on MFC operation have been previously reported to have a direct effect on electrochemical processes. This can be directly observed when MFC reactors are run at ambient temperatures where cell voltages have been reported to cycle up and down with the diurnal temperature fluctuations (Moon et al. 2006; Jadhav and Ghangrekar 2009; Ahn and Logan 2010; Kim et al. 2010). It is not only system constraints that will directly affect MFC operation but also how these factors influence reactor efficiency and power generation through the conversion of electrons in biomass to electricity. The percentage recovery of electrons, termed as the Coulombic Efficiency (CE), can often achieve levels of 70% or more (Kim et al. 2009) when non-fermentable substrate such as acetate is used. Low CEs reflect the activity of alternative electron sinks and non-electrogenic metabolic pathways being utilized by the anode biofilm and planktonic microbial populations. Possible sinks include the activity of methanogenic Archaea (both acetoclastic and hydrogen utilizing) in the catabolic generation of CH_4 and microbial anabolic production of biomass, of which the former has been reported to be the more significant (Lee et al. 2008) . Conventional anaerobic digestion (AD) optimally operates at mesophilic temperatures, when these systems are subjected to sub-mesophilic conditions methanogenic AD efficiency/activity decreases with the resultant elevated production of volatile fatty acids (VFAs); however it has been demonstrated that AD systems may also be adapted to operate at both high temperatures and low temperatures through long-term reactor acclimatisation (McHugh et al. 2006). MFCs have similarly been shown to operate and produce electricity over a range of psychrophilic and mesophilic operating conditions (Liu et al. 2005).

Psychrophiles, that only grow at temperatures below 10°C, and psychrotolerant bacteria, that can grow at less than 20°C but have optimal growth temperatures of greater than 20°C, have both been found in a wide variety of natural and processed environments e.g. wastewater, soil and sediment (Morita 1975). In these habitats cold adapted biofilm communities can consist of a diverse range of Archaeal and Bacterial populations and this observed variability may also include transitions between different thermal types. Indeed it has been found that bacteria isolated from cold boreal ground waters (4°C) may be predominantly psychrotolerant (Männistö and Puhakka 2002). This suggests there is an inherent adaptability of cold tolerant microorganisms to mesophilic environments and a capacity for growth over a wide temperature range.

BES devices such as sediment MFCs have been previously developed for in situ operation in cold marine sediments. They are able to generate electricity from anaerobic anode respiring bacteria (ARB) which are present in the sediment; these act as a biocatalyst on an anode whilst aerobic

isolated from electrodes in marine sediment fuel cells (Bond et al. 2002). This family of bacteria are also commonly found in mesophilic MFC anode biofilms (Logan and Regan 2006b), where *Geobacter spp.* have often been identified as the dominant and active ARB. Two psychrotolerant *Geobacteraceae* strains, A1(T) and A2 which grow over a range of 4 °C to 30°C have also been isolated from these types of sediment MFCs (Holmes et al. 2004), however adaptation and change of the ARB communities derived from mixed culture biofilms at different temperatures have not been extensively studied.

A number of studies have looked at low strength wastewater treatment at ambient and mesophilic temperatures (21-35°C), but since most waste treatment systems in temperate climates work and discharge effluents at temperatures much less than this (10-20°C) these processes would require a significant input of energy as heat (Lettinga et al. 2001). The capacity to run MFC reactors at temperatures of 10-20°C would substantially reduce operating costs by eliminating a substantial power input for heating. Thus, psychrophilic operation introduces the potential for MFCs to be an economically viable alternative to conventional aerobic processes in temperate sewage treatment operations. In addition to the generation of electricity these MFC systems also have the potential to produce substantially lower levels of stabilized sludge due to the activity of biofilms with a low growth yield.

As in AD systems MFC operation at thermophilic temperatures (50-60°C) can provide advantages in terms of increased rates of enzymatic activity and pathogen removal when compared with lower temperature systems (Suryawanshi et al. 2010). A few studies have looked at high temperature MFC operation and demonstrated that MFCs can be operated effectively at temperatures of 40-60°C with power densities of 375 mW m^{-2} (Jong et al. 2006; Carver et al. 2011) but MFC design was seen to be a potential issue due the increased rates of evaporation at higher operational temperatures. Where thermophilic reactors have been operated for long periods it has been found that a predominance (50%) of *Firmicutes thermicola* strains occurred in current producing MFCs (Wrighton et al. 2008). High reported CEs of 89% would seem to suggest that there was little alternative metabolic competition for electrons in these communities.

1.3.2 pH Effects

pH is an important parameter in the operation of MFCs as the chemical formation and movement of protons from the anode to the cathode is integral to system operation. The Nernst equation shows that each pH unit change across a cell membrane represent a potential loss

(overpotential) of 0.059V through the development of high anodic equilibrium potentials (Rozendal et al. 2006). Hence, in a MFC dual chamber system He et al (2008) found that reducing the anode chamber to pH 5 also reduced the current density 10-fold. The actual pH that develops in an MFC anode will be dependent on the type and concentration of buffering used and the composition of substrates; when high concentrations of fermentable carbohydrates are fed to an MFC the pH can rapidly drop due to the formation of acidic products by fermentative metabolism, but it has also been reported that even if low pH values cause a reduction in power production this power can again recover if the pH is again re-adjusted to 7 (Ren et al. 2007). The optimal operational pH level in an air cathode MFC system was found to be 6.5 by Jadhev et al (2009) , and when MFC anodes were run for a period of time at pHs 4, 5, 6 and 7 in dual chamber MFCs, Zhang et al (2011a) found that operation at pH 5 and 6 only reduced voltage production by 16% and 8% and power density by 32% and 0%, respectively: however these reactors were not acclimated from the initial enrichment step. Low pH can also have a direct effect on the respiratory activity of EAB and it has been demonstrated that this can be a particular concern in anodic biofilms where the build-up of protons due to mass transfer limitations can lead to significant localized drops in pH close to the electrode (Torres et al. 2008). However it has also been shown that bacteria such as *Shewanella spp.* can be acclimated to operation at pH levels as low as 5 (Biffinger et al. 2008).

1.3.3 The microbial oxidation of different substrates

The observed diverse nature of anode biofilms has been reflected by the diverse number of organic materials that have been reported to be successfully converted to electrical current. This includes a range of carbohydrates, proteins, fats, VFAs, alcohols and inorganic compounds (Pant et al. 2010). Pure substrate studies allow anodic metabolic processes to be studied but are not generally applicable to typical waste streams that could be used to power MFC systems. The treatment of mixed wastewaters requires the anode microbial communities to degrade a range of complex organic compounds i.e. domestic wastewaters, landfill leachates, brewery wastewaters, paper recycling wastewater and AD effluent (Liu et al. 2004; Aelterman et al. 2006; Feng et al. 2008; Huang and Logan 2008). Certain classes of substrate are known to adversely affect MFC power production i.e. wastewaters, however it was demonstrated that power production in hospital wastewater could be substantially improved through the addition of acetate (Rabaey et al. 2005b); it was thought this low power production was due to interfering sulphate ions and the non-degradability of some of the constituent components in the wastewater. This demonstrates the

need for efficient bacterial hydrolysis to occur as this step can be rate limiting when compared relatively to fermentation rates (Velasquez-Orta et al. 2011).

1.3.4 MFC anode potential

Artificially poising the anode potential has been reported to have an effect on the start-up and performance of EABs (Wang et al. 2009; Srikanth et al. 2010), this is typically done using an electrochemical interface but it is also possible to alter the external load applied to the MFC (Cheng et al. 2009; Woodward et al. 2009). However there are some conflicting results reported about MFC start-up times with anodes set over a range of potentials. Wang et al (2009) reported that a anode potential poised at +0.2V (vs Ag/AgCL) in a dual chamber reactors could shorten the acclimation period to 34 days compared to 59 days with a control under a 1000 ohm loading. However Aelterman et al (2008a) also reported that anode potential did not have an effect on start-up time, but this was attributed to the inoculum being sourced from an active MFC. Interestingly both reports noted that the operational performance of the reactor once they had attained steady state was similar regardless of the start-up poised potential. It is possible that some of the variability in the reported findings could be due cathodic and ohmic limitations inherent in 2 chamber reactors used in the experimentation.

By changing the load on the MFC it is also possible to change the cell and anode potentials. Using a dual type MFC reactor Jung et al (2011) also showed also that reducing the resistive loading from 9600 ohms to 150 ohms improved the current density by a factor of 7. It was additionally shown that changes in external resistive loading affected the anode biofilm community which developed. Lyon and et al (2010) were also able to demonstrate a similar result by altering the external loading, demonstrating that a relationship exists between biofilm ecology and load resistance.

Optimizing the anode potential is likely to optimize the electrogenic activity of EAB, indeed Woodward *et al.* (2009) employed a load varying technique using an optimization algorithm for maximum power point tracking (MPPT) to maximize power production during both MFC start-up and steady-state operation but the affect on biofilm development was not investigated.

1.3.5 Carbon anode material, flow conditions and substrate loading

Carbon/graphite is considered to be a good support material due to its inherent biocompatibility, high surface area and relative low cost (Morozan et al. 2007); electrical conductivity is also good but is significantly lower than typical metal conductivities. To improve the biocatalytic properties a number of surface modifications have been carried out which have resulted in improved anode performance, notably ammonium treatment produced a 46% improvement in power production (Cheng and Logan 2007), but carbon has also been modified with quinine groups and electrically active mediators such as neutral red (Park and Zeikus 2002) which have resulted in improvements in current production by a factor of up to 10. However, the three-dimensional structure of the carbon electrode has an equally great influence on anode performance. Surface area to volume properties of the carbon at the micron levels and above will vary according to the type of carbon in question, with graphite rods having a low surface area to volume ratio compared to carbon felt which is composed of a porous network of inter-linking carbon fibres. Indeed this approach was used by Logan et al (2007) to enhance the 'biologically' effective surface area by winding graphite fibres around a metal current collector to produce a 2.5 fold improvement in power production compared to standard carbon cloth electrodes. High surface area availability in porous carbon will also enhance the potential contact between substrate and bacteria through maximizing mass transfer. This approach was further investigated by looking at forced flow through porous anodes, this produced a 2.28 fold improvement in current densities and a reduction in the internal resistance (Sleutels et al. 2009). Interestingly in an MEC system the same group found that increasing the flow rate away from a porous anode actually produced the best current densities as this actually produced an improved buffering effect by apparently producing a smaller boundary diffusion layer (Sleutels et al. 2011).

1.4 MFC scale up and tubular architectures

The Industrial scale-up of MFCs requires a system that can be economically run continuously at high volumes (>1m^3). A number of different such scalable reactor designs have been investigated, including systems based on tubular up-flow graphite granule The potential inefficiency of large-scale reactors was investigated by Ieropoulus et al (2008). This study looked at the effects of both scalability and stack configuration on power density measurements and it was found that small scale units (6.3ml) out-performed medium (29ml) and large reactors (652ml) by factors of 1.5 and 3.5 respectively. It was then estimated that a projected stack of 80 units would out-perform a larger MFC unit, of equivalent volume, by a factor of 50. However, if relative electrode parameters such as electrode spacing and electrode surface areas are maintained then it should possible to maintain

power performance even with larger volume units (Liu et al. 2008). Whilst there have been no published reports of large volume pilot scale reactor (>1m^3) being operated, Logan et al (2010) discussed some issues and potential limitations thought to be associated with a pilot scale operation that was run at Foster's brewery in Yatala, Australia. The replication of power densities produced in small scale reactors in large scale reactors may not be feasible as it has been estimated that a logarithmic increase in electrode surface area would be required (Dewan et al. 2008).

Tubular microbial fuel cells (MFCs) have previously been investigated as an effective anaerobic treatment process for low strength wastewaters (Kim et al. 2010; Kim et al. 2011); these systems have the potential to benefit from economies of scale in the event of large scale deployment, reduce biomass production and recover electrical energy (Kim et al. 2011). Anaerobic treatment has the advantage of low levels of biomass production resulting from low biomass yields. Cell yields from activated sludge processes have been estimated to be 0.4-0.8 gVSS g^{-1} BOD5 compared to typical anaerobically respiring process yields of 0.035-0.057 gVSS g^{-1} BOD5 and this 10 fold difference has implications for decreasing the cost of downstream secondary treatment processes (Oh et al. 2010).

Power densities currently produced in MFCs and thermodynamic limitations associated with the technology mean that these reactor systems are unlikely to be used for the production of power as their primary function. Whilst commercial organizations have been looking at these systems as a potential wastewater treatment technology this has been on the basis of both reduced water treatment energy costs as well as bioenergy recovery, i.e. Emfcy bioenergy systems, Israel, but no product has yet been released by this company. Where MFCs have been currently applied to real systems these have tended to include 'niche' applications e.g., providing autonomous power to robotic systems and as river/deep water environmental sensors where system accessibility may be an issue during long term use (Logan and Regan 2006c; Melhuish et al. 2006). Indeed life cycle assessments have concluded that MFCs are only viable if they are used to produce high-value biosynthesized products i.e. hydrogen (Foley et al. 2010). The use of MFCs to mitigate the high costs involved in wastewater treatment would involve the development of a BES that is capable of optimizing a combination of high energy recovery and high COD removal. The balance of these two parameters will depend on the current economic situation, but Pant et al (2011) estimated that an economically viable energy production system would need to generate 1000 W/m^3 and/or a viable treatment system would need to remove COD at a rate of 1-10 kg/m^3/day.

1.5 Aims and objectives of the Research

Aim: To further the understanding of how MFC anodic biofilms develop over time and investigate how environmental parameters, pertinent to system scale-up, may affect electrogenic performance.

Objectives:

- To determine the effect of fermentable and non-fermentable substrate acclimation on microbial community development and anodic performance.
- To investigate the influence of psychrophilic, psychrotrophic and mesophilic temperatures on anodic biofilm performance and microbial community acclimation and understand how temperature influences electrogenic and non-electrogenic development over time.
- To examine how flow conditions and novel anode helical architectures can influence MFC anodic performance.
- Investigate the influence of carbon material type on electrogenic activity and understand how a control algorithm may be used to optimize MFC power production by changing the external loading of the cell.

2 Materials and Methods

2.1 Experimental Apparatus

2.1.1 Reactor design

Two MFC reactor types, tubular air cathode reactors and H-type reactors, were used as part of the experimentation in this study. Tubular air cathode reactors utilizing a wound carbon veil anode and a series of 3 spiral based anode configurations with small, medium and large configurations were used in the substrate, temperature and helical configuration experiments (Chapters 3, 4, 5 and 6). H-type MFC reactors were used in the material and control experiments (Chapters 7 and 8).

2.1.2 Tubular reactors – wound carbon design

The tubular experimental reactors were 280 mm long and 40 mm diameter and constructed using polypropylene tubing as a supporting structure. An air cathode (80 x 210 mm) with 0.5mg/cm^2 Pt platinum catalyst was prepared, fixed with activated carbon (Kim et al. 2009) and then combined with a cation exchange membrane (CMI-7000, Membrane International Inc. NJ, USA). The anode was constructed by winding a 260 x 450mm carbon veil cloth (PRF Composite Materials, Dorset, UK) around a central PVC rod of 1 cm diameter to form a multilayered anode electrode. The system was sealed to make it water secure, giving a total liquid reactor volume in the anode chamber of 245 ml. Tubular reactors in experiments 2-4 used engineered caps with 'o' ring sealing joins and 1cm screw fittings manufactured by the University of Glamorgan.

The MFC construction process is shown in Fig 1.

A)

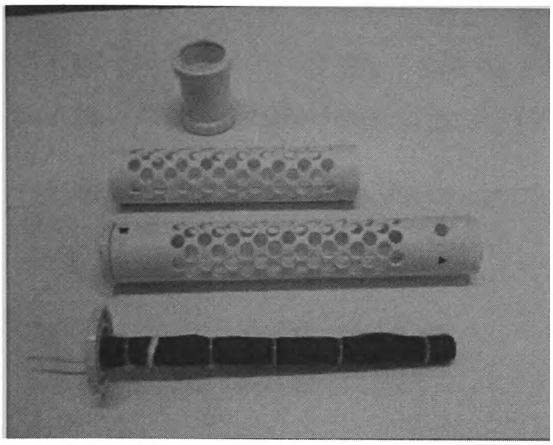

B)

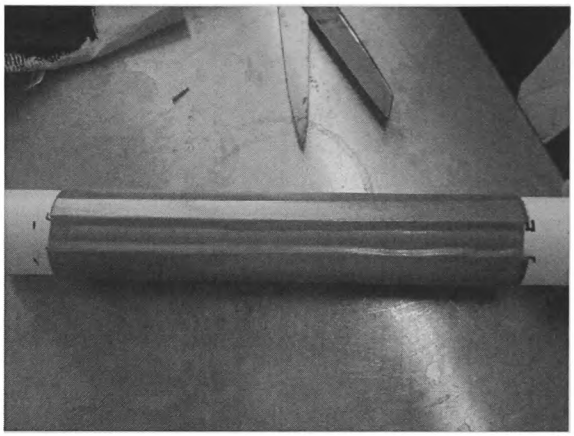

C)

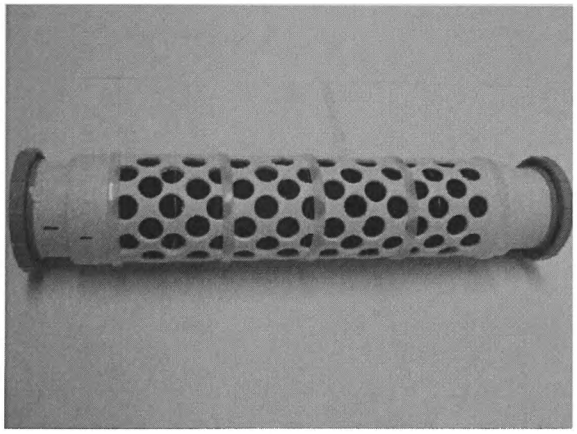

D)

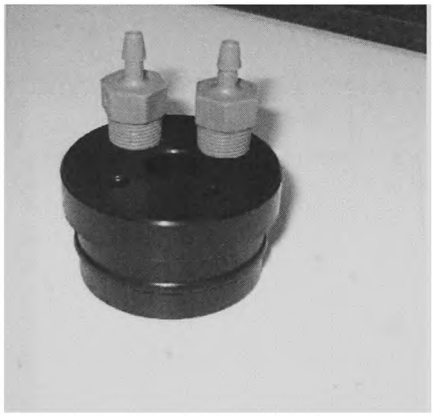

Figure 2-1. Construction and assembly of Tubular MFCs used as part of the experimentation. A) Engineered propylene tubing and plastic rod with carbon veil wrapped around. B) Ion exchange membrane fixed to the polypropylene tubing. C) Pt cathodes and polypropylene support added to the reactor and secured. D) End caps (manufactured by the University of Glamorgan)

2.1.3 Tubular reactors – Helical anode design

Helical tubular reactors were 280 mm long and 40 mm diameter and constructed using polypropylene tubing as a supporting structure. An air cathode (80 x 210 mm) with 0.5mg/cm2 Pt platinum catalyst was prepared, fixed with activated carbon (Kim et al. 2009) and then combined with a cation exchange membrane (CMI-7000, Membrane International Inc. NJ, USA). Three anode designs with supporting spokes were manufactured by the University of Glamorgan using a rapid prototyping process from a CAD solid model. The helical structure was made from acrylonitrile

butadiene styrene (ABS) plastic, 3 different helical constructs each with a different pitch were produced (helix structures 1, 2 and 3 had anode veil strip widths of 10mm, 13mm and 17mm respectively), Fig 2.2. Each helical anode frame contained a 10.5mm gap running through the centre to house a plastic support rod; the structure was designed to have the wound carbon veil separated by a fluid flow channel as determined by the helical pitch.

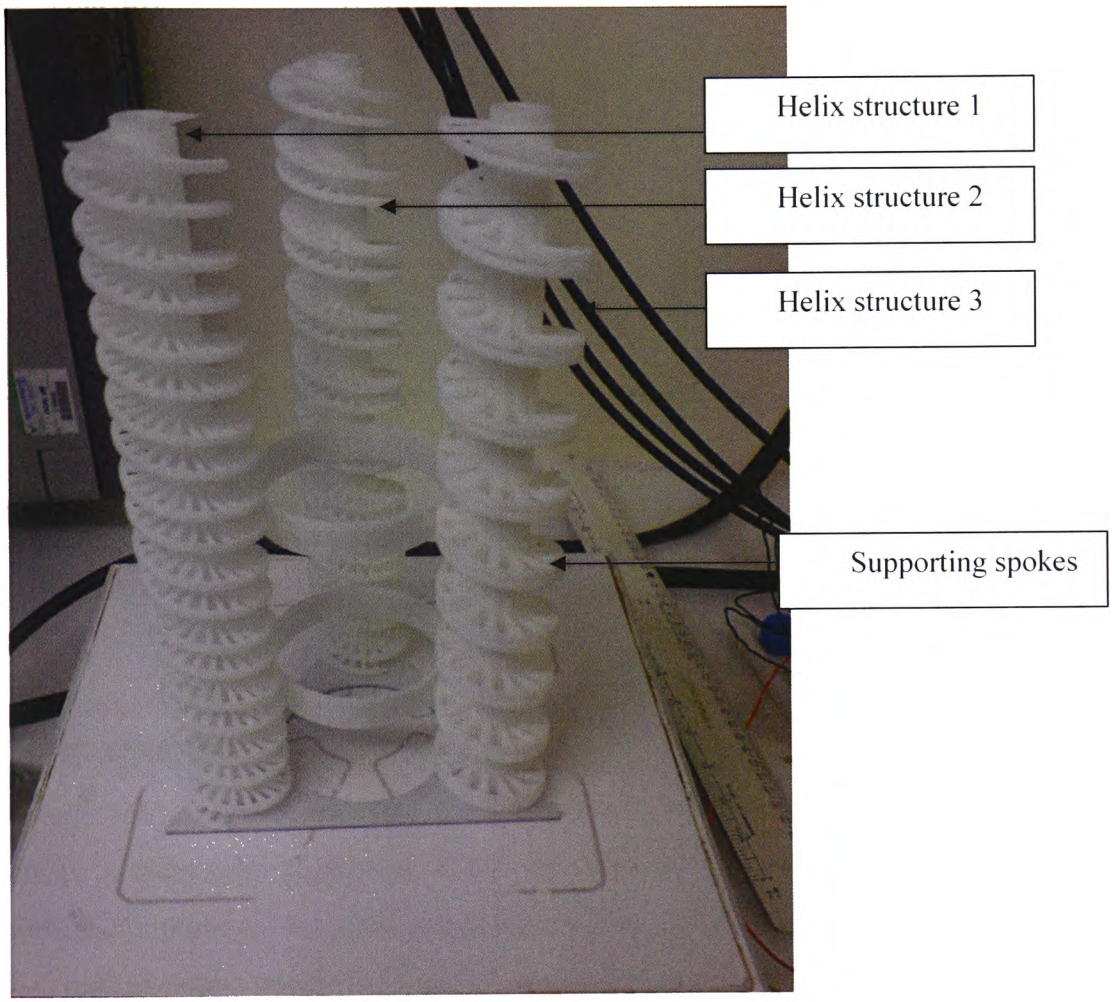

Figure 2-2. Three different spiral anode designs with different helical structures

The anodes was constructed by winding a carbon veil cloth (PRF Composite Materials, Dorset, UK) around the helical frames and then securing at either end with wire. A stainless steel mesh (Type 304, Lenntech BV, Netherland), woven from 0.56mm diameter type 304 wire with 1.5 mm aperture, was then used to overlay the carbon to maintain the carbon veil anode and improve conductivity/electron collection, Fig 2.3.

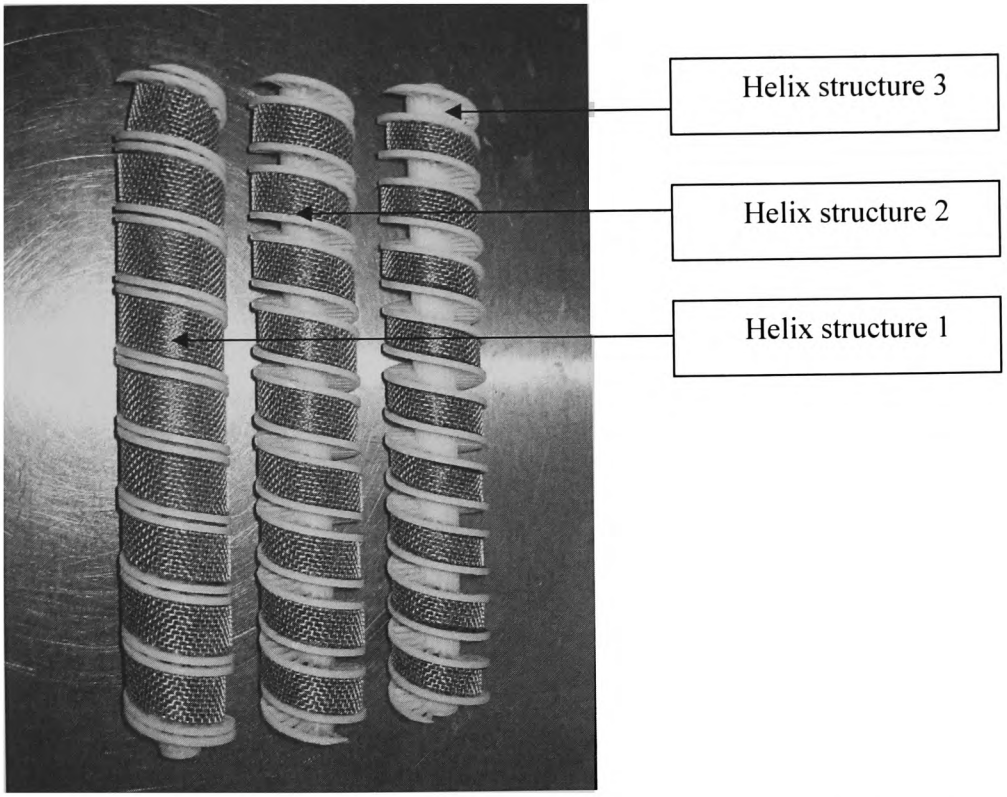

Figure 2-3. Three different helical anode designs with wound anode carbon and stainless steel support

2.2 Two chamber MFC reactors

H-type MFCs were constructed using two media bottles (320ml capacity, Corning Inc., NY), joined by a glass tube containing a 2.1 cm diameter cation exchange membrane (CMI-7000, Membrane International Inc. USA) as per Fig 2.4 (Kim et al. 2008b). Cathode electrodes were made of plain porous carbon paper (TGPH-120, Toray carbon paper, E-TEC, 2.5 cm × 4.5 cm, projected area of 22.5 cm^2) with an incorporated Pt catalyst (0.35 mg/cm2; 10% Pt; E-Tek, NJ). Ferricyanide solution (100 mM in phosphate buffer, 100 mM, pH 7) was used as catholyte in order to maintain cathode potential (Kim et al. 2005). The anode chamber was placed on a magnetic stirrer and this was used to provide vigorous mixing to ensure uniform conditions were maintained in the anode chamber and there was no affect due to the proximity of the anode to the cathode/ion exchange membrane.

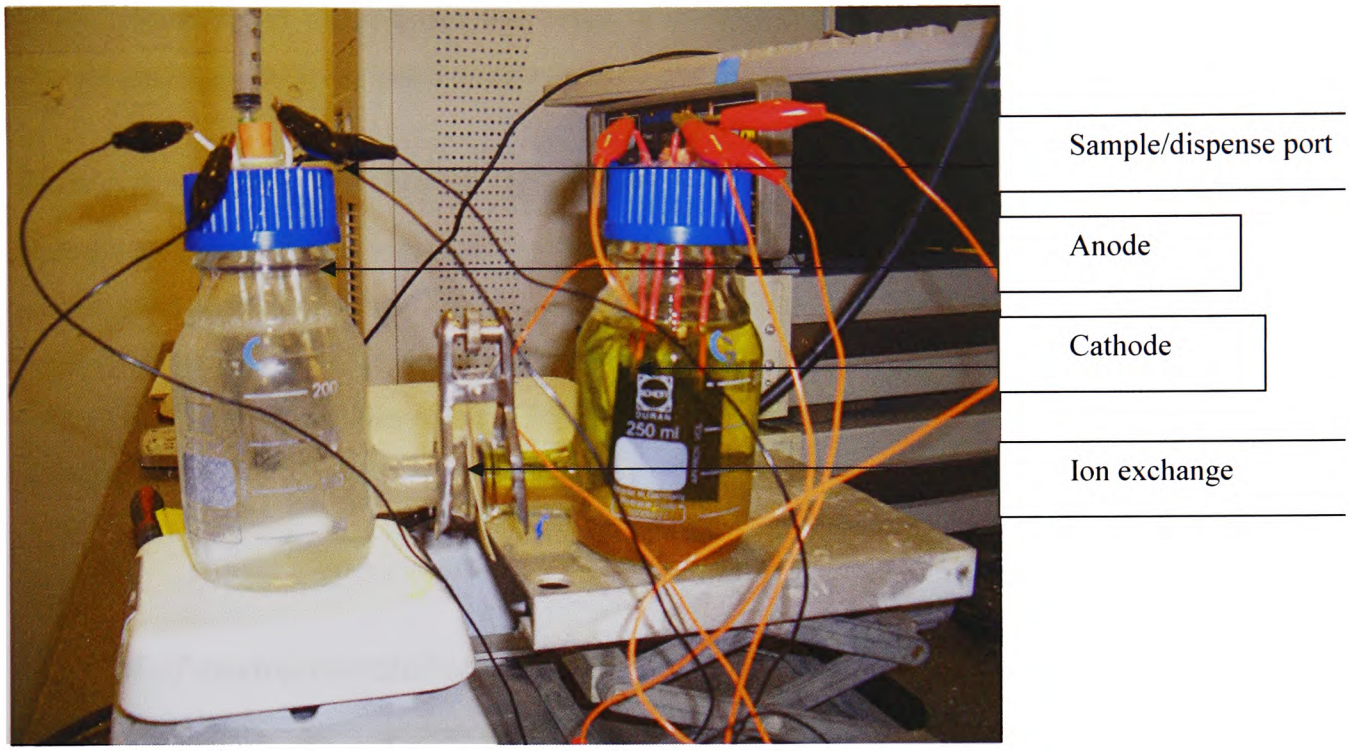

Figure 2-4. Dual chamber 'H' type MFC reactors

2.2.1 Carbon materials experiment

Four different anode carbon materials were tested during MFC operation – TGPH-120 Toray carbon paper, E-Tek, NJ, USA (2.5 cm × 4.5 cm); V2 Carbon felt (2.5 cm × 4.5 cm) Mast carbon advanced products ltd, (Devon, UK; Carbon rod cluster (4.5 cm length), Mast carbon advanced products ltd, Devon, UK; graphite rod (C-P Graphite GmbH, Germany). The carbon felt was mounted onto a clear plastic support to maintain structural integrity during testing. The four different materials were each suspended from the reactor cap and sealed in place with silicone glue, care was taken to ensure the materials were spaced equally apart within the chamber. Each material type was connected to a specific cathodic electrode located in the cathode chamber (Figs 2.4 and 7.4).

2.2.2 Controlled load experiment

Anode and cathode electrodes were made of plain porous carbon paper (TGPH-120 Toray carbon paper, E-Tek, NJ, USA), 2.5 cm × 4.5 cm, projected area of 22.5 cm^2. The cathode additionally contained a Pt catalyst (0.35 mg/cm2; 10% Pt; E-Tek, NJ, USA) (Kim et al. 2005). The controlled

reactor was connected to circuit board that acted to maximize system power by automatically adjusting the loading up or down based on an average of the previous power readings.

2.3 Flow rates during continuous operation

When the MFC reactors were run in continuous mode nutrient media and buffer was pumped to the reactors using a Watson Marlow 505U/RL or 505S pumps fitted with marprene tubing (Watson and Marlow, Falmouth, UK). System flow rates were calibrated by checking the flow (ml) over time and pump speeds were adjusted accordingly. During the course of continuous flow experiments flow rates were periodically checked.

2.4 Control of environmental conditions

Where appropriate, MFC temperatures were controlled by placing the reactors in heating/cooling incubators (Oxitop, WCW, Germany). Incubator temperatures were checked on a weekly basis using a mercury glass thermometer to ensure target temperatures were correctly maintained (± 1°C).

2.5 Data Acquisition

A desktop PC was used for capturing data from MFC reactors. Voltages across the MFCs were recorded typically at 10 minute intervals using LabVIEW™ software and a NI 16-Bit, isolated M Series MIO DAQ, (National Instrument Corporation Ltd. Berkshire UK). A custom interface was written using Labview 6 in order to capture, collect and display data from this device. The data was automatically written to a text file. See Appendix 2 for LabVIEW™ block diagram detailing program used for data display and capture.

2.6 Inoculum

The reactors were inoculated with a 10% anaerobic digestion sludge (Cog Moors wastewater treatment plant, Cardiff, Wales), consisting of 24.5ml sludge in 220.5 ml nutrient buffer media (TS = 24.8 ± 0.1g/L and pH = 7.52). The inoculum was stored in a sealed vessel for up to 7 weeks at 4°C and up to 2 weeks at room temperature.

2.7 Media

100 mM phosphate buffer was made up in 20L batches and diluted as necessary. Nutrients were as per the composition detailed in Appendix 1 and added to the nutrient media at a concentration of 12.5ml per litre, acetate, butyrate and or sucrose substrates were then added to the required concentrations.

2.8 Chemical analysis

2.8.1 pH

pH of fed-batch experiments was measured on a weekly basis using a Mettler-Toledo, Gmbh 8603 meter (Mettler-Toledo, UK).

2.8.2 Methane

In experiments 1, 2 and 3 a gas bag was connected to the MFC reactors and used to collect reactor gas production. A 1ml gas tight syringe (Varian Ltd, Walton-upon-Thames, UK) was used to inject the gas sample into the GC by activating the start option within the data handling package. A vacuum pump drew the gas sample through a loop (10 µl) and then the injector injected the gas sample from the sample loop into the carrier gas stream.

The level of gaseous methane composition was checked using a Varian CP-4900 Gas Chromatograph (Varian, Walton on Thames, UK). The GC was equipped with two columns, a "molecular sieve 5A plot" (10m x 0.32mm) (Varian) running at 150°C and 30 psi for the detection of hydrogen, nitrogen and methane, and a "Porapack Q column" (10m x 0.15) (Varian) running at 60°C and 20 psi for the detection of carbon dioxide. The carrier gas in both columns was argon. This instrument was also able to analyze the methane, nitrogen, carbon dioxide, and hydrogen content of the gas samples simultaneously and with no need for multiple samples to be taken from the instrument. The instrument was calibrated every three months using gas mixtures of known proportions (Air Products, UK). A QC sample was run before each day of use and consisted of a gas mixture of known proportions (Scientific and Technical Gases Ltd., Newcastle-under-Lyme).

The calibration of the GC for $H_{B2}B$, COB_2B, CHB_4B, and NB_2B was done using calibration gases of following compositions: 10.047% $H_{B2}B$, 30.256% NB_2B, 27.764% CHB_4B and 31.933% COB_2B (Scientific and Technical Gases Ltd., Newcastle-under-Lyme, UK)

2.8.3 Volatile Fatty Acids

VFAs were measured according to the method of Cruwys *et al.* (2002) using a Perkin Elmer headspace gas chromatograph (Model number HS40XL, Perkin Elmer, Beaconsfield, UK) in conjunction with a flame ionisation detector (FID) and a "Nukol" free fatty acid phase (FFAP) column (30m x 0.32mm) (Supelco Ltd, Poole, UK) running at 190°C and 14 psi. The carrier gas was nitrogen. The GC was connected to a headspace auto-sampling system (Perkin Elmer, Beaconsfield, UK). The machine was calibrated using standards of acetic, propionic, isobutyric, n-butyric, isovaleric and n-valeric acids with concentrations in the range of 0 mg L^{-1} to 1000 mg L^{-1}. In their paper Cruwys et al. (2002) state that the detection limit for these acids was below 4mg L^{-1} and analysis of replicates samples yielded a coefficient of variation between 0.039 and 0.065.

Preparation of samples followed the method in Cruwys et al. (2002). A 22.3 ml glass vial was used with a PTBE septum and a proprietary sealing system (Perkin-Elmer, Beaconsfield, UK). 1 ml of sample was pipetted into the vial together with 1ml of deionised water, 1 ml of $NaHSO_4$ and 0.1 ml of 2-ethylbutyric acid (1800mg L^{-1}) as an internal standard.

2.9 Electrochemical analysis

Power density plots and polarization curves were measured using a Solartron Instruments (Farnborough, UK) 1287 electrochemical interface with an Ag/AgCl reference electrode. A Potentiostatic method was used (CorrWare 2™, Scribner Associate Inc., NC), to apply a constant potential and then monitor current as a function of time. Polarisation curves were measured after 2 hours at OCV (open circuit potential). The slope of the ohmic (linear) portion of the polarisation curves was calculated, and the ratio of the cell potential to the current was then used to determine the internal resistance of the MFC. Each cell potential was measured after an interval of 10 minutes to allow stabilization of the current.

In experiments the voltage across a 1000Ω resistor in the circuit in the MFC was monitored (using 30 min intervals to allow for current stabilization) using a multimeter (Keithley Instruments,

Cleveland, OH, USA). The current (C/s) was calculated according to $I=V/R$, where V is the measured voltage and R (Ω) is resistance. The power density was obtained by normalizing power ($P=IV$) by the electrode surface area (22.5cm2) or the fuel cell volume (240ml).

Coulombic efficiencies (*CE%*) for each batch mode operation were calculated as previously described (Liu et al. 2004; Logan et al. 2006), Equation 11.

$$\mathbf{CE\ \%} = \frac{CEx}{CTh}.\ \mathbf{100.COD_{factor}}$$

Equation 11

Where *CEx* is the total coulombs calculated by integrating the current measured at each time interval (*i*) over time and COD_{factor} is the factor of 100/measured % COD removal. *CTh* is the theoretical amount of coulombs available from substrate oxidation, calculated as $C = F\ b\ M\ V\ Th$ where *F* is Faraday's constant (96,485 C/mol-e-), *b* the number of moles of electrons produced per mol of substrate (i.e. 8 mol e/mol acetate), *M* the substrate concentration (mol/L), and V the liquid volume (L).

2.9.1 Cyclic Voltammetry

Cyclic voltammetry (cv) analysis was performed using a Solartron Instruments (Farnborough, UK) 1287 electrochemical interface with an Ag/AgCl reference electrode. The working electrode potential was programmed to linearly ramp with through time in an oxidizing and reducing cycle. The cycle was conducted in triplicate during the experiments using a voltage range of -0.7 to +0.7 Volts, the scan rate was differed, but lay in the range between 0.1 - 50mV/S. The current at the working electrode (y axis) was plotted against the applied voltage to produce the cyclic voltammogram (x axis).

2.10 Molecular analysis

2.10.1 DNA/Biomass measurement

Genomic double stranded DNA (dsDNA) was isolated from $1cm^2$ samples of carbon veil that had been aseptically excised from the anode. Samples were mechanically disrupted by bead beating

and a phenol/chloroform/iso-amyl-alcohol extraction was carried out as the method described by Elferink et al (1997). DNA concentrations were measured using a NanoDrop™ 1000 Spectrophotometer (Thermo Scientific) and these values were used as a measure of biomass/biofilm growth. DNA concentration has been previously shown to be an indicator of bacterial cell counts present in potable waters (McCoy and Olson 1985), and correlations have also been established between DNA concentrations and levels of organic dry matter in reactor biofilms (Flemming et al. 2000). A conversion of DNA levels to carbon biomass (C biomass) concentrations have been previously calculated using a conversion factor of 16.6, based on an average 3% DNA concentration in bacterial cells by dry weight. In this study the following linear regression equation was used to calculate the microbial mass concentration (VSS (mg/l) in each $1cm^2$ anode sample, this conversion factor (VSS (mg/l) = 257.2 x DNA concentration (mg/l) + 250.4) was reported to provide a better correlation in active biological reactors (Kim et al. 2008a).

2.10.2 DNA calibration curve

To verify the correlation between DNA concentration (ng μl^{-1}) and the NanoDrop™ 1000 Spectrophotometer (Thermo Scientific), a calibration was carried out using Lambda Phage DNA, Methylated from *Escherichia coli* host strain W3110 (Sigma –Aldrich, UK), concentration 700 mg/ml. Calibration checks were carried out periodically using a -80°C frozen stock solution (Fig 2.1).

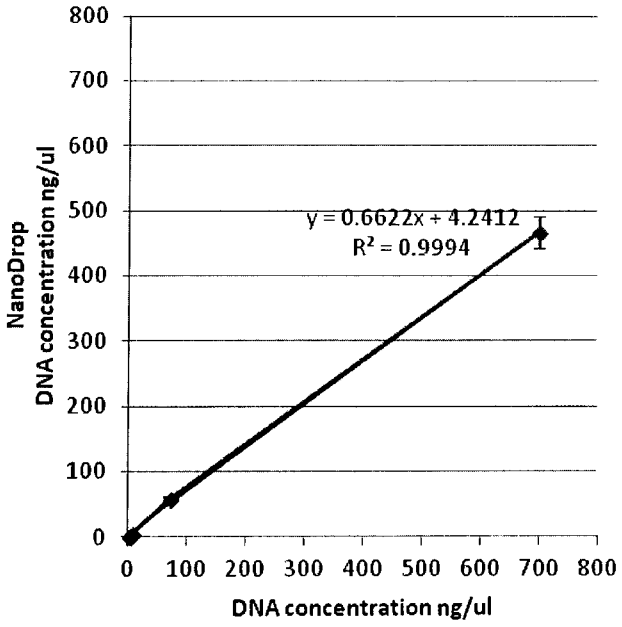

Figure 2-5. Nanodrop spectrophotometer and lambda phage DNA Calibration

2.10.3 Sampling and Analysis of Biofilm ecology

1cm^2 sections of anode carbon material were sampled in an anaerobic chamber (Coy Laboratory Products, Michigan, USA); by aseptically excising with scissors on a pre-sterilized glass plate and all test samples were immediately transferred for storage at -80°C prior to processing.

Amplification of DNA (16S rDNA) and PCR analysis were performed as previously described (Roest et al. 2005) using Archaeal primers 0968F-GC and 1401R, i.e. forward primer (5'-CGC CCG GGG CGC GCC CCG GGC GGG GCG GGG GCA CGG GGG G AAC GCG AAG AAC CTT AC -3') and reverse primer (5'-CGG TGT GTA CAA GAC CC -3'). and universal bacterial primers 0109F-T and 0515R-GC i.e. forward primer (5'-CGC CCG GGG CGC GCC CCG GGC GGG GCG GGG GCA CGG GGG G ATC GTA TTA CCG CGG CTG CTG GCA C-3') and reverse primer (5'-ACT GCT CAG TAA CAC GT-3'). For DGGE analysis a D-Code system (Bio-Rad, Hercules, CA, USA) was used with a 20% to 80% denaturing gradient (100% denaturant consisting of 7 M urea and 40% (v/v) formamide). 8% (w/v) polyacrylamide gels (acrylamide:bisacrylamide, 37.5:1, gel stock solution; Sigma, USA) in 1 × TAE (40 mM Tris, 20 mM acetic acid, 1 mM EDTA, pH 8.3), containing 0.11% (wt/v) APS (ammonium persulfate; Sigma) and 0.1% (v/v) TEMED (N',N,N,N'-tetra-methylethylenediamine; Sigma). Gels were run at 60°C at 200V for 5minutes, then 85V for 16 hours and were silver stained prior to gel imaging with a Fluor-S MultiImager (Bio-Rad, Hercules, CA, USA).

2.10.4 Computational analysis of DGGE banding patterns

Scanned DGGE gels were analysed using GelCompar II software (Applied Maths, Belgium). Test bands were viewed and compared in terms of intensity and position. To correct for variations in successive DGGE gels a standard marker sample was run with each gel, this was used to normalize the bands based on defined reference positions. Densitometric curves were calculated for each gel track using a best-fitting Gausian algorithm for each band.

Microbial ecological analysis of the DGGE band profiles (Archaeal and Bacterial communities) were analysed to evaluate the diversity of bacterial communities operated at different temperatures over time. The following band based and curve based nearest-neighbour correlation methods were used for the analysis, with UPGMA (average linking method) used as the hierarchical clustering method:

(i) The Dice index of similarity, $Cs = 2j/(a+b)$ was used. j is the number of common bands between samples A and B; a and b are the total number of bands in samples A and B, respectively.

(ii) Pearson based correlation using a formula based on the covariance of the band patterns divided by the product of their standard deviations.

Community dynamics were analysed through calculating population richness, microbial dynamics, functional organization and microbial clustering (Marzorati et al. 2008). The range-weighted richness (R_r) was calculated over time from the Archaeal and Bacterial DGGE biofilm profiles using $R_r = N^2 \times D_g$. Here N is the total number of bands in the profile (lane) and D_g is the denaturing gradient between the first and the last band of the pattern. Microbial dynamics were analysed over time by moving window analysis plots. These were calculated on a sequential weekly basis as percentage change values using:

change (%) = 100 - similarity (%).

Functional organization of the bacterial communities were graphically represented as Pareto-Lorenz evenness curves with bands from individual profiles ranked from high to low according to their cumulative intensities and number of the bands.

2.11 Microscopy

2.11.1 Scanning electron microscopy

Anode biofilm samples were fixed in 2.5% glutaraldehyde in 10mM HEPES (pH 7.4), overnight. The samples were dehydrated in a graded series of aqueous ethanol solutions (30–100%) and then critical point-dried using Bis(trimethylsilyl)amine (Sigma, UK). Sample were maintained in each solution for a period of 15 minutes (Sich and Van Rijn 1997) taking care to avoid excess sample agitation. Finally, samples were mounted on aluminum stubs, sputtered with gold and examined in a LEO 1430 SEM (Zeiss, Welwyn Garden City, UK).

2.11.2 FISH confocal scanning microscopy

An MFC was set up with different carbon materials (carbon felt, E-Tek carbon, engineered carbon and graphite rod) and inoculated with cell biomass from a working MFC reactor. The biomass was spun down and washed before inoculation in 100mM phosphate buffer containing a 1g L^{-1}

acetate substrate. Prior to initiating the experimentation the following FISH probes were ordered from Bioneer, Korea.

Table 2-1. FISH probes used as part of the fluorescent microscopy testing

probe	modifying fluorescence	sequence	Target bacterial group
EUB338	FAM	GCT GCC TCC CGT AGG AGT	Most bacteria
EUB338Ⅲ	FAM	GCT GCC ACC CGT AGG TGT	Verrucomicrobiales
Geo3-A	Texas-Red	CCG CAA CAC CTA GTA CTC ATC	Geobacter cluster
ARC915	Texas-Red	GTG CTC CCC CGC CAA TTC CT	Archaea
Gamma42a	Tamra	GCC TTC CCA CAT CGT TT	Gamma proteobacteria
Delta495a	FAM	AGT TAG CCG GTG CTT CCT	Most δ-proteobacteria

2.11.2.1 FISH Methodology

2.11.2.1.1 Cell fixation and hybridization

Cell fixation was carried out as per the method developed by Zarda et al (1991) with minor modifications. The anode biofilms/carbon materials from each anode were aseptically sampled on day 13 and fixed in 4% paraformaldehyde solution for 24 h at 4°C. Cell fixation was carried out by adding paraformaldehyde to give a 4% final concentration in PBS.

Gelatin coated slides were prepared as per the protocol of Wildeboer-Veloo et al (2003) with minor modifications. Microscope slides were treated with detergent solution for 30-60 minutes and then rinsed with MQ water. After allowing to dry the slides were then soaked for approximately 1 minute in a filtered solution of 0.1 % gelatin and 0.01 % CrK(SO4)2. After draining and the slides were air-dried overnight and then dried and stored at room temperature.

The sample was spot fixed (10 ul) onto the gelatin coated slide and the allowed to dry for 10 minutes at 46°C. Hybridisation buffer was prepared by adding 10 ul of lysosyme solution (lysosyme in 100 mM Tris HCl pH 7.5 and 5 mM EDTA). Hybridisation was carried out at for 10 min at 37°C and the samples were then rinsed with MQ water. Thereafter, the biofilms were washed three times with phosphate-buffered saline (PBS - 10 mM sodium phosphate buffer, 130 mM sodium chloride; pH 7.2) and then embedded in Tissue-Tek OCT compound (Sakura Finetek, Torrance, CA, USA) overnight to allow complete infiltration of the compound into the biofilm (Okabe et al. 1999). After rapidly

freezing the embedded sample at -20°C, 10-µm thick vertical thin sections were prepared using a cryostat microtome (Reichert-Jung Cryocut 1800, Leica, Bensheim, Germany). The sample was then stored at –80°C (by adding 1 volume of 96% ethanol) or were immediately dehydrated on the slide in an increasing and decreasing ethanol series (3 min each in 50, 80 and 96, 80 and 50% (v/v) ethanol) and then allowed to dry on the bench.

2.11.2.1.2 Oligonucleotide probes and fluorescence in situ hybridization

The 16S and 23S rRNA-targeted oligonucleotide probes used in this study are shown in Table 2. The probes were labeled with FAM, TAMRA and Texas Red at the 5' end. The oligonucleotide probes were thawed and 10 ul of hybridisation buffer was aliquoted onto the wells/slide. Hybridisation buffer was composed of 5 M NaCl - 180 ul, 1 M Tris/HCl (pH 8.0) - 20 ul ,50ul of SDS (10% v/v), 35% formamide (350ul) and MQ water (450ul), the stringency concentration were based on values cited in the product literature. 1 ul of each probe (working solution concentration of 50 ng/ul) was added whilst ensuring the slide surface was not scratched or marked. Hybridisation tubes (50 ml Falcon tube) were prepared by folding a piece of tissue, placing it in the tube and pipetting the remaining hybridisation buffer onto the tissue. The slide was then immediately transferred into the hybridisation tube and incubated at 46°C for 1.5 hours. Washing buffer was prepared using 5 M NaCl - 700 ul, 1 M Tris/HCl (pH 8.0) - 80 ul, 50ul of SDS (10% v/v) and MQ water up to 50ml. The solution was preheated to 48°C (in a water bath) and this was then used to rinse the hybridisation buffer for 5-10 mins in a preheated water bath (48°C). Distilled water was then used to remove the washing buffer with and the slide was allowed to air-dry before embedding the slide with anti-fade solution and placing a cover slip which was then secured using nail polish.

A confocal laser-scanning microscope (LSM510 Carl Zeiss, Oberkochen, Germany) equipped with an Ar ion laser (488 nm) and HeNe laser (543 nm) was used to carry out all the microscopy work.

2.12 Experiments

To further an understanding of how environmental parameters affect MFC anodic biofilm development and electrogenic performance over time, the influence of substrate type, temperature, anodic structure, anode material type and the automated control of anodic resistance were investigated. The experiments carried out as part of this study are summarized below:-

2.12.1 MFC anodic biofilm development and reactor performance with non-fermentable and fermentable substrates (Experiments 1, 2 and 3)

Experiment 1 - microbial development and performance of 3-dimensional carbon MFC anodes, using acetate and sucrose substrate

MFC reactors with a fixed load resistance of 1000Ω were fed weekly with 5000 ppm COD L^{-1} of acetate, and sucrose (5.26g and 4.46g per L). The system was operated for a period of 12 weeks at ambient temperatures and the microbial community development was investigated on a weekly basis. The performance of the MFC analyzed at the end of the test period by measuring the substrate polarization curves.

Experiment 2 – microbial development and performance of 3-dimensional carbon MFC anodes, using acetate, butyrate and sucrose

This experiment again looked at the effect of substrate on the MFC system. Microbial community development and MFC performance were investigated periodically over a period of 1 year. COD analysis and pH were monitored on a weekly basis; and the production of secondary metabolites, pH and COD was investigated for each substrate over the course of one batch cycle (1 week). The MFC reactors were run in batch mode, 5000 ppm COD L^{-1} of acetate, butyrate and sucrose were fed on a weekly basis (5.26g, 3.42g and 4.46g per L). Each reactor was connected independently to an external resistive load circuit (1000 ohm) and the voltages across the MFCs were recorded at 10 minute intervals using LabVIEW™ software via an external PC. The reactors were maintained in 35°C incubators at a fixed 45° angle with the anode always orientated in the same position within the chamber to facilitate gas collection and maintain the anode biofilms in fixed positions for standardized microbial community analysis. Biofilm development from the substrate acclimatized carbon veil anode electrodes were analysed using DNA extraction and

analysis from each sample layer. The carbon veil (1st layer) was aseptically sampled with a scalpel, and then trimmed by scissors to $1cm^2$ on a pre-sterilized glass plate to avoid cross-contamination. The second layer was then discarded and the third layer was also analysed as previously described. Layers 1, 3 5, 7 and 9 were sampled. The reactors were batch acclimated for a period of 76 weeks and were then run in continuous mode for 1 week before reverting back to fed-batch feeding. Each of the biofilms was then sequentially tested by substrate-switching with acetate, butyrate and sucrose; with the performance of each biofilm-substrate combination assessed using power curve analysis. Before starting each experiment it was ensured that a stable voltage baseline had been established using the acclimated biofilm-substrate combinations and that the reactor chamber had been washed through to avoid substrate carry-over. Each polarization curve was analysed at 2 days post-feeding to maximize potential power production, allowing time for enzymatic induction but minimizing the level of bacterial growth.

Experiment 3 – Substrate switch performance of acetate, butyrate and sucrose acclimated anode biofilms

MFC reactors were from experiment 2 batch-fed fed with 5000 ppm COD L^{-1} acetate, butyrate or sucrose over a period of 83 weeks. The reactors were maintained at a temperature of 35°C ± 1°C through-out the course of the experiment. During the substrate-switch testing each acclimated biofilm was first tested with corresponding acclimated substrate, with acetate run as the final test substrate with the sucrose and butyrate acclimated biofilms. All the acclimated biofilm reactors were rinsed and then operated with their corresponding acclimated substrate between test runs to ensure the reactors were running at steady-state voltage and there was no substrate carry-over prior to substrate switching.

2.12.2 The effect of start-up temperature on MFC operation

The MFC reactors were fed with 5000 ppm COD L^{-1} acetate and batch operated for a period 60 weeks. MFC reactors were maintained at 3 different temperatures; 10°C, 20°C and 35°C ± 1°C throughout the course of the experiment in heating/cooling incubators (Oxitop, WCW, Germany). Biofilms were aseptically collected as per the protocol carried out in Chapter 3.

2.12.3 MFC anodic biofilm development and biocatalytic performance using acetate as a substrate

2.12.3.1 Batch operation

MFC reactors were run in batch mode with a fixed load resistance of 1000Ω, being fed with 5000 ppm COD L^{-1} acetate on a weekly basis. The biofilm samples from the differentially temperature acclimatized carbon veil anode electrodes were used for DNA extraction and analysis. The carbon veil (1^{st} layer) was aseptically sampled with a scalpel, and then trimmed by scissors to $1cm^2$ on a pre-sterilized glass plate to avoid cross-contamination. Test samples were taken at 8 weeks (T1), 33 weeks (T2) and 56 weeks (T3) from inoculation of the reactors, consecutive sites separated by 150mm lengths along the column length of the anode were used for sampling.

2.12.3.2 Continuous operation

At the end of the batch experimentation the reactors were run in continuous operation. Peristaltic pumping was used to combine substrate and nutrient media maintained at 4°C and this media was then passed into reactor chambers. Substrate utilization was investigated by analyzing the effluent COD values.

2.12.4 Continuous MFC operation and the use of helical anode configurations

Helical reactors (SP1- small gap, SP 2 – medium gap and SP3 – large gap) were enriched with AD sludge for 4 weeks, the annular reactor (wound carbon veil) had already been run in fed-batch operation for a period of 76 weeks. The MFCs were then switched to continuous operation. Peristalic pumps (Watson and Marlow, Falmouth, UK) were calibrated to the appropriate flow rates, 10, 135, 240 and 540ml per min. The reactors were operated with 2 and 20mM acetate in a 50mM phosphate buffer. During continuous operation peristaltic pumps separately drew up buffer/nutrient media and the acetate solution (40mM acetate) and this was then mixed together in-line to give the final substrate concentrations of 2 and 20mM acetate. All stock solutions were refrigerated to 4°C to prevent bacterial growth during the course of the experiments.

2.12.5 Dual chamber MFC reactors used to investigate electrogenic biofilm development: the effect of carbon anode material and the application of an automated load control algorithm

Experiment 1. MFC reactors used to investigate open circuit and closed circuit MFCs operation with four different types of carbon anodes

2 MFC reactors were operated in batch mode, being fed with 1000 mg/L sucrose on a weekly basis during the course of experiment, one was maintained in open circuit conditions and a duplicate reactor was operated with a 1000 Omega external resistance: both MFCs were operated in batch mode with magnetic stirring and at room temperature (ranging between 15±2 °C and 30±2 °C). Biofilms were aseptically sampled using scissors and a scalpel at the end of the experiment for characterization of the bacterial communities and microscopy. To assess the effects of pH on the biofilms a syringe/needle placed in the sample port which allowed the step-wise manual (drop-wise) introduction of 1M HCl into the anode chamber. The pH drop was monitored by a pH probe which had been sealed and fitted into the anode cap. pH values in anode substrate/media were then sequentially adjusted to pH 6.0, 5.5, 5.0, and 4.5.

MFC reactors used to investigate open circuit and closed circuit MFCs operation with four different types of carbon anodes MFC reactors used to investigate open circuit and closed circuit MFCs operation with four different types of carbon anodes

Experiment 2. The effect of automated load control on electrogenic biofilm development

MFC reactors were operated in batch mode, being fed with 5000 mg/L acetate on a weekly basis before the start of the experiment. One of the duplicate MFCs was load controlled by connecting it to a monitoring and control system through an analogue/digital interface and real-time dynamic monitoring and control system; this was applied using an algorithm executed on a personal computer, as described below (Load controlled MFC, LC-MFC). The second MFC reactor was connected to a static load (200Ω) and monitored, but not controlled (Static load MFC, SL-MFC): both MFCs were operated in batch mode with magnetic stirring and at room temperature (ranging between 15±2 °C and 30±2 °C). Anodic biofilms were examined at the end of the experiment to investigate and compare the influence of control on the MFC microbial ecology, which had developed over almost 600 hours. LC-MFC and the SL-MFC reactors were operated anaerobically and

identification of 16S rDNA and PCR analysis were performed on the biofilm on the anode of both LC-MFC and SL-MFC were sampled in order to compare the microbial and archaeal communities that had developed over the entire 600 hour duration of the batch experiment.

3 MFC anodic biofilm development and reactor performance with non-fermentable and fermentable substrates

A diverse range of Bacterial and Archaeal microbial groups have been identified in MFCs. However, the microbial population dynamics of bacterial groups found in three-dimensional engineered anode electrode structures within single chamber MFCs have not been studied extensively. It was expected that diverse bacterial groups co-exist in the structurally designed anodic surfaces found in the tubular MFC anode veil, with fermentative and methanogenic processes competing and/or interacting with acetogenic pathways and the formation of hydrogen. The formation of biofilm itself further affects community structure by restricting physical access to anode surfaces and dictating mass transport flows of preferable electron donors (especially when complex substrates are metabolized) and subsequent flows of protons to the cathode. The MFC anode was constructed by winding a 260 x 450mm sheet around a central PVC rod (1 cm diameter) and this meant biofilm development through the depth of the porous carbon veil anode could be investigated by examining discrete anode layers. In experiment 1 analysis was carried out using sucrose and acetate and in experiment 2 the first experiment was repeated using butyrate as an additional and more complex non-fermentable substrate. Experiment 3 then investigated the efficacy of each substrate in each of the acclimated biofilms.

All tests were carried out in batch mode, with the reactors being fed on a weekly basis. The aim of these experiments was to establish how feeding tubular air cathode MFCs with fermentable and non-fermentable substrates affected the reactor performance, anode biofilm growth and microbial community development.

3.1 Results

The three experiments conducted can be summarized as follows (as described in section 2.12.1):-

- The microbial development and performance of 3-dimentional carbon MFC anodes, using acetate and sucrose substrates.
- The microbial development and performance of 3-dimentional carbon MFC anodes, with sucrose, butyrate and acetate substrates.

- Substrate switch performance of acetate, butyrate and sucrose substrate acclimated anode biofilms.

3.1.1 The microbial development and performance of 3-dimentional carbon MFC anodes, using acetate and sucrose substrates

Representative fermentable and non-fermentable substrates (acetate and sucrose at 5000ppm/L) were used to compare anode biofilm development in batch mode. After 10 weeks operation the acetate fed MFC produced a power density 5.5 W/m^3 but the sucrose reactor generated only very low power densities of 0.22 W/m^3 (Fig 3.1).

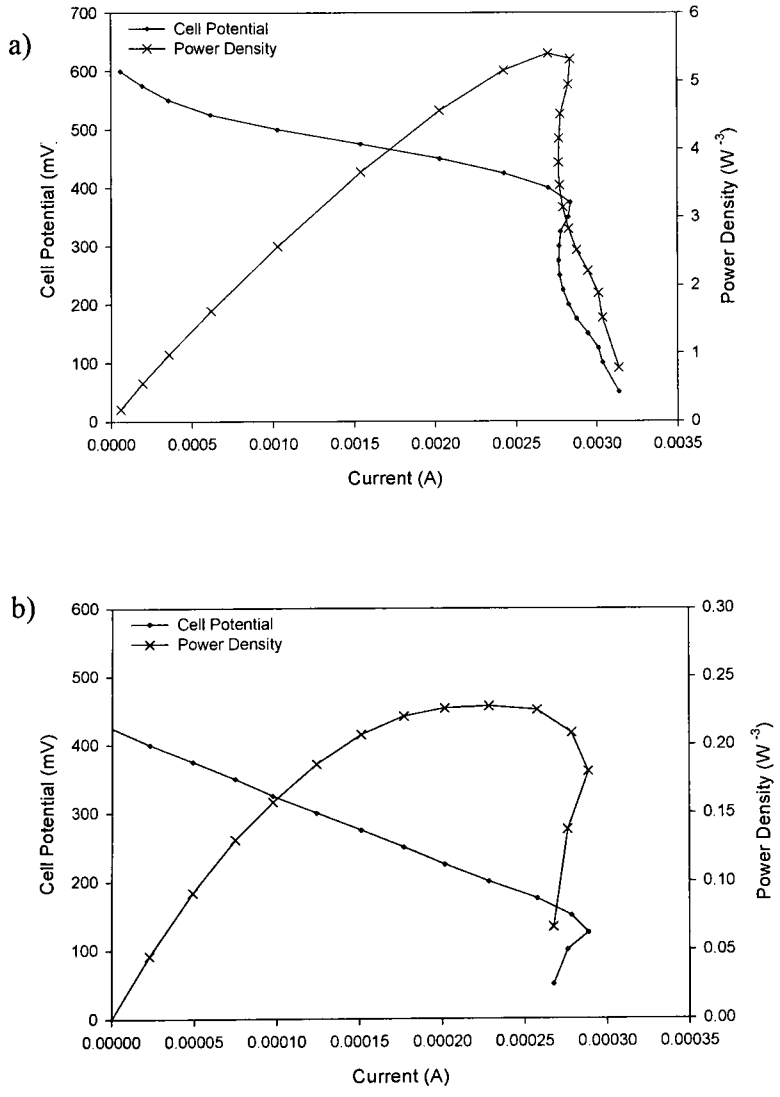

Figure 3-1. Cell potential and power density curves produced in tubular MFCs using fermentable and non-fermentable substrates (10 weeks operation) a) sucrose and b) acetate.

Examination of scanning electron micrograph (SEM) pictures by anode depth (carbon veil layer) in Fig 3.2 showed that at the 10 week operational time point, higher numbers of bacteria (cocci and rods) were present in the sucrose fed anode biofilm and this included clumps of bacteria developing in the upper anodic carbon layers. These types of clumps have been previously associated with surface anode biofilms fed with fermentable substrate. It has been hypothesized that clumps contain fermentative bacteria that oxidize substrate to fatty acids that can then be metabolized by EAB who syntrophically transfer electrons to the electrode (Lee et al. 2003). No such clumps were observed in any of the acetate fed reactors, only sparse numbers of isolated rods were observed in anode layers 2 – 10.

The levels of biofilm decreased with depth of the anode (by anode layers L1-L9) in both reactor types.

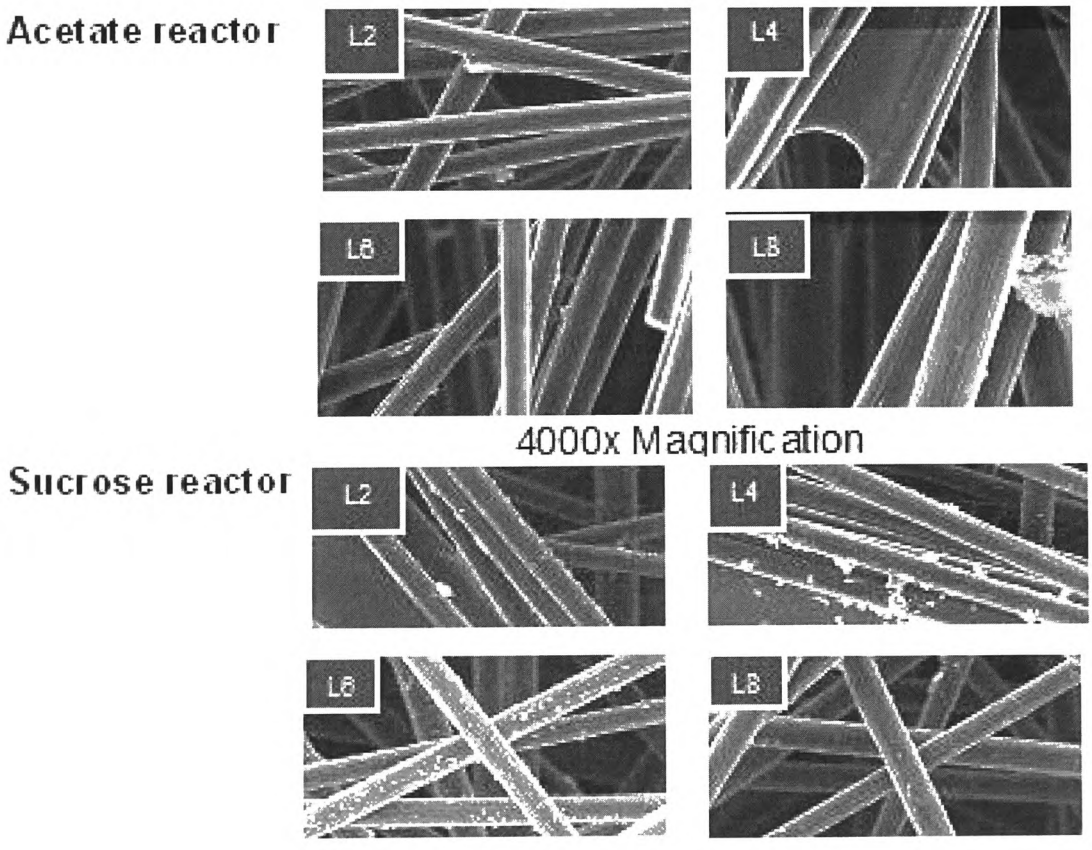

Figure 3-2. Sequence of SEM pictures in acetate and sucrose fed reactors – carbon veil layers 2 to 8 through the anode structure.

The reproducibility of the DGGE technique for the analysis of carbon veil anodic biofilm samples was tested by running replicate samples from 2 duplicate reactors using both Archaeal and Bacterial

primers (Fig 3.3). Cluster analysis shows that Archaea and Bacterial grouped into 2 distinct profiles with similarity scores of 88.6 and 78.8 respectively, with the AD sludge inoculum forming another distinct grouping. The results demonstrate that the development of both Archaeal and Bacterial community profiles was consistent between the two test reactors. Over the 1 week time period another cluster formed indicating that the process of biofilm acclimation was still progressing.

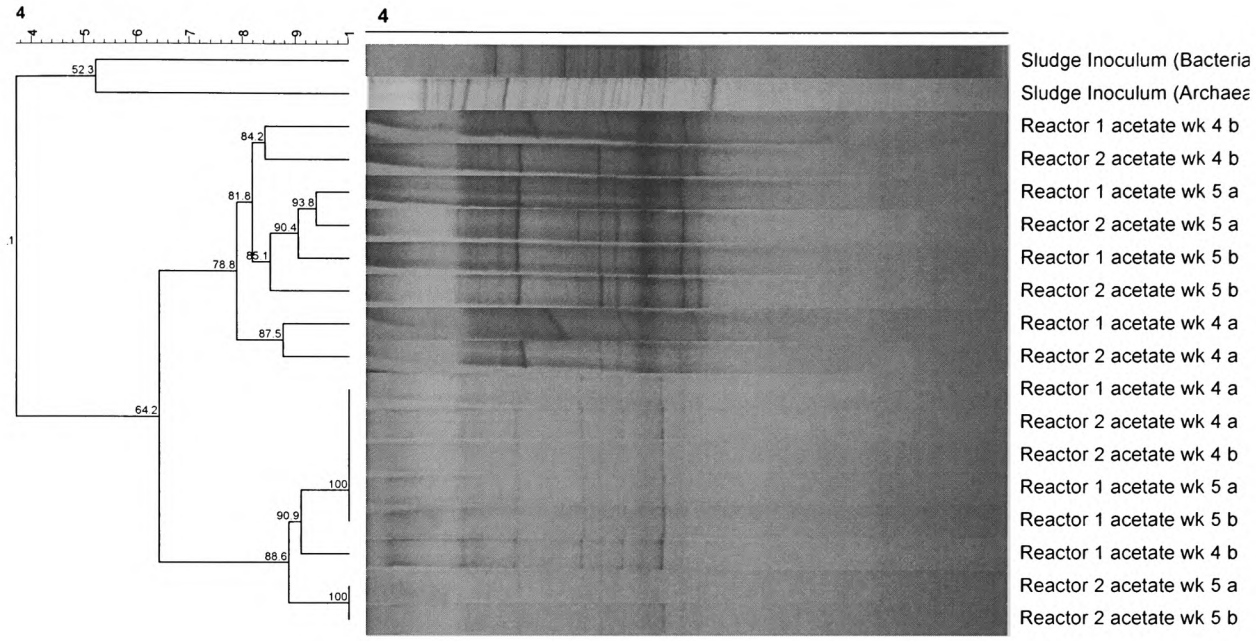

Figure 3-3. Bacterial and Archaeal DGGE profiles of acetate fed anode biofilm replicates (a and b) from 2 duplicate reactors at 2 time points (operational weeks 4 and 5).

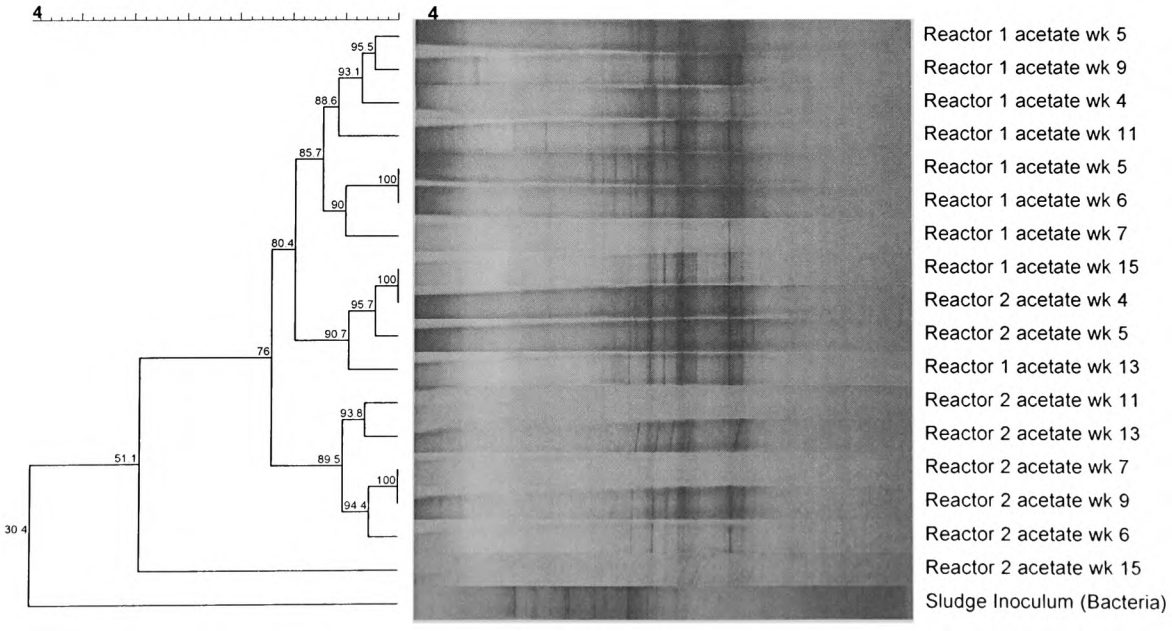

Figure 3-4. Bacterial DGGE profiles from 2 replicate acetate fed anode MFC biofilms over a 15 week time period.

The development of Bacteria in the acetate reactor was further monitored over a period of 15 weeks (Fig 3.4). Cluster analysis did show that over time replicate reactors 1 and 2 did maintain distinct profiles and levels of similarity were very high (76-100%) with key bacterial species being conserved between the two reactors. The acetate reactor 2-week 15 result significantly differed from the other band profiles as 'smiling effects' caused by the lane position (proximity) to the edge of the gel could not be fully compensated by the GelCompar II software.

From the starting profile of the sludge inoculum both acetate and sucrose fed reactor profiles changed dynamically with time, developed dominant bands and also increased in richness (Figs 3.5 and 3.6). Key Bacterial DGGE bands differed between acetate and sucrose MFC anodes showing the trophic development of bacterial communities as they adapted to on-going environmental-microbiological interactions.

By using a multilayered carbon veil anode electrode, novel aspects surrounding the spatial distribution of Bacterial and Archaeal groups through the electrode depth (by anode layer) and over time were investigated. DGGE banding profiles were observed through anodic carbon veil layers 1 to 9 in both sucrose and acetate fed reactors. These showed that microbial communities were consistent through depth of the anode (layers 1 to 9). In concordance with SEM results (Fig 3.2), the levels of DNA dilution prior to PCR and DGGE band intensities suggested that the numbers of bacteria decreased with depth (Figs 3.5 and 3.6). Hence, although the banding profile in the L5 Archaeal acetate profile from 01 July 2008 was noticeably more intense than the LI and L5 profiles the DNA had been diluted 1:10 for the PCR amplification step (Fig 3.7).

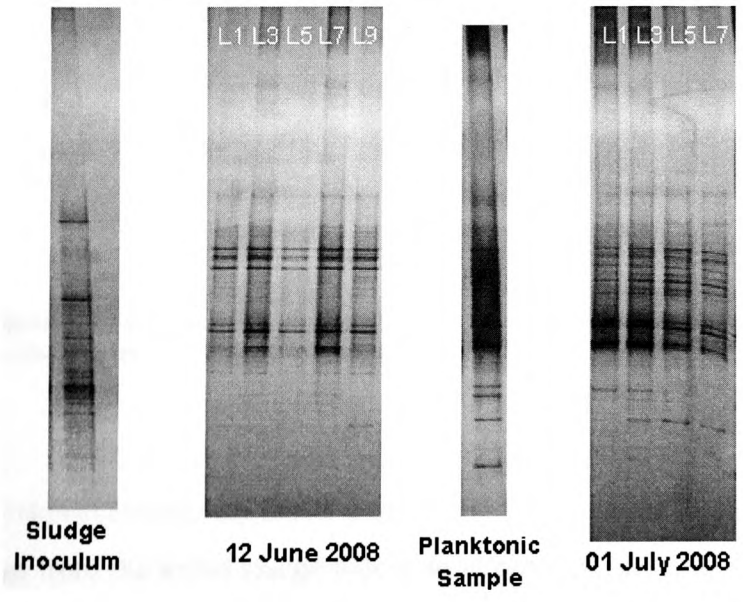

Figure 3-5. Bacterial DGGE profiles of the initial sludge inoculum and acetate fed MFC reactor at 2 different time points through anode layers.

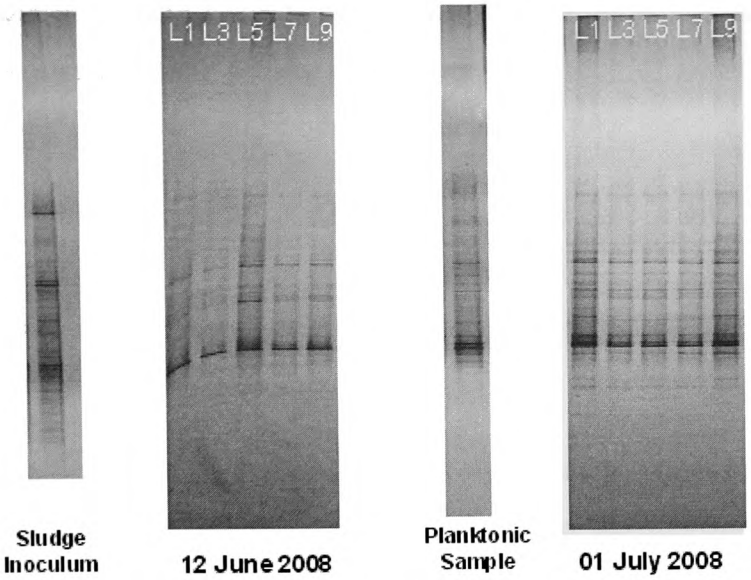

Figure 3-6. Bacterial DGGE profiles of the initial sludge inoculum and sucrose fed MFC reactor at 2 different time points through anode layers.

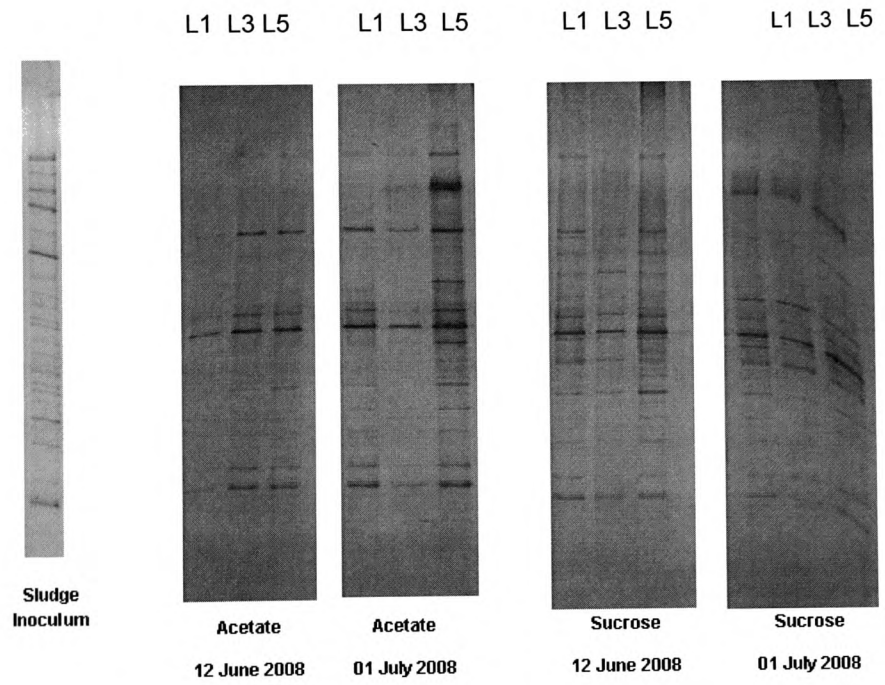

Figure 3-7. Archaeal DGGE profiles of the initial sludge inoculum and acetate / sucrose fed MFC reactors at 2 time points, showing layers 1, 3 and 5 in each reactor.

Archaeal community DGGE profiles (Fig 3.7) from the 2 sample dates also resulted in a dynamic change from the initial sludge inoculum in both acetate and sucrose reactors. The development of similar key bands highlights the presence of Archaeal populations active in association with both fermentative and non-fermentative substrates. This probably reflects the key activity of acetoclastic

methanogens in both reactors. More complex profiles in the sucrose reactor may reflect more complex methanogenic activity due to the production of hydrogen as a result of fermentative activity and subsequent metabolism by hydrogenotrophic bacteria.

The diffusion gradient of substrate into the porous anode material and protons out of the material (produced as a result of anaerobic respiration), did not seem to result in the development of different trophic groups and thus no change in population dynamics through the anode electrode layers was evident.

The utilization of the carbon veil layers making up the anode provides the potential for increased surface area for microbial colonization and biofilm development, and provides the possibility of increased electrochemical activity.

3.1.2 The microbial development and performance of 3-dimensional carbon MFC anodes, using acetate, butyrate and sucrose substrates

The development of electrogenic activity was monitored over time for each substrate fed reactor (Fig 3.8). The lag-time to attain steady-state voltage was 2-3 weeks for the acetate fed reactor but this was 12-14 weeks for both the butyrate and sucrose fed reactors. The acetate fed reactor also produced a significantly higher voltage which stabilized at 0.49 (± 0.02V) compared to both the sucrose and butyrate reactors which achieved a steady-state voltage of ~0.26V, with the former consistently higher by 0.01-0.03V.

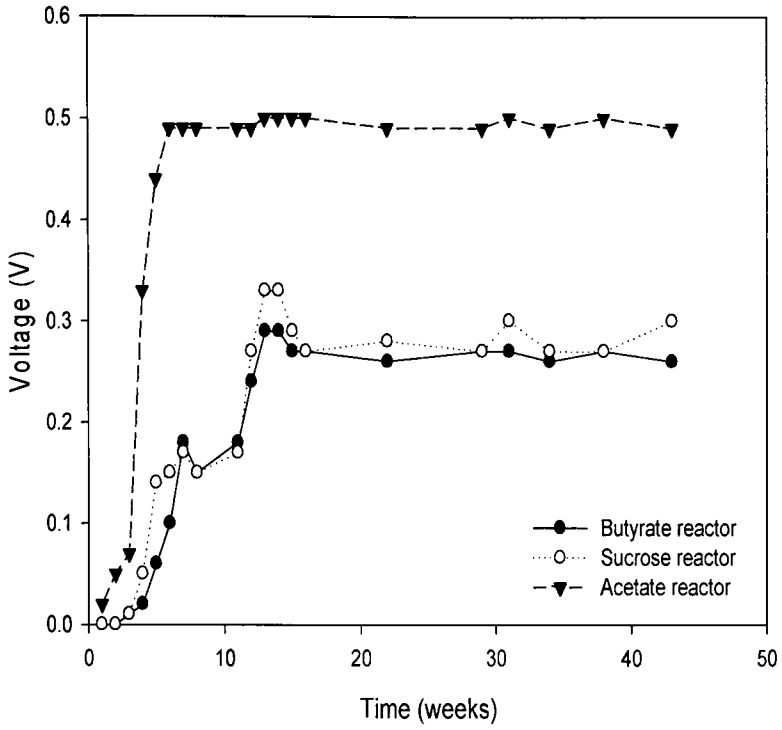

Figure 3-8. Voltage development during the enrichment of MFC reactors with 3 different substrates (acetate, butyrate and sucrose). Reactors were batch fed on a 1 week cycle with 5000 ppm COD L^{-1} substrate. External resistance was 1000Ω.

This data related to the maximum voltage obtained during each batch cycle but it was observed that where butyrate and acetate substrates facilitated the maintenance of a consistent voltage throughout the batch cycle, sucrose rapidly reached the level of maximum voltage but this was then followed by gradual decrease in voltage over the 1 week feeding cycle.

At 30 weeks operation time all the voltages in the different substrate acclimated reactors had stabilized and for each substrate type pH values, COD removal (%) and VFA production were profiled over a 1 week batch period. A 100 mM phosphate buffer was used in all the reactors, this had a pH of 6.9 and the butyrate reactor maintained this pH through-out the 1 week batch operation (Fig 3.9). However addition of sucrose caused a rapid decrease in pH to 5.5 as VFAs were produced through fermentative metabolism, this pH then increased from day 3 as VFAs were then consumed EAB. In contrast, the pH of the acetate fed reactor increased through-out the batch cycle, this is likely caused by a shift in the relative levels of sodium dihydrogen phosphate and disodium hydrogen phosphate. It is thought that as protons were transferred to and then consumed by the cathodic reaction this would favour production of disodium hydrogen phosphate which has a pH range of 8.7-

9.3; this pH increase is therefore reflective of relatively high rates of electrogenesis in the acetate reactor and how these respiratory products interacted with this particular buffer system.

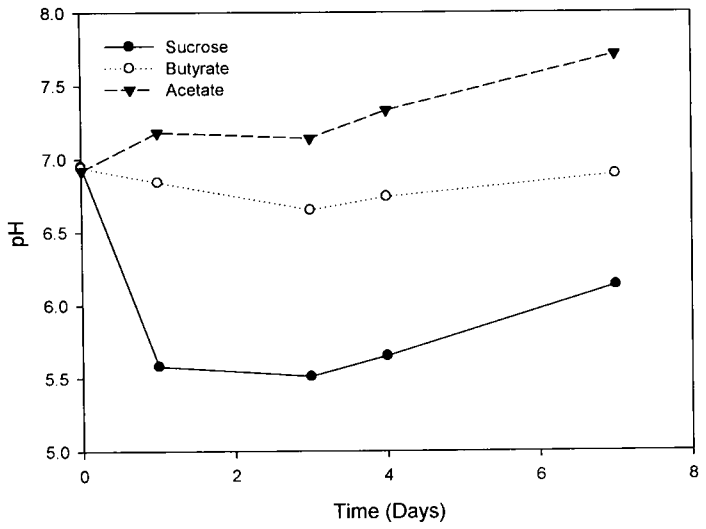

Figure 3-9. pH development during a 1 week batch cycle of MFC reactors fed with 3 different substrates (acetate, butyrate and sucrose). Reactors were batch fed with 5000 ppm COD L^{-1} acetate at 30 weeks operation.

When COD levels were investigated over the course of the batch cycle (Fig 3.10) acetate had the fastest removal rate and butyrate the slowest. Sucrose exhibited a very fast initial COD decrease as the substrate was rapidly fermented to VFAs but then this rate decreased after day 1 as COD removal after this point was increasingly reliant on VFA metabolism.

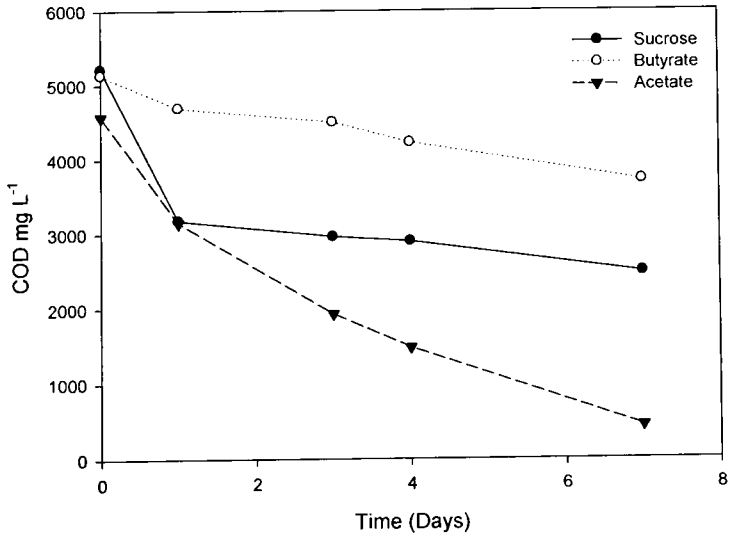

Figure 3-10. COD removal during a 1 week batch cycle of MFC reactors fed with 3 different substrates (acetate, butyrate and sucrose). Reactors were batch fed with 5000 ppm COD L^{-1} acetate at 30 weeks operation.

Analysis of VFAs produced in the sucrose reactor demonstrated that acetate and butyrate were the predominant fermentative metabolites produced along with propionate (Fig 3.11 a)). It can be observed that VFA levels continued to rise until day 5 when net VFA consumption exceeded VFA production via mixed fermentation; at which point all VFA levels decreased to day 7, notably the acetic and butyric acids but also propionate. The subsequent anaerobic respiration/metabolism of VFAs present and associated buffering effects can thus be related to the observed shifts in pH values with sucrose over the course of the batch cycle (Fig 3.9). Acetate concentrations in the acetate fed reactor decreased with time with no other VFAs detected. In contrast acetate was detected in the butyrate reactor, with levels increasing up to day 3 and then decreasing with time to day 7 (Fig 3.11 b) and c)). It is also interesting to note that valeric (pentanoic) acid was produced following the fermentation of sucrose (Fig 3.11); this could be due to micro-organisms (notably *Clostridia spp.*) carrying out the Strickland reaction and could denote the high levels of protein being present (bacterial biomass) in the sucrose biofilm, that was then subsequently metabolized.

a)

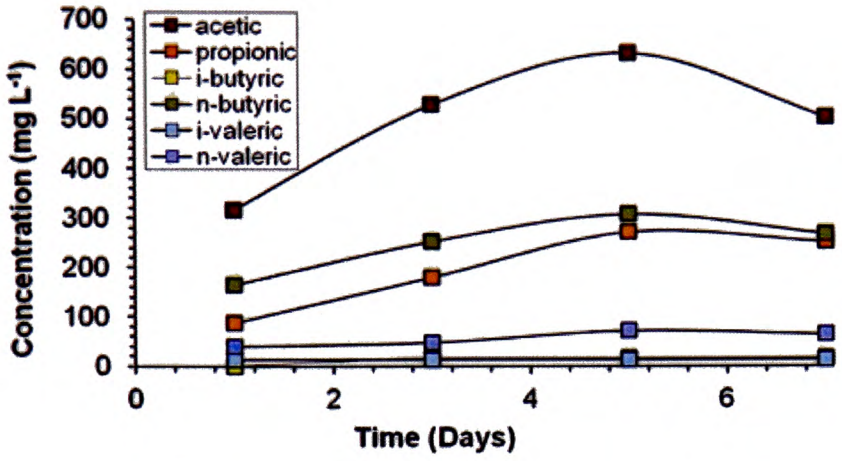

b)

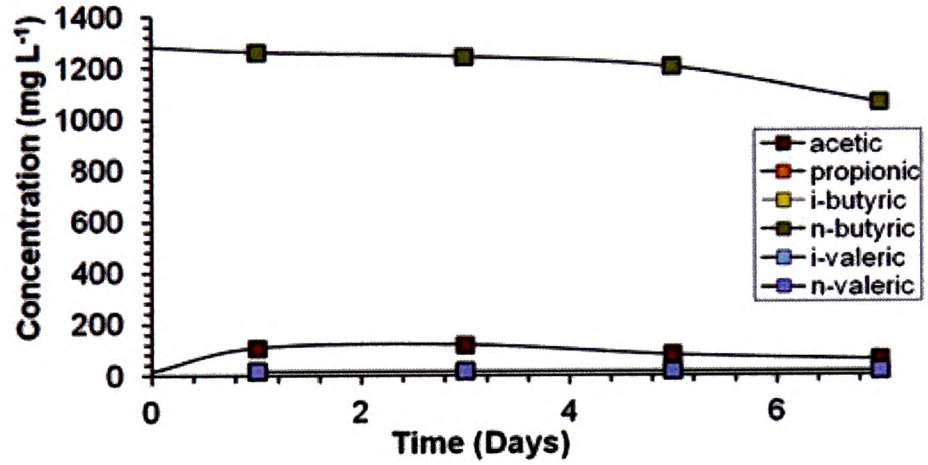

c)

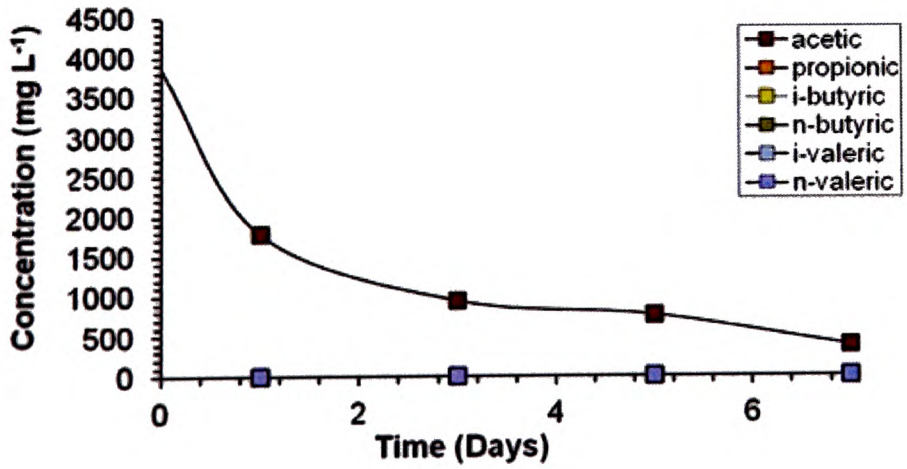

Figure 3-11. VFA production during a 1 week batch cycle of MFC reactors fed with 3 different substrates, a) sucrose b) butyrate and c) acetate. Reactors were each batch fed with 5000 ppm COD L^{-1} after 30 weeks fed-batch operation.

Throughout the course of the experiment, at the end of each batch sample, (weekly) samples were withdrawn and COD levels quantified, allowing % COD removal rates to be calculated over time (Fig 3.12).

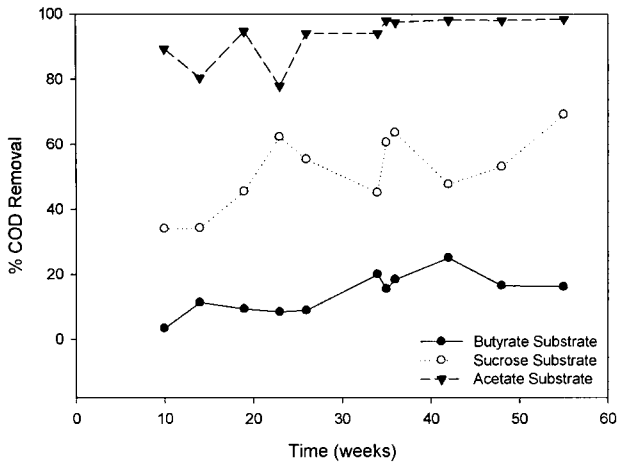

Figure 3-12. sCOD removal efficiency (%) at different reactor temperatures over time. Batch reactors were fed 5000 ppm COD L^{-1} acetate COD measurements were taken after 1 week operation 10 weeks post enrichment.

After 10 weeks operation the acetate fed reactor attained an 89% removal rate over the 1 week batch cycle and by the 35th week this reached 97% COD removal. The COD removal rates in both the sucrose and butyrate fed reactors increased over time but at significantly lower rates than the acetate reactor: COD removal in the butyrate reactor started at 10% and increased to 16-25%, COD removal in the sucrose reactor started at 34% and increased to 68%.

The production of methane was detected in the acetate fed MFCs but not the butyrate or sucrose reactors, the maximal rate of methanogenesis with acetate being 1.03 $mMol.d^{-1}$. Gas production was observed in the sucrose reactor but this was found to be carbon dioxide, no gas production was observed in the butyrate reactor.

Using a high initial substrate loading of 5000 ppm COD L^{-1} CEs were investigated for each of the substrate operated MFCs. After 3 months operation the CE of the acetate reactor was 3.12% but this decreased to 2.9% after 4 months operation. The CEs for the sucrose and butyrate reactors were 3.9% and 8.1% respectively after 4 months operation.

Figure 3.13 shows the DGGE archaeal community development at 8 weeks and 56 weeks operation. Archaeal species can be observed to have developed through all the layers of the wound anode (Layers 1 to 9), with a high degree of similarity between the profiles of each layer in each

given (substrate) reactor. It can be determined qualitatively that the L7 and L9 layers have less distinct banding indicating that less archaea were present in these samples. This was not observed in the butyrate sample, which may reflect the high initial DNA dilutions (bacterial numbers) of 1:10 and 1:100 used in the preparation of the sucrose and acetate reactors resulting in a proportionally greater biomass differentials occurring in these samples. Each substrate type produced distinct clusters, indicating that substrate type has a strong influence on the development and acclimation of the archaeal communities. Although the archaeal community profiles changed and developed over time from the initial inoculum, it can be observed that a similarity of 63.7% exists between the AD sludge and sucrose biofilm. It is possible that the wider range of fermentative metabolic products resulting from sucrose substrate (Fig 3.11) may support the wide range of Archaea that are likely to be found in sludge environments.

a)

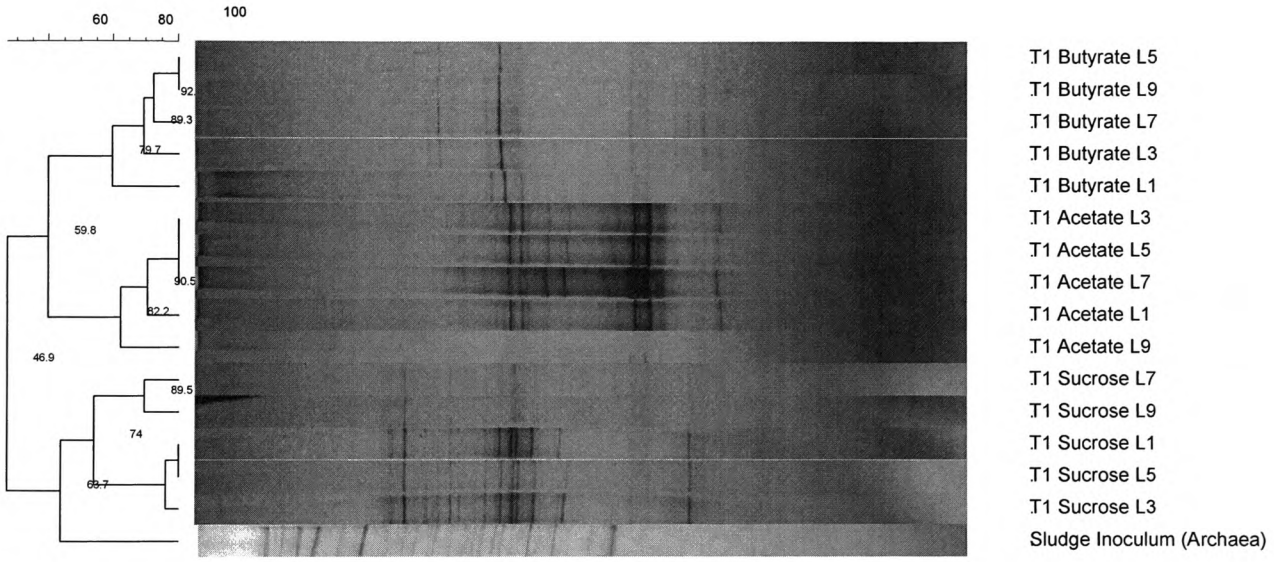

b)

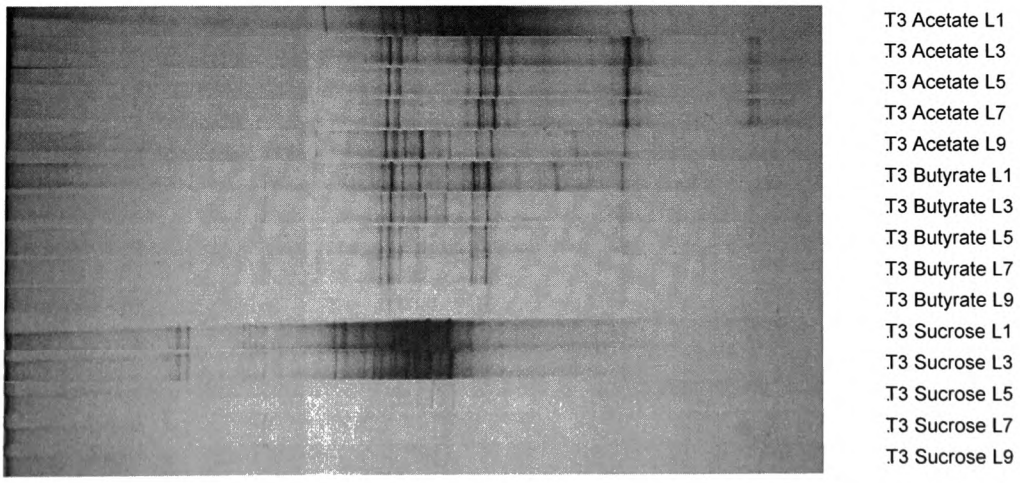

Figure 3-13. Archaeal DGGE biofilm profiles through anode depth at 2 time points using 3 different substrates (sucrose, butyrate and acetate), a) 8 weeks (T1) and b) 56 weeks (T3)

Bacterial populations were also observed to cluster according to substrate type (Fig 3.14). As per the archaeal population profiles, anode depth did not affect microbial population development. Again it was observed that lower anode depths produced less intense banding indicating that lower numbers of bacteria could grow in these positional environments. In contrast to the Archaeal community profiles all the Bacterial substrate biofilm profiles showed an equally divergent development from the initial AD sludge inoculum, this may indicate the selective drive to form electrochemically active communities.

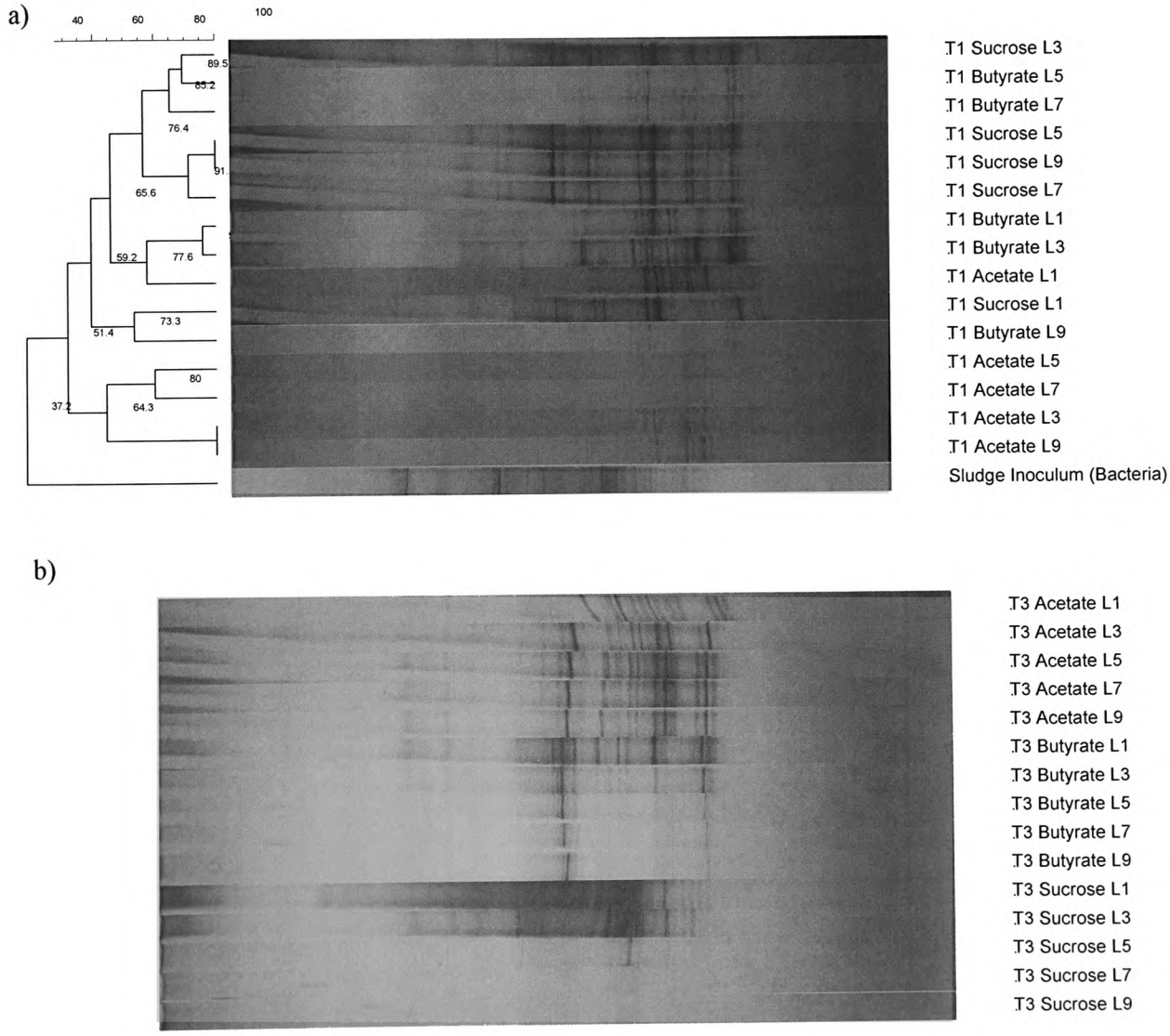

Figure 3-14. Bacterial DGGE biofilm profiles through anode depth at 2 time points using 3 different substrates (sucrose, butyrate and acetate), a) 8 weeks (T1) and b) 56 weeks (T3)

To quantify the growth of biofilm in each substrate fed reactor over time and by anode depth, levels of DNA (ng L^{-1}) were measured as an indicator of biomass (Fig 3.15). The butyrate reactor produced low levels of biomass in the L1 biofilm and no biomass was detected through the depth of the anode. In contrast the sucrose anode produced high levels of biomass, with significant levels detected up to L5 but biomass also detected up to L9. Biomass levels increased up to T2 and then stabilized. Biomass levels in the L1 biofilm of the acetate fed reactor increased over time but whilst biomass was detected in layers 3-9 these were not significantly high and did not increase over time. Factors that limit biofilm growth in the inner anode layers are likely to be either due to the ability of substrates/electron donors to diffuse into the biofilm or the potential inhibitory build-up of protons resulting from anaerobic respiration (Torres et al. 2008).

a) T1

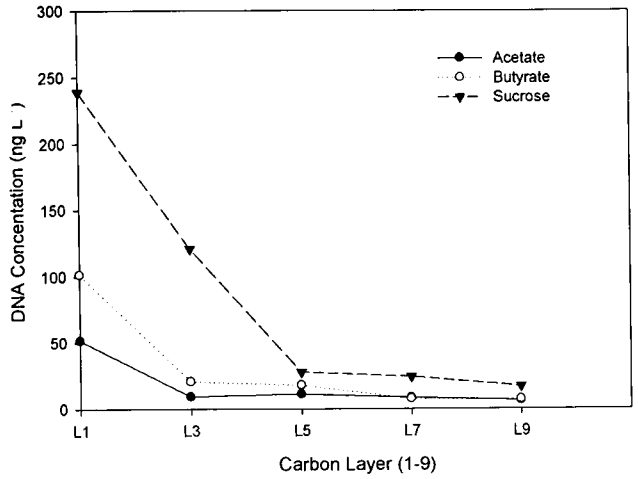

b) T2

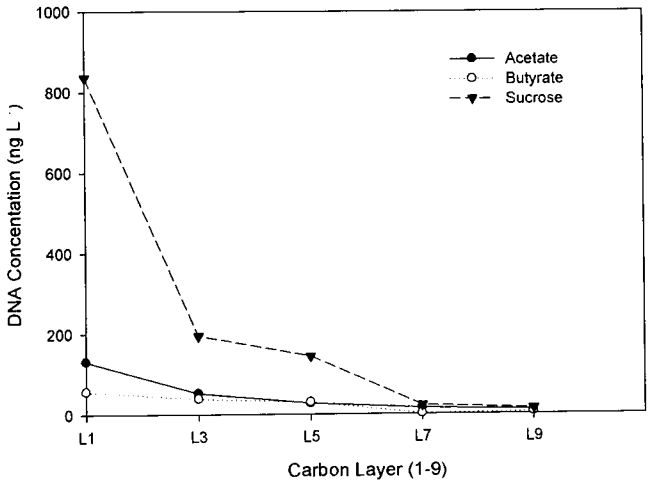

c) T3

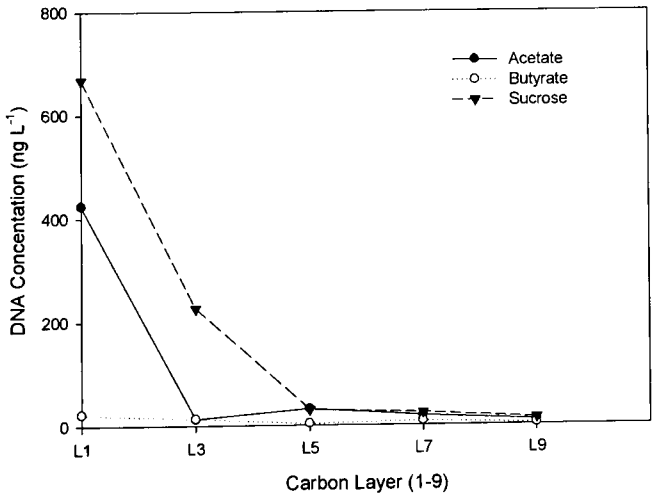

Figure 3-15. Biofilm profiles through anode depth (layers 1 to 9) at 3 time points using 3 different substrates (sucrose, butyrate and acetate), a) 8 weeks (T1) b) 33 weeks (T2) and c) 56 weeks (T3)

When the L1 biofilm development was examined over time this showed that sucrose produced the greatest levels of biofilm but total biomass levels peaked at 33 weeks operation. Acetate biomass levels continued to increase over the test period of 56 weeks but, in contrast, biomass levels in the butyrate reactor decreased over time (Fig 3.16). Thus it would seem that fermentation could sustain the production of high levels of bacteria/biomass up to a maximum set level, that acetate metabolism was undertaken by a rapidly replicating population of bacteria but butyrate metabolism could not sustain high population levels (from the initial inoculation event).

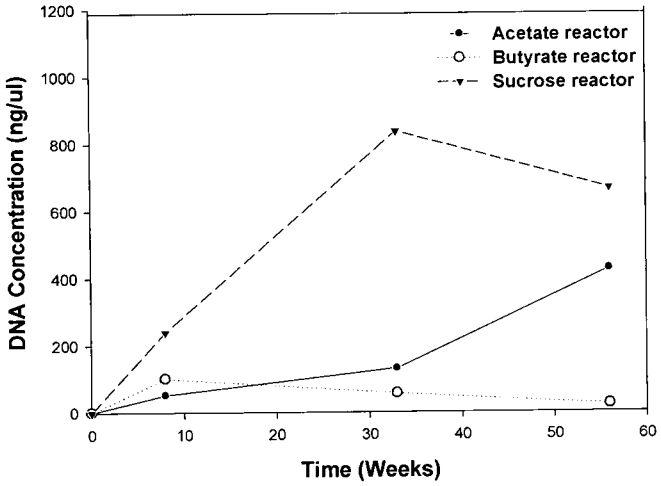

Figure 3-16. Biofilm development over time with in MFC reactors fed-batch with 3 different substrates (sucrose, butyrate and acetate).

When Layer 1 biofilm Bacterial profiles were monitored over time the early sucrose community clustered with butyrate biofilm communities but then further developed with time (T2 and T3) to cluster with the acetate fed reactor communities (Fig 3.17). It is likely that after the first sample time at 8 weeks the sucrose biofilm continued to select for EAB that could utilize VFAs produced via fermentation, particularly acetate. Butyrate degradation and subsequent electrogenesis will be reliant on syntrophic relationships between both bacteria and archaea (Schink and Stams 2005) and so the capacity for the biofilm acclimation is likely to be more limited than is the case with sucrose and acetate substrates.

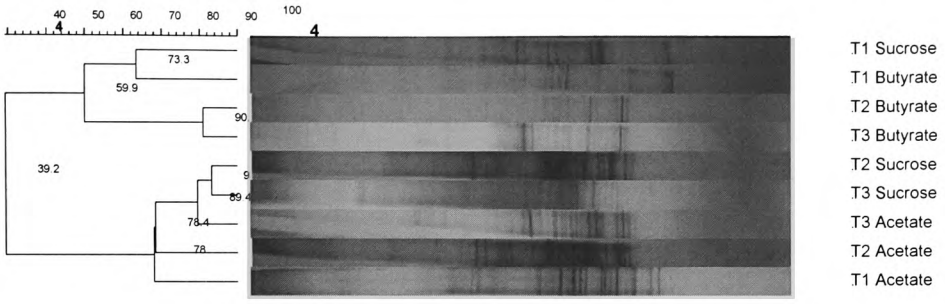

Figure 3-17. Cluster analyses of bacteria DGGE biofilm (L1) profiles at 3 time points using 3 different substrates (sucrose, butyrate and acetate).

When the range-weighted richness values were examined for Bacteria present in the acclimated biofilms it was found that the initial scores were low in the sucrose reactor biofilm and then increased to high values of >200; where-as the butyrate scores stayed low and decreased with time (Table 3.1). According to Marzorati et al (2008) a richness score of >30 is indicative of very habitable environments and scores of 10-30 a medium level of richness. This result shows the development of very diverse populations in the acetate and sucrose biofilms but not the butyrate biofilm.

Table 3-1. Richness scores at 3 time points using 3 different substrates (sucrose, butyrate and acetate).

Time (weeks)	Sucrose	Butyrate	Acetate
8	25.9	32.9	267
33	363	15.6	267
56	284	13.8	230

These results were also supported by visual examination of the carbon veil anodes which demonstrated the variable levels of biomass production at 56 weeks operation (Fig 3.15). In concordance with the DNA results (Fig 3.16) it was observed that the sucrose biofilm on the anode surface was thick and copious whereas the butyrate biofilm was absent. High levels of visible biomass may have been due to the production of dextrans. Species of the *Leucanostoc* and *Lactobacillus* are known to produce the extracellular enzyme dextransucrase which catalyses the glucose polymerization process (Karthikeyan et al. 1996). However as DNA was used as an indicator

of biomass in this study, this component of the biofilm would not have been reflected in the biomass/VSS measurements reported.

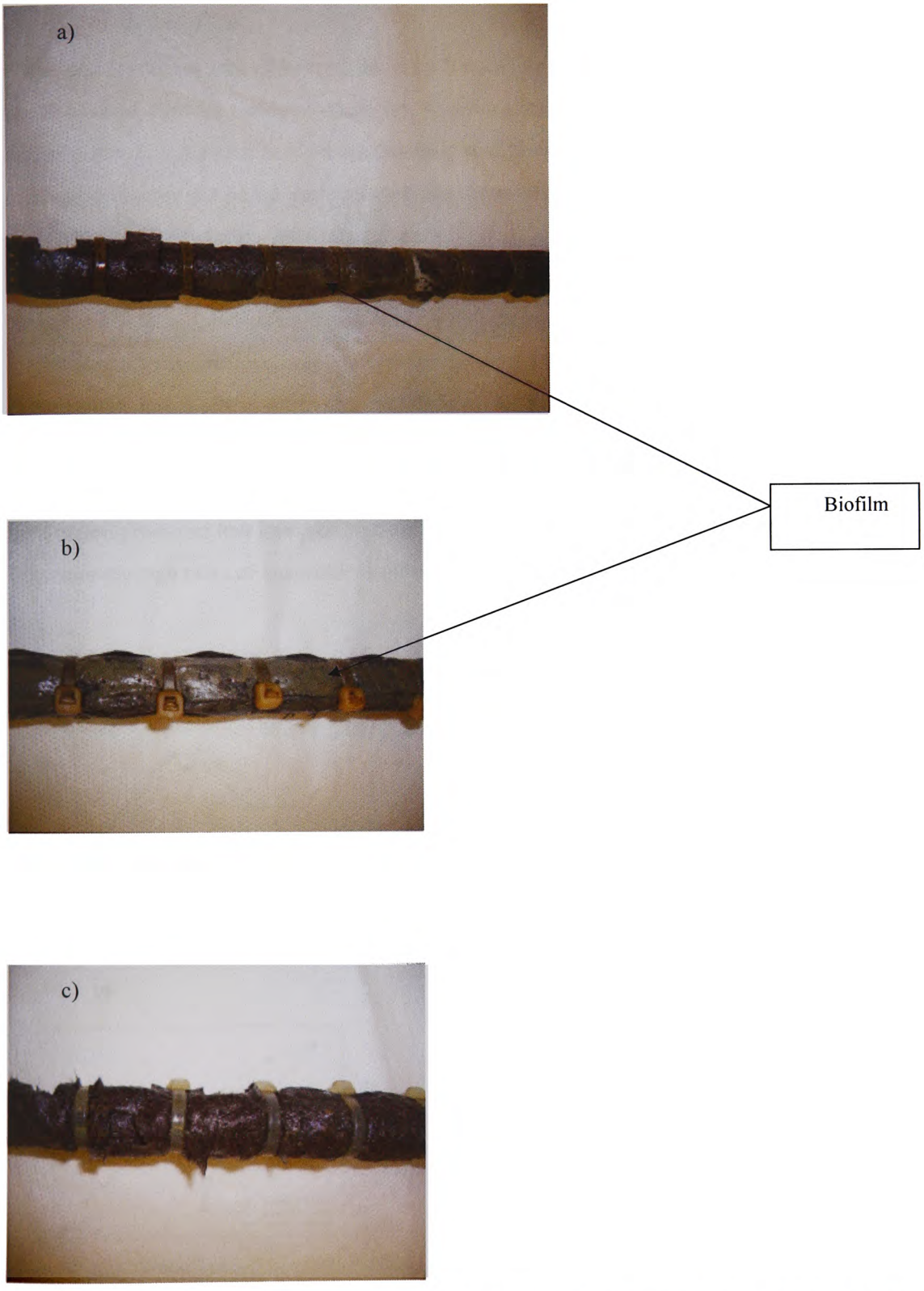

Figure 3-18. Visual examination of biofilm development on carbon veil anodes from a) acetate b) sucrose c) butyrate fed reactors (56 weeks)

3.1.3 *Substrate switch performance of acetate, butyrate and sucrose acclimated anode biofilms*

Power density curves with different substrates for acetate, sucrose and butyrate acclimated reactors were obtained after 83 weeks of operation. Acetate substrate produced the highest power in each of the different substrate acclimated biofilms, this being higher by a factor of 7 in the acetate acclimated reactor compared acetate substrate in the sucrose and butyrate reactors. In the sucrose acclimated biofilm butyrate substrate produced power densities comparable to those from acetate substrate (1 and 1.1 Wm^{-3} respectively) both higher than the power produced by the sucrose substrate (0.6 Wm^{-3}), indicating that a mixed bacterial population in the sucrose biofilm was able to metabolize both butyrate and acetate effectively but the wide range of mixed VFAs produced during fermentative metabolism were not metabolized as effectively by the electrochemically active bacteria (EAB) present (Fig 3.19 a). The butyrate biofilm (Fig 3.19 b) produced the lowest power measurement for each of the 3 different substrates tested, further demonstrating that butyrate acclimation produced low levels of biofilm/biomass and could not sustain high numbers of EAB and consequently high rates of anaerobic respiration.

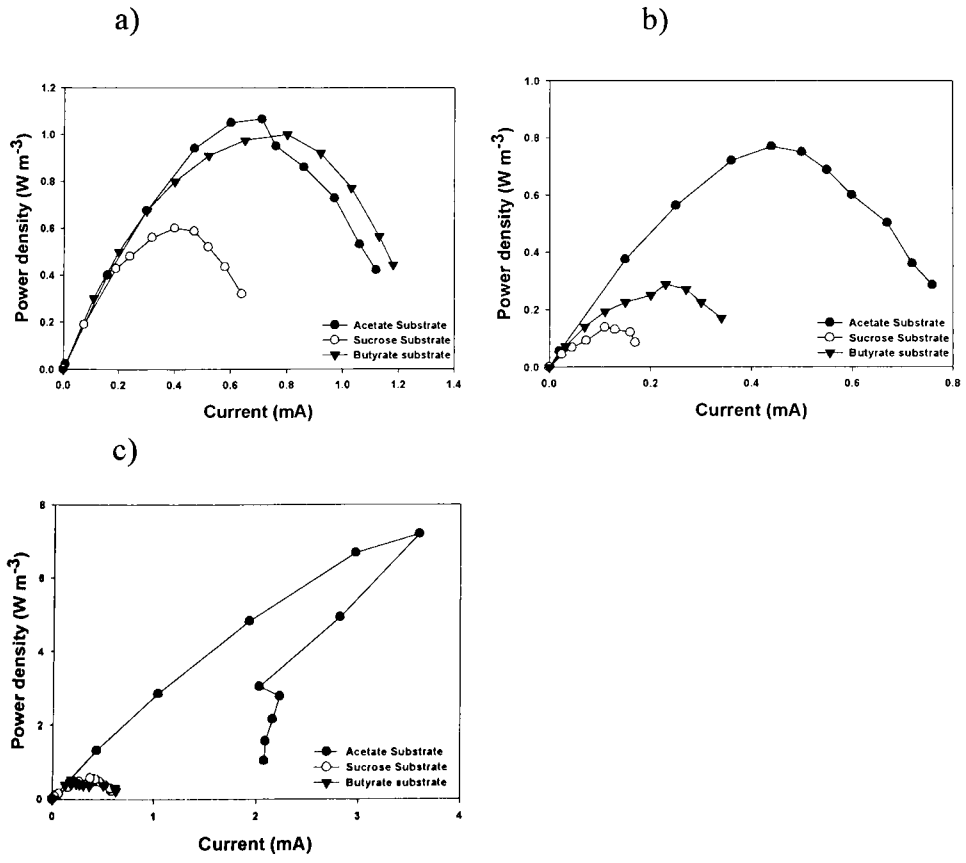

Figure 3-19. Power density curves using 3 different substrates (sucrose, butyrate and acetate) in 3 different substrate acclimated reactors with a) sucrose, b) butyrate and c) acetate

High numbers of EAB that could readily metabolize acetate were shown by the high acetate substrate power measurement in Fig 3.19 c; both sucrose and butyrate produced power readings of 0.5 Wm^{-3} with the acetate biofilm, however the butyrate power reading was half that recorded in the sucrose acclimated biofilm suggesting that a wide range of syntrophic associations were not available and was limiting overall power production.

The differential metabolic activities of the different acclimated biofilm were further evidenced by the relative COD removal rates which were calculated as the % COD loss over each 1 week batch cycle. Acetate and butyrate acclimated biofilms only reduced sucrose CODs by 57% and 54% respectively compared to 80% for the sucrose acclimated biofilm; this was probably due to limiting numbers fermentative microorganisms being present in the former biofilms. Whereas the acetate acclimated biofilm only produced butyrate and sucrose substrate COD removal rates of 22.6% and 19.6% respectively, showing that not only were fermentative trophic groups limiting substrate removal but also trophic groups associated with the metabolism of VFAs, specifically butyrate (Table 3.2).

Table 3-2. The % COD drop over a 1 week batch cycle using 3 different substrates (sucrose, butyrate and acetate) in 3 different substrate acclimated biofilms (sucrose, butyrate and acetate).

Acclimated reactor	Substrate	% COD drop
Acetate	Acetate	87.5
Butyrate	Acetate	22.6
Sucrose	Acetate	19.4
Acetate	Butyrate	41.6
Butyrate	Butyrate	41.7
Sucrose	Butyrate	58.2
Acetate	Sucrose	57.1
Butyrate	Sucrose	54.1
Sucrose	Sucrose	80.3

The COD results show a different trend to the power density results as these values relate to overall metabolic activity including non-electrogenic activity such as methanogenesis, the high % COD decreases observed in the sucrose reactors also demonstrate low rates of electron harvesting. Additionally the higher rate of COD removal of butyrate substrate from the butyrate biofilm compared to acetate substrate from the butyrate biofilm shows the development of (non-electrogenic) butyrate metabolic activity.

In Figure 3.20 sequential low temperature perturbations were used as a mechanism to test the functional robustness of the differentially acclimated biofilms. From a stable operating temperature of 35°C each reactor was sequentially subjected to 24 hours at 10°C, 20°C and then 35°C and the metabolic response was monitored in terms of electrogenic activity (cell voltage). It was found that only the sucrose reactor was adversely affected by the low temperature operation at 10°C.

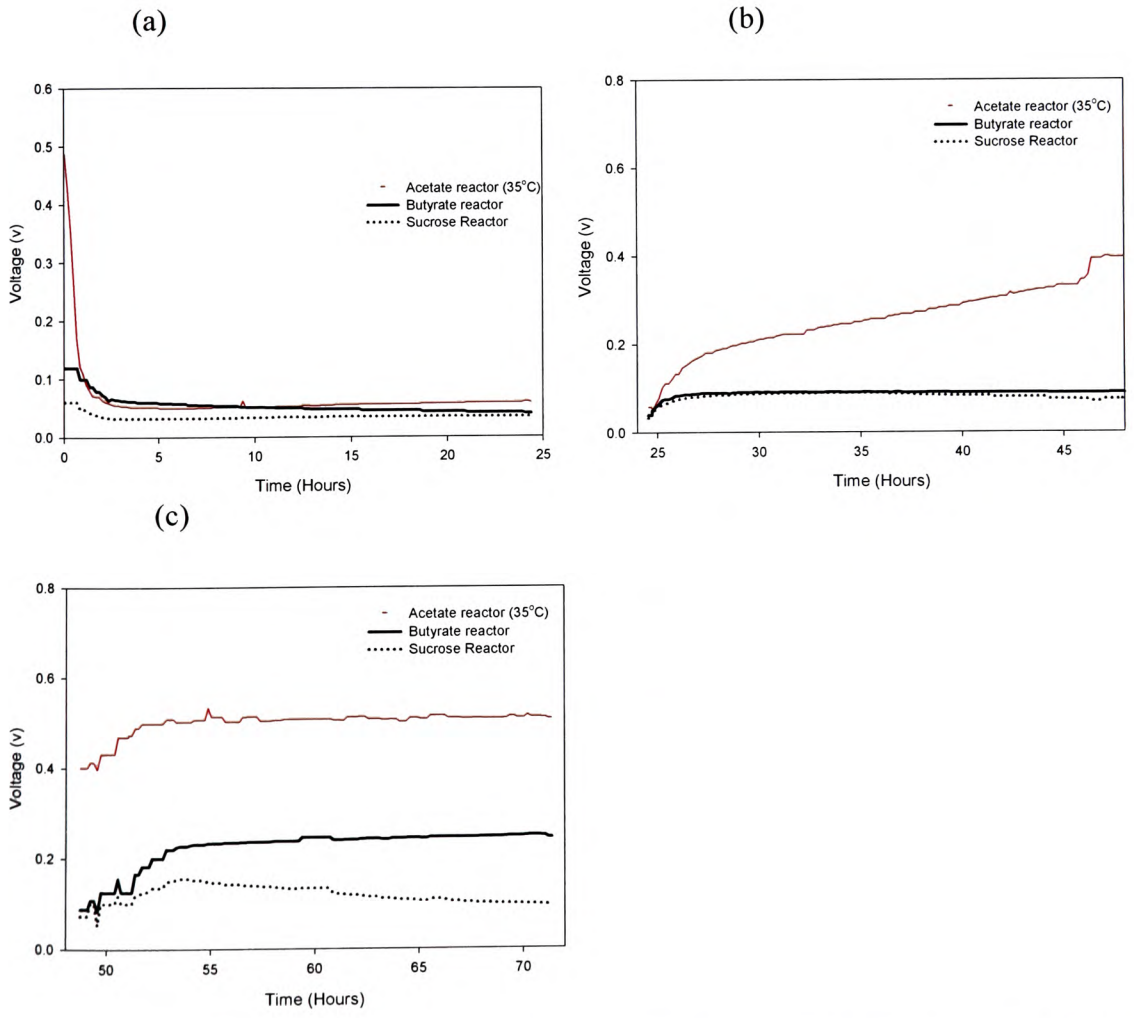

Figure 3-20. The effect of temperature perturbation on voltage development profiles of 3 differentially acclimatized MFC reactors using 3 different substrates (sucrose, butyrate and acetate). Reactors incubated at a) 10°C, b) 20°C and c) 35°C

3.2 Discussion

Acetate and butyrate are VFA substrates of particular interest as they are two of the key metabolic products of AD and dark fermentative processes, and MFCs provide an interesting opportunity for maximizing energy recovery from these systems (Guwy et al. 2011). Even though the molar Gibbs free energy of butyrate is higher than acetate (-524kJ vs -215kJ), acetate was observed to be readily metabolized by EAB whereas butyrate was metabolized at a slower rate producing lower power densities. Whilst it is accepted that acetate is readily able to stimulate a strong electrogenic response to produce carbon dioxide, electrons and protons (Bond et al. 2002), within the anodic biofilms the key question is how the butyrate is being metabolized by the EAB. This could occur either through the direct oxidation of butyrate to electrons or through the breakdown of butyrate first to hydrogen and acetate, which could then be further metabolized to electrons. Lovley et al (1993) describe how *Geobacter metallireductans* is able to completely oxidize both acetate and butyrate and it has been further demonstrated that *Geobacter sulfurreductans* is able to oxidize both acetate and hydrogen (Brown et al. 2005). However due to the metabolic pathways used in anaerobic butyrate oxidation it is likely that acetate and hydrogen are initially produced (Müller et al. 2010) as this process has a positive Gibbs free energy and the reaction can only proceed with a negative Gibbs free energy if there is an associated consumption of hydrogen (therefore maintaining low partial pressures) via a syntrophic microbial partner. This process is typically associated with methanogens but it is possible that electrogenic activity could account for the hydrogen removal; it has been reported that more free energy can be released under electron accepting conditions compared to methanogenic conditions which may explain why no methanogenesis was observed in the butyrate reactor (Jackson and McInerney 2002). The detection of acetate production and its subsequent utilization (Fig 3.11) during a butyrate fed batch cycle would suggest that the latter metabolic system was predominantly active. In a similar manner, a degree of syntrophy must exist to maximize the energetic conversion of glucose conversion of to electrical current through the removal of VFA end-products (Freguia et al. 2008).

The maximum power density results for butyrate and sucrose were low in this study relative to acetate. Using a single-chamber reactor systems Liu et al (2005) reported that acetate produced 66% more power than butyrate, a figure that far higher than the result from this study. This large differential in reported power outputs is likely to be due to the 83 week operational time period which saw an increase in acetate biofilm and decrease in butyrate biofilm over time (Fig 3.16). The low reported columbic efficiencies reflect the high levels of substrate, high electrical loading and ingress of air due to water evaporation occurring at the 35°C incubation temperature leading to electron flow away from current generation (Huang and Logan 2008; Pinto et al. 2010).

In agreement with previous studies it was found that substrate type had a profound effect on both bacterial and archaeal community profiles (Jung and Regan 2007; Chae et al. 2009). Whilst it has been previously reported that more complex fermentative substrates tend to have higher degrees of diversity (Kim et al. 2004), the high diversity scores in both sucrose and acetate fed reactors probably reflects the reactors in experiment 2 being operated for a period of over one year. However, low diversity values in the butyrate biofilm can probably be directly related to the low levels of biofilm that developed in this reactor, and that these biofilm levels also decreased over time. However it can also be observed in Figure 3.20 that both the acetate and butyrate reactors recovered activity after low temperature perturbation but the sucrose reactor did not. It has been previously reported that microbial diversity and functional redundancy can help microbial systems withstand perturbation events (Briones and Raskin 2003). Whilst acetate had a very high bacterial richness score (Table 3.1) and recovered activity quickly after the temperature was raised to 20°C (Fig 3.20 b)), sucrose also had a high richness score but lost activity at 35°C but the butyrate regained activity despite a very low bacterial diversity. This may seem anomalous but could be explained in the context of the levels of diversity that may exist in the different interacting levels of trophic groups that were key to EAB activity; measured in this case as voltage output. Whereas the acetate biofilm has high inherent diversity in the one step metabolism of acetate, the sucrose biofilm have a greater number of functional trophic steps which individually may not have a high degree of diversity (fermentation, syntrophic breakdown of different VFA products to acetate, acetate conversion to electrons); this therefore may impact on the electrogenic systems capacity to deal with the perturbation event.

3.3 Conclusion

This study demonstrates that substrate type has a dramatic effect on the microbial community dynamics, the level of biofilm development and the EAB activity. The trophic composition of the anodic biofilm was dictated by the substrate type and the capacity for microorganisms to develop syntrophic associations to degrade substrates of different complexities. The complex nature of these interactions was further demonstrated by temperature perturbation of the acclimated biofilms; this showed that despite the sucrose biofilm having a high bacterial diversity and high levels of biofilm it was also the most vulnerable to this perturbation event due to the complex syntrohpic interactions that must occur for electricity production to occur. The porous nature of the carbon veil meant that bacterial colonization could occur through the entire depth of anode but this

was focused on the layers 1 to 3. This provides the potential of an increased surface area for EAB activity but this could be limited by mass transfer characteristic associated with the biofilm.

4 *The influence of start-up temperature on microbial fuel cell reactor performance*

The effects of temperature on MFC operation have been previously reported to have a direct effect on electrochemical processes. This can be directly observed when MFC reactors are run at ambient temperatures where cell voltages have been reported to cycle up and down with the diurnal temperature fluctuations (Moon et al. 2006; Jadhav and Ghangrekar 2009; Ahn and Logan 2010; Kim et al. 2010). It is not only system constraints that will directly affect MFC operation but also how these factors influence reactor efficiency and power generation through the conversion of electrons in biomass to electricity. The percentage recovery of electrons, termed as the Coulombic Efficiency (CE), can often achieve levels of 70% or more (Kim et al. 2009) when non-fermentable substrate such as acetate is used. Low CEs reflect the activity of alternative electron sinks and non-electrogenic metabolic pathways being utilized by the anode biofilm and planktonic microbial populations. Possible sinks include the activity of methanogenic Archaea (both acetoclastic and hydrogen utilizing) in the catabolic generation of CH_4 and microbial anabolic production of biomass, of which the former has been reported to be the more significant (Lee et al. 2008) .

A number of studies have looked at low strength wastewater treatment at ambient and mesophilic temperatures (21-35°C), but since most waste treatment systems in temperate climates work and discharge effluents at temperatures much less than this (10-20°C) these processes would require a significant input of energy as heat (Lettinga et al. 2001). The capacity to run MFC reactors at temperatures of 10-20°C would substantially reduce operating costs by eliminating a substantial power input for heating. Thus, psychrophilic operation introduces the potential for MFCs to be an economically viable alternative to conventional aerobic processes in temperate sewage treatment operations. In addition to the generation of electricity these MFC systems also have the potential to produce substantially lower levels of stabilized sludge due to the activity of biofilms with a low growth yield.

The aim of this study was to examine the adaptive capability of MFC systems to operate at psychrophilic and mesophilic conditions and investigate the influence of temperature on rates of COD removal, CEs, microbial community dynamics and MFC performance. Acetate was used as a non-fermenting substrate to examine anode respiring bacteria (ARB) development within the biofilm and simulate conditions in secondary or tertiary waste streams. The development of voltage over

time and performance was investigated in relation to the development of both bacterial and archaeal communities and the feasibility of psychrophilic MFC operation.

The results in this chapter have been published (Michie et al. 2011b), see Appendix 4.

4.1 Results

4.1.1 Voltage development at different operational temperatures

The production of a stable steady-state voltage from MFCs incubated at different operating temperatures (10°C, 20°C and 35°C) took 47 weeks and stabilized at 0.49 V (± 0.02V), a figure consistent for all the reactors used in the experiment. It is expected that this is the maximum voltage at the 1000Ω resistive loading used with a tubular MFC design, this maximum figure being a factor of the internal resistances that are attributable to the individual characteristics of the anode, cathode and electrolyte. All eexperiemtnation was carried out in duplicate and the results supported previous work carried out by Kim et al (2010) which showed that comparative MFC performances can be observed in duplicate single chamber tubular systems. The acclimation time required to attain steady-state voltage varied with temperature, (at 10°C, 20°C and 35°C; 47 weeks, 41 weeks and 10 weeks respectively) (Fig 4.1), with slower ARB biofilm development at lower temperatures.

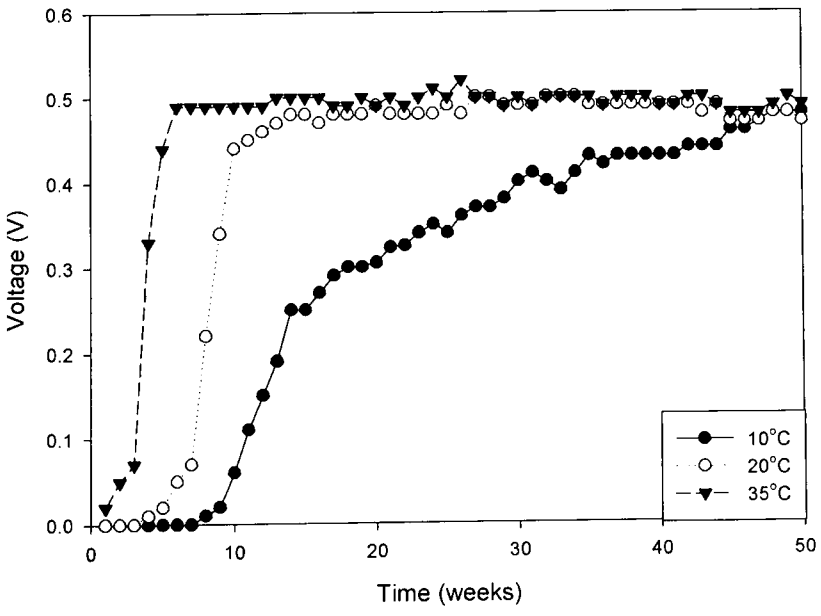

Figure 4-1. Voltage development during the enrichment of MFC reactors at 3 different temperatures (10°C, 20°C and 35°C). Reactors were batch fed on a 1 week cycle with 5000 ppm COD L^{-1} acetate. External resistance was 1000Ω.

A sequential temperature switch was used to understand the effect of the different operating temperatures on the temperature pre-acclimated biofilms (10°C, 20°C and 35°C) at 43 weeks operation, with each reactorbeing sequentially maintained at 10°C, 20°C and 35°C temperatures for 24 hours (Fig 4.2). It was observed that the voltage generation of the 35°C pre-acclimated reactor decreased significantly at 10°C (0.48 to 0.05V within 2.5hrs) with the voltage not recovering over 24 hrs whrn the reactors were held at this temperature. However, in contrast, it was also observed that incubation of the 10°C and 20°C pre-acclimatized reactors at 10°C only produced a small decrease in voltage (0.005V). A voltage differential of 0.02V was consistently observed between the 10°C and 20°C reactors and it is thought that this represented the difference between the maximum voltages achieved after 43 weeks of operation, and therefore reflected the fact that the 10°C reactor had not yet reached its maximum steady-state voltage: as per Fig 4.1, a voltage of 0.49 V (± 0.02V) was reached by the 10°C reactor only after 47 weeks of operation. An increase in the operating temperature to 20°C resulted in the 35°C pre-acclimated reactor biofilm producing a gradual increase in voltage to 0.4V over a period of 20hrs, in contrast both the 10°C and 20°C pre-acclimated reactors only increased by 0.02V whilst maintaining the 0.02V voltage differencepreviously observed at the 10°C test temperature. When the temperature was additionally raised to 35°C the 35°C pre-acclimated reactor rapidly attained a steady state voltage of 0.51V, a voltage similar to that produced by the 20°C reactor. However it was then observed that the 10°C acclimated reactor was adversely affected by the 35°C operating temperature as the voltage decreased from 0.48V to 0.45V. The 10°C reactor was held at 35°C and this resulted in the voltage further decreasing to 0.24V over the following week (data not shown). This reflects that the high (35°C) temperature shock had an adverse effect on the psychrophilically adapted ARB community.

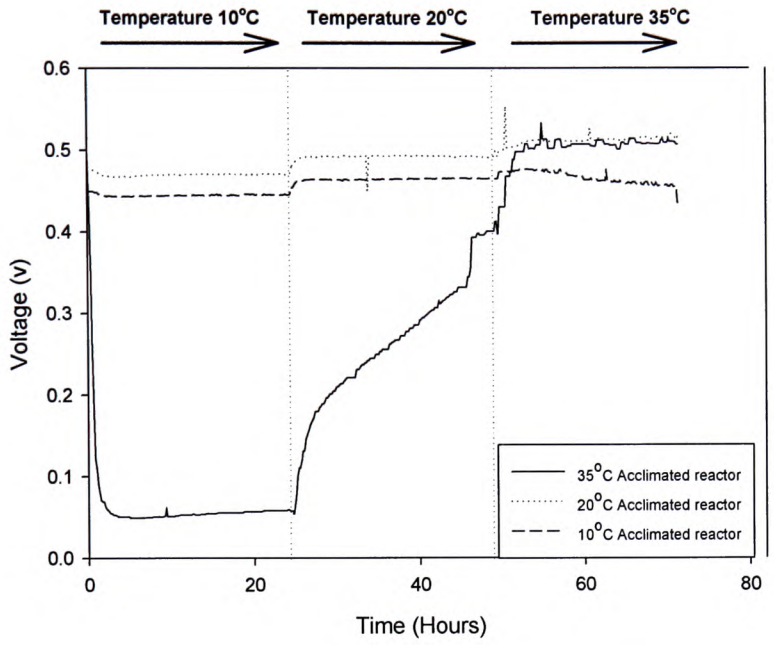

Figure 4-2. Voltage development profiles of 3 differentially acclimatized MFC reactors at 3 different temperatures (10°C, 20°C and 35°C). Reactors were fed with 5000 ppm COD L^{-1} acetate and incubated for 24 hours at each temperature. External resistance was 1000Ω.

The influence on voltage production by further lowering the temperature to 8°C was then investigated by incubating the reactors over time until substrate depletion occurred (Fig 4.3).

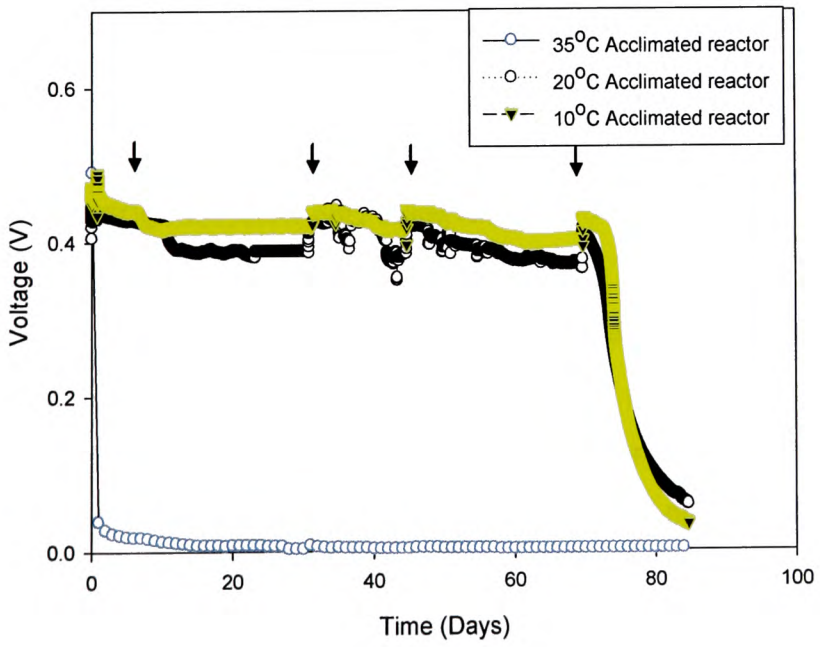

Figure 4-3. Batch cycle voltage generation (5000 ppm COD L^{-1} acetate) with 10°C, 20°C and 35°C pre-acclimated reactors at 8°C. Arrows indicate peaks observed in the 10°C and 20°C voltage profiles at 33, 46 and 77 days when the reactors were filled up with deionised water to compensate for water loss through the cathode.

The operation of the MFC reactors at 8°C had no significant effect on the performance of the 10°C and 20°C acclimatized anodic biofilms, with the former showing a small voltage decrease to 0.44V. However it was observed that the voltage in the 35°C reactor rapidly declined to 0.03V and did not recover. It was further observed that 10°C and 20°C acclimatized reactors could be operated at 4°C with no effect on the voltage output.

Table 4-1. Coulombic efficiency (%) and COD decrease (%) over 84 days at 8°C with differentially temperature acclimatized MFC reactors. MFC reactors were run in batch mode with a fixed load resistance of 1000Ω using an initial loading of 5000 ppm COD L^{-1} acetate. COD removal rates were used to calculate the actual CEs (%)

Acclimatisation Temperature	No. Coulombs	COD removal (%)	Coulombic Efficiency (%)
35°C	25.1	87	0.2
20°C	1756.3	94	15.7
10°C	2787.6	94	24.9

4.1.2 COD removal and microbial diversity at different temperatures

To ensure a the reactor systems were not substrate limited a high initial substrate loading of 5000ppm COD L^{-1} acetate was used in all the reactors. A pre-enrichment period of 10 weeks was used, with sCOD measurements being monitored over the course of the experiment for each 1 week batch cycle at the 3 test temperatures (Fig 4. 4). The percentage COD removal in the 35°C reactor after 10 weeks were at levels above 90% and after week 36 consistently increased to 98%. In the 20°C reactor there was a noticeable trend toward a higher % COD removal over time, moving from 14.3% (week 10) to 22.2% (week 55). The % COD removal of the 10°C acclimated reactors ranged from 5-15% but after 1 years operation this rate had not noticeably increased. A paired t-test (two-sided) was used to test whether the % COD removal in the 10°C and 20°C acclimated MFCs were statistically different, this gave a significant p value of 0.000138. The % COD removals at 56 weeks were 0.27, 0.67 and 2.98g COD $L^{-1}d^{-1}$ for the 10°C, 20°C and 35°C acclimated reactors respectively.

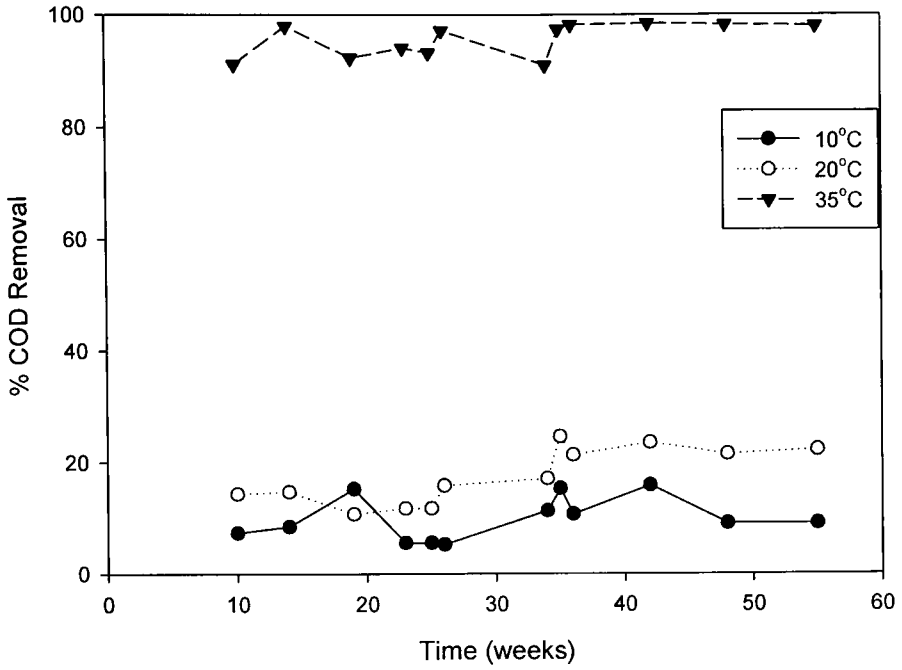

Figure 4-4. sCOD removal efficiency (%) at different reactor temperatures over time. Batch reactors were fed 5000 ppm COD L^{-1} acetate and COD measurements were taken at the end of each 1 week batch cycle.

The effect of prolonged low temperature operation on reactor performance was investigated and levels of COD removal and CEs were compared (Table 4.2). As high levels of substrate (COD) were fed to the reactors this resulted in the MFCs taking 84 days for the substrate to be fully consumed, at this point the voltage then dropped from a level of 0.42V in the 10°C reactor and 0.4V in the 20°C reactor. The 10°C acclimated reactor had the highest CE reflecting a more efficient electron recovery at low temperatures and lower activity levels of alternative electron sinks such as methanogenesis and the production of biomass. Rates of methanogenesis in the 35°C reactor were first measured at 17 weeks operation when the system produced 0.006 mmol d^{-1} methane (over a 1 week batch cycle), however by week 37 this rate had increased to 1.03 mmol d^{-1}. A low methogenic rate of 0.006 mmol d^{-1} (recorded over a 2 week batch cycle) after 30 weeks was detected in the 20°C reactor, however no methane production was detected in the 10°C reactor. These results are in general agreement with results obtained from AD systems which also indicate that methanogenesis will preferentially occur at mesophilic temperatures and is generally less active at sub- mesophilic temperatures. Within the MFC reactors lower rates of methanogenesis at lower temperatures will directly lead to higher rates of electron recovery via the electrode as the electrons are not being lost via the production of methane. It is interesting to note that in contrast to AD technology MFCs may be particularly applicable to domestic wastewater treatment. This is because these particular waste

streams typically include low COD wastewaters and also environments where low and variable temperatures (10-20°C) may exist (Pham et al. 2006).

A cluster analysis was carried on the PCR-DGGE microbial community profiles acclimated at the three different operating temperatures, using Dice similarity matrices to analyze and track changes over time (T1, T2 and T3). The bacterial population clustering (Fig 4.5) shows that a convergence of banding profiles occurred after 12 months (T3) at all three acclimatisation temperatures. The highest similarity of 84.6% was between the T3 10°C and T3 20°C reactors, with the T3 35°C reactor having the next closest similarity of 81.8%. The T1 and T2 35°C reactors formed the next cluster with similarities of 77.1% and 73.5% indicating that these reactors had developed an electrogenically active biofilm before the T2 10°C and T2 20°C reactors which had similarity values of 69.9% and 65.9%.

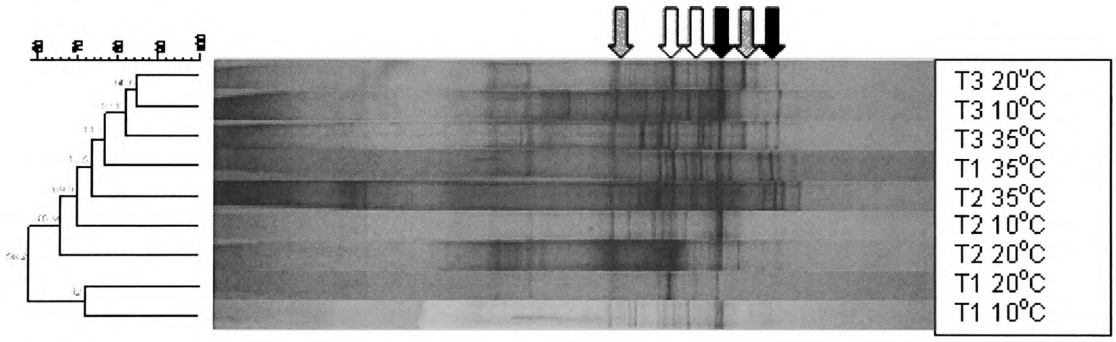

Figure 4-5. Cluster analyses of bacteria DGGE profiles at 3 different temperatures and 3 time points. The trees were generated using Dice similarity coefficient and UPGMA clustering algorithms. At T3 bands common to the temperature acclimatized reactors were identified: solid black arrows between the 10°C, 20°C and 35°C reactors (T3 10°C, 20°C and 35°C), solid grey arrows between the 20°C and 35°C reactors (T3 20°C and T3 35°C) and solid white arrows between the 20°C and 10°C reactors (T3 20°C and T3 10°C).

It is thought that the T1 10°C and 20°C reactors then formed another cluster reflecting an early stage of anode biofilm development. MFCs have been previously shown to actively select for ARB communities over time (Rabaey et al. 2004), the community profile development at the different acclimation temperatures therefore reflects the growth of electrogenically selective anode biofilms.

Analysis of the archaeal cluster profiles (Fig 4.6) show that three distinct groups were formed. Group 1 - T2 20°C, T3 10°C and T2 10°C reactors, Group 2 - 35°C reactors and T3 20°C, and Group 3 - T1 10°C and T1 20°C reactors. The profiles suggest that over time there was a differential development of biofilm Archaeal methanogenic communities.

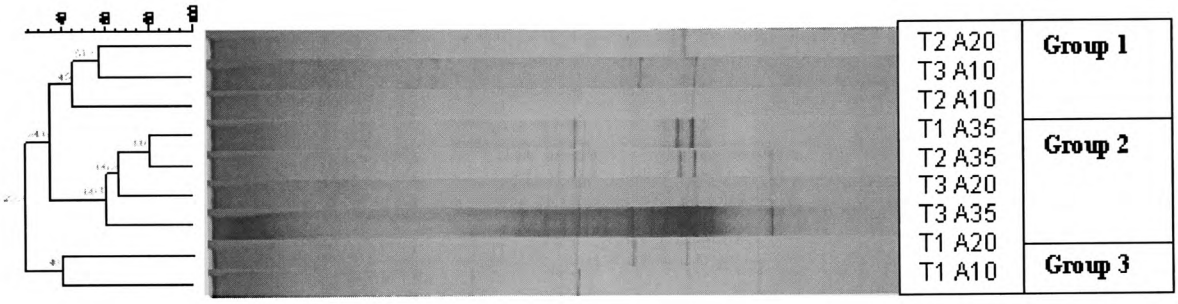

Figure 4-6. Cluster analyses of archaeal DGGE profiles at 3 different temperatures and 3 time points. The trees were generated using Dice similarity coefficient and UPGMA clustering algorithm. 3 cluster groups were identified from the profiles: Group 1 – T2 10°C and T3 10°C and 20°C, Group 2 T1, T2, T3 at 35°C and T3 at 20°C, Group 3 - T1 10°C and 20°C.

It is thought that the slow microbial colonization of the anode occurring at lower operating temperatures might reflect the slow initial attachment and low growth rates of methanogenic Archaea at 10°C and 20°C (as indicated by the T1 10°C and T1 20°C reactors in group 1, forming a cluster). However, the development of more complex Archaeal communities in Group 2 might be associated with a higher reactor temperature and longer incubation times i.e. T1, T2, T3 at 35°C and T3 at 20°C (56 weeks incubation). Thus it is thought that the Group 1 cluster reflects an interim stage between the Groups 2 and 3 described above.

To graphically represent the dynamic adaptation of the microbial communities at each temperature over time, an averaged weekly moving image analysis (Fig 4.7) method was applied. This method calculated changes occurring in the microbial community profiles over time, with the results being normalized to give a percentage change per week. The initial dynamics at 8 weeks (T1) were measured relative to the initial AD sludge inoculum profile. The data represented in Fig 4.7 show that a low-to-medium degree of change (6-10% population change) occurred in all the reactors at 8 weeks (T1) but by 33 weeks (T2) the 10°C reactor showed a 3% level of dynamic change compared to 0.35-0.9% for 20°C and 35°C reactors. However, by week 56 (T3) all the reactors

exhibited a very low level of population change (all less than 1% change per week). This suggests that as each of the bacterial communities reached a stable and consistant electrogenic operation the microbial communities were also stable and thus resistive to the emergence and establishment of newly emergent species. Lower bacterial growth rates in the psychrophilic 10°C reactor imply that the adaptation period required as part of the establishment of a stable electrogenic biofilm was also extended, this would seem to support the voltage development profiles (Fig 4.1) which showed longer lag times for the 10°C reactors and also reflected a relatively higher population dynamic value of 9.2 which was maintained until week 33. When this technique of analyzing the percentage rate of change has been applied to other microbial systems using DGGE profiles it has been suggested that a value of 12.6 ± 5.2 % represents a medium level of dynamic change where new microbial species may be able multiply within a community but will not necessarily interfere with system functionality (Wittebolle et al. 2008). It can be observed that all the reactors at T3 have low rates of dynamic change and steady-state voltage production. This is consistent with previous work which established a relationship between stabilized bacterial populations (3% dynamic change) and stable wastewater treatment plant operation (Wittebolle et al. 2005). The low rates of population change obtained here relative to the latter study may reflect in part lower microbial growth rates at sub-mesophilic temperatures found in some of the reactors and also longer experimental time frames which would have resulted in the accumulation of biofilm/biomass over time.

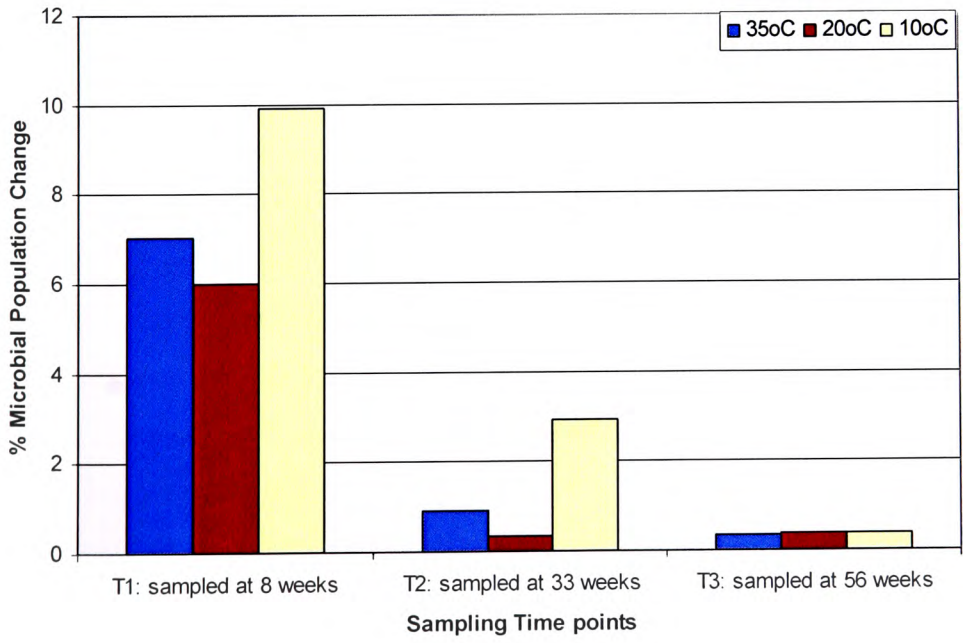

Figure 4-7. Moving image analysis. Microbial dynamics at each reactor temperatures were analysed over time using moving window analysis plots based on a Pearson based correlation.

Range-weighted Bacterial richness scores were calculated from the DGGE profiles (Table 4.2). It was found that the score in the 35°C reactor increased rapidly to 31.6 at 8 weeks (T1), peaked at 80 at week 33 (T2) and then fell back to 45 at 56 weeks (T3). In contrast the richness measures in both the 10°C and 20°C reactors increased more slowly with time, resulting in scores of 35 and 37.5 respectively at 56 weeks (T3). Wittebolle suggested that a richness of greater than 30 is indicative of a diverse community exisitng in a habitable environment, these scores therefore indicate the development of stable ARB biofilms which have a capacity to resist environmental change (2008). It can also be observed that range-weighted richness development of Archaea (Table 4.2) shows a diverse population of methanogens developed in the 35°C reactor after 56 weeks. The population diversity in the 10°C reactor did not increase over the course of the experiment, having a score of only 0.8 at 56 weeks; he richness in the 20°C reactor only increased to 3.1 over the same time period. These results support the suggestion that low temperature operation may adversely affect the ability of the methanogens to establish a stable biofilm population over time.

Table 4-2. Microbial community richness development with time. Bacterial and Archaeal community profiles were studied by DGGE analysis of PCR amplified partial fragments of the 16s rDNA gene, richness measurements were scored using Dice's index of similarity

Bacterial community			
Temperature	T1	T2	T3
10°C	3.5	17.2	35
20°C	8	31	37.8
35°C	31.6	80	45

Archaeal community			
Temperature	T1	T2	T3
10°C	0.7	0.04	0.8
20°C	1.6	0.4	3.1
35°C	2.7	7.4	19.7

T1: sampled at 8 weeks

T2: sampled at 33 weeks

T3: sampled at 56 weeks

However it was observed that growth at mesophillic temperatures allowed a diverse methanogenic population to establish on the anode. Pareto-Lorenz evenness data (Fig 4.8) was investigated for the 10°C, 20°C and 35°C reactors after 56 weeks (T3). From the Pareto-Lorenz plot it can be observed that the 20°C reactor has the highest degree of evenness, with a plot close to Y=X perfect evenness. The 0.2 intercept value on the X-axis of Pareto-Lorenz plots have previously been used as a comparative measure of evenness (Verstraete et al. 2007); from Fig 4.8 these were 29.9, 24.1 and 41.5 for the 10°C, 20°C and 35°C reactors respectively. The use of sequential temperature shock parameters with the 10°C, 20°C and 35°C acclimatized reactors (Fig 4.4) resulted in the 20°C reactor having the highest evenness and the 35°C reactor the lowest evenness. An evenness value of 41.5 in the 35°C reactor can be thought of as being in the 'medium' range and suggests that a functional organization exists that is dominated by bacterial species adapted to those environmental conditions but with a degree functional capacity available which then could help the bacterial

communities present to be resistsant to any given environmental change (Marzorati et al. 2008). It is also possible that the high evenness score of 24.9 in the 20°C reactor could suggest a sub-optimal functionality, but this was not observed in this study, and could also mean a high degree of functional capacity. It should be recognized that as this data was based on semi-quantitative DGGE band intensities these results should be viewed as being indicative of functional status of the community profiles.

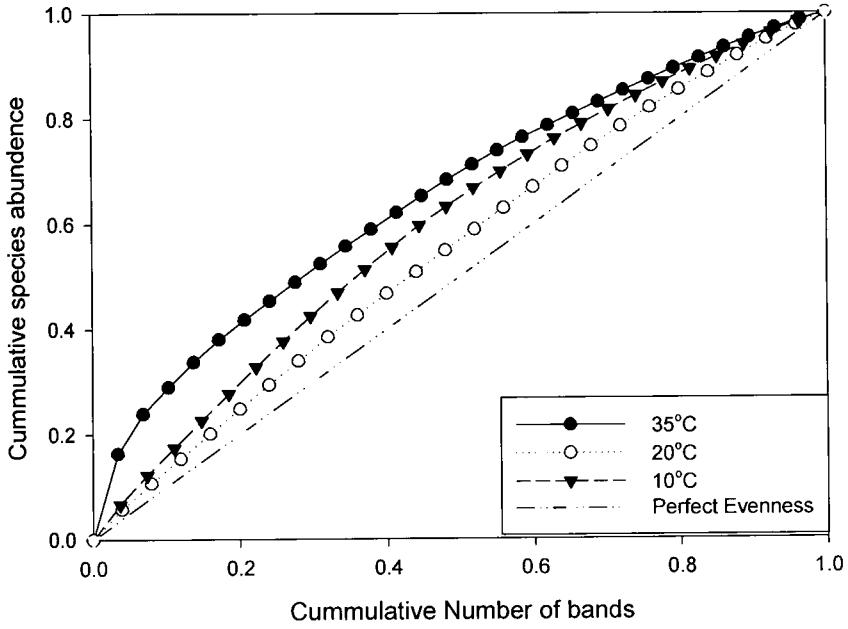

Figure 4-8. Lorenz evenness graph at 56 weeks operation (T3) at 3 different temperatures - 10°C, 20°C and 35°C. 16s DGGE bands profiles were ranked from high to low according to their cumulative intensities and cumulative number the of band results (scored using Dice's index of similarity).

4.2 Discussion

4.2.1 The influence of acclimation temperature on MFC performance

The effect of temperature on MFCs and their ability to metabolize substrate and produce electricity at low and ambient temperatures has been previously reported (Moon et al. 2006; Jadhav and Ghangrekar 2009; Ahn and Logan 2010). In contrast to these studies this work demonstrated that over time 10°C, 20°C and 35°C acclimated reactors all reached comparable steady-state power values of 1.2 Wm^{-3} (± 0.02 Wm^{-3}), the respective internal resistances of these MFCs were 112Ω, 115Ω and 151Ω. CEs measured in the 10°C, 20°C and 35°C reactors after 47 weeks operation were 25.9%, 11.1% and 2.2% respectively. A consistency in the CE measurements at low temperatures was demonstrated by the 10°C reactor having a CE of 25.9% at 10°C as compared to a 24.9% CE produced during MFC operation at 8°C (Fig 4.3), with the 20°C reactor at 20°C recording a 4.8% decrease relative to the CE at 20°C. Bacteria present in the electrogenic biofilms were shown to be able to adapt to respiratory metabolism at low temperatures as well as those bacteria that were operated under mesophilic conditions. Previous MFC studies using reactors that haven ot been temperature acclimated have shown that lower reactor temperatures will decrease the power output in MFCs (Moon et al. 2006). In batch mode it was shown that a temperature change from 30°C to 23°C was reported to cause a 12% decrease in power (Ahn and Logan 2010) and Liu et al (2005) also reported a 10% decrease in power when the operational temperature in a single-chamber MFC reactor was changed from 30°C to 20°C. However the influence of the microbial biocatalyst may also be important as a decrease in temperature was also shown to produce an increase in voltage (Jadhav and Ghangrekar 2009).

A measurement of voltage can be viewed as an indicator of the total electrochemical respiratory processes and thus total electrogenic metabolism. ARB may either respire directly to the anode to generate energy or simply use the anode as an electron sink to remove intracellular reducing equivalents formed during anaerobic substrate oxidation. Hence the level of electrogenic activity will depend on both the microbial groups present and the biochemical strategies utilized during metabolism. However, this measurement of electrogenic activity will not include metabolic activity associated with the ingress of oxygen, the use of other alternative electron acceptors or methanogenic activity.

The production of a stable voltage at 10°C and 20°C with the 10°C and 20°C acclimated reactors shows that these anode biofilms contain low temperature adapted psychrophilic and psychrotolerant ARB, and that these microorganisms have the necessary enzymes, cell walls and

membrane structures to allow growth and anaerobic respiratory metabolism at low temperatures. At 10°C, the 35°C acclimated reactor produced a rapid voltage drop due to inhibition of microbial metabolism indicating that this biofilm only contained active mesophilic microorganisms which had no capacity for respiration at the lower temperature (10°C). When the temperature increased to 20°C both the 10°C and 20°C acclimated reactors resulted in a slight voltage increase due to thermodynamic properties inherent in the system, this could be accounted for by the Arhennius and Nernst equations (Bard and Faulkner 2001). However with a rise in temperature to 35°C this voltage increase was augmented in the 20°C adapted reactor but had an adverse effect on voltage in the 10°C acclimated reactor. It is thought that psychrophilic bacteria were predominantly present within the 10°C adapted anode biofilm. Hence, the small increase in voltage at 20°C was due to these psychrophiles having an optimal metabolic rate at a temperature above their optimal growth rates. Obligate psychrophiles can be defined as having maximum growth rates at temperature of less than 15°C (Morita 1975); but it is known that these bacteria will often have maximum metabolic rates of 6-10°C above their optimal growth rates (Knoblauch et al. 1999) which would support the finding of increased respiratory activity at 20°C but not at 35°C reported here. The likely presence of both psychrophilic and psychrotrophic bacterial communities in the 20°C reactor meant this anode biofilm was well adapted to microbial activity over the full 10-35°C temperature range, consequently the diverse bacterial population could effectively metabolize and adapt to the changing environmental conditions. The 35°C adapted reactor only recovered full metabolic activity when it was restored to mesophilic 35°C operation. Where MFCs have been operated under thermophilic conditions (55°C) analysis of community profiles have shown that bacteria will also adapt to high temperature environments. In these situations the adaptation process will cause a decrease in diversity compared to the initial inoculum, indicating that the temperature selective nature of this environment will support fewer species but those present are capable of thermophilic electrochemical activity (Jong et al. 2006). This suggests that MFCs might well be capable of operation over an even wider range of temperatures and that some mesophilically adapted communities could feasibly be able to function at both psychrophilic and thermophilic conditions, thus providing the potential for even greater operational flexibility. It is known that some *Bacillus* species found in the heat treated milk products can survive and grow over temperature ranges of 10-20 °C to 55-60°C i.e. *Bacillus coagulans*.

4.2.2 MFC coulombic efficiency and COD removal at different temperatures

It was found that methane production was a significant electron sink in the 35°C reactor and this led to high rates of COD removal. When the MFC reactor temperature was decreased the COD

removal rates also decreased due to lower rates of methanogenesis, however other factors such as biomass production may also be affected by operational temperature. The 35°C acclimated reactor reomoved the COD at a rate of 2.98 kg $m^{-3}d^{-1}$ which is comparable to removal rates found in Anaerobic Digesters (AD) (Connaughton et al. 2006). It is interesting to note that in common with AD systems, rates of COD removal in MFCs also decreased with decreasing temperatures (Elmitwalli et al. 2002). MFC COD removal rates at 10°C were 0.27 kg $m^{-3}d^{-1}$ representing 9.1% activity compared to removal rates at 35°C, removal rates at 20°C were 0.67 kg $m^{-3}d^{-1}$ representing a 59.7% higher activity than the 10°C operation, these values are comparable to COD removal rates previously reported by Larrosa-Guerrero et al (2010). In typical black domestic wastewaters containing sewage, treatment reactors which have not been acclimated were studied by Zeeman and Lettinga (1999) and it was reported that lower total COD removal efficiencies (52-54%) occurred at temperatures of less than 20°C compared with 90-93% removal rates at temperatures greater than 20°C. However long-term psychrophilic acclimation has been investigated in anaerobic hybrid reactors operating over a temperature range of 12°C to 20°C, this demonstrated that rates of COD removal can be maintained at psychrophilic temperatures: a drop of temperature from 20°C to 12°C was shown to result in a subsequent 30% decrease in COD removal (McHugh et al. 2006), however this decrease is less than but comparable with the 59.7% drop observed in the MFC reactors in this study when the operating temperature was similarly decreased from 20°C to 10°C.

At an operational temperature of 8°C a CE of 24.9% was prodcued in the 10°C acclimated reactor as compared to a 15.7% CE in the 20°C acclimated reactor even though COD removal rates were both recorded as being 94% (Table 4.2). This indicates that the recovery of electrons at lower temperatures is a more efficient, and suggests that low temperatures act to affect on the net overall metabolic activity of the ARB at higher temperatures due increased activity of other potential electron sinks i.e. methanogenesis or the production of biofilm biomass. The detection of significant levels of methane being prodcued in the 20°C and 35°C reactors is also supported by the development of enriched archaeal DGGE profiles that showed richness levels increased over time (Table 4.1). The association of low operational temperatures applied to MFC anodic biofilms with low rates of COD removal and high CEs further supports results produced by Ahn and Logan which have were carried out at combined ambient and mesophilic temperatures (2010). The CEs' observed in this study were relatively low and this probably reflects the operation condition used as part of the experimental set-up i.e. long term batch operation and high COD loading rates used in the single chamber reactor. It is also thought that further coulombic losses were likely caused by oxygen ingress, however other similar tubular single chamber reactors have been shown to produce CEs of 70% when operated with with lower substrate conditions and continuous flow operations (Kim et al.

2009). The use high substrate loading rates in the MFC reactors was designed to mitigate against the potential effects of COD depletion in the anode chamber and create batch substrate conditions that were as uniform as possible over the complete batch cycle. However it is also likely that these high substrate levels also favoured methanogenic activity and high levels of biofilm formation.

MFCs have recently been viewed as a technology that may be able to provide a polishing step for the treatment of AD effluents; this could be used as an alternative method to energy intensive aerated activated sludge processes and could integrated as a post AD treatment (Kim et al. 2010),. The effluent from AD systems will contain VFAs due to acidogenic metabolism that have not been utilized by the methanogenic archaea but the actual composition and concentration of VFAs produced will be dependent on operating conditions such as temperature and OLRs (Grady et al. 1999). It may be possible that AD systems that are operated at sub-mesophilic temperatures or are subject to temperature operational shocks could utilize MFCs as a second stage operation to both recover additional energy and treat AD effluents.

4.2.3 Microbial community dynamics and diversity at different temperatures

PCR-DGGE analytical techniques were used to assess the dynamic development of bacterial and archaeal biofilm community profiles over time. The development of these microbial community profiles were then related to the performance of the reactors and the development of anodic biofilm communities at different operational temperatures. The Bacterial DGGE profiles (Fig 4.5) show how potential electrogenic bacterial populations developed over time at the different operational temperatures, this was demonstrated by the clustering of the 3 reactors acclimatized at the 10°C, 20°C and 35°C temperatures after 56 weeks (T3). The profile at T3 shows that several bands are common at each temperature (solid black arrows Fig 4.6), but some bands are also common between the 20°C and 35°C reactors (T3 20°C and T3 35°C solid grey arrows Fig 4.6) and also between the 20°C and 10°C reactors (T3 20°C and T3 10°C solid white arrows Fig 4.6). It is possible that the development of these banding profiles reflect the growth of electrogenic psychrophilic and psychrotolerant bacteria at 10°C and 20°C, and that these bacteria were absent from 35°C anodic biofilm as specific mesophilic species were only able to grow at temperatures 20°C-35°C. However it can also be observed that a number of common bands exist between all the reactors and this shows that a number of psychrotolerant electrogenic bacterial species must be able to grow and respire over the 10-35°C temperature range used in the study. The bacterial profiles suggest that more distinct and separate bands developed at temperature extremes of 10°C and 35°C when compared

to the 20°C reactor profile and it can be observed that at 56 weeks (T3) there was only one major DGGE band/bacterial specie that was exclusively present in the 10°C and 35°C reactors and also found in the 20°C reactor. Identification of the species prevalent at the different temperatures was not carried out in this study but further work may provide useful insights into the types of bacteria involved in low temperature MFC operation. It should be recognized that using DGGE to monitor ecological developments in the anodic biofilm will mean that these results are subject to limitations inherent in the PCR-DGGE methodology (as discussed in Section 1.2.2.5).

As the number of species (species richness) and degrees of evenness (relative abundance of the species) can be viewed as a function of the biodiversity of the anodic biofilm system, these parameters will then have a direct influence how an ecosystem functions. Hence it is thought that increasing biodiversity in engineered systems may provide more robust systems (Bell et al. 2005) that are more resistant to environmental change, suggesting that those anodic biofilms with a higher functional diversity may also be more robust to perturbation events. This also means that the development of stable electrogenic biofilms might also be observed in terms of microbial community dynamics in each reactor over time, with the development of low rates of population change relating to stable voltage output and reactor performance. A diverse ecological community can be seen as supporting the robustness of the system and promoting flexibility of MFC applications in different operating conditions. The main advantages of the MFC process over conventional bioenergy recovery systems (e.g. AD and dark fermentation) will likely be the wide operational temperature range, capacity to process high and low COD loading rates and stability of performance using a fixed biofilm. This then may provide a degree of flexibility when these systems are potentially applied to wastewater treatment systems and are required to cope with a range of potential perturbations that could affect the electrogenic performance.

4.3 Conclusions

Using biofilms acclimated at 3 different temperatures (10°C, 20°C and 35°C) it was shown that temperature has a significant effect of on MFC system performance. It was found that MFCs that were operated at psychrophilic and mesophilic temperatures (8°C-35°C) each produced similar maximum steady-state voltages of 0.49 V ± 0.02V and a steady-state power output of 1.2 Wm^{-3} (± 0.002 Wm^{-3}). However the acclimation time/lag time required to attain steady-state voltage varied with temperature and only finally occurred after an operational period of 47 weeks: at 10°C, 20°C and 35°C the lag times were 47 weeks, 41 weeks and 10 weeks respectively. It was observed that the

highest COD removal rates of 2.98g COD $L^{-1}d^{-1}$ were produced in the 35°C reactor but higher coulombic efficiencies (CE) were significantly higher at 10°C operational temperatures, with CEs of 24.9% and a COD removal rate of 0.27g COD $L^{-1}d^{-1}$. Temperature response studies demonstrated that high temperature operation of psychrophilic MFC reactors and low temperature operation of mesophilic acclimated MFC reactors both adversely affected MFC performance. Only the 20°C acclimated reactor was capable of optimal steady-state voltage operation (0.49 V ± 0.02V) over a 10-35°C temperature range, COD removal rates at this temperature were 0.67g COD $L^{-1}d^{-1}$, 59.7% higher than 10°C operation. In this study Denaturing Gradient Gel Electrophoresis (DGGE) profiles and dynamic analysis were used to demonstrate the differential development over time of archaeal and bacterial ARB communities at psychrophilic and mesophilic temperatures.

5 Anodic biofilm development and biocatalytic performance using MFC reactors operated at different temperatures

Chapter 3 showed that different levels of biofilm were produced by different substrate types but this did not seem to have a large influence on overall the MFC performance from each reactor. Therefore, this study looked to compare anode biofilms grown at 10°C, 20°C and 35°C, using acetate as the sole substrate, in order to investigate the operational effects on power generation, biomass development and biofilm activity. The impact of batch and continuous MFC operation on biofilm formation and electrogenic activity were also investigated.

The results in this chapter have been published (Michie et al. 2011a), see Appendix 4.

5.1 Calculation of anodic biofilm specific growth rate measurements

It is possible to calculate the rate of bacterial growth that occurs in the anode biofilm and this can be described as being based on the increase in the biofilm biomass which occurs over time. The following equation (12) was used to describe the accumulation of biofilm biomass in MFC batch reactors where the net increase in biofilm is modeled by the specific growth rate (μ), the cellular viability ratio (γ) and biofilm growth and losses due to biofilm detachment: x is the cell number and x_{bio} and x_{det} are the bacterial concentrations present in the biofilm and those detaching from the biofilm to the planktonic phase respectively and x_{attach} is the attachment of micro-organisms from the planktonic phase,:-

$$\frac{dx}{dt} = \mu x_{bio} + x_{attach} - x_{\det}$$

Equation 12

Cell attachment as a process was not considered to be significant as measurements were taken after an enrichment period of 8 weeks (using an initial 10% AD sludge loading that was subsequently diluted out over a period of 3 weeks), with the planktonic having been replaced every 7 days with fresh medium. At this point it was assumed that the rate of attachment was occurring at a steady rate. Marstorp and Witter (1999) used the concentration of extracted dsDNA as a direct indicator of biomass when investigating growth of microorganisms in soils. A similar approach was used to

determine biomass growth in anodic biofilms, for the purposes of this investigation dsDNA concentrations were measured and then converted into VSS (mg/l). This calculation process was described in section 2.10.1. the DNA VSS calculation was based on a conversion factor (VSS (mg/l) = 257.2 x DNA concentration (mg/l) + 250.4) which has been reported to provide a better correlation in active biological reactors (Kim et al. 2008a).

The total biofilm biomass after attachment and detachment losses were considered together as an overall specific growth rates , this meant that the rate of biomass accumulation could then be more simply understood as the net bacterial growth rate (μ_{net}) and total biofilm ($x_{VSS,total}$) to give equation 13:-

$$\frac{dx}{dt} = \mu_{net} x_{VSS,total}$$

Equation 13

Integration of equation 13 was then used to determine the net growth of bacteria in the system, where $x_{VSS,0}$ and $x_{VSS,t}$ are the total biomass measurements $x_{VSS,,total}$ at time (t) t = 0 and t = t_1.

$$\mu_{net} = \frac{1}{t} \ln\left(\frac{x_{VSS,total,t_1}}{x_{VSS,total,0}} \right)$$

Equation 14

It had been previously reported by Stenstrom et al (1998) that exponential increases in biomass that was present in a biofilm could be represented by not only exponentially growing microorganisms but also any non-growing microorganisms present. It was thought by Stenstrom et al that these microorganisms may also respire at a high rates and this response was indeed described in soil samples whenthey were fed with easily degradable substrates such as glucose. Hence, a constant term that represents non-growing but actively respiring microorganisms, the EPS biomass (K), could be combned with the exponential growth term ($x = x_{,0}\, e^{\mu net t}$) representing the growing microorganisms by using equation 13: it was assumed that the rate of inert biomass accumulation was maintained at a constant rate. In order to estimate the levels of electrochemically inert or potentially electrogenically inhibitory biomass development at different operational temperatures it was further assumed that an increase in the level of extractable dsDNA during exponential growth was proportional to $x_{VSS,}$ and this was then employed to determine the K_{VSS}, $x_{0,VSS}$

and μ_{net} terms (Marstorp and Witter 1999). These values were calculated using SigmaPlot 10.0 regression analysis (Systat Software, Inc) according to equation (15).

$$x_{VSS} = K_{VSS} + x_{oVSS} e^{\mu_{net} t}$$

Equation 15

5.2 Results

5.2.1 The development of anodic biofilmsat different temperatures

The development of MFC anode current densities over time at 3 operational temperatures (35°C, 20°C and 10°C) is shown in figure 5.1.

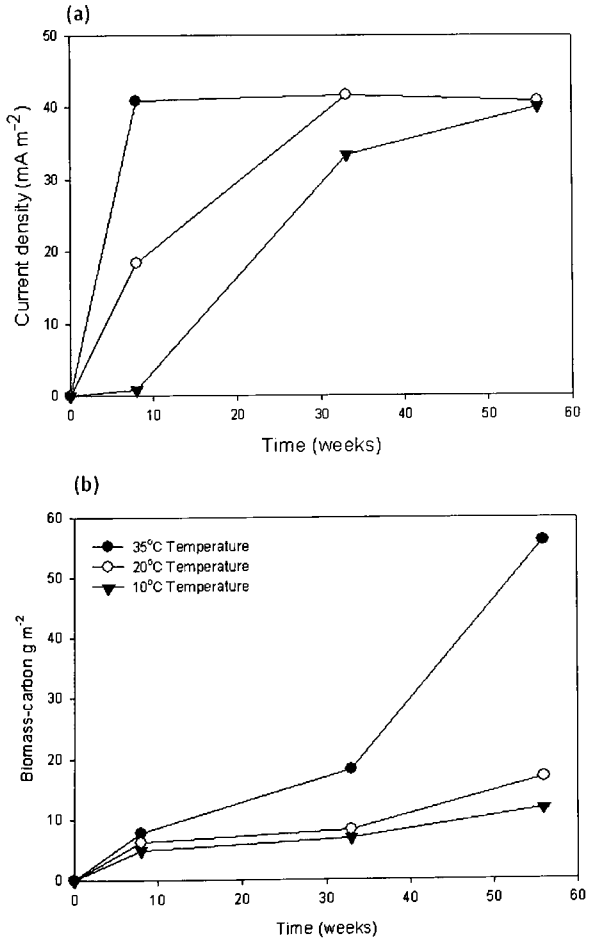

Figure 5-1. Effect of temperature on current density (mA m^{-2}) (a) and biomass Carbon (g m^{-2}) development (b) over a test period of 56 weeks at 3 different temperatures (35°C, 20°C and 10°C). A fixed load resistance of 1000Ω was maintained in all reactors.

All the reactors were run in batch mode using an initial acetate substrate loading of COD 5000 mg $L^{-1}$with a fixed load resistance of 1000Ω. The recorded power density measurements represented the maximum steady-state voltage value achieved in each batch cycle and represented the maximum achieved before any substrate depletion effects, using the COD removal profile which had been determined in Section 3.1.2. Maximum power development in the 35°C reactor anode biofilm occurred at week 8 post-inoculation, but maximum power was only attained at week 33 in the 20°C reactor and at week 56 in the 10°C reactor. All the MFC reactors then maintained a steady-state current density of 40 mA m^{-2} (± 2), equivalent to a power density of 1.20 Wm^{-3} (± 0.05). The development of the anode biofilm in each reactor was monitored via fluorometric analysis with values calculated as levels of dsDNA present per cm^2 (expressed as ng L^{-1}); dsDNA measurements were taken at 8, 33, and 56 weeks operation (Fig 5.1). A number of studies have previously used dsDNA as an indicator of biomass, with Marstorp et al (2000) using this technique to investigate Biomass C development in soils as an indicator of biofilm growth. Indeed, there is mounting evidence that dsDNA present in biofilms has a key structural function within the biofilm matrix and may even be an actively anabolized component of the exocellular matrix (Whitchurch et al. 2002). During the course of the experiment the levels of biofilm increased over time. It was observed that by week 8 the 35°C reactor had reached maximum steady-state voltage with a DNA concentration of 0.0514 g m^{-2} and this value continued to increase over the course of the experiment finally rteaching a figure of 0.425 g m^{-2}. It was however found that biofilm development was much slower at both the 20°C and 10°C temperatures, with dsDNA concentrations slowly increasing to 0.601 g m^{-2} and 0.403 g m^{-2} respectively by week 56. The 20°C reactor consistently maintained a higher level of biofilm build-up on the electrode compared to the 10°C reactor. DNA concentrations were then converted to levels of VSS biofilm biomass per litre (Table 5.1). The differential effect of 10°C, 20°C and 35°C operational temperatures on biofilm development was further demonstrated when carbon veil anode samples were analysed by scanning electron microscopy at 56 weeks operation (Fig 5.2). It could be observed that biological material had formed across the carbon fibres demonstrating the active production of biofilm EPS both on and across the anode. Although biofilm formation could be observed on carbon fibres at all three test temperatures, significantly greater amounts of biomass were found in the 35°C anode (Fig 5.2). It can be observed in the lower SEM magnification (400x) that large clumps or agglomerations of biomass had accumulated in the 35°C biofilm but not at 10 and 20°C. These observations are in agreement with and support the high dsDNA biomass measurements recorded at week 56 (Fig 5.1). The growth of anodic microorganisms associated with this EPS biofilm production can also be observed at all the temperatures we tested (Fig 5.2).

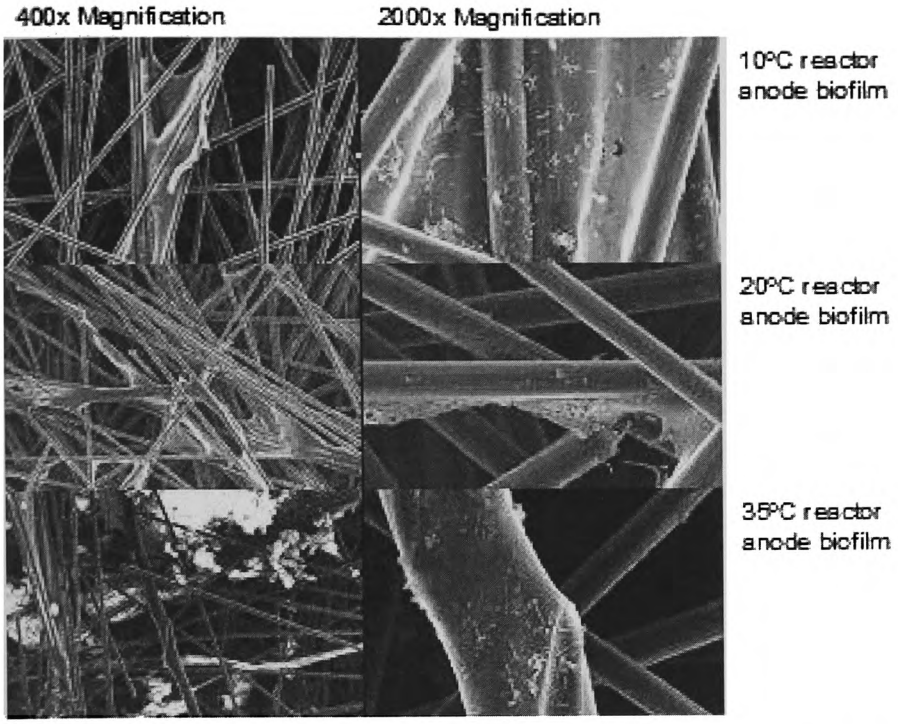

Figure 5-2. SEM microscope images of carbon veil anode biofilms after acclimation at 10°C, 20°C and 35°C (56 weeks operation)

5.2.2 Anodic biofilm activity at different temperatures

DNA concentrations measured using a spectrophotometer were converted to g VSS L^{-1} using the calculation outlined in Section 2.10.1. The specific anodic current densities were based on the total VSS adjusted for the total anodic surface area of 120.1 cm^2: the total current was then calculated from the maximum steady-state voltage generated in each respective batch cycle (Fig 5.3). Whilst it can be observed that as the 35°C reactor rapidly attained a steady-state voltage and the level of biofilm continued to increase throughout the course of the experiment, it can also be observes that the current density per VSS dropped from 2.8 mA.g^{-1} VSS at 8 weeks to 0.3 mA g^{-1}VSS at 56 weeks. The highest current density per Biomass (VSS) was prodcued in the 20°C reactor with a measured value of 6.2 mA g^{-1} VSS (week 8) but this then dropped to 2.3 mA g^{-1} VSS at week 56 (Fig 5.3). This was a consequence of continued biofilm growth slowly developing on the anode but without any further increases in MFC power occurring. Consequently, at 56 weeks the 10°C reactor had the highest activity level of 3.44 mA g^{-1}VSS.

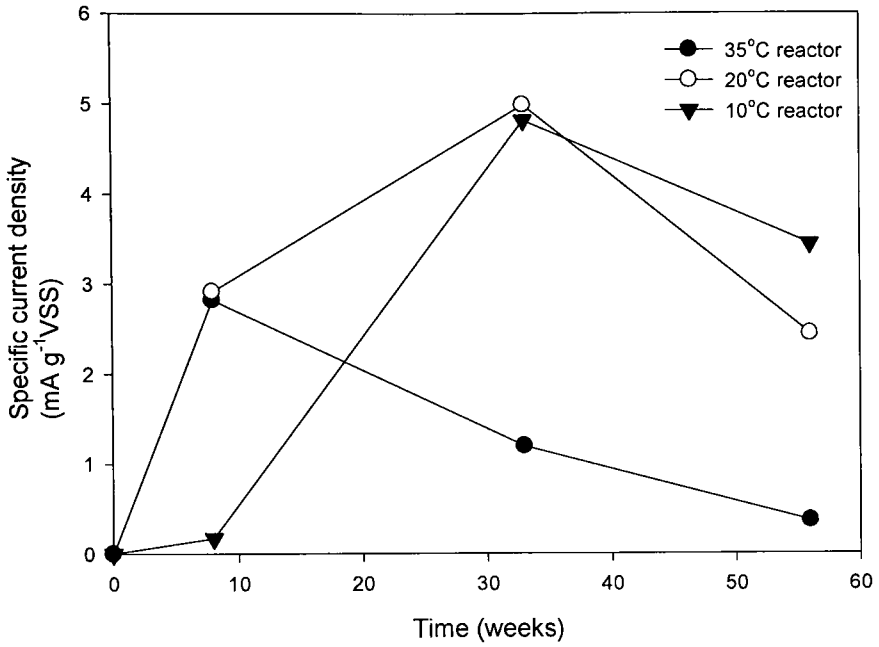

Figure 5-3. Current density development per VSS (g) over time. The maximum steady-state voltage generated in each respective batch cycle was used to calculate the total anodic current density (1000Ω resistive loading) per gram of biomass (VSS)

The total g COD removal was calculated from COD measurements before and after the batch cycle for each reactor at each time point. Using the total calculated amount of biomass present on the anode, the specific biomass COD removal activities were determined (Table 5.1).

Table 5-1. The change in biomass (as g VSS L^{-1} reactor), specific biomass activities (as g COD g VSS^{-1} day^{-1}) and power (mW) over time in MFC reactors incubated at 10°C, 20°C and 35°C temperatures.

Time (weeks)	35°C			20°C			10°C		
	g VSS L^{-1} reactor	g COD g VSS^{-1} day^{-1}	Power mW	g VSS L^{-1} reactor	g COD g VSS^{-1} day^{-1}	Power mW	g VSS L^{-1} reactor	g COD g VSS^{-1} day^{-1}	Power mW
0	0	0	0	0	0	0	0	0	0
8	0.71	0.39	0.24	0.31	0.04	0.05	0.24	0.04	0.0001
33	1.71	0.39	0.25	0.40	0.13	0.24	0.33	0.06	0.15
56	5.43	0.12	0.23	0.82	0.09	0.24	0.57	0.05	0.23

The amount of acetate substrate used over the different time periods was calculated based on the levels of COD removal and these were then related to the increase in biomass (VSS) to give a measurement of the maximum biomass yield over time, this was calculated as g Biomass-VSS per g substrate consumed. Although it was found that initial biomass yields varied with MFC operating temperature it was observed by week 56 that all 3 reactors (incubated at 10°C, 20°C and 35°C) had biomass yields that ranged between 0.013-0.019 g Biomass-VSS per g substrate C (Fig 5.4). Using equation 3 the specific growth rates (μ_{net}) were calculated using the dsDNA values as an indicator of the total biomass present. SigmaPlot software (Systat Software Inc, USA) was then used to fit the exponential part of the curve from the entire experimental period (0 at 56 weeks) and this gave specific growth rate measurements of 0.0015, 0.0019 and 0.0031 day^{-1} for the 10°C, 20°C and 35°C reactors respectively.

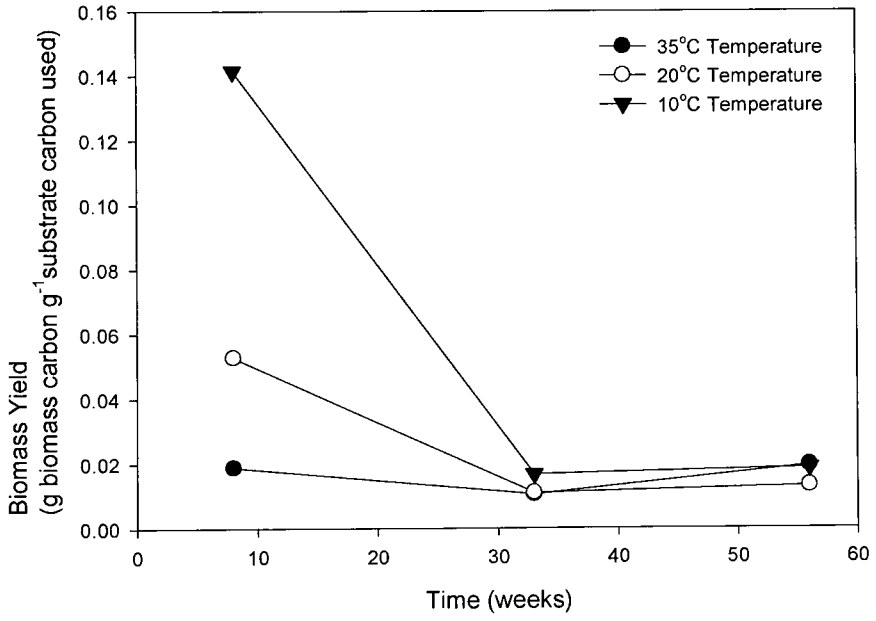

Figure 5-4. Growth yield development over time expressed as biomass VSS per substrate (carbon) used - 35°C, 20°C and 10°C temperature reactors

However by using equation (15) this then allows the introduction of non-exponential K_{vss} term so that the non-growing biofilm biomass can also be accounted for when calculating μ_{net}. This calculation was then found to produce higher specific growth rate values as reported in Table 5.2.

Table 5-2. Comparison of parameters calculated from dsDNA concentrations based on MFC reactors incubated at 10°C, 20°C and 35°C temperatures. Values of all standard errors were <1E^{-3}.

	Parameters			
	K_{VSS}	$X_{0\ VSS}$	μ_{net}	R^2
Temperature (°C)	mg VSS cm^{-2} anode	mg VSS cm^{-2} anode	day^{-1}	
35	0.84	0.38	0.0084	1.0
20	0.58	0.03	0.0095	1.0
10	0.38	0.073	0.0060	1.0

The use of dsDNA in the calculation of specific growth rates was suggested by Marstorp et al (1999): in this study by Marstorp et al it was found that results from dsDNA measurements were nearly identical to those values calculated from respiration rates, this then can provide a good measure of biofilm growth over time. It was assumed that substrate limitation was not a factor during the batch operation as high substrate concentrations were utilized and the reactors were fed on a weekly basis by discarding all the remaining media and replaceing with fresh substrate. During the experiement rates of biofilm detachment were not accounted for.

The production of methane was detected in both the 35°C and 20°C MFC reactors but not the 10°C reactor. The maximal rates of methanogenesis at 35°C was 1.03 mmol.d^{-1} and but this was only 0.006 mmol d^{-1} at 20°C operation. When gas production in the 35°C and 20°C reactors was related to levels of biofilm biomass carbon present in the biofilms, this gave specific methane production rates based on anode associated biomass in the 35°C and 20°C reactors of 10.1 mmol CH_4 biofilmVSSg^{-1} d^{-1} and 0.28 mmol CH_4 biofilmVSSg^{-1} d^{-1} respectively.

5.2.3 Electrochemical performance of anode biofilms at two different time points

The anodic biofilms incubated at temperatures of 10°C, 20°C and 35°C were analyzed electrochemically by measuring power density plots and polarisation curves of the MFC systems at 43 and 60 weeks of operatio (Fig 5.5).

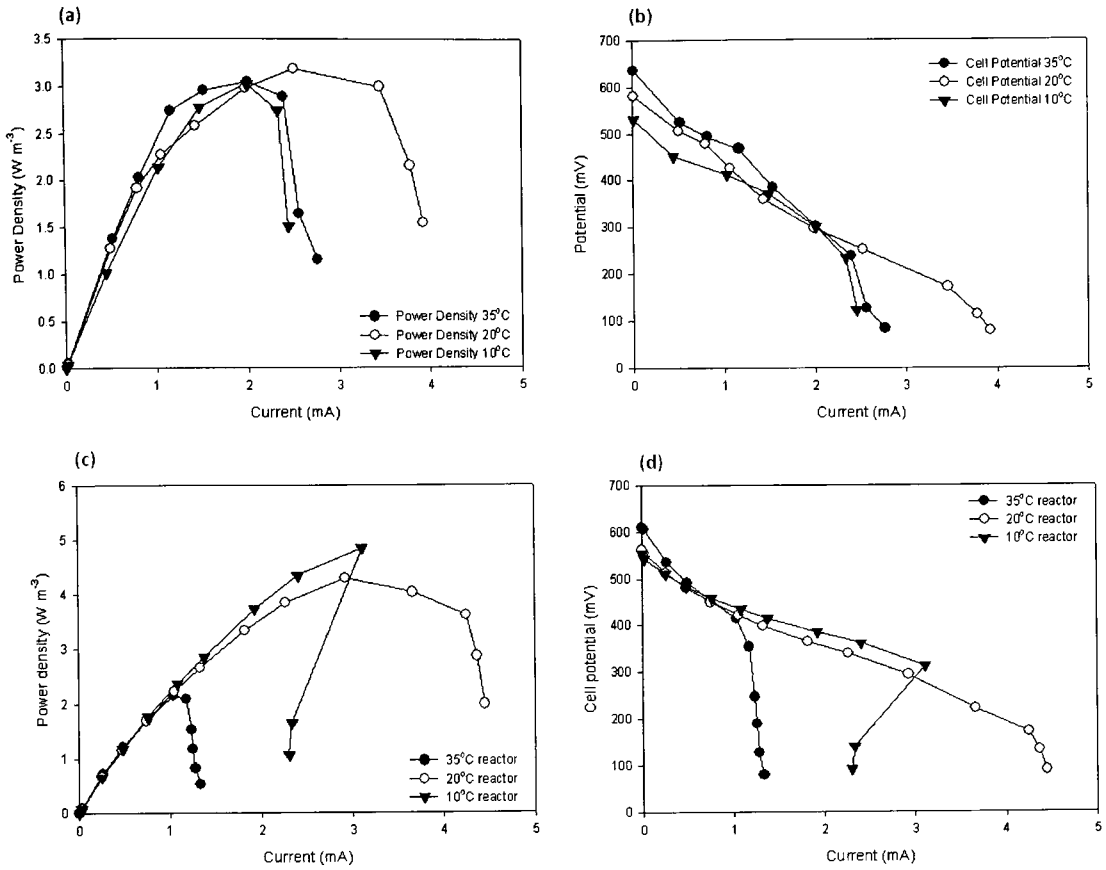

Figure 5-5. Power density and cell potential at 3 different temperatures (35°C, 20°C and 10°C). Reactors were tested at 2 operational time points; 43 weeks (a) and (b); 60 weeks (c) and (d)

The open circuit voltage (OCV) of the MFCs operated at different temperatures showed that a range of OCVs were produced in the 10°C, 20°C and 35°C reactors, measuring 530, 561 and 630mV respectively at 43 weeks and 554, 563 and 611 mV at 60 weeks. Using the polarization curve data the internal resistances were calculated, these were found to be 112, 115 and 151 Ohms respectively for the 10°C, 20°C and 35°C reactors at 43 weeks and then changing to 72, 68 and 198 Ohms internal resistance at 60 weeks. It was observed that the eactor temperature did not have a large effect on maximum power production at 43 weeks operation as all reactors produced 3.08 W m^{-3} (± 0.09), with the 10°C, 20°C and 35°C reactors each producing 3.02, 3.18 and 3.04 W m^{-3} power respectively. However when the maximum power densities were calculated at 60 weeks the power density in the 35°C reactors had dropped to 2.14 W m^{-3}, whereas maximum power in the 10°C and 20°C reactors had gradually increased to 4.84 W m^{-3} and 4.29 W m^{-3} respectively. It was observed at 43 weeks that the power density plots from the 10°C and 35°C reactors had similar curve profiles. However the 20°C reactor was additionally able to produce more power at higher currents, as from the polarisation curve it can be observed that more electrons could be extracted at lower system potentials. This would indicate that although the 20°C and 35°C biofilms had both matured and were

operating at a state-state voltage, the 20°C anode had actually developed a greater electrogenic activity with a subsequently greater potential to produce more current at lower electrode potentials. The 10°C anode reached maximum steady state power production after 56 weeks (Fig 5.1), with this power density level being comparable to the two higher temperatures reactors (20°C and 35°C) also tested. The decrease in the performance of the 35°C MFC after 60 weeks operation did not seem to be a function of a compromised cathodic performance which may have developed over time as runnning the reactor in continuous mode at a flow rate of 10ml hr^{-1} showed that the maimum power reading then increased to 9.14 W m^{-3}. To test whether the batch mode power density had also increased, the maximum power density was subsequently determined to be 7.2 W m^{-3}. This then suggests that the power development was directly linked to the performance of the anodic biofilm and factors associated with its composition and structure.

CEs were investigated for the MFCs operated at different temperatures over time (Fig 5.7). It can be observed that the CE of the 35°C reactor exhibited a gradual decrease to 2.2% at 48 weeks but the CE of the 20°C reactor increased to 11.1%. However, the results show that the 10°C MFC reactor prodcued the highest CE with a value 25.9% after 48 weeks operation. It was thought that the drop in CE% in the 20°C reactor at 18 weeks was an artifact arising from the reactors operating with poor electrical contacts during this period.

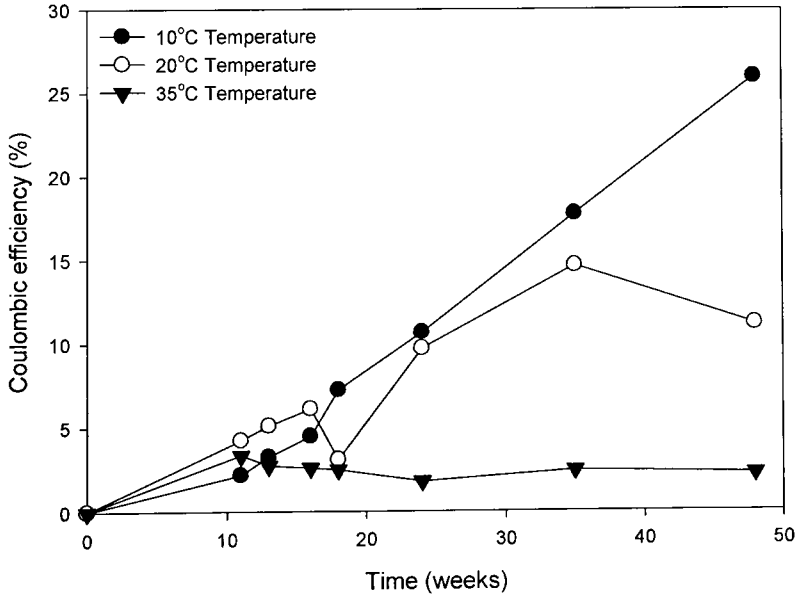

Figure 5-6. The development of MFC coulombic efficiency (%) rates over time at 3 different reactor temperatures - 10°C, 20°C and 35°C

To further understand whether the compromised power production in the 35°C reactor was due to a permanent change in the electrogenic capacity of the tubular MFC (i.e. decreased cathodic performance occurring over time), or whether this was due to mass transfer limitations associated with the anode biofilm structure, the MFC reactor was run in continuous mode at flow rates of 10 - 540ml per minute. The level of biofilm (DNA ng/ul) was then measured and the batch performance (power production) was reassessed (Table 5.3). The power readings are high compared to power results produced in Table 5.1 as these are maximal measurements and were not measured using a fixed external loading of 1000Ω.

Table 5-3. The development of layer 1 Biofilm biomass (DNA ng/ul) and maximum power production (W m^{-3}) over time.

Time (weeks)	Batch /continuous	Maximum Power (mW)	Maximum Power (W m^{-3})	Biofilm biomass (DNA ng/ul)
43	Batch	0.75	3.15	240
60	Batch	0.49	2.05	471
76	Continuous	2.94	12.33	110
77	Batch	1.71	7.2	110

5.3 Discussion

5.3.1 Influence of temperature on biofilm growth and development of electrogenic activity

The start-up of the MFC reactors in this study showed that whilst temperature influenced time taken to reach the steady-state maximum voltage it did not affect the final voltage attained. This result supports the work carried out by Ahn and Logan (2010), in this study the tubular single chamber MFC reactors which were operated at mesophillic temperatures of 23 and 30°C: at these operating temperatures the reactors reached comparable steady-state voltage outputs to those achieved in this study i.e. a voltage 0.43-0.44V using a 1000 Ω resistive load. However, we demonstrated that the ability yo attain steady-similar state maximum voltages was also applicable to sub-mesophilic and psychrophilic operated MFC systems. Hence although the absolute lag time and maximum power densities will always be a function of the MFC system in question and the microbiological composition of the system, it is clear that temperature affects the electrogenic biofilm development but not necarrily the final electrogenic capacity.

From the polarisation curves shown in Figure 5.6 it can be seen that the open circuit potential (OCP) was highest for 35°C reactor reflecting higher system activation energies present in this system, these higher cell potentials can be described by the Nernst equation (Bard and Faulkner 2001). However, the power curves also show that the maximum electrogenic power (P_{max}) of 3.08 W m^{-3} (± 0.09) at 43 weeks was comparable in all three temperature acclimated reactors showing that even when these reactors were run at low temperatures there was no effect on overall power production. Analysis of the power curves showed the 20°C reactor plot profile was elongated compared to the 10°C and 35°C temperature plots, this would seem to demonstrate that this bacterial community that developed within the 20°C electrogenic biofilm was better able to provide current at low potentials. This may suggest that a wider or richer electrogenic population was present which could mean that this bacterial community present was more able to shift their collective metabolic activities or those bacteria present could better facilitate electron transfer to the anode.

The carbon material utilized in this experiment was a carbon veil anode material which has been previously shown to provide a large microbially-accessible surface area by having an open 3-dimensional network of carbon fibres (Liu et al. 2010). Hence it is thought that this material structure was able to facilitate high levels of biofilm growth compared to other types of carbon material i.e. graphite rods. However in contrast with the Liu et al study which found an 80% increase in current density with a temperature increase of 30 to 40°C we found that from 43 to 60 weeks operation there was an increase in the maximum power (P_{max}) of 59% and 39% in the 10°C and 20°C reactors respectively, however it can also be observed that the 35°C reactor recoded a 30% decrease in maximum power (Fig 5.6). Measurement of biofilm biomass levels after 56 weeks found that the 10°C and 20°C reactors were lower by factors of 7.1 and 10.6 respectively when compared to the 35°C reactor (Fig 5.1). This indicates that electrogenic development and EAB growth continued to take place at 10°C and 20°C, but also shows that increased biomass production had a direct adverse effect of on electrogenic activity in the 35°C biofilm (Table 5.2). The effects of temperature have been previously investigated in non-temperature acclimated anode biofilms and it has been found that over a range of 4-35°C power production had a direct relationship with the operational temperature (Moon et al. 2006; Cheng et al. 2010). However there is little work been carried out on low temperature MFC reactors, Cheng et al (2010) reported no MFC voltage development at temperatures of <10°C but it is likely that these reactors were not allowed to acclimate for a sufficient time to allow microbial growth to occur. Where reactors have been acclimated for growth at 10°C, voltage production was shown to develop to a level equivalent to that of mesophilic operation and it is thought this is due to the development of psychrophilic and psychrotrophic

microbial populations, as discussed in Chapter 4. Therefore, although higher temperatures will provide more energy to initiate metabolic redox reactions and drive growth rates, low temperature tolerant electrogenic biofilms can develop over time that are able to respire at rates equivalent to or higher than those bacteria at mesophilic temperatures. Interestingly in arctic marine sediments it has been found that rates of dissimilatary anaerobic respiration were equivalent to corresponding mesophilic rates which were measured. It was thought that this was achieved through higher specific metabolic activities when the cells metabolized at the lower temperatures (Knoblauch et al. 1999). The decrease in the maximum power produced at 60 weeks in the 35°C reactor shows that over time the biocatalytic capacity was actually compromised compared to the 10°C and 20°C reactors that exhibited an improved electrochemical performance over time.

When the levels of biofilm were measured in the 35°C reactor at 56 weeks this showed that the biomass levels had increased significantly to 5.43g VSS L^{-1}. When compared measurements by Aelterman et al (2008a) using a graphite granule anode this figure was found to be high as the latter study produced an average biomass concentration after 30 days of ~0.58g VSS L^{-1} or 0.288 biomass-C L^{-1}. However this figure was comparable with the levels of biomass produced in the 10°C reactor at 56 weeks. The importance of developing active electrogenic anode populations is clear as this is the biocatalytic agent present in MFC systems and provides the key to electricity production from the biofilm, this importance has been demonstrated by electrochemical impedance spectroscopy (EIS) studies. Ramasamy et al. (2008) have used EIS to show that biofilm growth acts to reduce anode polarisation resistance whilst facilitating electrochemical kinetics. However it is also thought that the poor formation of conductive layer at the biofilm anode interface could restrict direct electron transfer and limit current densities (Torres et al. 2009b). It was observed that the 35°C reactor had developed an internal (Ohmic) resistance of 151 Ω at 43 weeks, higher than both the 10°C and 20°C MFCs, which then continued to increase to 198 Ω at week 60; this was in contrast to both the 10°C and 20°C MFCs and exhibited a decrease in ohmic resistance over the same period. Thus, biomass development over time in the 35°C biofilm had a negative effect on power production as system over-potentials increased. It is thought that this was probably due to the formation and development of non-electrogenic biofilm on the anode. Increasing levels of biomass could be observed from the SEM pictures taken at different time points and at different operational temperatures (Fig 5.1 and Fig 5.2). These are likely to introduce mass transfer and diffusive limitations and it is likely that effect would be predominate in the 35°C biofilm, where the presence of large biomass clumps will also mean that many microorganisms present are sited remotely from the anode and are therefore less likely to be able to undertake anodic respiratory activity. This was demonstrated in specific current density measurements highlighted in Figure 5.3, this showed that

after 8 weeks there was a subsequent decrease in values over time. These results are in general agreement with conduction based biofilm modeling by Picioreanu et al (2007) where it was suggested that thick biofilms may have a negative impact on power density measurements due to the potential increases in resistive limitations that may develop in the biofilm. It seems that higher biomass concentrations were sustained at higher temperatures and this then likely resulted in an increased competition for direct and indirect contact with the anode surface where optimal rates of electron transfer could not occur.

5.3.2 The effect of temperature on electrogenic activity

In order to assess levels of anaerobic respiratory activity in the MFCs at different temperatures over time, current density measurements were investigated relative to the development of anode biomass (as a proportion of the biofilm as g VSS) after an 8 week pre-enrichment phase. It was observed that although the amount of biomass increased over time at each test temperature this did not subsequently produce higher current densities (per g VSS) once the reactors had reached their maximum steady-state voltages. This did however result in higher maximum power density values at 10°C and 20°C, these being 4.84 W m^{-3} and 4.29 W m^{-3} respectively as described in Section 5.2.3. This indicates that after 60 weeks operation the 35°C reactor biofilm, and to a lesser degree the 10°C and 20°C biofilms, accumulated an electrochemically inert biomass matrix and dead or dormant cells. This biomass was not able to contribute to electrogenesis and may have also actively facilitated tpo methanogenic and non-electrogenic metabolism, the accumulation of dead and non-viable cells in anode biofilms has been previously reported by Ren et al (2011). Although microorganisms such as *G. sulphurreducens* may be able to transfer electrons through up to a 50nm matrix (Reguera et al. 2006), it is likely that the build-up of large amounts of biomass observed in the 35°C biofilm disrupts the electrogenic mechanisms and strategies involved in bacterial electron transfer to the anode surface. Where-as Patil et al (2010) reported that the age of the biofilm and its thickness had no effect on current densities this study demonstrates that the accumulation of biomass over time can lead to the overall electrogenic activity of the biofilm being compromised. The improvement in 35°C reactor performance during and after the application of continuous flow conditions shows that the application of a shear force to the biofilm by apply flow conditions led to improved mass transfer conditions; it it likely that this force induced both compositional and structural changes that enabled an improvement in overall electrogenic activity (Pham et al. 2008).

The calculation of specific growth rates (μ_{net}) showed that the 35°C reactor produced the highest microbial growth rates overall. However, it ws further demonstrated that if non-growing biomass was considered as a separate factor in the mass balance (Equation 15) the 20°C reactor had the highest specific growth rate, with the 35°C reactor having the greatest level of inactive biomass (Table 5.2). This may suggest that within the 35°C biofilm a proportionally smaller fraction of the biomass was actively growing at a faster rate. It can be oberseved that the growth rates calculated in this study were low, being approximately 5-8 fold lower than results obtained from batch water systems (Boe-Hansen et al. 2002). This may reflect the establishment of mature biofilms due to the high substrate concentrations used and the long time-frame of the experiment. This may have led to significant detachment losses to the planktonic phase during batch feeding process and were not accounted for in the calculations. The high initial biofilm value $X_{o,\ vss}$ (mg VSS cm^{-2} anode) measured in the 35°C reactor relates to the high level of biomass accumulation which occured during the first eight weeks operation.

Anode biofilm biomass yield values, calculated as biomass-C per substrate-C used, were comparable with results presented by Aelterman et al (2008a) who reported yields of 0.05 and 0.02 biomass-C per substrate-C used, and were in agreement with other previously reported values of 0 to 0.54 biomass-C per substrate-C used (Freguia et al. 2007). Operational temperature did not affect the biofilm yield once the reactors had established steady-state operation (Fig 5.4). This meant that the relative biomass conversion rates into biofilm of the 10°C, 20°C and 35°C reactors were similar even if the total levels of biomass (biofilm and suspended) differed. The higher yields produced by the 10°C and 20°C biofilms at 8 weeks operation highlights the initial establishment of the electrogenic biofilm, with the 10°C reactor at an earlier stage in the biofilm maturation process.

Biomass production and methane production have been previously shown to be significant electron sinks (Lee et al. 2008) and this is also reflected by the range of CEs reported in this study (Fig 5.7). The CE values produced in this study are comparable with other studies using tubular air cathode MFC systems (Ahn and Logan 2010) with the highest CE values recorded at the lowest reactor temperatures. However with decreased MFC operating temperatures the COD removal rates also decreased due to the lower rates of methanogenesis and biomass production. Rates of methanogenesis were significantly higher at 35°C, with no methane production detected at 10°C operation. It is thought that this directly led to the 35°C reactor having a COD removal rate of 2.98 $g^{-1}L^{-1}d^{-1}$ compared to the 10°C reactor which had a COD removal rate of 0.27 g^{-1} L^{-1} d^{-1}, however the latter reactors CE reached 25.9% after 56 weeks. The CE increased in the 10°C and 20°C reactors over time as the electrogenic populations developed, but slowly decreased at 35°C as biomass

accumulation and methanogenic activity increased as the numbers of methanogens increased. The observation that low temperature operational conditions are linked to low rates of COD removal and high CEs also further supports the results from Ahn and Logan (2010).

It was observed that even though the 10°C biofilm had the lowest specific growth rate and lowest level of biomass it also produced the highest CE and P_{max} values at 60 weeks of reactor operation; this was further demonstrated by the high current density produced per biomass VSS. This shows that by operating the biofilms at reduced temperatures it is possible to retain an anode that promotes an anodic biofilm that favours electrogenesis over methanogenesis and thus acts to divert electrons present in substrate from biosynthesis to energy demanding non-growth activities. This process has also been observed when operating aerobic wastewater treatment reactors at low organic loading rates, in these biofilms a higher proportion of substrate chemical energy was found to be used in the maintenance of bacterial activities at the expense of lower growth rates and less biomass production (Low and Chase 1999). High adenylate levels have been observed to accumulate in bacterial cells at low temperatures which may be utilized for cellular maintenance and repair as part of enhanced bacterial catabolic activities (Amato and Christner 2009). This suggests that the electrogenic potential of anode biofilms may be dictated by its operating temperature. It would additionally seem that electrochemical and biological limitations can be imposed on the MFC systems during biofilm maturation processes which may have implications for the operation of batch MFC systems or those reactors which may be operated at low flow rates.

5.3.3 The influence of continuous flow conditions on electrogenic performance

Operating the 35°C tubular reactors at MFC in continuous mode demonstrated that mass transfer limitations which developed due to the build-up of electrogenically inert biomass could be overcome through the application of high system flow rates (540ml per minute). This resulted in a six fold increase in maximum power output. High shear rates used to enriched electrogenic biofilms have been reported to increase active biomass density and thickness, improving MFC anodic performance (Pham et al. 2008); however in this study prolonged batch operation likely produced a thick biofilm with low relative tensile strength (as observed in Figs 3.15 and 3.18, Chapter 3) which was able to be detached by the internal stresses caused by the hydrodynamic flow (Picioreanu et al. 2001). This then resulted in biofilm sloughing, as evidenced by the decrease in biofilm biomass (Table 5.3). EAB retained in close proximity to the anode were then able increase electrogenic activity due to improved substrate/proton mass transfer flows. This was further demonstrated by

the improvement in maximum power performance exhibited by the batch operation post-continuous flow, an improvement by a factor of 3.5.

5.4 Conclusions

This study demonstrates that the operational temperature of MFC reactors directly influences the biocatalytic capacity of biofilms. Whilst it was observed that the 10°C and 20°C temperatures led to slower start-up times compared to 35°C, less biomass accumulation occured as the biofilms matured. This meant that lower anode overpotentials developed at the lower temperatures likely due to improved mass transfer within the biofilm. The build-up of biomass can lead to a conductive barrier forming between the anode interface and EAB present in the biofilm and this was associated with increased rates of methanogenesis at 35°C of 10.1 mmol CH_4 g^{-1} d^{-1} compared to 0.28 mol CH_4 g^{-1} d^{-1} at 20°C. This resulted in the maximum power recorded at 60 weeks operation in the 35°C reactor being 2.14 W m^{-3} whereas the 10°C and 20°C reactors produced 4.84 W m^{-3} and 4.29 W m^{-3} respectively. It was further demonstrated that exposure of the 35°C biofilm to high hydrodynamic forces caused biofilm sloughing to occur, which then subsequently led to improvements in MFC performance. These results provide an important insight into the link between anode biofilm development and electrochemical performance and highlight the potential effects of temperature on biocatalytic performance of EAB, which also has implications for the design and practical application MFC technology in temperate regions.

6 Continuous MFC operation and the influence of novel helical anode designs on reactor performance

Continuous flow systems utilizing fixed biofilms offer the potential of cost-effective bioprocess treatment (Ieropoulos et al. 2010). Chapter 5 demonstrated that mass transfer limitations due to the build-up of non-electrogenic biomass can lead to low system performance due to the probable build-up of high proton concentrations within electrogenic biofilms and low substrate diffusion rates. In order to reduce over-potentials associated with mass transfer effects, decrease HRTs and increase the potential surface area available for biocatalytic activity, 3 different tubular helical anode reactors were constructed. On each helical anode the pitch or constructed gap/liquid flow channel between the helicoids was varied i.e. the carbon veil width (Table 5.1). This change in the physical parameters of the anode will thus change the hydrodynamic properties under continuous flow conditions. The spoke configuration of the helix walls and the narrow gap will change the relative velocities in the anode chamber which will then influence both the type and the degree of turbulent flow and also the multi-directional flow characteristics. To test this influence, the 3 different helical anodes were operated at a range of flow rates and at 2 different substrate loadings. A comparison was also made with a wound annular carbon veil electrode; this had a biofilm that had been previously established over a period of > 1 year (as per Chapter 3).

Some of the results in this chapter have been published (Kim et al. In Press), see Appendix 4.

6.1 Results

Flow rates over a range of 10 – 540 ml per minute were used to investigate the influence of different anode designs on reactor performance in continuous operation mode. A low acetate concentration of 2mM was first used to test the different anode systems (Fig 6.1). The anode reactor types (annular, SP1, SP2, SP3) produced maximum power densities of 12.4, 11.63, 9.2 and 6.73 Wm^{-3} respectively. It can be observed that an increase in flow rate produced an increase in power in the annular reactor and the SP1 and SP2 reactors, although the SP1 reactor produced a higher maximum power result with the 240ml per min flow rate not the 540ml per min flow rate. However the SP3 reactor produced the highest power density at 130ml per min, with 540ml per min and 10ml per min flow rates producing similar power densities at half the maximum power value.

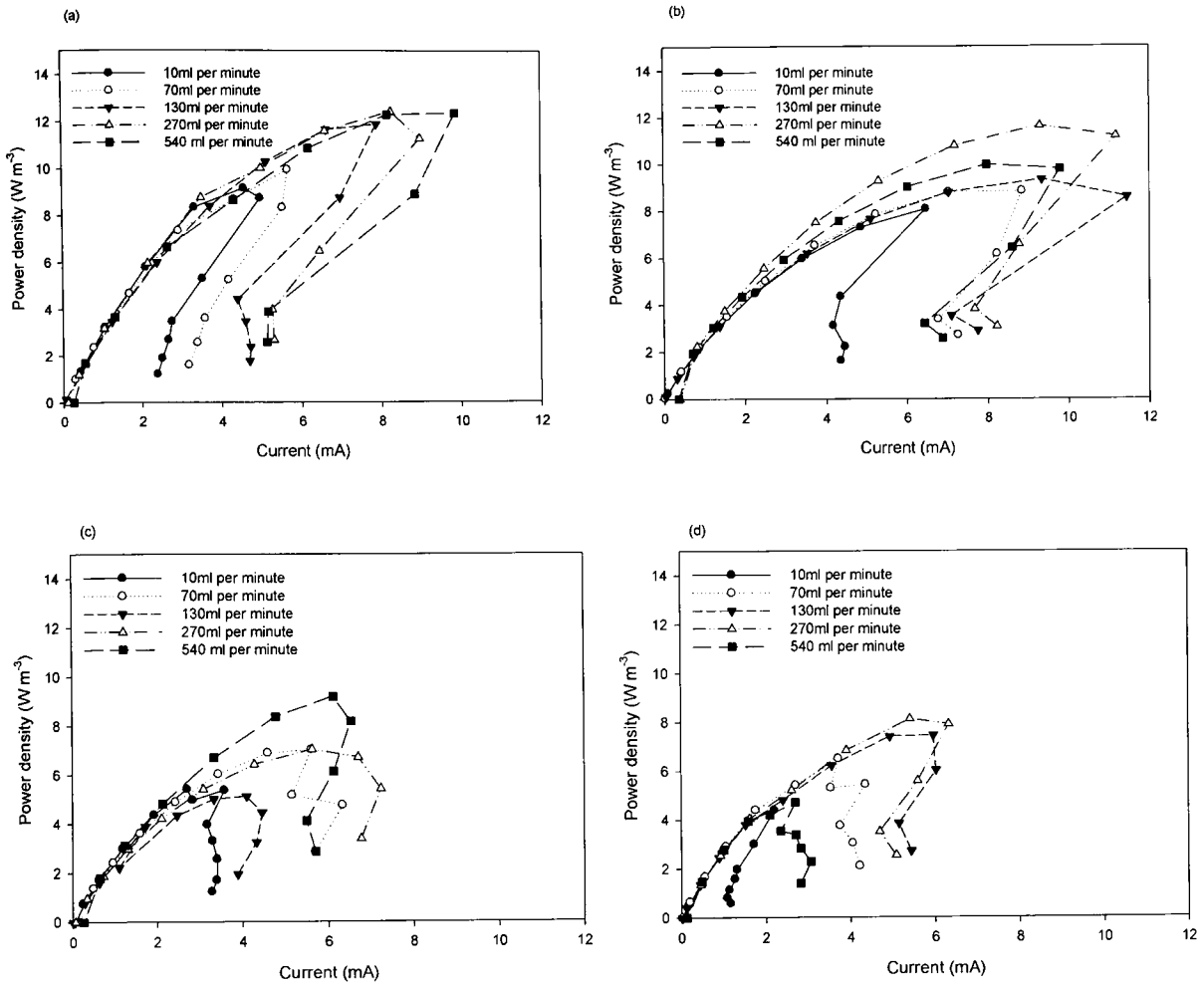

Figure 6-1. Effect of flow rate on power density performance using a 2mM acetate substrate. (a) Annular (b) SP1 (c) SP2 (d) SP3.

The maximum power densities obtained at a 10 fold higher substrate concentration (20mM acetate) were 14.75, 10.0, 9.2 and 7.4 W m^{-3} for the annular, SP1, SP2, SP3 reactors respectively. Although the annular, SP1 and SP2 maximum power densities generally increased with flow rate, with the annular 135ml per minute result as a notable exception, the SP3 reactor again produced the highest power density at 130ml per min, with 540ml per min and 10ml per min flow rates also showing similar and low maximum power values. Thus high flow rates into the anode chambers and high internal flow rates induced by the anode configuration seemed to have influenced the power densities produced in each reactor. High velocities can induce high levels of turbulence which will have a direct effect on mass transfer of protons out of electrogenic biofilms and substrate into the biofilm. Indeed it has been reported that proton accumulation is a major limitation to electrogenic activity within biofilms (Torres et al. 2008). As the carbon veil is porous, consisting of interlinked woven fibres, turbulence will also act to facilitate diffusion deeper into the anode.

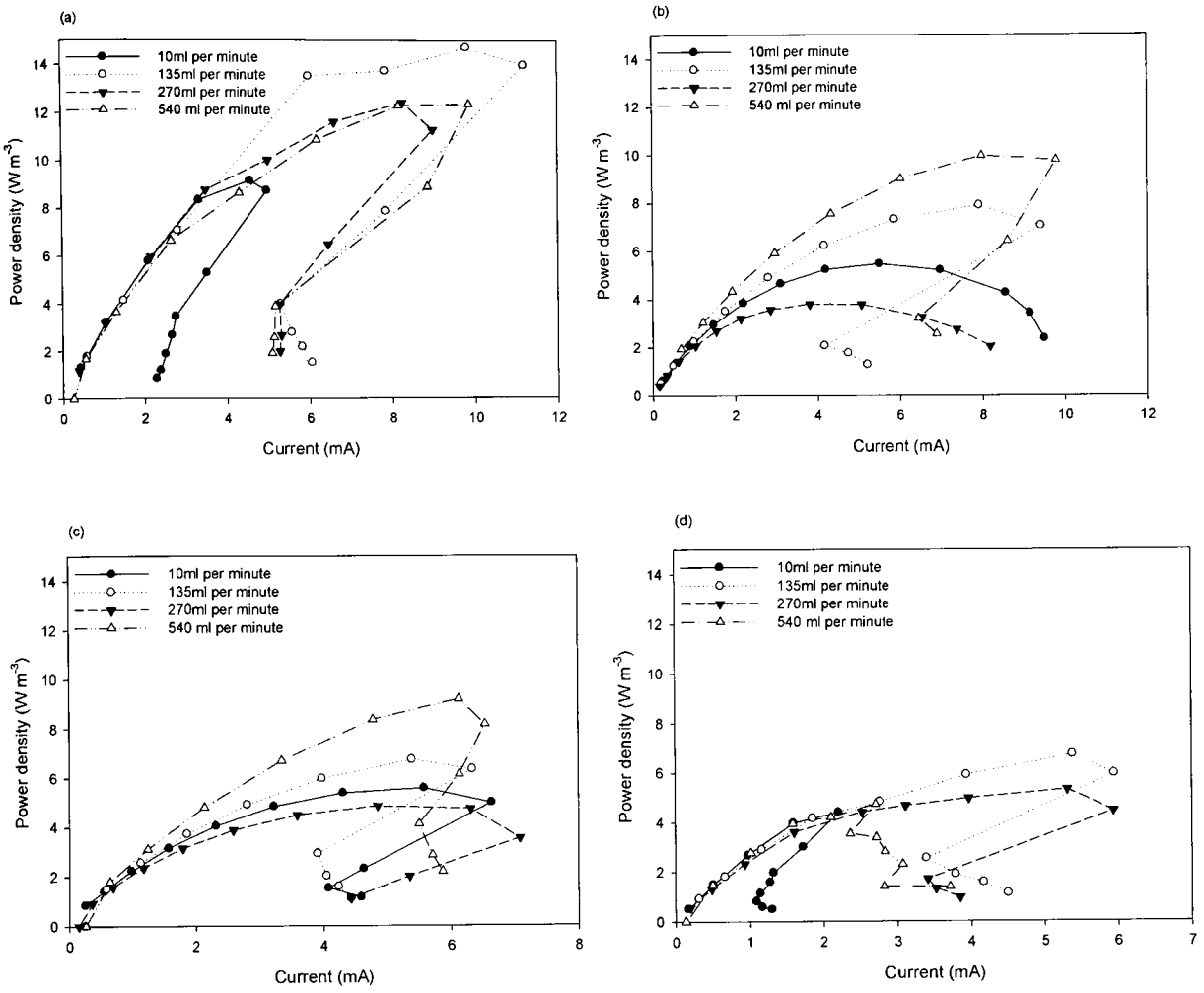

Figure 6-2. Effect of flow rate on power density performance using a 20mM acetate substrate. (a) Annular (b) SP1 (c) SP2 (d) SP3.

It can be observed that the maximum power density in the annular reactor decreased when operated with a lower acetate concentration. However the maximum power density in the helical anode reactors was either equivalent to or lower with 20mM acetate as the feed substrate compared to 2mM acetate. The power curves produced in this study show a strong power overshoot phenomenon, which is occurs when both the current and power decrease together causing the distinctive inward curve before the system recovers. A similar power overshoot was observed by Ieropoulos et al (2010) over a slower range of flow rates, 1.5 – 120 ml per hour. It can also be observed that the SP3 power curves exhibit a double power overshoot at the 540ml per min flow rate.

The physical parameters of the different anode configurations were analysed in terms of maximum current produced (Table 6.1). Due to the higher mass of carbon present in SP1, this reactor had a wider strip of carbon which meant a smaller gap (for liquid flow) and therefore a lower

operating volume. When performance was considered in terms of either surface area of carbon biomass the SP3 results were higher than the SP1, indicating that the SP1 had a higher specific activity. The annular anode with the established biofilm had the highest specific activities.

Table 6-1. Comparison of physical and performance characteristics of different anode tubular reactor designs

Parameter	Anode construction			
	Annular Wound anode	Helix SP1 small gap	Helix SP2 medium gap	Helix SP3 large gap
Operating fluid volume (ml)	225	148	177	202
Maximum current (mA) - 2mM acetate substrate	9.9	11.5	7.0	6.3
Total anode carbon mass (g)	10.8	35.41	25.75	21.85
Maximum current per carbon mass (mA g^{-1})	0.9167	0.3247	0.2718	0.5263
Carbon veil width (mm)	N/a	17	13	10
Surface area of carbon (cm^2)	113	447	421	398
Maximum current density per anode carbon cm^2 (mA cm^{-2})	0.0876	0.0257	0.0166	0.0289

The rate of COD removal (%) was related to the HRT with each different reactor design (Fig 6.3). Due to higher liquid/substrate residence times, longer HRTs resulted in increased (COD) removal rates of acetate. With the low (2mM) acetate solution there was a baseline removal of 55-70% suggesting that a significant proportion of the acetate was being quickly removed in the planktonic phase after flowing from or to the anode chamber. However at the highest HRTs the SP1 and SP2 reactors facilitated a 90% COD removal.

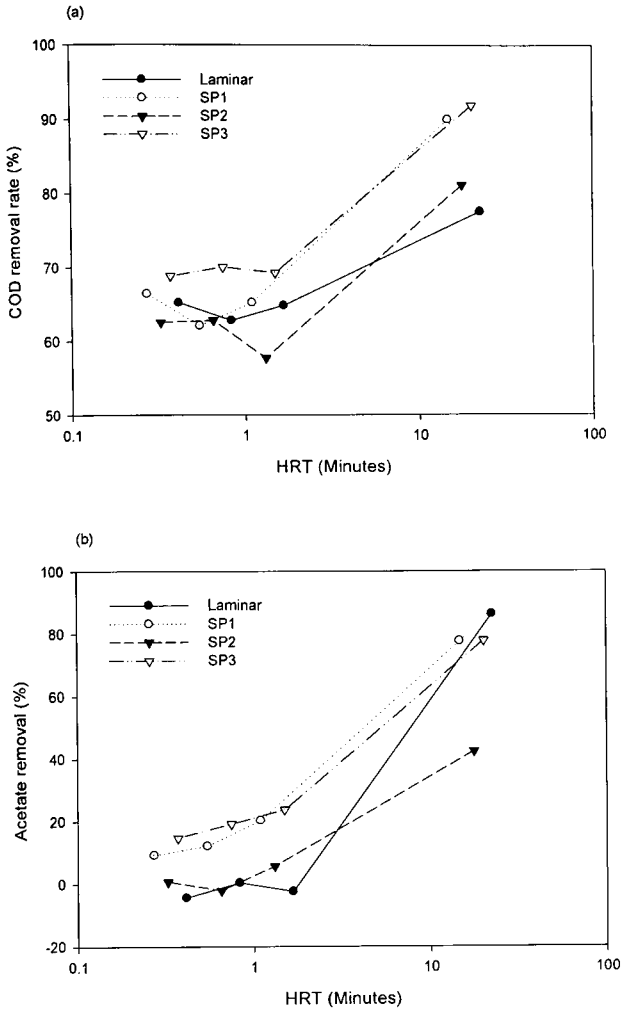

Figure 6-3. Rates of COD removal (%) related to HRT (minutes) for annular, SP1, SP2 and SP3 reactors using 2 concentrations of acetate (a) 2mM (b) 20mM

At the 20mM acetate concentration the annular anode did not remove any COD until a high HRT was used, indeed as the HRT was decreased (flow rate increased as per Table 6.2) negative COD removal rates were produced. This is indicative of biofilm sloughing due to increasing shear rates as the flow rate was increased. COD removal rates in the helical anode reactors increased with increasing HRT with the SP1 and SP3 achieving a 20% removal at an HRT of ~1 minute and 75-80% at higher HRTs. The annular reactor also removed ~80% at an HRT of 22.5, but the non-linear relationship indicates that mixing at the low flow rates was limiting biofilm activity. Although the SP2 reactor increased removal rate with HRT, % removal at 17 minutes retention time was only 40%, again showing that this system was not as active in substrate removal.

Table 6-2. Relationship between flow rate and HRT for annular, SP1, SP2 and SP3 reactors

	HRT (minutes) at different flow rates (ml min^{-1})			
	10	135	270	540
Annular	22.50	1.67	0.83	0.42
SP1	14.80	1.10	0.55	0.27
SP2	17.70	1.31	0.66	0.33
SP3	20.20	1.50	0.75	0.37

Analysis of Bacterial communities showed that the established biofilm from the annular reactor had the richest and most diverse population. Whilst there was an 82% similarity between the SP2 and SP3 anode communities, the similarity was much lower with the SP1 and annular anodes which shared a relatively closer association (Fig 6.4(a)). The Archaea population was very developed in the established annular reactor but population diversity was low in the helical anode reactors (Fig 6.4(b)).

(a)

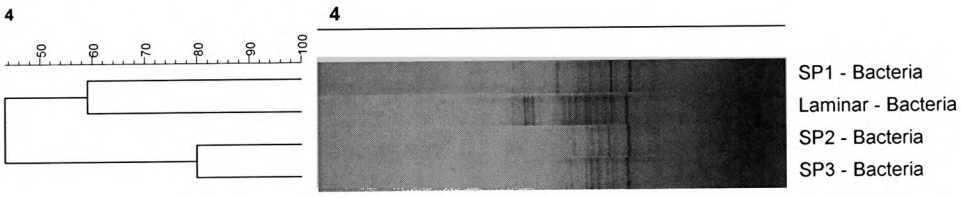

(b)

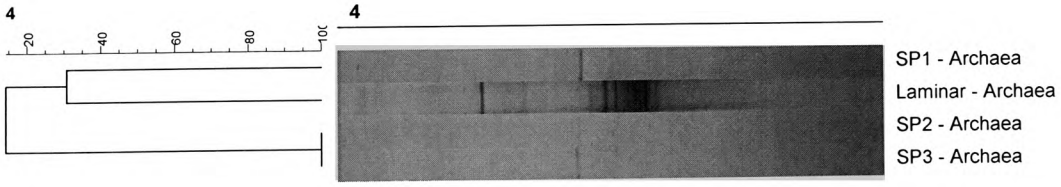

Figure 6-4. Biofilm DGGE community analysis of layer 1 carbon veil anode samples from annular, SP1, SP2 and SP3 reactors (a) Bacteria and (b) Archaea

Analysis of the levels of biofilm present in the carbon veil anodes as assessed by the quantity of DNA (DNA ng μl^{-1}) again showed that the established and mature annular biofilm contained the highest levels of biomass, a factor of 4 to 5 higher than the helical anode reactors (Table 6.3). The

SP1 reactor accumulated the highest levels of biofilm, 40% higher than the SP2 and SP3 anodes. However all the helical anode reactors had biofilm/biomass levels higher than that in the annular reactor in the 3rd carbon veil layer, in the case of SP1 this was 3 times higher.

Table 6-3. Development of biofilm biomass (DNA ng μl^{-1}) through carbon veil anode layers 1 to 5

Anode	Biofilm development (DNA ng μl^{-1})			
Layer	Annular	SP1	SP2	SP3
1	110	28.2	20.3	19.3
3	4.2	13	5.2	9.3
5	2.9	2.2	2.1	2.4

To understand how continuous flow impacted on the performance of the different reactor types over time, the MFCs were run in re-circulation loops over a period of 10 days using 20mM acetate substrate and a 270ml per minute flow rate (Fig 6.5). Whilst the SP3 and A35 reactors produced high initial voltages of 0.58V these voltages dropped-off at 6 and 4 days respectively. The SP1 reactor produced a consistent voltage of 0.53V over the course of 9 days, whilst the SP2 reactor ran at 0.51 V for 8 days. The different levels of electrogenic activity were also reflected in % CE results for the annular, SP1, SP2 and SP3 MFC reactors, these being 4,2%, 7.0%, 5.8% and 5.5% respectively. Low CEs achieved over the 10 day recirculation reflect the effect of the high initial substrate loading (Aelterman et al. 2008b), but more significantly oxygen ingress into the 1 litre reservoir bottle and a proportionally high planktonic phase. In a typical flow through systems high flow rates will wash non-electrogenic planktonic bacteria out if the flow rate is sufficiently higher than the cellular growth rate, however as the liquid was re-circulated in this experiment this could not occur (Borole et al. 2009).

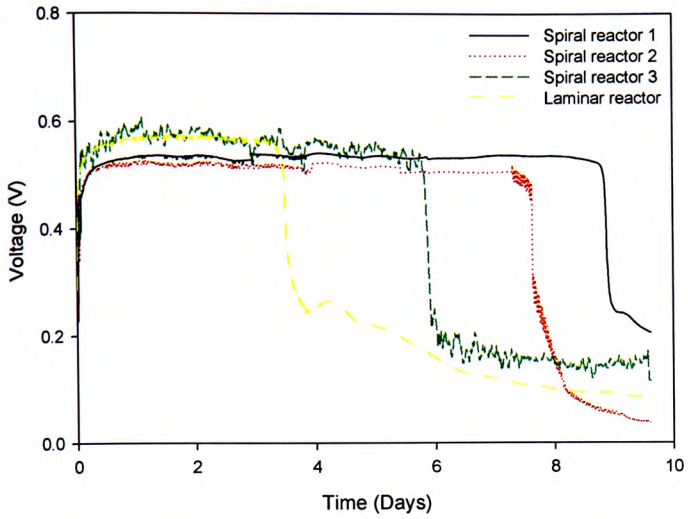

Figure 6-5. Using annular, SP1, SP2 and SP3 MFC reactors a 20mM acetate substrate was re-circulated at a 270ml per minute flow rate. A 1000 Omega loading was used on all the MFCs.

Power density measurements were taken after the 10 day re-circulation test, the maximum (peak) values from the annular, SP1, SP2 and SP3 MFC reactors were 7.6, 8.2, 8.2 and 6.9 Wm^{-3}, respectively. It can be seen that subjecting the different anodes to a prolonged high flow rate environment had a negative impact on performance of all the reactors, however this effect was particularly pronounced in the annular reactor.

6.2 Discussion

This study used high flow rates to examine the effect on of different spiral anode architectures on MFC performance. Decreasing HRTs have been previously shown to increase power densities up to a maximum point, after which further decreases result in lower power densities. The HRT at which this shift occurs will be determined by the MFC/anode architecture, but both Huang et al (2008) and Li et al (2008) reported maximum power figures at 10-20 hours and 15.5 hours respectively. This work showed that using longitudinal tubular reactors with 100 fold lower HRTs still resulted in increased power densities. Other work has also reported that high flow rates/low HRTs can cause a reduction in power as it was thought that dissolved oxygen levels will also proportionally increase within the anode chamber (Ieropoulos et al. 2008; Li et al. 2008). This means that even with the very high flow rates used in this study there was sufficient planktonic bacterial population/activity present to be capable of metabolizing the oxygen at high enough rates so as not to affect MFC power production.

As the maximum power produced by MFCs is determined by the activity and quantity of biocatalyst available, and the capacity of the biofilm to facilitate electron transfer to the solid carbon anode, the high level of power produced by the annular reactors demonstrates that high numbers of EAB were enriched during the >1 year fed-batch process (As per Chapter 3). The removal of loosely bound biofilm was also shown by the negative COD removal values produced as the HRT was decreased (Fig 6.3). This then left a highly active electrogenic biofilm that was robust to flow rates of up to 540ml per minute.

As there is a direct link between liquid velocity and internal pipe diameter, increasing flow rates will increase the possibility of turbulence occurring as defined by the Reynolds number (N_{re}); where υ is the fluid velocity, ρ the fluid density, D the pipe diameter and μ the fluid viscosity as per equation 16:-

$$N_{re} = \rho\upsilon D/\mu$$

Equation 16

Increasing Reynolds numbers are thus associated with the initiation of turbulent mixing and improved mass transfer (Lin and O'Brien 1974). As the 3 different spiral anode configurations have different gap sizes and different helical pitches this may have a direct effect on fluid velocities and mixing through the system. The construction of the spokes will also promote multi-direction liquid flow due to the induction of eddies. Increasing a Reynolds number from 900 to 4900 has been previously demonstrated to increase current densities by 30% in a stirred MEC anode chamber (Ajayi et al. 2010). It is possible that the very low performance in the SP3 reactors at 540ml per minute may be related to a hydrodynamic effect on the mass transfer events in this particular anode. Lower cell maintenance energies with high shear rates have also been reported as a reason for high energy recoveries (Pham et al. 2008). A high substrate concentration had an equal or detrimental effect on power production in the helical anode reactors as would be expected in an electrogenic biofilm system where electron transfer is limited. Hence higher substrate flows into the carbon veil may be metabolized to produce electrons and protons, but thermodynamic limitations associated with proton and electron flows at high external loadings (1000 Omega) could lead to limitations on EAB metabolic rates and the accumulation of end-products leading to a negative impact on power production (Aelterman et al. 2008a). The higher numbers of EAB in the annular reactor may have mitigated this effect and there may also have been a lower penetration of substrate through the biofilm into the carbon veil depth. Limitations in exocellular electron transfer to the electrode may also account for the observed power over-shoot curves (Nien et al. 2011),

although the double power over-shoot curves at 540ml per minute in the SP3 reactor probably reflects a relatively sparse biofilm that was not able to cope with increased mass transfer rates under these flow conditions (Winfield et al. 2011).

Operating conditions such as substrate concentration and flow/shear rates will have a direct effect on electrogenesis by directly influencing mass transfer and indirectly by determining biofilm development over time. The results in this study show that turbulent conditions induced higher biofilm formation within the carbon veil, potentially increasing the available surface area for EAB growth and electrogenic activity (Table 6.3). Higher turbulence may also account for high biomass levels occurring in the SP1 reactor. Different flow conditions in the 3 helical anode configurations also produced different bacterial community profiles (Fig 6.4), enrichment at range of different shear rates has previously been shown to significantly alter biofilm composition and bacterial community development (Liu and Tay 2002; Pham et al. 2008). High flow conditions also seemed to limit biofilm archaeal growth.

It has been previously reported that increasing the anode surface area also leads to an increase in power density (Li et al. 2008). This study demonstrates that by using novel helical anode configurations and high flow rates it is possible to maximize the available volumetric surface area available to EAB by enhancing mass transfer flows. This resulted in 68% higher accumulation of coulombic charge from the SP1 reactor compared to the annular reactor during the re-circulation experiment (Fig 6.5). Whilst energy consumption from pump usage would be high it may be possible to balance out these costs with improved system performance. It is likely that extended operation would further enhance performance as further EAB enrichment would occur over time.

6.3 Conclusion

Anodic structure clearly had a large impact on system performances. This may reflect the surface area available for electrogenic activity, a function of not only the actual surface area but also the hydrodynamic forces that impact on mass transfer into the biofilm and porous carbon veil. The spiral reactor with the smallest gap produced the highest coulombic efficiency of 7% and a maximum power density of 11.63 Wm^{-3}. This was however lower than the annular reactor indicating that for high power production the electrogenic biofilm may need to be enriched over a longer time period. Turbulent conditions in the SP1 reactor may have stimulated increased biomass production in the depth of the carbon veil anode.

7 *Dual chamber MFC reactors used to investigate electrogenic biofilm development: the effect of carbon anode material and the application of an automated load control algorithm.*

Whilst it has been shown in Chapter 5 that biofilm growth on MFC anodes are associated with the growth of EAB and the development of electrogenic activity, it has been further demonstrated that the three dimensional structure and the porosity of the carbon also increase the surface available for this bacterial growth (Chapter 3). The first aim of this experiment was to investigate how porosity and material structure of different types of carbon influences anodic biofilm development and thus MFC operation; to ensure consistent experimental conditions all carbon materials were sited adjacent to each other in the same anode reactor chamber. Dual chamber reactors were used as part of this experimentation, as described in the methods and materials chapter (Chapter 2). MFC reactors were constructed with four different types of carbon material sited in the anode chamber, each with a projected surface area of $4cm^2$. All four material types were placed together during testing, with one reactor run as an open circuit control and the other in closed circuit conditions using a fixed external load of 1000Ω. The anode material provided the support for initial attachment of microorganisms and subsequent electrogenic biofilm growth. Different physical properties are associated with different anode materials and their corresponding three-dimensional properties at the micro scale will affect how microorganisms within an electrogenic biofilm attach, develop and facilitate exocellular electron transfer. Before the start of the experiment the mass (g) of each carbon material was determined along with the carbon material resistance (at ambient temperature).

Power density results from Chapters 4 to 6 demonstrated that the 1000Ω external loading used was not optimal for MFC operation and was likely limiting the systems by restricting the flow of electrons. Therefore, dual chamber reactors were used to investigate how MFC external loading control influenced anodic biofilm development and thus MFC operation, and also how a control algorithm could be used to optimize power production by optimizing the external load on the system. The dual chambers reactors were used in this testing as described in the method and materials chapter (Chapter 2.2). It has been previously discussed that system power can be theoretically optimized by matching the internal resistance to the external resistance (Logan et al. 2006), further to this Pinto et al (2010) modeled this approach and found that even small differences in internal and external impedances could cause large differences in the power produced. However

any change in loading/voltage will also have an effect on the EAB present in the anode biofilm, indeed it has been shown that voltage acts to regulate the activity of electron-transferring microorganisms. The effect of changing external resistance on microbial community development may not be clear, as Lyon et al (2010) reported that changes in external resistance did cause changes in microbial profiles but did not result in any change in MFC performance in terms of power production. Using carbon paper as the anode material a control algorithm was developed in Labview that used Boolean logic to assess whether the external resistance should be raised or lowered so as to optimize system power via a data acquisition card; this was determined by measuring the voltage (*V*) across the load, such that power $P = V^2/R$. The control strategy was implemented by using a single CMOS Intersil® 100 step 1kΩ digitally controlled potentiometer, X9C102 (Farnell UK Ltd., Leeds) as the load resistance. Some of the results in this chapter have been published (Premier et al. 2011), see Appendix 4.

7.1 Results

7.1.1 Open circuit and closed circuit operation with four different types of carbon anode material

4 weeks post-inoculation the anode biofilm was established in the closed circuit MFC. At this point it could be observed that carbon materials 1 and 2 produced the highest maximum voltage of 0.29 V (Fig 7.1), compared to 0.27 V and 0.23V from materials 3 and 4 respectively (Table 7.1). Material 1 sustained a higher voltage even when substrate depletion occurred indicating that this biofilm contained a more efficient electrogenic biofilm and/or the porous material was able to retain substrate to continue anaerobic respiration at a higher rate for a longer period.

Table 7-1. Carbon mass (g) used in each of the 4 different experimental and control anode materials

Carbon Material type	Control reactor mass (g)	Experimental reactor mass (g)	Material Resistance (ohms per $4cm^2$)
Material 1 Felt	0.16	0.15	53.9 Dry 39.7 wet
Material 2 E-Tek carbon paper	0.11	0.11	0.7
Material 3 Engineered carbon tubes	1.3	1.3	0.2
Material 4 Graphite rod	2.25	2.29	1.2

Results were not adjusted for the resistance of the different electrodes as a high fixed resistance of 1000 Ω was used and this meant the margin of error was <4% for the carbon felt electrode (the material with the highest inherent resistance, Table 7.1).

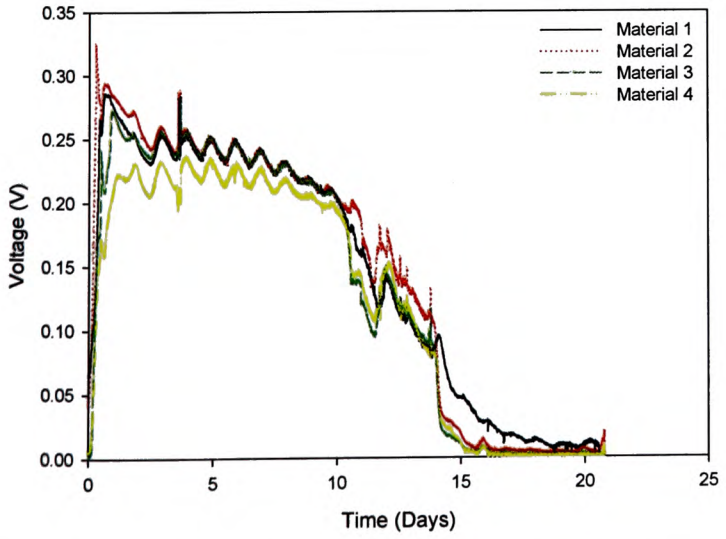

Figure 7-1. MFC potential development of 4 different carbon material types (1- felt, 2 – E-Tech, 3- graphite rods, 4 – graphite) fed with 5mMol sucrose. Closed circuit MFC with a fixed resistance of 1000Ω.

After 3 months batch fed operation archaeal and bacterial community profiles were investigated in both the open circuit and closed circuit MFCs (Figs 2 and 3). The archaeal profiles of materials 1-4 (Fig 7.2) showed that material type did not affect archaeal species development in materials 2, 3 and 4, as these profiles shared 95.7-100% similarity scores. However material 1 shared only a 78.1% similarity having developed a richer archaeal profile. A profile from the open circuit reactor (material 1) also produced a 75.9% similarity with the other closed circuit material types, sharing a number a common bands with the closed circuit anode biofilms; both open and closed circuit anode biofilms digressed significantly from the sludge inoculum. The planktonic profile from the closed circuit MFC had very low amounts of archaeal DNA and, subsequently, low numbers of visible bands which accounts for its low profile similarity score.

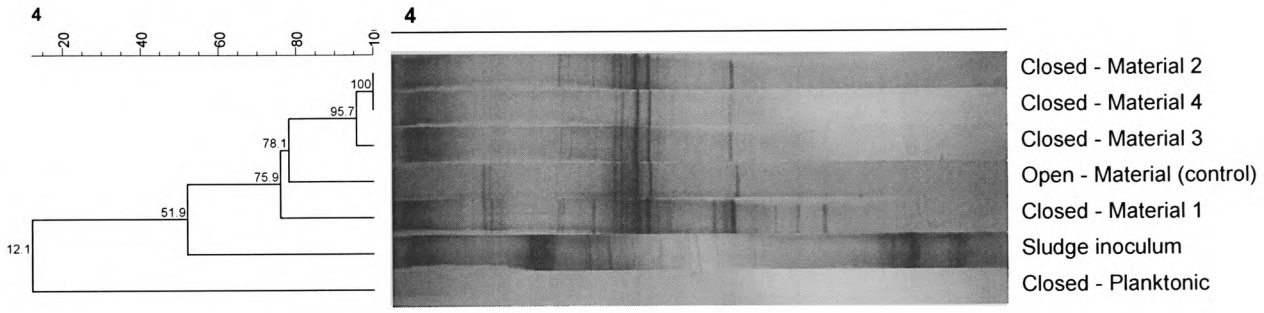

Figure 7-2. DGGE archaeal community profiles from closed MFC with 4 different carbon material types (1- felt, 2 - E-Tek, 3- graphite rods, 4 - graphite). Cluster analysis was carried out using the Jaccard coefficient of similarity measurement. An open circuit control (material 1) is included.

In contrast to the Archaea community development, the bacterial profiles developed differently between open and closed circuit conditions, with a similarity score of 62.1 between the 2 clusters (Fig 7.3). It can be observed that the similarity between the closed circuit materials (1 to 4) was 88.7 to 96.2% but this was 70 to 86.4% between the open circuit materials. It can also be seen that the closed circuit planktonic profile was significantly different from the material biofilm profiles (32.7%); this was in direct contrast with the open circuit planktonic profile which had a similarity value of 75.1%.

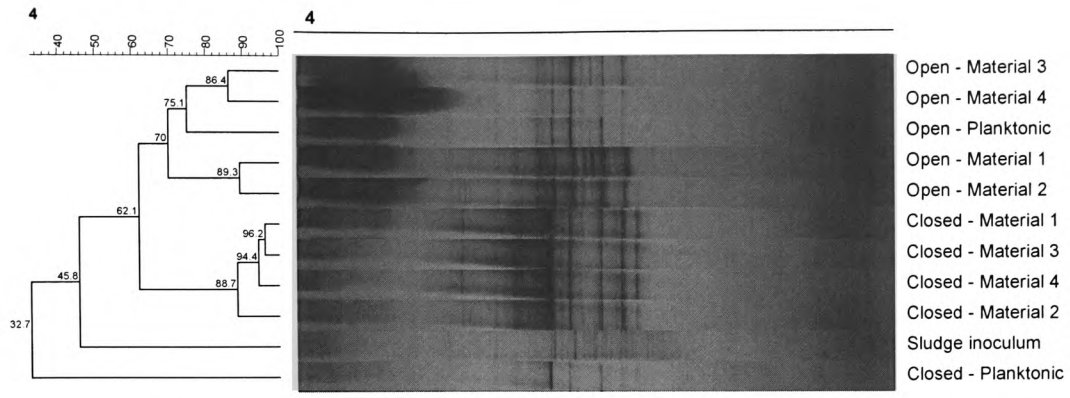

Figure 7-3. DGGE bacterial community profiles from closed and open circuit MFCs with 4 different carbon material types (1- felt, 2 - E-Tek paper, 3- graphite rods, 4 - graphite). Cluster analysis was carried out using the Jaccard coefficient of similarity measurement.

It has been previously shown that anodic biofilms operated in closed circuit conditions facilitate the selective growth of electrogenic bacteria that are able to mediate electrogenic activity and the transfer of electrons to a solid anode (Rabaey et al. 2004). The selective nature of this electrogenic growth meant that materials 1-4 bacterial communities incubated in closed circuit conditions were more closely associated than the respective materials incubated in open circuit conditions. However, the level of difference between the open and closed circuit archaeal populations was very low suggesting a low degree of selection occurred for the archaeal populations during MFC operation. Thus, it seems that the type of carbon material did not greatly influence the selection or development of electrogenic bacteria. However in terms of the amount of biofilm/biomass produced open and closed operation did have a significant effect (Table 7.2), with the level of closed circuit biomass being higher by factors of 11 and 8 in materials 4 and 2 respectively. This suggests that closed circuit conditions provide a key benefit to bacteria existing within anodic biofilms as they are able to exploit electrogenic metabolic activity, thus facilitating EAB growth.

Table 7-2. Biofilm biomass (DNA ng μL^{-1}) in open and closed circuit materials 1, 2, 3 and 4.

	DNA (ng ul^{-1})	
Material	Open circuit	Closed circuit
1	582	1209
2	142	1107
3	597	767
4	70	819
Planktonic	158	120

A visual examination of the different carbon materials showed that extensive biofilm growth occurred on all the anodes (Fig 7.3).

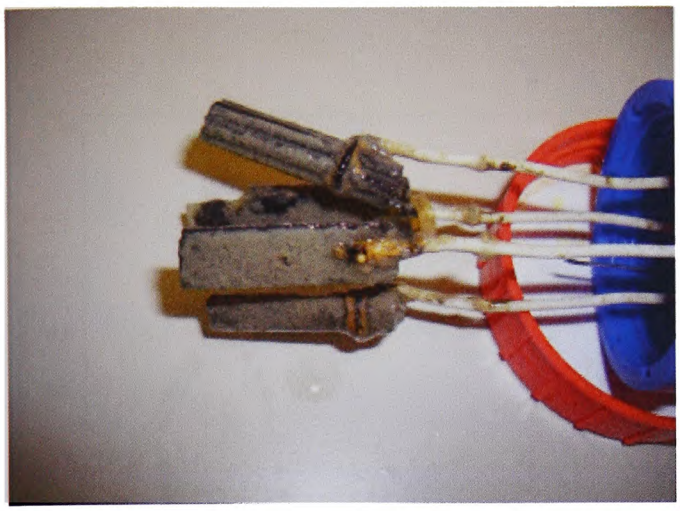

Figure 7-4. Extensive biofim growth occurred on all 4 different carbon anode materials.

In concordance with the lower planktonic biomass levels recorded in Table 7.2, it was visually observed that the turbidity levels in the closed circuit reactor were consistently lower than the open circuit reactor.

Power curve analysis of the different material types in closed circuit (Fig 7.5) showed that material 1 produced the highest power density reading of P_{max} 1.4 W m^{-3} or 0.7 W m^{-2}. However material 2 closely matched this reading with a measurement of 1.2 W m^{-3}, but both materials 3 and 4 generated successively lower power densities. When the internal resistances or ohmic overpotentials were calculated from the polarisation curves (Fig 7.5) this produced internal resistance values of 526 Ω, 526 Ω, 833Ω and 2460 Ω for materials 1 to 4 respectively. As all other factors in the MFC were the same for all the material types i.e. ionic resistances in the electrolyte and electronic resistances in the components and cathode, these differences must relate to the properties of the anode material and the levels of electrogenic biofilm development and its facility to accommodate electron transfer to the electrode. Materials 1 and 2 had the same internal resistances but different power results, this shows that the former material had a lower charge transfer overpotential. This can be related to the associated properties of the biocatalytic biofilm and how this interacts with the microstructure of the anode material itself. Hence, it may be that

material 1 facilitated more EAB to be present in a closer association with the carbon anode, enhancing electrogenesis and reducing activation losses. Fig 7.6 shows the power curves of anode materials 1 to 4 from the open circuit control reactor. The P_{max} of material 1 was 0.95 W m^{-3} or 0.475 W m^{-2} two thirds the value achieved in closed circuit but higher than the maximum closed circuit power densities achieved by materials 3 and 4. The other open circuit materials (2, 3 and 4) all produced power densities of < 0.06 W m^{-3}.

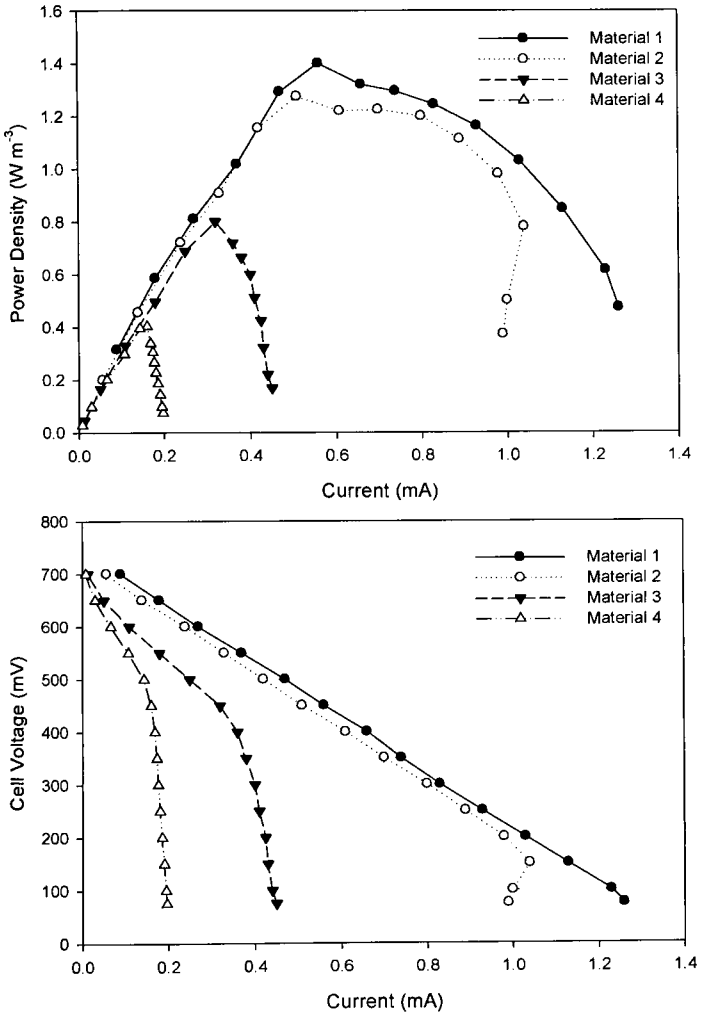

Figure 7-5. Cell potential and power density curves produced in the closed circuit MFC with Materials 1,2,3 and 4 (8 weeks operation). MFC with a fixed resistance of 1000Ω.

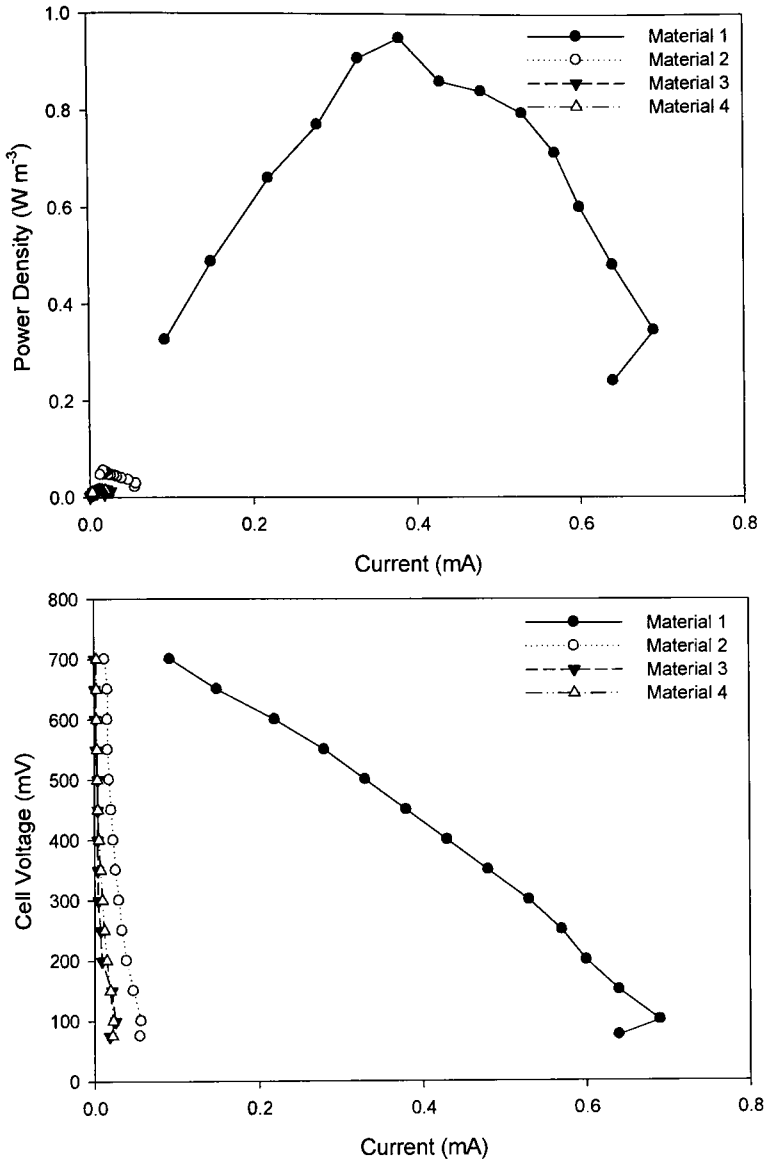

Figure 7-6. Cell potential and power density curves produced in the open circuit MFC with Materials 1, 2, 3 and 4 (8 weeks operation).

From Fig 7.3 it can be seen that even though a high number of bacterial species are common to the open and closed circuit biofilms, there is a higher degree of similarity between materials 1 and 2 open circuit than that of material 1 in open and closed circuit. This means that acclimation or selection of EAB species cannot be considered as the sole reason for the higher power density reading from the open circuit material 1 system compared to the closed circuit material 2.

Cyclic voltammetry (cv) has been previously used to examine electron transfer mechanisms and the redox species involved in interactions between anode biofilms and carbon MFC anodes (Rabaey et al. 2004; Fricke et al. 2008). In this study cyclic voltammograms were run on different anode materials (1 to 4) using both open and closed circuit MFCs. An initial examination of material

1 from the closed circuit reactor found that high scan rates of 10-50 mV/s produced atypical '2-pointed spike' cv plots (Fig 7.7), the maximum current density of which decreased with decreasing scan rates. This did not occur with materials 2, 3 and 4 but the plot profile was repeated with the open circuit material 1 scan. It was reported by Marsili et al (2008b) that at high scan rates slow electrochemical reactions may not have time to occur before the potential shifts to the next step; therefore at these high scan rates as the potential was stepped-up the current also accumulated over time. The material 1 cv profile at high scan rates thus reflects redox agents that are able to undergo multiple redox turnovers; this has been previously demonstrated in immobilized enzyme systems (Heering et al. 1998; Armstrong 2005) and shows the masking of the redox kinetics due to the accumulation of current. The Randles-Sevcik equation (Equation 17) describes the effect of scan rate on the peak current (i_p) for reversible systems at room temperature; this demonstrates that both concentration and diffusional terms will affect i_p.

$$i_p = \left(2.687 \times 10^5\right) n^{3/2} v^{1/2} D^{1/2} AC \qquad \textbf{Equation 17}$$

Where n = the number of electrons in the redox reaction, v = the scan rate in V s^{-1}, A = the electrode area cm^2, C = concentration in mol/cm^3 and D = the analyte diffusion coefficient cm^2 s^{-1} (Bard and Faulkner 2001).

Fricke et al (2008) have previously reported a non-linear relationship between scan rates and peak current, and suggested that this effect could be caused by diffusion control characteristics, which can then be explained by a change in the electrochemical process from quasi-reversible to reversible by decreasing the scan rate. Thus the atypical build up charge with time is indicative that either a large number of redox agents are present and/or they are remotely sited from the carbon anode.

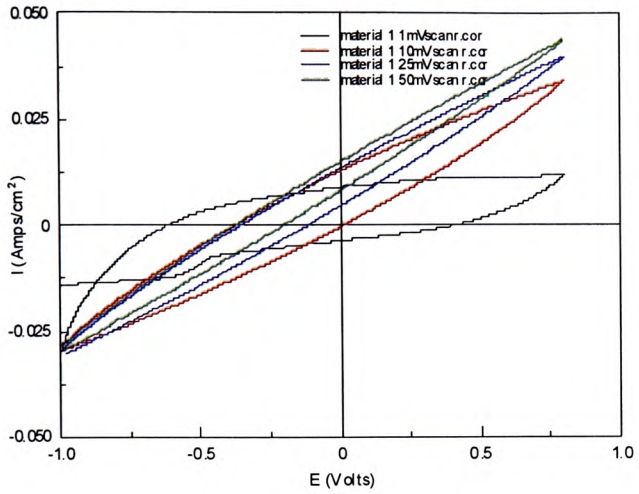

Figure 7-7. Cyclic voltammogram sweeps of material 1 (closed circuit) using 1, 10, 25 and 50 mV/s scan rates. E (V) versus Ag/AgCl.

Figure 7.7 shows the comparative cv scans for closed circuit MFC materials after 3 months MFC operation. Material 1 exhibits the greatest current densities (maximum peaks between oxidizing and reducing sweeps) followed by materials 2, 3 and 4. A comparison between the material 1 open and closed cvs' (Fig 7.8) also demonstrate that material 1 (open circuit) is able to generate comparatively high current densities; this data supports power density results produced in Figs 7.5 and 7.6.

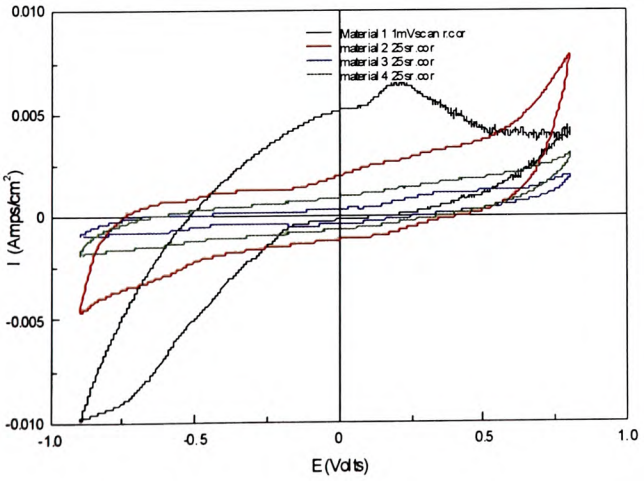

Figure 7-8. Cyclic voltammogram sweeps of materials 1, 2, 3 and 4 (closed circuit) using 1 mV/s scan rates for material 1 and 25 mV/s scan rates for materials 2, 3 and 4. E (V) versus Ag/AgCl.

Cvs performed on the open circuit biofilms (Fig 7.9) also demonstrated the development of electrogenic capacity in the material 1 biofilm only, these results being in accordance with power density measurements (Fig 7.6)

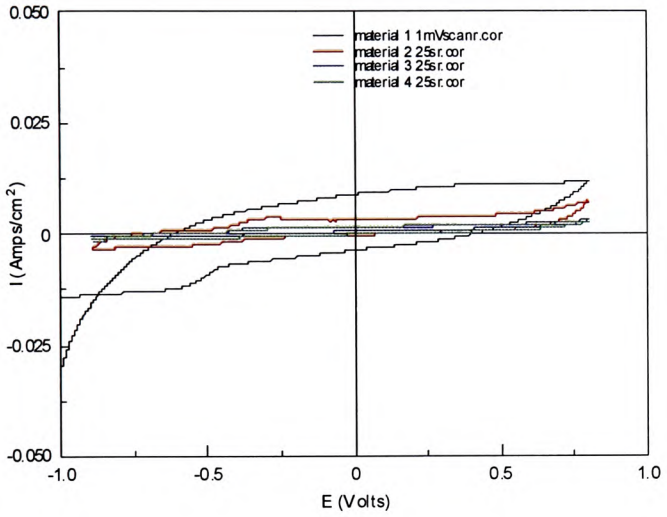

Figure 7-9. Cyclic voltammogram sweeps of materials 1, 2, 3 and 4 (open circuit) using 1 and 25 mV/s scan rates. E (V) versus Ag/AgCl.

Comparative open and closed circuit cvs using material 1 demonstrate the capacity of both the open and the closed circuit biofilms to undergo electron transfer (Fig 7.10).

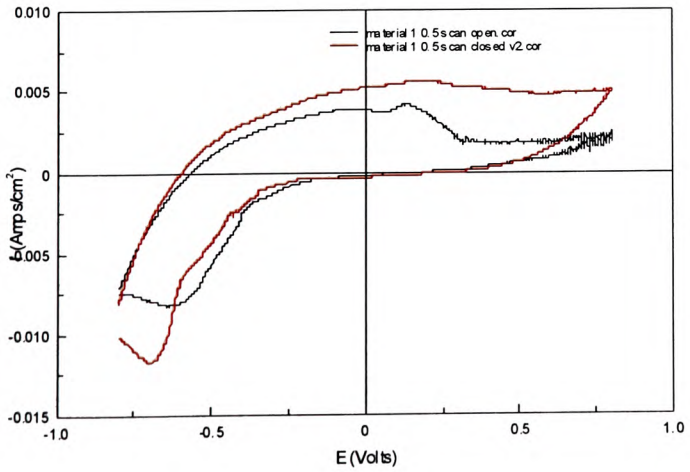

Figure 7-10. Cyclic voltammogram sweeps of material 1 open and closed circuit using 0.5 mV/s scan rate. E (V) versus Ag/AgCl.

As a visual examination of the oxidative and reductive sweeps did not reveal any clear redox peaks (Figs 6, 7 and 8) first order derivatives ($(\Delta I/\Delta V)$ were calculated in order to estimate both the potentials at which any inflections occurred and their given amplitude (Table 7.3). See Appendix 3 to view the actual first derivative graphs.

Table 7-3. First derivative potentials and amplitudes for closed and open circuit oxidative and reductive sweeps. E (V) versus Ag/AgCl.

	Open circuit				Closed circuit			
	Reductive sweep (towards a positive E_{an})		Oxidative sweep (towards a negative E_{an})		Reductive sweep (towards a positive E_{an})		Oxidative sweep (towards a negative E_{an})	
Material	Voltage E_{an} (V)	$\Delta I/\Delta V_{max}$ $(\Delta I/\Delta V_{An})$	Voltage E_{an} (V)	$\Delta I/\Delta V_{max}$ $(\Delta I/\Delta V_{An})$	Voltage E_{an} (V)	$\Delta I/\Delta V_{max}$ $(\Delta I/\Delta V_{An})$	Voltage E_{an} (V)	$\Delta I/\Delta V_{max}$ $(\Delta I/\Delta V_{An})$
	n/a	n/a	-0.6 to -0.15	-0.01	n/a	n/a	-0.49	-0.03
	-0.5	0.004	-0.55	-0.005	-0.39	0.021	-0.44	-0.011
	n/d	n/d	-0.53	-0.0025	-0.39	0.016	-0.4	-0.006
	-0.51	0.002	-0.55	-0.0025	-0.38	0.006	-0.39	-0.003

The reductive sweeps reveal higher $\Delta I/\Delta V_{max}$ values indicating higher levels/rates of electron transfer to the electrode compared with from the electrode. This would indicate that electron transfer was from cytochrome enzymes as these have been shown to be inactive on the reverse cv sweep (Zhao et al. 2009). No results were obtained for the material 1 forward sweeps as the derivative values were observed to decrease from a very high value to a low value over the course of applying the potentials (See Appendix 3 for graphs). It is thought that this again relates to a capacitive build-up of current with the scan rates used in this experiment. The potentials produced in this study can be compared to the midpoint potentials of multiheme cytochromes which have been determined from *Geobacter spp.* The open circuit reactor midpoint potentials are comparable with the measured potentials from OmcB and OmcZ purified from *G. sulfurreducens*, these being of -0.39 and -0.42 V (*vs.* Ag/AgCl) respectively (Magnuson et al. 2001; Inoue et al. 2010). The maximum potential in the carbon felt open circuit material (1) ranged from -0.6 to -0.15 (E (V) versus

Ag/AgCl), showing that there was no optimal mid-point anode potential but rather a range of active potentials capable of electron transfer. Interestingly, although the other open circuit materials showed low current generation their mid-point anode potentials were lower (-0.53 to -0.55).

The different biofilms formed on the 4 different materials were tested in order to investigate their response to low pH perturbation. Changing the pH to 6.00 immediately affected the electrogenic activity of the material 3 and 4 biofilms.

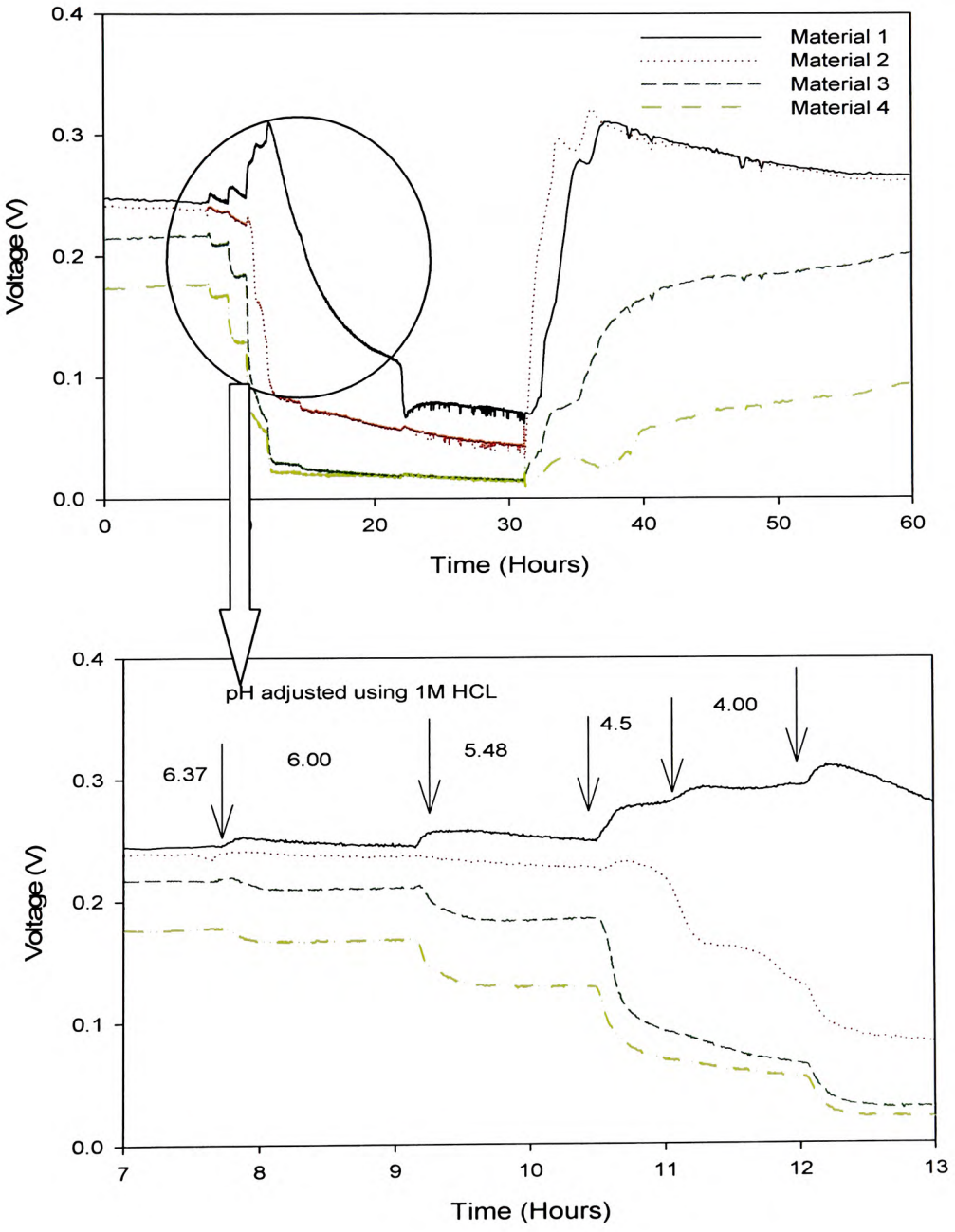

Figure 7-11. The effect of pH shifts on biofilms formed on materials 1, 2, 3 and 4.

The material 2 biofilm was adversely affected at pH 5.5 but voltage from the material 1 biofilm reduced when pH 4.0 was introduced into the reactor. Materials 2, 3 and 4 stabilized to steady-state voltage readings until pH 5.00 was introduced into the reactor, after which voltage dropped rapidly in all 3 material types. This could suggest that down to pH 5.0 the voltage limitation was purely thermodynamic, but after this point the physiology of the bacteria in the biofilm were being affected. The voltage of material 1 was observed to increase as the other voltages decreased. This is likely because the dual chamber MFC was cathode limited due to the small surface area of the AEM, although it is also possible that the low bulk pH may have been advantageous for the system by promoting proton transfer and minimizing any potential pH gradients that may have developed between the anode and cathode chambers. Whilst pH 4.0 caused a complete cessation of electrogenic activity in the material 3 and 4 biofilms, the material 1 and 2 biofilms maintained some activity. When the pH was then restored to 7.0 materials 1 and 2 recovered their initial voltage within 4 hours, demonstrating that the bacterial cells had not been adversely damaged. In contrast the material 3 and 4 voltages took > 4 days to recover showing that bacterial cell death had occurred.

Scanning electron microscopy was used to assess the levels biofilm growth on the different material structures (Fig-7.12).

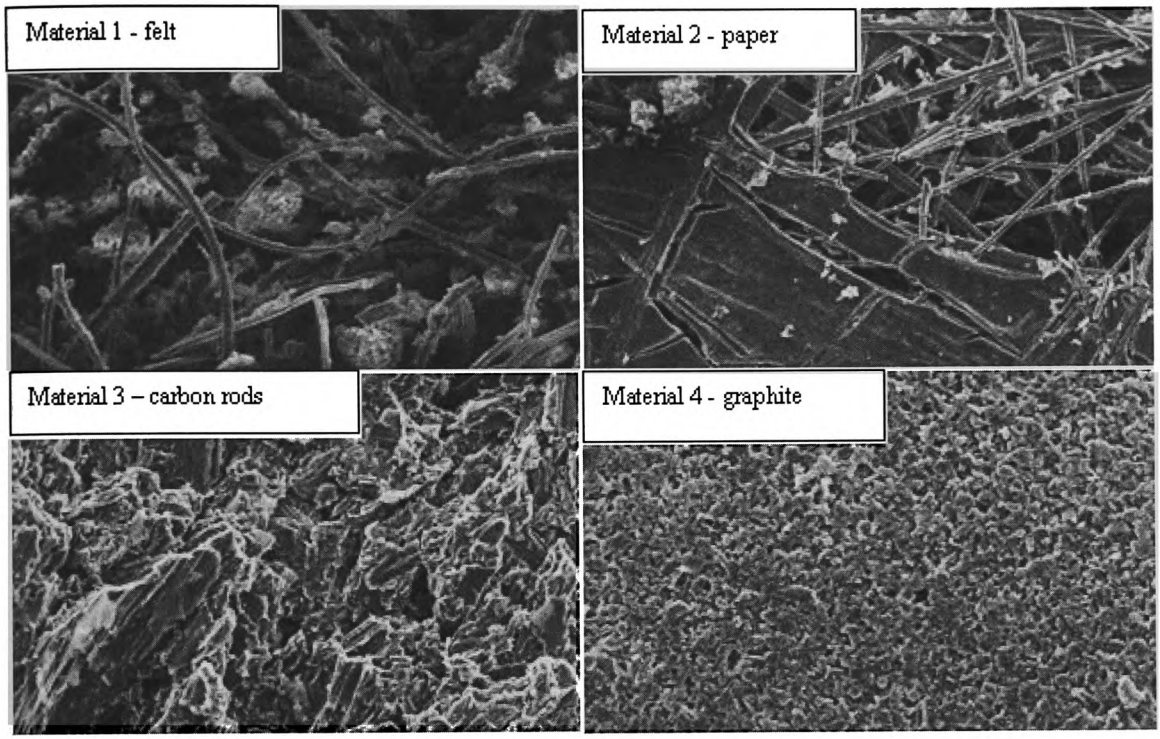

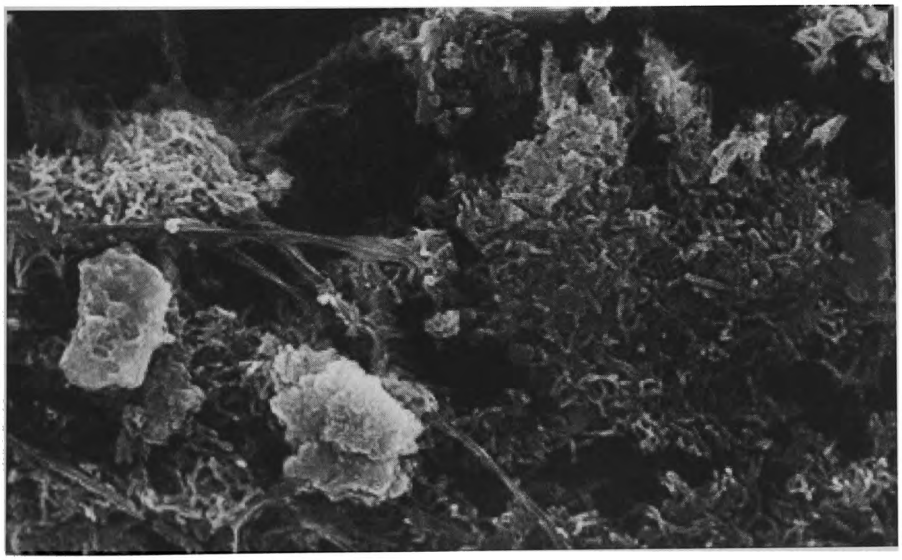

Figure 7-12. SEM pictures showing biofilm build-up and microbial growth on different test carbon materials (a) 450 X and (b) 4000 X magnification (carbon felt).

Using SEM microscopy to view the felt material it was possible to observe a thick and dense biofilm had formed, with copious levels of biomass developing along the carbon fibres (Fig 7.12); the development of this biomass was further observed in CSLM images of the felt materials (Fig 7.14). Increasing the SEM magnification showed that a large number of bacteria were attached both over the surface of the carbon material but also within the porous structure. High levels of biomass were also present on the fibres associated with the carbon paper, although less biofilm seemed to have accumulated within the depth on the anode due to the more compact nature of the carbon paper. It can be clearly seen that materials 2, 3 and 4 provide a less active surface area (available for microbiological attachment and growth).

As carbon felt biofilms were found to facilitate the highest power densities and could provide some protection from low pH perturbation, it was decided to examine the material (1) using a CLSM microscope to understand how the porous carbon structure affected bacterial phylogeny, colonization and growth.

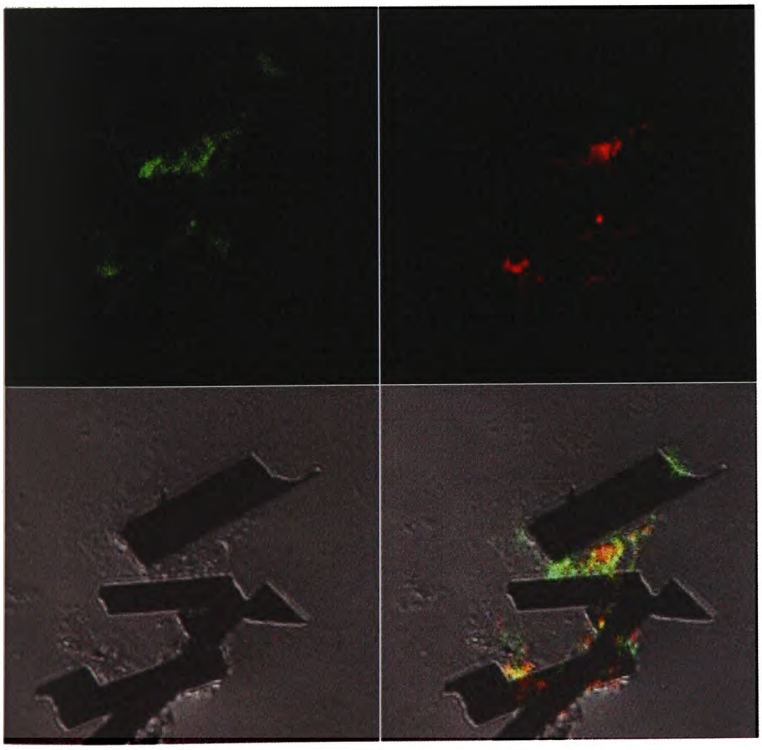

Figure 7-13. CLSM split images of Archaeal (red) and Eubacterial (green) bacteria within the biofilm

Biofilm development from carbon felt samples were analysed for the presence and spatial organization of Archaeal and Eubacterial species (EUB I and III) (Fig 7.13). Light microscopy showed

that significant biofilm developed both on and between the carbon fibres. Although significant levels of Archaea (red colour) were observed these were found to be generally located remotely from the carbon anode; in contrast, Eubacteria tended to be more closely associated with the anode carbon surfaces (Fig 7.13).

When the same carbon fibres were then analysed using a probe set targeting gamma and δ Proteobacteria this again showed differences in the localized distribution of the bacterial groups, with the gamma Proteobacteria (green) being more associated with diffuse biofilm remotely sited from the anode and delta Proteobacteria tending towards a closer proximity along the length of the carbon fibres (Fig 7.14).

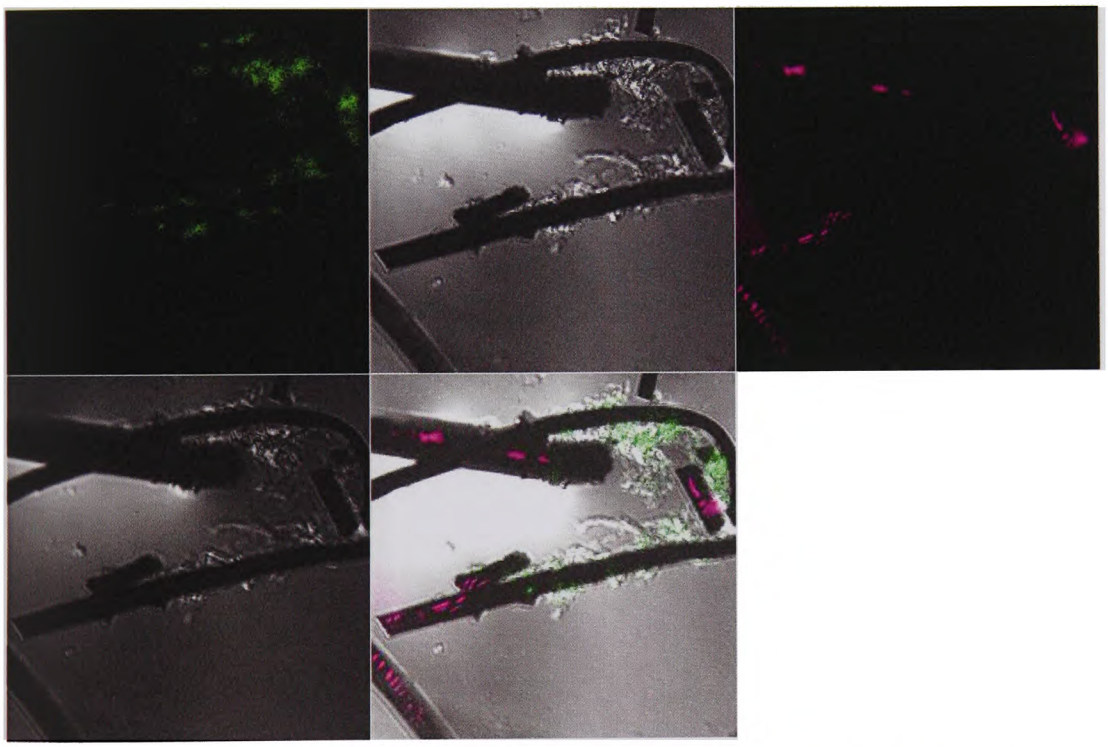

Figure 7-14. CLSM split images of γ Proteobacteria (purple) and δ Proteobacteria (green) bacteria

Prominent members of enriched MFCs have been often found to be members of the Geobacteraceae cluster of species (Chae et al. 2009; Torres et al. 2009a) and these bacteria have demonstrated the ability to respire directly to a solid anode (Mehta et al. 2005). The delta Proteobacteria observed here may represent a pre-dominance of this Genus, as has been previously reported (Lee et al. 2003; Kiely et al. 2010). In contrast family members of the γ Proteobacteria group such as *Shewanella spp.* and Pseudomonaceae have a greater tendency to respire

anaerobically by producing exogenous mediators such as flavins and pyocyanins to facilitate electron transfer to a remote anode surface (Rabaey et al. 2004; Marsili et al. 2008a).

To investigate whether the δ Proteobacteria cells, that were observed to be in close proximity with/sited along the length of the carbon fibres, could be capable of direct electron transfer to the carbon anode through being part of the Geobacter group of organisms, a specific FISH probe for a Geobacter cluster of the δ proteobacteria was used for microscopic analysis. This specific probe confirmed the presence of the *Geobacter spp.*, and in accordance with Fig 7.15, these were also found to reside in close proximity to the anode along the length of the carbon fibres.

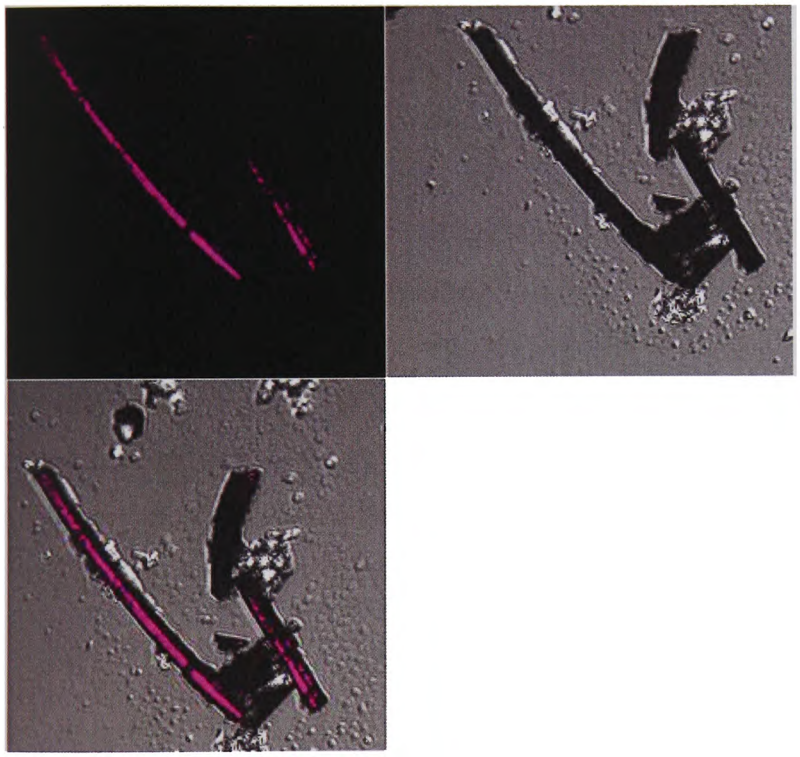

Figure 7-15. CLSM split images of Geobacter cluster bacteria (purple) located on carbon felt fibres.

It was similarly found that *Geobacter spp.* were also present in the other anode materials that were found to produce high current densities. Figure 7.16 shows graphite rod particles stained with the Geobacter cluster FISH probe, this shows *Geobacter spp.* present in lower numbers than observed on the carbon felt fibres.

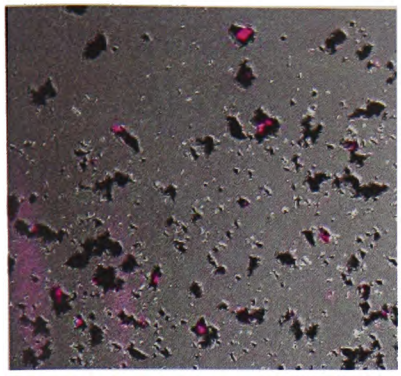

Figure 7-16. CLSM split images of Geobacter cluster bacteria (purple) located on particles of graphite carbon.

7.1.2 The effect of controlled external load on anodic biofilm development

The application of a controlled load (LC-MFC) algorithm to the test MFC reactor resulted in an improvement in the reactor performance when compared with the uncontrolled reactor (SL-MFC) where no control was applied (Fig 7.17). The former generated 1600±400 coulombs producing a CE range of 15.1% to 22.7%, compared to 300±10 coulombs generated with the fixed load system and a CE range of 3.3% to 3.7%. This showed that constant control of the loading and power optimization led to improved biocatalytic activity, as demonstrated by a higher proportion of electrons being harvested via the anode as opposed to other potential electron sinks i.e. methanogenesis. This means that within the LC-MFC the EAB are more active, have less metabolic competition, are better acclimated and/or are more optimally organized within the electrogenic biofilm.

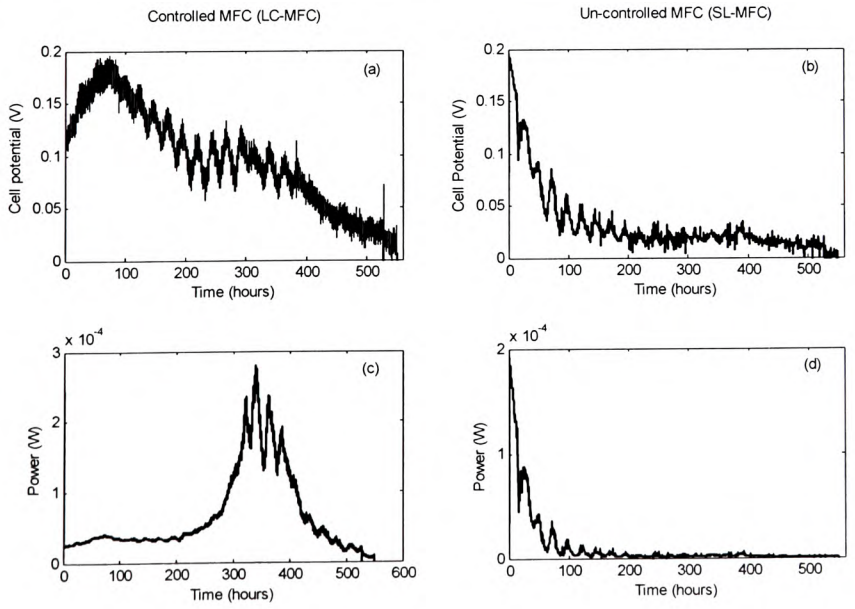

Figure 7-177. Evolution of MFC potential and power generation in LC-MFC (a&c) load controlled and SL-MFC (b&d) un-controlled MFC (load is constant 200Ω). Graphs supplied by Dr.Jung-Rae Kim.

Contents

To further understand differences in acclimation between the controlled and uncontrolled operation the biofilm samples were analysed by DGGE using both bacteria and archaeal primers. Community profiles of bacteria and archaea reveal distinct differences developed between LC-MFC and SL-MFC biofilms (Fig. 7.18).

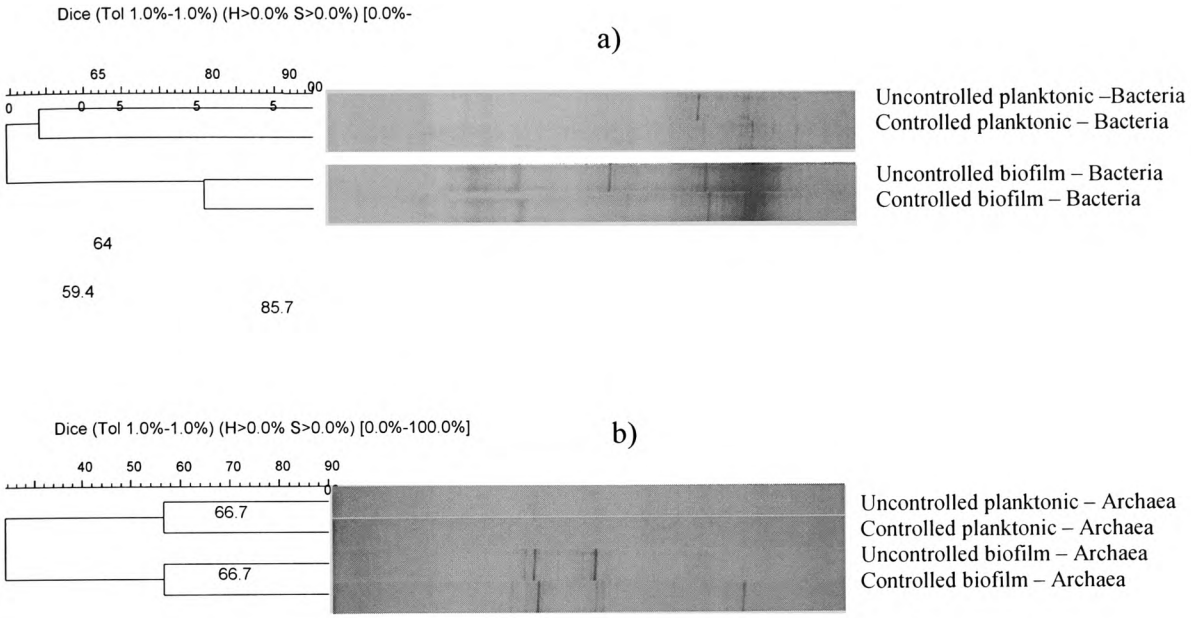

Figure 7-18. DGGE bacterial and archaeal community profiles from controlled and uncontrolled MFCs. Cluster analysis was carried out using the Dice coefficient of similarity measurement: a) Bacterial banding profile (LC-MFC and SL-MFC); b) Archaeal banding profile (LC-MFC and SL-MFC.

Cluster Analysis was carried out to analyze the levels of similarity that existed between between DGGE bands produced by both anode electrode biofilm and planktonic populations of bacteria and archaea. Fig 7.18 indicates that the similarity index values between LC- and SL-MFC bacteria biofilms was relatively high (85.7%) when compared with that of the planktonic suspension (64%), but the level of similarity between the archaeal biofilm and suspension was at an equally low level of 66.7% for both profiles (Fig 7.18). This result suggests that the load control activity influences both bacterial and archaeal community development, but archaeal communities were more affected. This may reflect the low selective influence on this population group especially with regard to the application of the control algorithm. In support with the finding that SL-MFC resulted in a lower coulombic efficiency when compared with the LC-MFC Chae et al (2010) reported that lower methanogenic populations (in gene copy number) were obtained in the lower resistance (50 Ω) systems than at higher resistances (600 Ω), implying that load affects methanogen development on

anode electrode. Therefore, it is possible that automatically optimizing the external resistance and potential power output might successfully reduce non-electrogenic side reactions (e.g. methanogenesis and biomass production), so improving the overall performance of MFC system.

The functional organization of the bacterial biofilm communities was investigated through Pareto-Lorenz evenness plots (Fig. 7.19). The 20% intercept point on the x-axis can be used as an evenness score measurement; it can be observed that the LC-MFC measured 32% indicating a higher degree of evenness as compared with the SL-MFC which measured 48%. A higher evenness value of 32% in the LC-MFC indicates of a higher functional spread of Bacteria may have been present in this biofilm community. This could suggest an increased functional flexibility to environmental change relating to the constant changes in external load resistance initiated in LC-MFC when compared to the static load conditions present in the SL-MFC reactor.

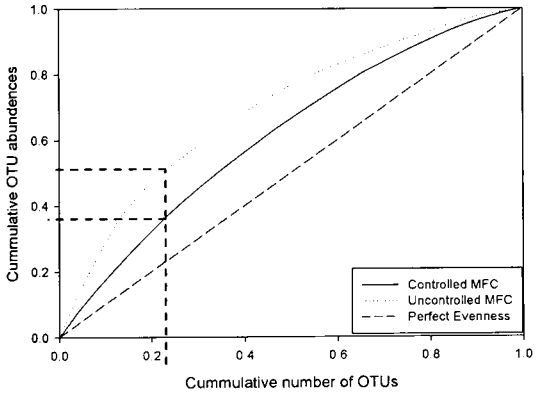

Figure 7-19. Pareto-Lorenz evenness graph for LC-MFC and SL-MFC bacterial biofilm populations. DGGE bands profiles were ranked from high to low according to their cumulative intensities and cumulative number the of band results (scored using Dice's index of similarity).

The total amount of biomass was monitored as an indicator of biological activity; specifically by quantifying the level of DNA present at the end of the experiment (Table 7.4).

Table 7-4. Total biomass (DNA ng/µl) in LC-MFC and SL-MFC reactors

Reactor Sample	Total Biomass (ng/µl DNA)
SL-MFC Biofilm	314
LC-MFC Biofilm	144
SL-MFC Planktonic	3.5
LC-MFC Planktonic	10.9

The biomass present in the LC-MFC biofilm was observed to be less than half that in the SL-MFC biofilm (Table 7.17). This shows that these microorganisms were more electrogenically active and thus this further suggests that load control had an adverse affect on biomass formation and/or methanogenesis. The diversity of microbial (both archaeal and bacterial) species determined by Dice's index of similarity was observed to be higher in the LC-MFC than SL-MFC (bacterial community, 185.9 *c.f.* 150.9; archaeal community, 73.5 *c.f.* 43.4). This may further support the idea that a higher level of activity was facilitated in the controlled reactor.

7.2 Discussion

The importance of the carbon anode material derives from it providing the support structure for EAB biocatalytic activity and also because it acts to harvest electrons generated as part of the bacterial metabolism (Rabaey et al. 2005b). Table 7.1 demonstrates the differences in carbon density for each of the different carbon materials, with the relatively high resistance of the carbon felt also indicating poor electrical connectivity between the carbon fibres in this material. SEM pictures showed that the three dimensional structures of the 4 different materials differed considerably, with the felt having a loose porous network of fibres and the graphite having a solid structure with roughness exhibited only at the micro level. This then influenced the active surface area available for bacterial attachment and more generally influenced structure of electrogenic biofilm development. Hence the fact that carbon paper gave a lower power density compared to the carbon felt may be related to how tightly bound the carbon fibres were on a macroscale (Xie et al.

2011). It is important to determine the surface area that is accessible for microbial growth as BET surface area measurements have shown very high surface area in graphite due to its micro-porous structure (Liu et al. 2010) but the material also produced the lowest power density measurements (Fig 7.5). The power produced from the open circuit biofilm may in part be related to the levels of biomass that developed in the biofilm, as this was 4.5 fold higher than the carbon paper. The high open circuit biomass produced in the carbon rods may relate to large amounts of biomass building up in the internal tubes that made up the structure.

Cyclic voltammetry demonstrated that the material 1 produced biofilms (open and closed circuit) that had high levels of capacitive current and this may account for the open circuit performance in material 1. It is interesting to note the wide range anode potentials in the open circuit biofilm in contrast to defined potentials of −0.39 and −0.42 V (*vs.* Ag/AgCl) highlighted in closed circuit operation (Table 7.3). This would suggest that closed circuit operation selected for *Geobacter spp.* or bacteria with active cytochromes with similar mid-point potentials to those of *Geobacter spp.* cytochrome C proteins. Community analysis on anodic MFCs fed with acetate and packed with either carbon felt or granular graphite have shown that *Geobacter spp.* are selected for in both materials but the proportion is higher in the former material (Sun et al. 2011). Hence even with the similar bacterial community profiles produced in the closed circuit materials the proportions of active bacteria may differ between them. Results from FISH microscopy seemed to support this result. It would seem that colonization of the carbon material using an enriched MFC effluent facilitates the growth of Geobacter cluster bacteria that are suited to direct anaerobic respiration by electron transfer via c-type cytochromes externally sited on cell membranes or possibly 'nanowire' conductive appendages. Other bacterial groups which may not possess a strong capability for direct electron transfer or are able to mediate remote electron transfer were observed to be more remotely located from the carbon electrode surfaces.

Previous studies on the influence of pH perturbation on MFC/anodic performance have shown that pH 7.0 is generally a preferred pH for high power production (He et al. 2008; Yuan et al. 2011), but pH 6.0 has also been found to be optimal in one dual chamber MFC reactor (Raghavulu et al. 2009). However, this study demonstrates that pH effects on electrogenic biofilms may be mediated by the three dimensional structure of the carbon material and its influence on biofilm development. pH affects the biofilm by changing electrostatic molecular interactions (Stoodley et al. 1997) with a drop of pH 7.0 to 6.0 being reported to severely limit growth and metabolism *of Geobacter Sulfurreductans* (Franks et al. 2009*)*. However high numbers of EAB close to the electrode and large amounts of biofilm between fibres may have acted to reduce pH effects, it is also possible

that there may also have been a cell density based modulated adaption to the low pH conditions (Li et al. 2001).

When a control algorithm was applied to MFC reactors in order to optimize the system power output the effect on the anodic biofilm communities was invstigated. Operation of load controlled (LC-MFC) and static load MFC (SL-MFC) systems resulted in similarity a score of 85.7 between both respective bacterial biofilm communities. These gel profiles show that a common range of electrogenically active bacteria existed in both controlled and uncontrolled reactors but some differences in the operational conditions may have been reflected in the development of some distinct bands.

High levels of microbial diversity were measured in both the LC-MFC and SL-MFC reactors, a figure of >30 being indicative of habitable environments (Marzorati et al. 2008). The higher diversity value in the former MFC may be a result of increased levels of electrochemical perturbation in the system as indicated by the control process producing more variable shifts in cell voltage and loading (Fig 7.17). It has been previously reported that perturbation can lead to increased microbial diversity in actively growing microbial populations (Rashit and Bazin 1987) and that this diversity can promote stability in engineered systems (Briones and Raskin 2003). The 'evenness' of the community also plays a role in maintaining functional stability and the higher level of evenness observed in the controlled reactor would indicate that this reactor was supporting a wider range of species capable of electrogenic activity.

A wider range of active bacteria may provide an optimized electrogenic activity over the range of anode potentials produced in the LC-MFC reactor. The ability of the microbial community to adapt to maximum power production in the controlled reactor would seem to be driven by microbial growth as this process took ~12 days, as opposed to being solely an adjustment of bacterial metabolic pathways or different respiratory cytochromes.

Whilst the growth of biofilm is often associated with increased current densities (Torres et al. 2009b) biomass accumulation can also be a significant electron sink along with other non-respiratory side reactions such as methanogenesis (Virdis et al. 2009), which then act to reduce CEs. The LC-MFC reactor in this experiment produced less than half the total biomass produced in the SL-MFC reactor (Table 8.1) but produced substantially more accumulated coulombic charge (Figure 8.1).

7.3 Conclusions

Dual chamber reactors were used to investigate the effect of carbon material and an optimized load on anodic biofilm development and MFC performance. The three dimensional structure of the carbon anode determined the power density achieved from each type of carbon material by modulating the electrogenic biofilm development. However it was found that open circuit incubation using carbon felt as an anode material contained bacteria capable of electrogenesis. Power density in the open circuit felt biofilm was 0.95 W m^{-3} compared to 1.40 W m^{-3} in closed circuit operation. *Geobacter spp.* were enriched in closed circuit operation, with mid-point anode potentials close to values reported for cytochromes from *Geobacter sulfurreductans*. The biofilm structure produced in the felt was also observed to protect the EABs from the effects of low pH perturbation.

Operation of the fuel cell under load control meant that the LC-MFC performance was enhanced when compared with the SL-MFC reactor, the system was also more robust to environmental perturbations such as substrate depletion and temperature fluctuation. The increased power production, coulombic efficiency and operational stability of the LC-MFC over the SL-MFC were derived from the automatic control of a resistive load. Improved performance of the EAB was derived from the selective pressure on the biofilm which favoured EAB that were capable of maximizing electrogenic activity in Lieu of alternative metabolic activities. Further development of the control algorithm, giving consideration to operating condition and system configuration could facilitate MFC technology implementation into real-world applications such as wastewater treatment and bioenergy recovery.

8 Conclusions and further work

8.1 Summary of work

The anode biofilm plays a crucial role in the operation and functional stability of MFC reactors and it is the optimization of this biocatalytic capacity that can be viewed as a key factor in improving the performance of BES systems. The development of this anodic electrogenic activity is dependent on the ability of the constituent microbial species to uptake substrates, metabolize them and then facilitate electron transfer from the bacterial membranes though the biofilm matrix to the anode and cathode electrodes. This study examined the interaction of environmental factors such as temperature, substrate type, pH, anodic carbon material and optimized external loading on the development of anodic biofilms and how this then influenced MFC system performance.

Chapters 3 and 4 showed that anodic bacterial optimization with non-fermentable/fermentable substrates and a range of operational temperatures were associated with the selection of electrochemically active microbial consortia. As it was observed that acetate was both formed and consumed during MFC operation with butyrate and sucrose substrates and power production was highest with acetate as a sole substrate, it is possible that all electrical current was generated via this route. This would mean that the role of the anodic biofilm consortia could be to not only facilitate syntrophic wastewater hydrolysis and fermentation but also acetogenic metabolism prior to anaerobic respiration. *Geobacter spp.* have been commonly associated with MFCs generating high current densities, notably *Geobacter sulfurreducens* species and it is known that these bacteria preferentially metabolize acetate as an electron donor (Bond and Lovley 2003; Reguera et al. 2006; Kiely et al. 2010). The prominent role of *Geobacter spp.* in electrochemical activity in this study was further suggested by the FISH results in Chapter 7, these images showed a predominance of Geobacter group organisms closely associated with the anode electrode surface. However the requirement for diverse and complex metabolic interactions was recently demonstrated by the construction of an "artificial consortium" of bacteria isolated from an estuarine environment (Zhang et al. 2012). Interestingly analysis of the isolated bacteria showed that only 34% of the species were electrochemically active but that the mixed consortia still produced higher levels of power compared to the pure cultures isolated and tested.

Chapters 3 and 4 also demonstrated that substrate type and temperature have a dramatic effect on microbial community dynamics, the level of biofilm development and EAB activity. The trophic composition of the anodic biofilms was thus dictated by the substrate feed type and the capacity for microorganisms to develop syntrophic associations to degrade substrates of different

complexities. The complex nature of these interactions was further demonstrated by low temperature perturbation of the acclimated biofilms, where sucrose biofilms were found to be susceptible to this type of perturbative shock. However, biofilm acclimation at sub-mesophilic temperatures may provide a strategy to extract electrical energy from mixed wastewaters in temperate climates. The interaction of temperature and MFC operation especially during the enrichment step is likely to be an important factor in the low cost operation of MFC systems in temperate climates. Whilst it may be possible to acclimate anodic biofilms for robust MFC operation over the cyclic temperature ranges typically found in temperate climates, it seems that complex bacterial interactions in complex substrate types may make these systems more vulnerable to environmental shocks. This may have implications for scaled-up systems using real wastewaters, indeed Cusick et al (2011) reported that it was necessary during enrichment to add additional heat and acetate to a 1000L bioelectrochemical system designed to produce hydrogen from winery wastewaters to ensure a successful enrichment. A start-up temperature of 20°C would seem to allow the development of psychrotrophic electrogenic bacteria that are capable of operation over a typical temperature range but with time-frame that is not operationally prohibitive.

AD sludge was used as the inoculum in all experiments; the use of this inoculum type (generated from mesophilic operation) was not an impediment to the biofilm selection process, notably in the temperature controlled start-up experiments in Chapter 4 using acetate as a substrate. In this experiment the enrichment process was elongated at psychrophilic temperatures but the final voltage out-put was the same for each MFC reactor. It is likely that this elongated enrichment was due to the low numbers of psychrophilic bacteria as well as their lower relative growth rates, this result concurs with previous observations by Rabaey et al (2005) that inoculum source was not a strong factor in final EAB development and that sufficient inherent diversity was present to facilitate acclimation. However differences in MFC batch performance were observed to occur over time and this was attributed to structural aspects of the biofilm development, notably differential accumulation of non-electrogenic biomass affecting mass transfer characteristics and the electrogenic efficacy (Chapter 5). It is also likely that improved mass transfer as well as increased available surface areas available for bacterial colonization can account for improved performance observed at higher flow rates and when using helical architectures (Chapter 6). Although the comparison with an annular system which had been operational for >1 year showed that suitable enrichment of electrogenic bacteria was likely to an equally important factor.

The use of multiple layered anodes showed that the potential for anodic colonization and electrogenic activity was not necessarily limited to the outermost/top layers of the electrode when

using a porous carbon veil material (Chapter 3, 5 and 6). Hence the influence of different carbon structures on biofilms development and electrogenic performance was tested in chapter 7. Here it was shown that the use of a very porous carbon felt material could be used to improve mass transfer events by providing an anode environment with large pore sizes suitable for colonization at a microbiological scale, thus promoting biofilm formation and total electrogenic activity. Controlling the circuit loading to optimize power production (Chapter 8) also led to an increase in biofilm levels compared to a control suggesting a selective increase in the numbers of EAB. Optimizing the system power means that bacterial electron transfer is also optimized such that the net electron gain is balanced against the system conditions and the metabolic activity of the bacteria. Recent results also suggest that controlling (poising) anode potentials to improve anodic performance must be maintained beyond the enrichment phase in order to retain these acclimated benefits (Sun et al. 2012) indicating that this operation should be maintained to retain optimal EAB activity.

It has been demonstrated that a number of factors will affect both the structure and the composition of the anodic biofilms and thus influence MFC performance. The results from this study help to advance our knowledge on how these electrogenic biofilms are able to function at ambient temperatures (typically experienced in temperate climates), are able to form consortia that can metabolize a range of substrate types and how anodic performance can be improved through optimization of anode architecture, type of carbon material and manipulation of the external loading.

Whilst this work addresses some of the key known obstacles associated with the anodic operation and the commercial scale-up of MFCs, others groups are also targeting other factors which may limit the commercial application of these types of systems : this includes the replacement of expensive ion exchange membranes with low cost separators (Zhang et al. 2011b), the development of low cost functionally efficient cathodes (Chen et al. 2012) and the potential chemical modification of carbon anode materials to facilitate enhanced electron transfer rates and suitable strategies to increase the transfer of protons to the cathode (Lai et al. 2011).

8.2 Conclusions

- When different fermentable and non-fermentable substrate types were tested in MFCs it was found that this had an effect on the microbial community dynamics, the level of biofilm development and the EAB activity. The type and complexity of the substrate dictated the trophic composition of the anodic biofilms and the capacity for a consortia of microorganisms to develop syntrophic associations in order to degrade these substrates. The complex nature of these interactions was further demonstrated by low temperature perturbation of the substrate acclimated biofilms, which showed that the sucrose reactor (anodic biofilm) was the most vulnerable to this perturbation event; this was possibly due to the more complex metabolic syntropic interactions that were active within the sucrose biofilm.

- To develop a robust microbial biocatalyst on the anode single-chamber tubular reactors were acclimated for operation at 10°C, 20°C and 35°C. This showed an adaptive capability of the temperature acclimated biofilms and demonstrated how MFC operation at different pyschrophilic and mesophilic temperatures affected rates of power generation, organic removal and levels of energy recovery. It was found that only those MFC systems acclimated at 20°C were capable of operating at maximum voltage (as per by the MFC system used in this experiment) over a 8-35°C temperature range and this capacity was facilitated by the selective activity of psychrotolerant microorganisms. This work suggests that it may be possible to develop MFCs that are both scalable and functionally stable at a range of operating temperatures; this could then allow systems the capability of water treatment and bioenergy recovery in temperate climates without the need for a substantial power input in terms of an external heat source.

- Substrate type and operational temperature were found to affect the development of biofilm biomass and biocatalytic capacity of anodic biofilms. Lower anode overpotentials developed at lower temperatures due to better mass transfer capabilities of the biofilm; at 60 weeks the 10°C, 20°C and 35°C reactors had internal resistance values of 72, 68 and 198 Ohms respectively. The build-up of biomass can lead to an impeded conductive barrier forming between the anode interface and EAB present in the biofilm and this was associated with increased rates of methanogenesis at 35°C of 10.1 mol CH_4 g^{-1} d^{-1} compared to 0.28 mol CH_4 g^{-1} d^{-1} at 20°C. It was further demonstrated that exposure of the 35°C biofilm to high hydrodynamic forces caused biofilm sloughing to occur and subsequently led to improvements in MFC performance by a factor of 3.5.

- The three dimensional structure of the carbon anode determined the power density achieved from different types of carbon anode material by modulating electrognic biofilm development. Carbon felt with a porous loose network of carbon fibres produced the highest current density of 1.40 Wm^{-3} in closed circuit operation. However it was also found that open circuit incubation using carbon felt as an anode material produced a power density of 0.95 Wm^{-3}. *Geobacter spp.* were enriched in closed circuit operation, with mid-point anode potentials close to values reported for cytochromes from *Geobacter sulfurreductans*. The carbon felt biofilm was also observed to protect these EAB from the effects of low pH perturbation. Thus the choice of anode material was found to have a large impact on MFC performance in terms of enrichment, operational stability and power output.

- Anodic structure and configuration had a large impact on carbon veil anode performance. The porous nature of the carbon veil meant that bacterial colonization could occur through the entire depth of anode but the majority of the biocatalytic activity was focused on carbon veil layers 1 to 3. This meant that multiple carbon veil layers within the anode could provide an increased surface area for EAB activity, however this activity could be limited by mass transfer characteristic associated with the biofilm development. The spiral reactor with the smallest gap produced the highest coulombic efficiency of 7% and a maximum power density of 11.63 W m^{-3}. Turbulent conditions induced at high flow rates in the SP1 reactor (small gap) stimulated increased biomass in layers 1 to 3 of the carbon veil anode. This reflected the surface area available for electrogenic activity being a function of not only the actual surface area but also the hydrodynamic forces that impacted on mass transfer into the biofilm and porous carbon veil. However the importance of a long enrichment step was also indicated by the high power densities produced by the annular reactor which had been enriched for a period of > 1year.

- Operation of the fuel cell under load control meant that the LC-MFC performance was enhanced when compared with the SL-MFC reactor. The increased power production, coulombic efficiency and operational stability of the LC-MFC over the SL-MFC were derived from the automatic control of a resistive load. Improved performance of the EAB was derived from the selective pressure on the biofilm which favoured EAB that were capable of maximizing electrogenic activity in lieu of alternative metabolic activities.

- The process of acclimation is crucial to the production of anodic biofilms that are robust to environmental perturbations and can produce high levels of power. Electrogenic biofilm development is integral to MFC performance as this dictates the activity and capacity of biocatalytic activity, but this process will also be subject to the environmental operating conditions and the design of individual types of BES reactor.

8.3 Further work

Although it was demonstrated that MFC reactors/anodic biofilms could be acclimated for pychrophilic, psychrotrophic and mesophilic operation, the bacterial species that were selected for during the acclimation process should be characterized. Pyrosequencing or clone library analysis techniques could provide a full and detailed examination of the phylogenic range of Bacteria and Archaea present in the anodic biofilms and provide an understanding and relative abundances of the active bacterial species present. This would look to support results obtained using DGGE community analysis. Similarly, sequencing of substrate acclimated biofilms would yield more specific information about the trophic groups present, the potential syntrophic relationships that might exist in different substrate fed reactors and how these microbial communities might have affected MFC performance results when substrate-switch experiments were run. MFCs acclimated with acetate, butyrate and sucrose substrates should be tested in continuous flow operations and the performance monitored. It would then be possible to test the applicability of operating the differentially acclimated MFC reactors when connected in series under different continuous flow conditions. The efficacy of this system should be monitored in terms of COD removal and electron recovery using sucrose as a substrate and be tested against systems acclimated using sucrose and acetate as single enrichment substrates. The performance of each module could then be assessed relative to VFA production, COD removal and power generation. The performance of these systems should then be tested with a range of different wastewater types and the effect of complex substrates on trophic population development be further assessed. The possibility of using MFC reactors as integrated second or third stage wastewaters processing operations using effluent from biohydrogen and/or AD fermentations could then also be investigated.

Modeling simulations of three dimensional velocity plots should be carried out on the three spiral anode configurations used in this study. From these results, shear rates and

levels of turbulence could be calculated to assess the effect on community development and electrochemical performance. Further anode configurations could also be designed to maximize internal turbulence rates as a way of increasing mass transfer rates with the aim of increasing electrical productivity and/or treatment capacity, and increasing the effective surface areas whilst minimizing the energy inputs i.e. costs associated with pumping. The effects of different turbulent conditions on biofilm growth in different porous carbon materials and how this influences the bacterial growth through the depth of these anodes could be examined using quantitative molecular/microscopy techniques.

Further work should be carried out to examine the composition of the EPS and its effect on electron transfer through the biofilm. It would be useful to understand which components of the biofilm are actively involved in this process. It is known that DNA can be actively produced as a structural component of the biofilm but how extensive this process is in electrogenic biofilms is unclear, as is contribution of EPS DNA to exocellular electron flows to the anode.

This study demonstrated that acclimation strategies can be used to develop MFC anodic biofilms that are able to operate under a range of environmental conditions which are associated with the potential commercial scale-up of these reactor systems. To test the feasibility of single-chamber tubular system for scale-up, a plurality of MFCs systems could be constructed for continuous operation based on helical designs that are able to optimize mass transfer effects. These would undergo an extended enrichment at 20°C using acetate and the target wastewater as enrichment substrates. The control algorithm may also be modified to enhance the enrichment process and a modified control algorithm could be used to both monitor and optimize the electrogenic activities of individual chambers that make up the complete reactor system. This would mean that any issues to do with voltage reversal or sub-optimal activity in any given chamber could be addressed to maximize power output of the overall system. The system could be operated under temperate ambient conditions using a number of wastewater applications, but the creation of an integrated bioenergy/treatment system for biological fermentation effluents would be of particular interest. Acclimated anodes could also be developed for use in other BES applications such as microbial electrolysis cells for the production hydrogen, where high coulombic efficiencies and low rates of methanogenic activity could be expected to improve system performance. Although MFC technology has developed significantly in the last 10 years further work is required to both further improve the performance of the reactors and also reduce

associated costs. It is hoped that by enhancing the treatment/electrogenic efficacy and rationalizing the reactor systems it will enable MFC technology to be utilized as part of an environmental and cost effective solution for the treatment of wastewaters.

9 References

Aelterman, P., Freguia, S., Keller, J., Verstraete, W. and Rabaey, K. (2008a) The anode potential regulates bacterial activity in microbial fuel cells. *Appl. Microbiol. Biotechnol.* **78**(3), 409-418.

Aelterman, P., Rabaey, K., Clauwaert, P. and Verstraete, W. (2006) Microbial fuel cells for wastewater treatment. *Water Science & Technology* **Vol 54** (No 8), 9-15.

Aelterman, P., Versichele, M., Marzorati, M., Boon, N. and Verstraete, W. (2008b) Loading rate and external resistance control the electricity generation of microbial fuel cells with different three-dimensional anodes. *Bioresource Technology* **99**(18), 8895-8902.

Ahn, Y. and Logan, B.E. (2010) Effectiveness of domestic wastewater treatment using microbial fuel cells at ambient and mesophilic temperatures. *Bioresource Technology* **101**, 469-475.

Ajayi, F.F., Kim, K.-Y., Chae, K.-J., Choi, M.-J. and Kim, I.S. (2010) Effect of hydrodymamic force and prolonged oxygen exposure on the performance of anodic biofilm in microbial electrolysis cells. *Int. J. Hydrog. Energy* **35**(8), 3206-3213.

Allen, R. and Bennetto, H. (1993) Microbial fuel-cells. *Applied Biochemistry and Biotechnology* **39-40**(1), 27-40.

Amato, P. and Christner, B.C. (2009) Energy Metabolism Response to Low-Temperature and Frozen Conditions in Psychrobacter cryohalolentis. *Appl. Environ. Microbiol.* **75**(3), 711-718.

Anon (2005). Regional electricity consumption statistics. Change, D.o.E.a.C.

Anon (2007). Energy and Sewage. Technology, P.o.f.S.a. **282**.

Armstrong, F.A. (2005) Recent developments in dynamic electrochemical studies of adsorbed enzymes and their active sites. *Current Opinion in Chemical Biology* **9**(2), 110-117.

Baker, G.C., Smith, J.J. and Cowan, D.A. (2003) Review and re-analysis of domain-specific 16S primers. *Journal of Microbiological Methods* **55**, 541- 555.

Bard, A.J. and Faulkner, L.R. (2001) Electrochemical methods : fundamentals and applications. John Wiley, New York.

Baron, D., Labelle, E., Coursolle, D., Gralnick, J.A. and Bond, D.R. (2009) Electrochemical Measurement of Electron Transfer Kinetics by Shewanella oneidensis MR-1. *Journal of Biological Chemistry* **284**(42), 28865-28873.

Bell, T., Newman, J.A., Silverman, B.W., Turner, S.L. and Lilley, A.K. (2005) The contribution of species richness and composition to bacterial services. *Nature* **436**, 1157-1160

Biffinger, J.C., Pietron, J., Bretschger, O., Nadeau, L.J., Johnson, G.R., Williams, C.C., Nealson, K.H. and Ringeisen, B.R. (2008) The influence of acidity on microbial fuel cells containing Shewanella oneidensis. *Biosensors and Bioelectronics* **24**(4), 900-905.

Boe-Hansen, R., Albrechtsen, H.J., Arvin, E. and Jorgensen, C. (2002) Bulk water phase and biofilm growth in drinking water at low nutrient conditions. *Water Research* **36**(18), 4477-4486.

Bond, D.R., Holmes, D.E., Tender, L.M. and Lovley, D.R. (2002) Electrode-Reducing Microorganisms That Harvest Energy from Marine Sediments *Science* **295**(5554), 483 - 485.

Bond, D.R. and Lovley, D.R. (2003) Electricity Production by *Geobacter sulfurreducens* Attached to Electrodes. *Applied and Environmental Microbiology* **69**(3), 1548-1555.

Boon, N., De Windt, W., Verstraete, W. and Top, E.M. (2002) Evaluation of nested PCR-DGGE (denaturing gradient gel electrophoresis) with group-specific 16S rRNA primers for the analysis of bacterial communities from different wastewater treatment plants. *FEMS Microbiology Ecology* **39**(2), 101-112.

Borole, A.P., Hamilton, C.Y., Vishnivetskaya, T., Leak, D. and Andras, C. (2009) Improving power production in acetate-fed microbial fuel cells via enrichment of exoelectrogenic organisms in flow-through systems. *Biochemical Engineering Journal* **48**(1), 71-80.

Briones, A. and Raskin, L. (2003) Diversity and dynamics of microbial communities in engineered environments and their implications for process stability. *Current Opinion in Biotechnology* **14**(3), 270-276.

Brown, D.G., Komlos, J. and Jaffe, P.R. (2005) Simultaneous Utilization of Acetate and Hydrogen by *Geobacter sulfurreducens* and Implications for Use of Hydrogen as an Indicator of Redox Conditions. *Environmental Science & Technology* **39**(9), 3069-3076.

Busalmen, J.P., Esteve-Nunez, A. and Feliu, J.M. (2008) Whole Cell Electrochemistry of Electricity-Producing Microorganisms Evidence an Adaptation for Optimal Exocellular Electron Transport. *Environmental Science & Technology* **42**(7), 2445-2450.

Busscher, H.J., Cowan, M.M. and Van Der Mei, H.C. (1992) On the relative importance of specific and non-specific approaches to oral microbial adhesion. *FEMS Microbiology Letters* **88**(3-4), 199-209.

Carver, S.M., Vuoriranta, P. and Tuovinen, O.H. (2011) A thermophilic microbial fuel cell design. *J. Power Sources* **196**(8), 3757-3760.

Chae, K.-J., Choi, M.-J., Lee, J.-W., Kim, K.-Y. and Kim, I.S. (2009) Effect of different substrates on the performance, bacterial diversity, and bacterial viability in microbial fuel cells. *Bioresource Technology* **100**(14), 3518-3525.

Chen, Y., Lv, Z., Xu, J., Peng, D., Liu, Y., Chen, J., Sun, X., Feng, C. and Wei, C. (2012) Stainless steel mesh coated with MnO2/carbon nanotube and polymethylphenyl siloxane as low-cost and high-performance microbial fuel cell cathode materials. *J. Power Sources* **201**(0), 136-141.

Cheng, K.Y., Cord-Ruwisch, R. and Ho, G. (2009) A new approach for in situ cyclic voltammetry of a microbial fuel cell biofilm without using a potentiostat. *Bioelectrochemistry* **74**(2), 227-231.

Cheng, S. and Logan, B.E. (2007) Ammonia treatment of carbon cloth anodes to enhance power generation of microbial fuel cells. *Electrochemistry Communications* **9**(3), 492-496.

Cheng, S., Xing, D. and Logan, B.E. (2010) Electricity generation of single-chamber microbial fuel cells at low temperatures. *Biosensors and Bioelectronics* **26**(5), 1913-1917.

Childers, S.E., Ciufo, S. and Lovley, D.R. (2002) Geobacter metallireducens accesses insoluble Fe(III) oxide by chemotaxis. *Nature* **416**(6882), 767-769.

Clauwaert, P., Aelterman, P., Pham, T.H., De Schamphelaire, L., Carballa, M., Rabaey, K. and Verstraete, W. (2008) Minimizing losses in bio-electrochemical systems: the road to applications. *Appl. Microbiol. Biotechnol.* **79**(6), 901-913.

Cohen, B. (1931) The Bacterial Culture as an Electrical Half-Cell. *Journal of Bacteriology* **21**, 18-19.

Compare, C., Bellonâe-Fontaine, M., Bertrand, P., Costa, D., Marcus, P., Poleunis, C., Pradier, C., Rondot, B. and Walls, M.G. (2001) Kinetics of conditioning layer formation on stainless steel immersed in seawater. *Biofouling* **17**(2), 129-145.

Connaughton, S., Collins, G. and O'flaherty, V. (2006) Psychrophilic and mesophilic anaerobic digestion of brewery effluent: A comparative study. *Water Research* **40**, 2503 - 2510.

Cruwys, J.A., Dinsdale, R.M., Hawkes, F.R. and Hawkes, D.L. (2002) Development of a static headspace gas chromatographic procedure for the routine analysis of volatile fatty acids in wastewaters. *Journal of Chromatography A* **945**(1-2), 195-209.

Cusick, R., Bryan, B., Parker, D., Merrill, M., Mehanna, M., Kiely, P., Liu, G. and Logan, B. (2011) Performance of a pilot-scale continuous flow microbial electrolysis cell fed winery wastewater. *Appl. Microbiol. Biotechnol.* **89**(6), 2053-2063.

Davis, J.B. and Yarbrough, H.F. (1962) Preliminary Experiments on a Microbial Fuel Cell. *Science* **137**(3530), 615-616.

Dewan, A., Beyenal, H. and Lewandowski, Z. (2008) Scaling up Microbial Fuel Cells. *Environmental Science & Technology* **42**(20), 7643-7648.

Elferink, S.J.W.H.O., Rinia, H.A., Bruins, M.E., Vos, W.M.D. and Stams, A.J.M. (1997) Detection and quantification of Desulforhabdus amnigenus in anaerobic granular sludge by dot blot hybridization and PCR amplification. *J. Appl. Microbiol.* **83**, 102-110.

Elmitwalli, T.A., Oahn, K.L.T., Grietje Zeeman and Lettinga, G. (2002) Treatment of domestic sewage in a two-step anaerobic filter/anaerobic hybrid system at low temperature *Water Research* **36,**(9), 2225-2232.

Feng, Y., Wang, X., Logan, B. and Lee, H. (2008) Brewery wastewater treatment using air-cathode microbial fuel cells. *Appl. Microbiol. Biotechnol.* **78**(5), 873-880.

Flemming, H.-C., Szewzyk, U. and Griebe, T. (2000) Title Biofilms : investigative methods & applications In, Lancaster, Pa. : Technomic Pub. Co.

Foley, J.M., Rozendal, R.A., Hertle, C.K., Lant, P.A. and Rabaey, K. (2010) Life Cycle Assessment of High-Rate Anaerobic Treatment, Microbial Fuel Cells, and Microbial Electrolysis Cells. *Environmental Science & Technology* **44**(9), 3629-3637.

Franks, A.E., Nevin, K.P., Jia, H., Izallalen, M., Woodard, T.L. and Lovley, D.R. (2009) Novel strategy for three-dimensional real-time imaging of microbial fuel cell communities: monitoring the inhibitory effects of proton accumulation within the anode biofilm. *Energy & Environmental Science* **2**(1), 113-119.

Freguia, S., Rabaey, K., Yuan, Z.G. and Keller, J. (2007) Electron and carbon balances in microbial fuel cells reveal temporary bacterial storage behavior during electricity generation. *Environmental Science & Technology* **41**(8), 2915-2921.

Freguia, S., Rabaey, K., Yuan, Z.G. and Keller, J. (2008) Syntrophic Processes Drive the Conversion of Glucose in Microbial Fuel Cell Anodes. *Environmental Science & Technology* **42**, 7937-7943.

Fricke, K., Harnisch, F. and Schroder, U. (2008) On the use of cyclic voltammetry for the study of anodic electron transfer in microbial fuel cells. *Energy & Environmental Science* **1**(1), 144-147.

Girvan, M.S., Campbell, C.D., Killham, K., Prosser, J.I. and Glover, L.A. (2005) Bacterial diversity promotes community stability and functional resilience after perturbation. *Environmental Microbiology* **7**(3), 301-313.

Gorby, Y.A. (2006) Bacterial nanowires: Electrically conductive filaments and their implications for en ergytrans formation and distribution in natural and engineered systems. *2006 Bio- Micro- and Nanosystems Conference*, 20-20.

Gorby, Y.A. (2007) Bacterial nanowires: Extracellular electron transfer and mineral transformation. *Geochim Cosmochim Ac* **71**(15), A345-A345.

Gorby, Y.A., Yanina, S., Mclean, J.S., Rosso, K.M., Moyles, D., Dohnalkova, A., Beveridge, T.J., Chang, I.S., Kim, B.H., Kim, K.S., Culley, D.E., Reed, S.B., Romine, M.F., Saffarini, D.A., Hill, E.A., Shi, L., Elias, D.A., Kennedy, D.W., Pinchuk, G., Watanabe, K., Ishii, S.I., Logan, B., Nealson, K.H. and Fredrickson, J.K. (2006) Electrically conductive bacterial nanowires produced by Shewanella oneidensis strain MR-1 and other microorganisms. *Proceedings of the National Academy of Sciences.* **103**(30), 11358-11363.

Grady, C.P.L., Daigger, G.T. and Lim, H.C. (1999) Biological wastewater treatment. Marcel Dekker, New York.

Gray, N.D. and Head, I.M. (2001) Linking genetic identity and function in communities of uncultured bacteria. *Environmental Microbiology* **3(8)**, 481-492.

Guwy, A.J., Dinsdale, R.M., Kim, J.R., Massanet-Nicolau, J. and Premier, G. (2011) Fermentative biohydrogen production systems integration. *Bioresource Technology* **102**(18), 8534-8542.

Hall-Stoodley, L., Costerton, J.W. and Stoodley, P. (2004) Bacterial biofilms: from the Natural environment to infectious diseases. *Nature Reviews Microbiology* **2**, 95-108.

Harnisch, F., Schrã¶Der, U. and Scholz, F. (2008) The Suitability of Monopolar and Bipolar Ion Exchange Membranes as Separators for Biological Fuel Cells. *Environmental Science & Technology* **42**(5), 1740-1746.

Harnisch, F. and Schroder, U. (2010) From MFC to MXC: chemical and biological cathodes and their potential for microbial bioelectrochemical systems. *Chemical Society Reviews* **39**(11), 4433-4448.

He, Z., Huang, Y., Manohar, A.K. and Mansfeld, F. (2008) Effect of electrolyte pH on the rate of the anodic and cathodic reactions in an air-cathode microbial fuel cell. *Bioelectrochemistry* **74**(1), 78-82.

Heering, H.A., Hirst, J. and Armstrong, F.A. (1998) Interpreting the catalytic voltammetry of electroactive enzymes adsorbed on electrodes. *J. Phys. Chem. B* **102**(35), 6889-6902.

Heidelberg, J.F., Paulsen, I.T., Nelson, K.E., Gaidos, E.J., Nelson, W.C., Read, T.D., Eisen, J.A., Seshadri, R., Ward, N., Methe, B., Clayton, R.A., Meyer, T., Tsapin, A., Scott, J., Beanan, M., Brinkac, L., Daugherty, S., Deboy, R.T., Dodson, R.J., Durkin, A.S., Haft, D.H., Kolonay, J.F., Madupu, R., Peterson, J.D., Umayam, L.A., White, O., Wolf, A.M., Vamathevan, J., Weidman, J., Impraim, M., Lee, K., Berry, K., Lee, C., Mueller, J., Khouri, H., Gill, J., Utterback, T.R., Mcdonald, L.A., Feldblyum, T.V., Smith, H.O., Venter, J.C., Nealson, K.H. and Fraser, C.M. (2002) Genome sequence of the dissimilatory metal ion-reducing bacterium Shewanella oneidensis. *Nat Biotech* **20**(11), 1118-1123.

Hernandez, M.E. and Newman, D.K. (2001) Extracellular electron Transfer. *CMLS Cell. Mol. Life. Sci* **58**, 1562 - 1571.

Holmes, D.E., Nicoll, J.S., Bond, D.R. and Lovley, D.R. (2004) Potential role of a novel psychrotolerant member of the family Geobacteraceae, Geopsychrobacter electrodiphilus gen. nov., sp nov., in electricity production by a marine sediment fuel cell. *Applied and Environmental Microbiology* **70**, 6023-6030.

Huang, L. and Logan, B. (2008) Electricity generation and treatment of paper recycling wastewater using a microbial fuel cell. *Appl. Microbiol. Biotechnol.* **80**(2), 349-355.

Ieropoulos, I., Greenman, J. and Melhuish, C. (2008) Microbial fuel cells based on carbon veil electrodes: Stack configuration and scalability. *International Journal of Energy Research* **32**(13), 1228-1240.

Ieropoulos, I., Winfield, J. and Greenman, J. (2010) Effects of flow-rate, inoculum and time on the internal resistance of microbial fuel cells. *Bioresource Technology* **101**(10), 3520-3525.

Inoue, K., Qian, X., Morgado, L., Kim, B.-C., Mester, T.N., Izallalen, M., Salgueiro, C.A. and Lovley, D.R. (2010) Purification and Characterization of OmcZ, an Outer-Surface, Octaheme c-Type Cytochrome Essential for Optimal Current Production by Geobacter sulfurreducens. *Applied and Environmental Microbiology* **76**(12), 3999-4007.

Intergovernmental, Solomon, S., Qin, D., Manning, M., Chen, Z., Marquis, M., Averyt, K.B., Tignor, M. and Miller, H.L. (2007) Climate Change 2007 - The Physical Science Basis: Working Group I Contribution to the Fourth Assessment Report of the IPCC. Cambridge University Press.

Jackson, B.E. and Mcinerney, M.J. (2002) Anaerobic microbial metabolism can proceed close to thermodynamic limits. *Nature* **415**(6870), 454-456.

Jadhav, G.S. and Ghangrekar, M.M. (2009) Performance of microbial fuel cell subjected to variation in pH, temperature, external load and substrate concentration. *Bioresource Technology* **100**, 717-723.

Jong, B.C., Kim, B.H., Chang, I.S., Liew, P.W.Y., Choo, Y.F. and Kang, G.S. (2006) Enrichment, performance, and microbial diversity of a thermophilic mediatorless microbial fuel cell. *Environmental Science & Technology* **40**(20), 6449-6454.

Jung, S. and Regan, J.M. (2007) Comparison of anode bacterial communities and performance in microbial fuel cells with different electron donors. *Appl. Microbiol. Biotechnol.* **77**(2), 393-402.

Jung, S. and Regan, J.M. (2011) Influence of External Resistance on Electrogenesis, Methanogenesis, and Anode Prokaryotic Communities in Microbial Fuel Cells. *APPLIED AND ENVIRONMENTAL MICROBIOLOGY* **77**(2), 564-571.

Karthikeyan, R., Rakshit, S. and Baradarajan, A. (1996) Optimization of batch fermentation conditions for dextran production. *Bioprocess and Biosystems Engineering* **15**(5), 247-251.

Kiely, P., Call, D., Yates, M., Regan, J. and Logan, B. (2010) Anodic biofilms in microbial fuel cells harbor low numbers of higher-power-producing bacteria than abundant genera. *Appl. Microbiol. Biotechnol.* **88**(1), 371-380.

Kim, B.H., Park, H.S., Kim, H.J., Kim, G.T., Chang, I.S., Lee, J. and Phung, N.T. (2004) Enrichment of microbial community generating electricity using a fuel-cell-type electrochemical cell. *Appl Microbiol Biotechnol* **63**, 672-681.

Kim, H.J., Park, H.S., Hyun, M.S., Chang, I.S., Kim, M. and Kim, B.H. (2002) A mediator-less microbial fuel cell using a metal reducing bacterium, Shewanella putrefaciens. *Enzyme Microb. Technol.* **30**(2), 145-152.

Kim, J., Lee, C., Shin, S. and Hwang, S. (2008a) Correlation of microbial mass with ATP and DNA concentrations in acidogenesis of whey permeate. *Biodegradation* **19**(2), 187-195.

Kim, J.R., Boghani, H.C., Amini, N., Aguey-Zinsou, K.-F.O., Michie, I., Dinsdale, R.M., Guwy, A.J., Guo, Z.X. and Premier, G.C. (In Press) Porous anodes with helical flow pathways in bioelectrochemical systems: The effects of fluid dynamics and operating regimes. *J. Power Sources*(0).

Kim, J.R., Cheng, S., Oh, S.E. and Logan, B.E. (2007) Power generation using different cation, anion, and ultrafiltration membranes in microbial fuel cells. *Environmental Science & Technology* **41**(3), 1004-1009.

Kim, J.R., Dec, J., Bruns, M.A. and Logan, B.E. (2008b) Removal of Odors from swine wastewater by using microbial fuel cells. *Applied and Environmental Microbiology* **74**(8), 2540-2543.

Kim, J.R., Min, B. and Logan, B.E. (2005) Evaluation of procedures to acclimate a microbial fuel cell for electricity production. *Appl. Microbiol. Biotechnol.* **68**(1), 23-30.

Kim, J.R., Premier, G.C., Hawkes, F.R., Dinsdale, R.M. and Guwy, A.J. (2009) Development of a tubular microbial fuel cell (MFC) employing a membrane electrode assembly cathode. *J. Power Sources* **187**, 393-399.

Kim, J.R., Premier, G.C., Hawkes, F.R., Rodriguez, J., Dinsdale, R.M. and Guwy, A.J. (2010) Modular tubular microbial fuel cells for energy recovery during sucrose wastewater treatment at low organic loading rate. *Bioresource Technology* **101**(4), 1190-1198.

Kim, J.R., Rodriguez, J., Hawkes, F.R., Dinsdale, R.M., Guwy, A.J. and Premier, G.C. (2011) Increasing power recovery and organic removal efficiency using extended longitudinal tubular microbial fuel cell (MFC) reactors. *Energy & Environmental Science* **4**(2), 459-465.

Knoblauch, C., Jorgensen, B.B. and Harder, J. (1999) Community Size and Metabolic Rates of Psychrophilic Sulfate-Reducing Bacteria in Arctic Marine Sediments. *Applied and Environmental Microbiology* **65**(9), 4230-4233.

Lai, B., Tang, X., Li, H., Du, Z., Liu, X. and Zhang, Q. (2011) Power production enhancement with a polyaniline modified anode in microbial fuel cells. *Biosensors and Bioelectronics* **28**(1), 373-377.

Lapara, T.M., Zakharova, T., Nakatsu, C.H. and Konopka, A. (2002) Functional and Structural Adaptations of Bacterial Communities Growing on Particulate Substrates under Stringent Nutrient Limitation. *Microbial Ecology* **44**(4), 317-326.

Larrosa-Guerrero, A., Scott, K., Head, I.M., Mateo, F., Ginesta, A. and Godinez, C. (2010) Effect of temperature on the performance of microbial fuel cells. *Fuel* **89**(12), 3985-3994.

Leang, C., Qian, X., Mester, T.N. and Lovley, D.R. (2010) Alignment of the c-Type Cytochrome OmcS along Pili of Geobacter sulfurreducens. *Applied and Environmental Microbiology* **76**(12), 4080-4084.

Lee, H.-S., Prathap Parameswaran, Andrew Kato-Marcus, Ce´Sar I. Torres and Rittmann, B.E. (2008) Evaluation of energy-conversion efficiencies in microbial fuel cells (MFCs) utilizing fermentable and non-fermentable substrates. *Water Research* **42**, 1501-1510.

Lee, J., Phung, N.T., Seopchang, I., Kim, B.H. and Sung, H.C. (2003) Use of acetate for enrichment of electrochemically active microorganisms and their 16S rDNA analyses. *FEMS Microbiology Letters* **223** 185-191.

Lettinga, G., Rebac, S. and Zeeman, G. (2001) Challenge of psychrophilic anaerobic wastewater treatment. *Trends in Biotechnology* **19**(9), 363-370

Li, Y.-H., Hanna, M.N., SvensãTer, G., Ellen, R.P. and Cvitkovitch, D.G. (2001) Cell Density Modulates Acid Adaptation in Streptococcus mutans: Implications for Survival in Biofilms. *Journal of bacteriology* **183**(23), 6875-6884.

Li, Z., Yao, L., Kong, L. and Liu, H. (2008) Electricity generation using a baffled microbial fuel cell convenient for stacking. *Bioresource Technology* **99**(6), 1650-1655.

Lies, D.P., Hernandez, M.E., Kappler, A., Mielke, R.E., Gralnick, J.A. and Newman, D.K. (2005) Shewanella oneidensis MR-1 Uses Overlapping Pathways for Iron Reduction at a Distance and by Direct Contact under Conditions Relevant for Biofilms. *Applied and Environmental Microbiology, August* **71**(8), 4414-4426.

Lin, C.-H. and O'brien, E.E. (1974) Turbulent shear flow mixing and rapid chemical reactions: an analogy. *Journal of Fluid Mechanics* **64**, 195-206.

Liu, H., Cheng, S., Huang, L. and Logan, B.E. (2008) Scale-up of membrane-free single-chamber microbial fuel cells. *J. Power Sources* **179**, 274-279.

Liu, H., Cheng, S. and Logan, B. (2005) Production of Electricity from Acetate or Butyrate Using a Single-Chamber Microbial Fuel Cell. *Environ. Sci. Technol.* **39**, 658-662.

Liu, H., Ramnarayanan, R. and Logan, B.E. (2004) Production of Electricity during Wastewater Treatment Using a Single Chamber Microbial Fuel Cell. *Environmental Science & Technology* **38**(7), 2281-2285.

Liu, W.-T., Marsh, T.L., Cheng, H. and Forney, L.J. (1997) Characterization of Microbial Diversity by Determining Terminal Restriction Fragment Length Polymorphisms of Genes Encoding 16S rRNA. *Applied and Environmental Microbiology* **Vol. 63,** (No. 11), 4516-4522.

Liu, Y., Harnisch, F., Fricke, K., Schroder, U., Climent, V. and Feliu, J.M. (2010) The study of electrochemically active microbial biofilms on different carbon-based anode materials in microbial fuel cells. *Biosens. Bioelectron.* **25**(9), 2167-2171.

Liu, Y. and Tay, J.-H. (2002) The essential role of hydrodynamic shear force in the formation of biofilm and granular sludge. *Water Research* **36**(7), 1653-1665.

Logan, B. (2008) Microbial fuel cells. Wiley-Interscience, Hoboken, N.J.

Logan, B. (2010) Scaling up microbial fuel cells and other bioelectrochemical systems. *Appl. Microbiol. Biotechnol.* **85**(6), 1665-1671.

Logan, B., Cheng, S., Watson, V. and Estadt, G. (2007) Graphite Fiber Brush Anodes for Increased Power Production in Air-Cathode Microbial Fuel Cells. *Environmental Science & Technology* **41**(9), 3341-3346.

Logan, B. and Regan, J. (2006a) Electricity-producing bacterial communities in microbial fuel cells. *Trends in Microbiology* **14**(12), 512-518.

Logan, B.E. (2009) Exoelectrogenic bacteria that power microbial fuel cells. *Nat Rev Micro* **7**(5), 375-381.

Logan, B.E., Hamelers, B., Rozendal, R., Schröder, U., Keller, J., Freguia, S., Aelterman, P., Verstraete, W. and Rabaey, K. (2006) Microbial Fuel Cells: Methodology and Technology. *Environ. Sci. Technol.* **40**(17), 5181-5192.

Logan, B.E. and Regan, J.M. (2006b) Electricity-producing bacterial communities in microbial fuel cells. *Trends in Microbiology* **14**(12), 512-518.

Logan, B.E. and Regan, J.M. (2006c) Microbial Fuel Cell: "Challenges and Applications. *Environmental Science & Technology* **40**(17), 5172-5180.

Lonergan, D.J., Jenter, H.L., Coates, J.D., Phillips, E.J.P., Schmidt, T.M. and Loveley, D.R. (1996) Phylogenetic Analysis of Dissimilatory Fe(III)-Reducing Bacteria. *J. Bacteriol* **178**, 2402 - 2408.

Lovley, D.R. (1997) Microbial Fe(III) reduction in subsurface environments. *Fems Microbiol Rev* **20**(3-4), 305-313.

Lovley, D.R., Giovannoni, S.J., White, D.C., Champine, J.E., Phillips, E.J.P., Gorby, Y.A. and Goodwin, S. (1993) Geobacter metallireducens gen. nov. sp. nov., a microorganism capable of coupling the complete oxidation of organic compounds to the reduction of iron and other metals. *Archives of Microbiology* **159**(4), 336-344.

Lovley, D.R., Holmes, D.E. and Nevlin, K.P. (2004) Dessimilatory Fe (III) and Mn (IV) Reduction *Advanced Microbial Physiology* **49**, 219 - 286.

Low, E.W. and Chase, H.A. (1999) The effect of maintenance energy requirements on biomass production during wastewater treatment. *Water Research* **33**(3), 847-853.

Lyon, D.Y., Buret, F., Vogel, T.M. and Monier, J.M. Is resistance futile? Changing external resistance does not improve microbial fuel cell performance. *Bioelectrochemistry* **78**(1), 2-7.

Lyon, D.Y., Buret, F., Vogel, T.M. and Monier, J.M. (2010) Is resistance futile? Changing external resistance does not improve microbial fuel cell performance. *Bioelectrochemistry* **78**(1), 2-7.

Madigan, M.T. and Brock, T.D. (2009) Brock biology of microorganisms. Pearson/Benjamin Cummings, San Francisco, CA.

Madsen, E.L. (2005) Identifying microorganisms responsible for ecologically significant biogeochemical processes. *Nature Reviews Microbiology* **3**, 439-446.

Magnuson, T.S. (2011) How the xap Locus Put Electrical Zap in Geobacter sulfurreducens Biofilms. *Journal of bacteriology* **193**(5), 1021-1022.

Magnuson, T.S., Isoyama, N., Hodges-Myerson, A.L., Davidson, G., Maroney, M.J., Geesey, G.G. and Lovley, D.R. (2001) Isolation, characterization and gene sequence analysis of a membrane-associated 89 kDa Fe(III) reducing cytochrome c from Geobacter sulfurreducens. *Biochem. J.* **359**(1), 147-152.

Männistö, M.K. and Puhakka, J.A. (2002) Psychrotolerant and microaerophilic bacteria in boreal groundwater *FEMS Microbiology Ecology* **41**(1), 9-16

Marsili, E., Baron, D.B., Shikhare, I.D., Coursolle, D., Gralnick, J.A. and Bond, D.R. (2008a) Shewanella secretes flavins that mediate extracellular electron transfer. *Proceedings of the National Academy of Sciences* **105**(10), 3968-3973.

Marsili, E., Rollefson, J.B., Baron, D.B., Hozalski, R.M. and Bond, D.R. (2008b) Microbial Biofilm Voltammetry: Direct Electrochemical Characterization of Catalytic Electrode-Attached Biofilms. *Applied and Environmental Microbiology* **74**(23), 7329-7337.

Marstorp, H., Guan, X. and Gong, P. (2000) Relationship between dsDNA, chloroform labile C and ergosterol in soils of different organic matter contents and pH. *Soil Biology and Biochemistry* **32**(6), 879-882.

Marstorp, H. and Witter, E. (1999) Extractable dsDNA and product formation as measures of microbial growth in soil upon substrate addition. *Soil Biology & Biochemistry* **31**(10), 1443-1453.

Marzorati, M., Wittebolle, L., Boon, N., Daffonchio, D. and Verstraete, W. (2008) How to get more out of molecular fingerprints: practical tools for microbial ecology. *Environmental Microbiology* **10(6)**, 1571-1581.

Mccoy, W.F. and Olson, B.H. (1985) Fluorometric Determination of the DNA Concentration in Municipal Drinking Water. *Applied and Environmental Microbiology* **Vol. 49**(No. 4), 811-817.

Mchugh, S., Collins, G. and O'flaherty, V. (2006) Long-term, high-rate anaerobic biological treatment of whey wastewaters at psychrophilic temperatures. *Bioresource Technology* **97**, 1669-1678.

Mehta, T., Coppi, M.V., Childers, S.E. and Lovley, D.R. (2005) Outer Membrane c-Type Cytochromes Required for Fe(III) and Mn(IV) Oxide Reduction in Geobacter sulfurreducens. *Applied and Environmental Microbiology* **71**(12), 8634-8641.

Melhuish, C., Ieropoulos, I., Greenman, J. and Horsfield, I. (2006) Energetically autonomous robots: Food for thought. *Autonomous Robots* **21**(3), 187-198.

Methe, B.A., Nelson, K.E., Eisen, J.A., Paulsen, I.T., Nelson, W., Heidelberg, J.F., Wu, D., Wu, M., Ward, N., Beanan, M.J., Dodson, R.J., Madupu, R., Brinkac, L.M., Daugherty, S.C., Deboy, R.T., Durkin, A.S., Gwinn, M., Kolonay, J.F., Sullivan, S.A., Haft, D.H., Selengut, J., Davidsen, T.M., Zafar, N., White, O., Tran, B., Romero, C., Forberger, H.A., Weidman, J., Khouri, H., Feldblyum, T.V., Utterback, T.R., Van Aken, S.E., Lovley, D.R. and Fraser, C.M. (2003) Genome of Geobacter sulfurreducens: Metal Reduction in Subsurface Environments. *Science* **302**(5652), 1967-1969.

Michie, I.S., Kim, J.R., Dinsdale, R.M., Guwy, A.J. and Premier, G.C. (2011a) Operational temperature regulates anodic biofilm growth and the development of electrogenic activity. *Appl. Microbiol. Biotechnol.* **92**(2), 419-430.

Michie, I.S., Kim, J.R., Dinsdale, R.M., Guwyb, A.J. and Premier, G.C. (2011b) The influence of psychrophilic and mesophilic start-up temperature on microbial fuel cell system performance. *Energy & Environmental Science* **4**(3), 1011-1019.

Mitchell, P. (1961) Coupling of Phosphorylation to Electron and Hydrogen Transfer by a Chemi-Osmotic type of Mechanism. *Nature* **191**(4784), 144-148.

Moon, H., Chang, I.S. and Kim, B.H. (2006) Continuous electricity production from artificial wastewater using a mediator-less microbial fuel cell. *Bioresource Technology* **97**, 621-627.

Morita, R.Y. (1975) Psychrophilic Bacteria. *Bacteriological Reviews* **39**(2), 144-167.

Morozan, A., Stamatin, I., Stamatin, L., Dumitru, A. and Scott, K. (2007) Carbon electrodes for microbial fuel cells. *Journal of Optoelectronics and Advanced Materials* **9**(1), 221 - 224.

Müller, N., Worm, P., Schink, B., Stams, A.J.M. and Plugge, C.M. (2010) Syntrophic butyrate and propionate oxidation processes: from genomes to reaction mechanisms. *Environmental Microbiology Reports* **2**(4), 489-499.

Muyzer, G. and Smalla, K. (1998) Application of denaturing gradient gel electrophoresis (DGGE) and temperature gradient gel electrophoresis (TGGE) in microbial ecology. *Antonie van Leeuwenhoek* **73**, 127-141

Nevin, K.P., Richter, H., Covalla, S.F., Johnson, J.P., Woodard, T.L., Orloff, A.L., Jia, H., Zhang, M. and Lovley, D.R. (2008) Power output and columbic efficiencies from biofilms of Geobacter sulfurreducens comparable to mixed community microbial fuel cells. *Environmental Microbiology* **10**(10), 2505-2514.

Nien, P.-C., Lee, C.-Y., Ho, K.-C., Adav, S.S., Liu, L., Wang, A., Ren, N. and Lee, D.-J. (2011) Power overshoot in two-chambered microbial fuel cell (MFC). *Bioresource Technology* **102**(7), 4742-4746.

Oh, S.T., Kim, J.R., Premier, G.C., Lee, T.H., Kim, C. and Sloan, W.T. (2010) Sustainable wastewater treatment: How might microbial fuel cells contribute. *Biotechnol. Adv.* **28**(6), 871-881.

Okabe, S., Satoh, H. and Watanabe, Y. (1999) In Situ Analysis of Nitrifying Biofilms as Determined by In Situ Hybridization and the Use of Microelectrodes. *Applied and Environmental Microbiology* **65**(7), 3182-3191.

Osborne, C.A., Galic, M., Parveen Sangwan and Janssen, P.H. (2005) PCR-generated artefact from 16S rRNA gene-specific primers. *FEMS Microbiology Letters* **248**, 183-187.

Pant, D., Singh, A., Van Bogaert, G., Gallego, Y.A., Diels, L. and Vanbroekhoven, K. (2011) An introduction to the life cycle assessment (LCA) of bioelectrochemical systems (BES) for sustainable energy and product generation: Relevance and key aspects. *Renewable & Sustainable Energy Reviews* **15**(2), 1305-1313.

Pant, D., Van Bogaert, G., Diels, L. and Vanbroekhoven, K. (2010) A review of the substrates used in microbial fuel cells (MFCs) for sustainable energy production. *Bioresource Technology* **101**(6), 1533-1543.

Park, D.P. and Zeikus, J.Z. (2002) Impact of electrode composition on electricity generation in a single-compartment fuel cell using <SMALL>Shewanella putrefaciens</SMALL&gt. *Appl. Microbiol. Biotechnol.* **59**(1), 58-61.

Patil, S.A., Harnisch, F., Kapadnis, B. and Schroder, U. (2010) Electroactive mixed culture biofilms in microbial bioelectrochemical systems: The role of temperature for biofilm formation and performance. *Biosens. Bioelectron.* **26**(2), 803-808.

Pham, H.T., Boon, N., Aelterman, P., Clauwaert, P., De Schamphelaire, L., Van Oostveldt, P., Verbeken, K., Rabaey, K. and Verstraete, W. (2008) High shear enrichment improves the performance of the anodophilic microbial consortium in a microbial fuel cell. *Microbial Biotechnology* **1**(6), 487-496.

Pham, T.H., Rabaey, K., Aelterman, P., Clauwaert, P., Schamphelaire, L.D., Boon, N. and Verstraete, W. (2006) Microbial Fuel Cells in Relation to Conventional Anaerobic Digestion Technology. *Eng. Life Sci.* **6**(3), 285-292.

Picioreanu, C., Head, I.M., Katuri, K.P., Van Loosdrecht, M.C.M. and Scott, K. (2007) A computational model for biofilm-based microbial fuel cells. *Water Research* **41**(13), 2921-2940.

Picioreanu, C., Van Loosdrecht, M.C.M. and Heijnen, J.J. (2001) Two-dimensional model of biofilm detachment caused by internal stress from liquid flow. *Biotechnology and Bioengineering* **72**(2), 205-218.

Pinto, R.P., Srinivasan, B., Manuel, M.F. and Tartakovsky, B. (2010) A two-population bio-electrochemical model of a microbial fuel cell. *Bioresource Technology* **101**(14), 5256-5265.

Prathap Parameswaran, Ce'Sar I. Torres, Hyung-Sool Lee, Rosa Krajmalnik-Brown and Rittmann, B.E. (2009) Syntrophic Interactions Among Anode Respiring Bacteria (ARB) and Non-ARB in a Biofilm Anode: Electron Balances. *Biotechnology and Bioengineering* **In Press.**

Premier, G.C., Kim, J.R., Michie, I., Dinsdale, R.M. and Guwy, A.J. (2011) Automatic control of load increases power and efficiency in a microbial fuel cell. *J. Power Sources* **196**(4), 2013-2019.

Rabaey, K. (2007) Mirobial ecology meets electrochemistry: electricity-driven and driving communities. *The ISME Journal* **1**, 9-18.

Rabaey, K., Boon, N., Hofte, M. and Verstraete, W. (2005a) Microbial phenazine production enhances electron transfer in biofuel cells. *Environmental Science & Technology* **39**, 3401-3408.

Rabaey, K., Boon, N., Siciliiano, S., Verhaege, M. and Verstraete, W. (2004) Biofuel cells select for consortia that self-mediate electron transfer. *Applied and Environmental Microbiology* **70(9)**, 5373-5382.

Rabaey, K., Clauwaert, P., Aelterman, P. and Verstraete, W. (2005b) Tubular Microbial Fuel Cells for Efficient Electricity Generation. *Environ. Sci. Technol* **39**, 8077-8082.

Rabaey, K. and Rozendal, R. (2010) Microbial electrosynthesis - revisiting the electrical route for microbial production. *Nat Rev Micro* **8**(10), 706-716.

Rabaey, K. and Verstraete, W. (2005) Microbial fuel cells: novel biotechnology for energy generation. *Trends in Biotechnology* **23**(6), 291-298.

Raghavulu, S.V., Mohan, S.V., Goud, R.K. and Sarma, P.N. (2009) Effect of anodic pH microenvironment on microbial fuel cell (MFC) performance in concurrence with aerated and ferricyanide catholytes. *Electrochemistry Communications* **11**(2), 371-375.

Ramasamy, R.P., Ren, Z., Mench, M.M. and Regan, J.M. (2008) Impact of Initial Biofilm Growth on the Anode Impedance of Microbial Fuel Cells. *Biotechnology and Bioengineering* **101**(1).

Rashit, E. and Bazin, M. (1987) Environmental fluctuations, productivity, and species diversity: An experimental study. *Microbial Ecology* **14**(2), 101-112.

Reguera, G., Mccarthy, K.D., Mehta, T., Nicoll, J.S., Tuominen, M.T. and Lovley, D.R. (2005) Extracellular electron transfer via microbial nanowires. *Nature* **435**(7045), 1098-1101.

Reguera, G., Nevin, K.P., Nicoll, J.S., Covalla, S.F., Woodard, T.L. and Lovley, D.R. (2006) Biofilm and nanowire production leads to increased current in Geobacter sulfurreducens fuel cells. *Applied and Environmental Microbiology* **72**(11), 7345-7348.

Ren, Z., Ward, T.E. and Regan, J.M. (2007) Electricity Production from Cellulose in a Microbial Fuel Cell Using a Defined Binary Culture. *Environmental Science & Technology* **41**(13), 4781-4786.

Ren, Z.Y., Ramasamy, R.P., Cloud-Owen, S.R., Yan, H.J., Mench, M.M. and Regan, J.M. (2011) Time-course correlation of biofilm properties and electrochemical performance in single-chamber microbial fuel cells. *Bioresource Technology* **102**(1), 416-421.

Rittmann, B.E. (2006) Microbial ecology to manage processes in environmental biotechnology. *Trends in Biotechnology* **24**(6), 261-266.

Roest, K., Heilig, H., Smidt, H., Vos, W., Stams, A. and Akkermans, A. (2005) Community analysis of a full-scale anaerobic bioreactor treating paper mill wastewater. *System Appl. Microbiol* **28(2)**, 175-185.

Rozendal, R., Hamelers, H.V.M. and Buisman, C.J.N. (2006) Effects of Membrane Cation Transport on pH and Microbial Fuel Cell Performance *Environmental Science & Technology* **40**(17), 5206-5211.

Schink, B. and Stams, A.J.M. (2005) Syntrophism among prokaryotes. Springer, New York.

Shirtliff, M.E., Mader, J.T. and Camper, A.K. (2002) Molecular Interactions in Biofilms. *Chemistry & Biology* **9**(8), 859-871.

Shizas, I. and Bagley, D.M. (2004) Experimental Determination of Energy Content of Unknown Organics in Municipal Wastewater Streams. *Journal of Energy Engineering* **130**(2), 45-53.

Sich, H. and Van Rijn, J. (1997) Scanning electron microscopy of biofilm formation in denitrifying, fluidised bed reactors. *Water Research* **31**(4), 733-742.

Sleutels, T.H.J.A., Hamelers, H.V.M. and Buisman, C.J.N. (2011) Effect of mass and charge transport speed and direction in porous anodes on microbial electrolysis cell performance. *Bioresource Technology* **102**(1), 399-403.

Sleutels, T.H.J.A., Lodder, R., Hamelers, H.V.M. and Buisman, C.J.N. (2009) Improved performance of porous bio-anodes in microbial electrolysis cells by enhancing mass and charge transport. *Int. J. Hydrog. Energy* **34**(24), 9655-9661.

Spormann, A.M. and Romeo, T. (2008) Physiology of Microbes in Biofilms

Bacterial Biofilms. In. 322, pp 17-36, Springer Berlin Heidelberg.

Srikanth, S., Mohan, S.V. and Sarma, P.N. (2010) Positive anodic poised potential regulates microbial fuel cell performance with the function of open and closed circuitry. *Bioresource Technology* **101**(14), 5337-5344.

Stams, A.J.M., Bok, F.A.M.D., Plugge, C.M., Eekert, M.H.A.V., Dolfing, J. and Schraa, G. (2006) Exocellular electron transfer in anaerobic microbial communities. *Environmental Microbiology* **8**(3), 371-382.

Stenstrom, J., Stenberg, B. and Johansson, M. (1998) Kinetics of substrate-induced respiration (SIR): Theory. *Ambio* **27**(1), 35-39.

Stewart, P.S. and William Costerton, J. (2001) Antibiotic resistance of bacteria in biofilms. *The Lancet* **358**(9276), 135-138.

Stoodley, P., Debeer, D. and Lappin-Scott, H.M. (1997) Influence of electric fields and pH on biofilm structure as related to the bioelectric effect. *Antimicrobial Agents and Chemotherapy* **41**(9), 1876-9.

Summers, Z.M., Fogarty, H.E., Leang, C., Franks, A.E., Malvankar, N.S. and Lovley, D.R. (2010) Direct Exchange of Electrons Within Aggregates of an Evolved Syntrophic Coculture of Anaerobic Bacteria. *Science* **330**(6009), 1413-1415.

Sun, D., Call, D.F., Kiely, P.D., Wang, A. and Logan, B.E. (2012) Syntrophic interactions improve power production in formic acid fed MFCs operated with set anode potentials or fixed resistances. *Biotechnology and Bioengineering* **109**(2), 405-414.

Sun, Y., Wei, J., Liang, P. and Huang, X. (2011) Electricity generation and microbial community changes in microbial fuel cells packed with different anodic materials. *Bioresource Technology* **102**(23), 10886-10891.

Suryawanshi, P.C., Chaudhari, A.B. and Kothari, R.M. (2010) Thermophilic anaerobic digestion: the best option for waste treatment. *Critical Reviews in Biotechnology* **30**(1), 31-40.

Tanaka, N. (2010). World Energy Outlook 2010, International Energy Agency

Thauer, R.K., Jungermann, K. and Decker, K. (1977) Energy conservation in chemotrophic anaerobic bactria. *Bacteriological Reviews* **41**(1), 100-180.

Torres, C.I., Kato Marcus, A. and Rittmann, B.E. (2008) Proton transport inside the biofilm limits electrical current generation by anode-respiring bacteria. *Biotechnology and Bioengineering* **100**(5), 872-881.

Torres, C.I., Krajmalnik-Brown, R., Parameswaran, P., Marcus, A.K., Wanger, G., Gorby, Y.A. and Rittmann, B.E. (2009a) Selecting Anode-Respiring Bacteria Based on Anode Potential:

Phylogenetic, Electrochemical, and Microscopic Characterization. *Environmental Science & Technology* **43**(24), 9519-9524.

Torres, C.I., Marcus, A.K., Lee, H.-S., Parameswaran, P., Krajmalnik-Brown, R. and Rittmann, B.E. (2009b) A kinetic perspective on extracellular electron transfer by anode-respiring bacteria. *FEMS Microbiol Rev* **34**(1), 3-17.

Velasquez-Orta, S., Yu, E., Katuri, K., Head, I., Curtis, T. and Scott, K. (2011) Evaluation of hydrolysis and fermentation rates in microbial fuel cells. *Appl. Microbiol. Biotechnol.* **90**(2), 789-798.

Verstraete, W., Wittebolle, L., Heylen, K., Vanparys, B., Vos, P.D., Wiele, T.V.D. and Boon, N. (2007) Microbial Resource Management: The Road To Go for Environmental Biotechnology (p). *Eng. Life Sci.* **7**(2), 117-126.

Virdis, B., Rabaey, K., Yuan, Z.G., Rozendal, R.A. and Keller, J. (2009) Electron Fluxes in a Microbial Fuel Cell Performing Carbon and Nitrogen Removal. *Environmental Science & Technology* **43**(13), 5144-5149.

Wang, X., Feng, Y., Ren, N., Wang, H., Lee, H., Li, N. and Zhao, Q. (2009) Accelerated start-up of two-chambered microbial fuel cells: Effect of anodic positive poised potential. *Electrochimica Acta* **54**(3), 1109-1114.

Watson, V.J. and Logan, B.E. (2009) Power production in MFCs inoculated with Shewanella oneidensis MR-1 or mixed cultures. *Biotechnology and Bioengineering* **105**(3), 489-498.

Weber, K.A., Achenbach, L.A. and Coates, J.D. (2006) Microorganisms pumping iron: anaerobic microbial iron oxidation and reduction. *Nat Rev Micro* **4**(10), 752-764.

Whitchurch, C.B., Tolker-Nielsen, T., Ragas, P.C. and Mattick, J.S. (2002) Extracellular DNA Required for Bacterial Biofilm Formation. *Science* **295**(5559), 1487.

Wildeboer-Veloo, A.C.M., Harmsen, H.J.M., Degener, J.E. and Welling, G.W. (2003) Development of a 16S rRNA-based Probe for Clostridium ramosum, C. spiroforme and C. cocleatum and its Application for the Quantification in Human Faeces from Volunteers of Different Age Groups. *Microbial Ecology in Health and Disease* **15**(2-3), 131-136.

Winfield, J., Ieropoulos, I., Greenman, J. and Dennis, J. (2011) The overshoot phenomenon as a function of internal resistance in microbial fuel cells. *Bioelectrochemistry* **81**(1), 22-27.

Wittebolle, L., Boon, N., Vanparys, B., Heylen, K., De Vos, P. and Verstraete, W. (2005) Failure of the ammonia oxidation process in two pharmaceutical wastewater treatment plants is linked to shifts in the bacterial communities. *Journal of Applied Microbiology* **99**(5), 997-1006.

Wittebolle, L., Vervaeren, H., Verstraete, W. and Boon, N. (2008) Quantifying Community Dynamics of Nitrifiers in Functionally Stable Reactors. *Applied and Environmental Microbiology* **74**(1), 286-293.

Woodward, L., Perreir, M., Srinivasan, B. and Tartakovsky, B. (2009) Maximizing power production in a stack of microbial fuel cells using multiunit optimisation method. *Biotechnol. Prog.* **25**(3).

Wrighton, K.C., Agbo, P., Warnecke, F., Weber, K.A., Brodie, E.L., Desantis, T.Z., Hugenholtz, P., Andersen, G.L. and Coates, J.D. (2008) A novel ecological role of the Firmicutes identified in thermophilic microbial fuel cells. *Isme J.* **2**(11), 1146-1156.

Xie, X., Hu, L., Pasta, M., Wells, G.F., Kong, D., Criddle, C.S. and Cui, Y. (2011) Three-Dimensional Carbon Nanotubeâ^'Textile Anode for High-Performance Microbial Fuel Cells. *Nano Letters* **11**(1), 291-296.

Yuan, Y., Zhou, S., Xu, N. and Zhuang, L. (2011) Electrochemical characterization of anodic biofilms enriched with glucose and acetate in single-chamber microbial fuel cells. *Colloids and Surfaces B: Biointerfaces* **82**(2), 641-646.

Zarda, B., Amann, R., Wallner, G.N. and Schleifer, K.-H. (1991) Identification of single bacterial cells using digoxigenin-labelled, rRNA-targeted oligonucleotides. *Journal of General Microbiology* **137**(12), 2823-2830.

Zeeman, G. and Lettinga, G. (1999) The role of anaerobic digestion of domestic sewage in closing the water and nutrient cycle at community level. *Water Science and Technology* **39**(5), 187-194.

Zhang, J.W., Zhang, E.R., Scott, K. and Burgess, J.G. (2012) Enhanced Electricity Production by Use of Reconstituted Artificial Consortia of Estuarine Bacteria Grown as Biofilms. *Environmental Science & Technology* **46**(5), 2984-2992.

Zhang, L., Li, C., Ding, L., Xu, K. and Ren, H. (2011a) Influences of initial pH on performance and anodic microbes of fed-batch microbial fuel cells. *Journal of Chemical Technology & Biotechnology* **86**(9), 1226-1232.

Zhang, X., Cheng, S., Liang, P., Huang, X. and Logan, B.E. (2011b) Scalable air cathode microbial fuel cells using glass fiber separators, plastic mesh supporters, and graphite fiber brush anodes. *Bioresource Technology* **102**(1), 372-375.

Zhao, F., Slade, R.C.T. and Varcoe, J.R. (2009) Techniques for the study and development of microbial fuel cells: an electrochemical perspective. *Chemical Society Reviews* **38**(7), 1926-1939.

Zobell, C.E. (1943) The Effect of Solid Surfaces upon Bacterial Activity. *Journal of bacteriology* **46**(1), 39-56.

Appendix 1 Composition for nutrient media used in all experiments

Ingredients 50mM Phosphate Buffer Media

(per liter)

H_2O	~1000	mL
NH_4Cl	0.31	g
$NaH_2PO_4 \bullet H_2O$	2.69	g
Na_2HPO_4	4.33	g
KCl	0.13	g
Minerals	12.5	mL
Vitamins	12.5	mL

Vitamins

	mg/L
biotin	2.0
folic acid	2.0
pyridoxine HCl	10.0
riboflavin	5.0
thiamin	5.0
nicotinic acid	5.0
pantothenic acid	5.0
B-12	0.1
p-aminobenzoic acid	5.0
thioctic acid	5.0

Appendix 2 LabVIEW™ block diagram detailing program used for data display and capture

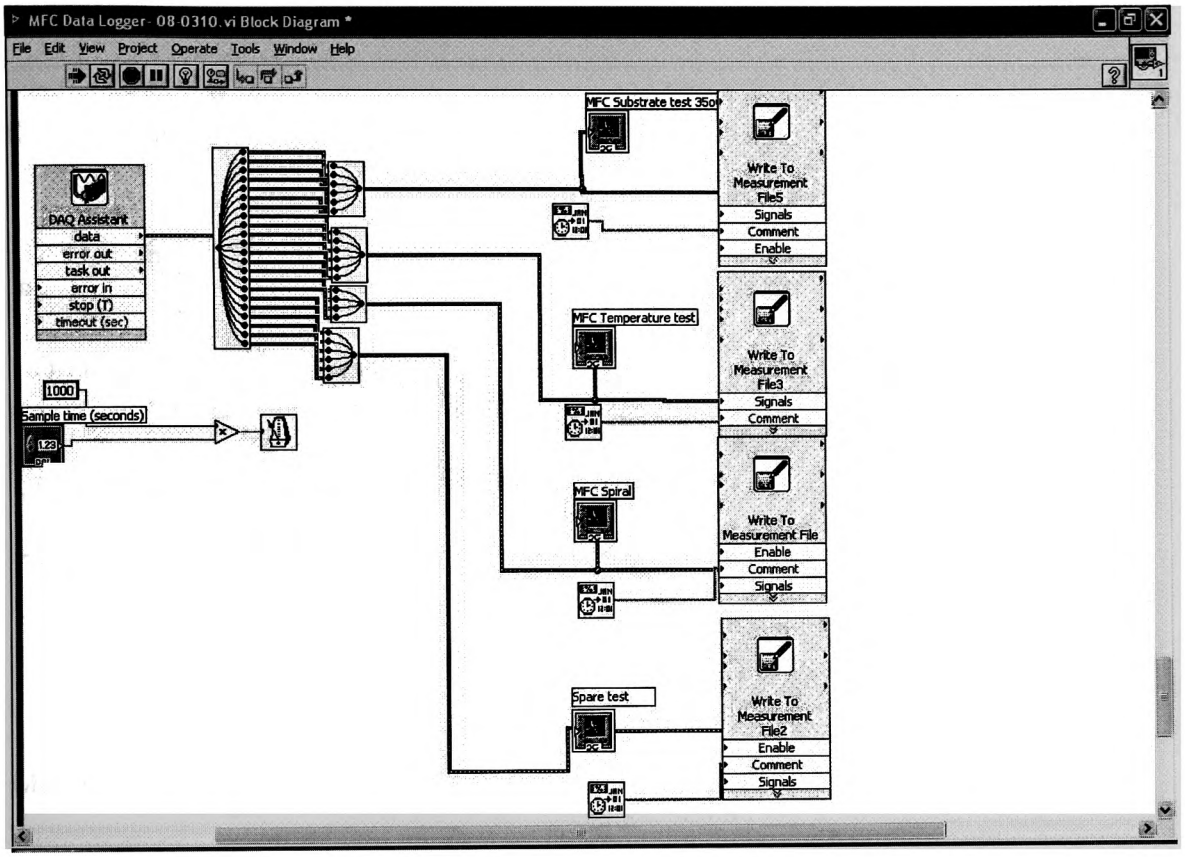

Appendix 3 Open and closed circuit first derivative plots from carbon anode materials 1, 2, 3 and 4

Closed circuit

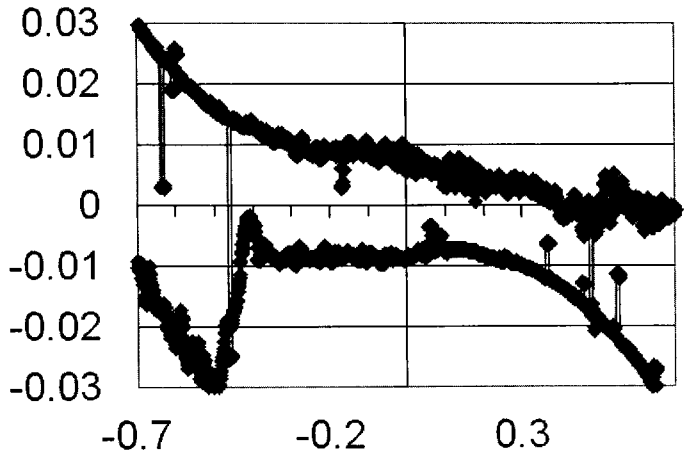

Material 1

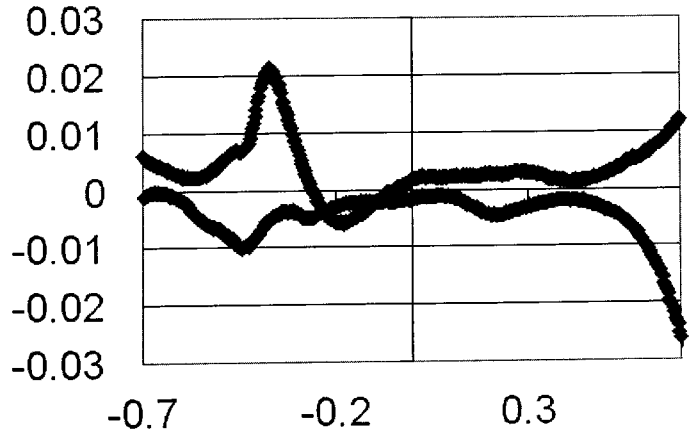

Material 2

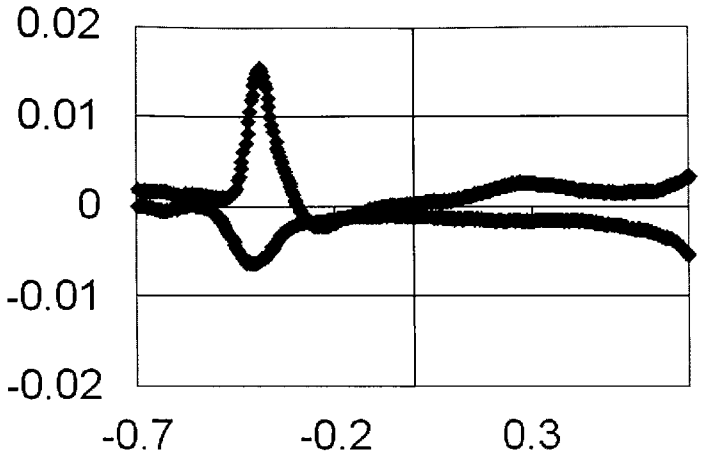

Material 3

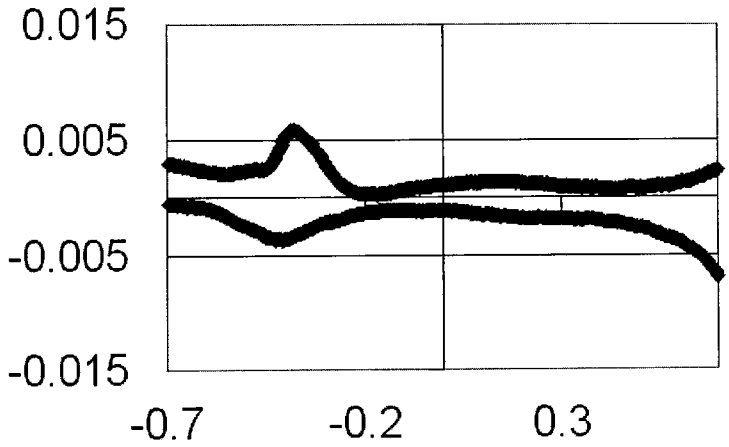

Material 4

open circuit

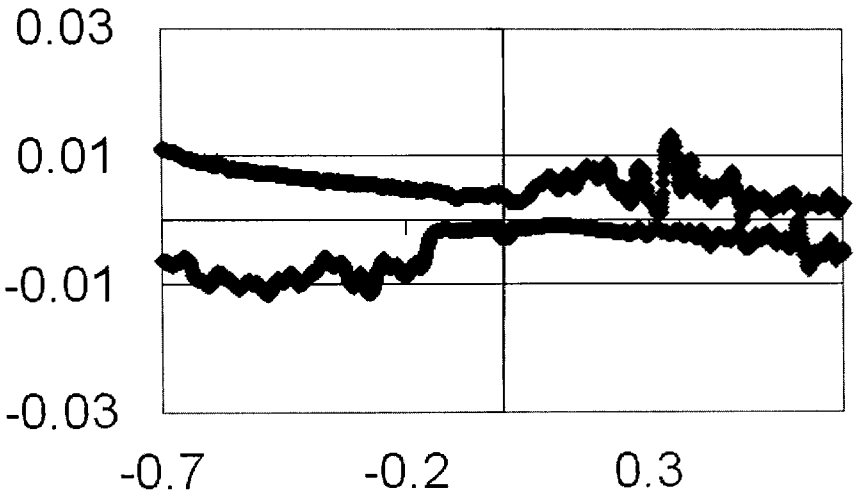

Material 1

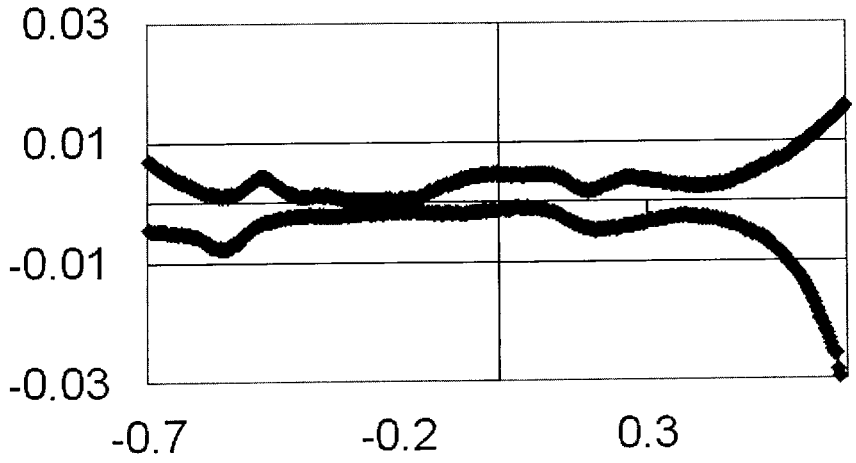

Material 2

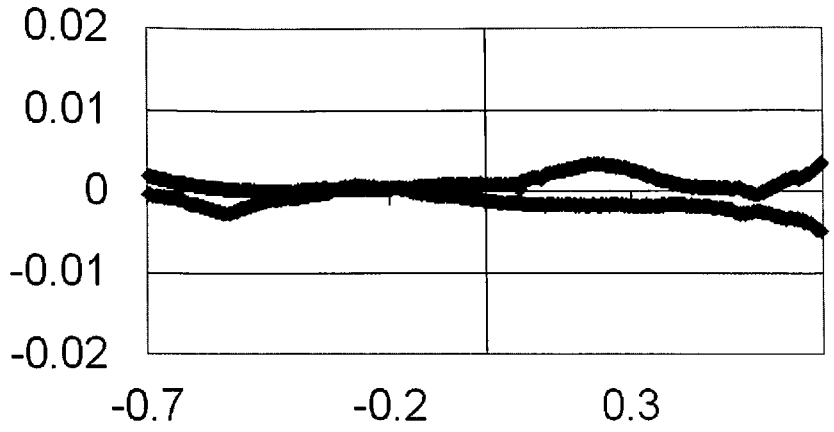

Material 3

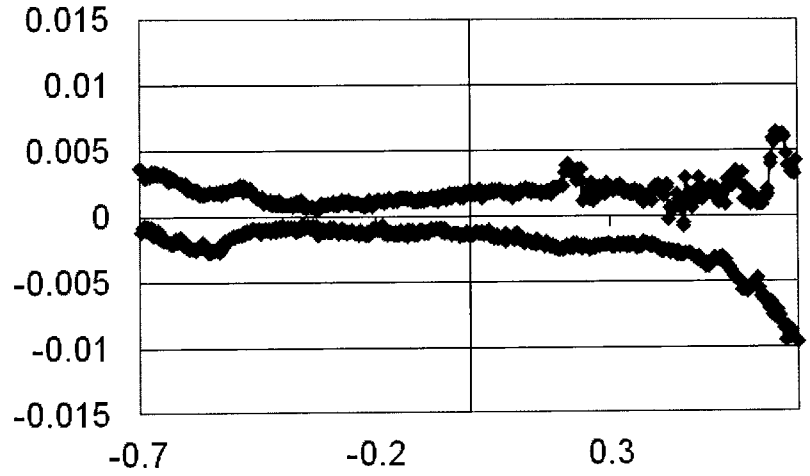

Material 4

Appendix 4 List of publications

Michie, I.S., Kim, J.R., Dinsdale, R.M., Guwy, A.J., Premier, G.C. (2011). Operational temperature regulates anodic biofilm growth and the development of electrogenic activity *Applied Microbiology and Biotechnology* Volume: 92 Issue: 2 Pages: 419-430 DOI: 10.1007/s00253-011-3531-9

Michie, I.S., Kim, J.R., Dinsdale, R.M., Guwy, A.J., Premier, G.C. (2011). The influence of psychrophilic and mesophilic start-up temperature on microbial fuel cell system performance. *Energy & Environmental Science*, 4 (3): 1011-1019.

Premier, G.C, Kim, J.R., Michie, I, Dinsdale, R.M, and Guwy, A.J. (2011) Automatic control of load increases power and efficiency in a microbial fuel cell. *Journal of Power Sources*. 196 (4) 2013-2019.

Kim, J.R., Boghani, H.C., Amini, N., Aguey-Zinsou, K.-F.o., Michie, I., Dinsdale, R.M., Guwy, A.J., Guo, Z.X., Premier, G.C., In Press. Porous anodes with helical flow pathways in bioelectrochemical systems: The effects of fluid dynamics and operating regimes. *Journal of Power Sources* 213: 382-390.

Platform presentations

Michie, I.S., Kim, J.R., Dinsdale, R.M., Guwy, A.J., Premier, G.C. Factors affecting microbial fuel cell acclimation and operation in temperate climates. *IWA World Water Congress 2012, Busan, Korea (accepted).*

Michie, I.S., Kim, J.R., Dinsdale, R.M., Guwy, A.J., Premier, G.C. Performance of temperature selected electrogenic biofilms in Microbial fuel cells: adaptation and stabilization, power and organic removal. *3rd International Microbial Fuel Cell Conference (2011), Leuwarden, Netherlands.*